The Control of Food Intake

and Bitter Taste Information Processing

in the *Drosophila* Larval Brain

Kumulative Dissertation

zur

Erlangung des Doktorgrades (Dr. rer. nat.)

der

Mathematisch-Naturwissenschaftlichen Fakultät

der

Rheinischen Friedrich-Wilhelms-Universität Bonn

vorgelegt von

Sebastian Hückesfeld

aus

Bad Bergzabern

Bonn, Mai 2016

Angefertigt mit Genehmigung der Mathematisch-Naturwissenschaftlichen Fakultät der Rheinischen Friedrich-Wilhelms-Universität Bonn

1. Gutachter: Prof. Dr. Michael J. Pankratz
2. Gutachter: PD Dr. Reinhard Bauer

Tag der Promotion: 07.11.2016

Erscheinungsjahr: 2016

To Heike, Marie and Luise

Acknowledgements

I would like to express my sincere gratitude towards Prof. Michael J. Pankratz for the excellent scientific guidance throughout my doctorate. He offered the combination of experimental freedom and lively discussions, leading to this work. Coming to his lab with a unique friendly atmosphere was a pleasure for me and I appreciated his idea of combining research fields.

I thank PD Dr. Reinhard Bauer for acting as my second referee and Prof. Dr. Gerhard von der Emde and Prof. Dr. Clemens Simmer for participation in the PHD committee.

Special thanks to Dr. Andreas Schoofs with whom I started to work in the Pankratz Lab. It was a great time with you not only scientifically but also as a friend. This kind of blindly working together is rare. Thank you.

The publications presented in this thesis would not have been possible without the cooperation with good colleagues. Special thanks go to Philipp and Anton, who provided together with Andreas and former lab members, Torsten and Marc, a pleasant and lively work atmosphere.

I want to thank the whole Pankratz lab for all the good times we had together. Especially Dr. Ingo Zinke for keeping everything under control and for always being our good cop.

To my parents. Ich danke euch für jahrelange Hilfe (nicht nur finanziell) und Eure bedingungslose Bereitschaft jederzeit für mich dazusein. Man könnte nicht besser aufwachsen und unterstützt werden in allem was man sich so denkt.

To my wife and kids. Ohne euch wäre ein Alltag außerhalb des Labors nicht mehr denkbar. Ich danke dir Heike für das Verständnis das du mir entgegen bringst wenn es mal wieder "spät" wird und für die notwendige Ablenkung sorgst, wenn der Laborfrust mal überwiegt. Marie und Luise, danke dass ihr mein Leben um ein so vieles lebenswerter macht. Durch euch weiß ich, wofür sich die Arbeit auszahlt.

To my parents-in-law and friends. Danke euch allen für die jahrelange moralische und seelische Unterstützung und die Tatsache, dass keiner gefragt hat was für einen Sinn es macht sich Fliegengehirne anzuschauen.

Abstract

The regulation of feeding behavior by central neural circuits is crucial for every organism to survive. Hierarchical organized motor systems are responsible for the execution of appropriate feeding movements and can be subdivided into higher brain centers modulating the activity of central pattern generators (CPGs), which in turn control the activity of motor neurons. Motor neurons innervate muscles whose contractions lead to the final behavioral outcome. Focus of this thesis was the deconstruction of feeding regulatory elements like motor neurons innervating the muscles specific for the *Drosophila* larval feeding cycle and neural populations modulating their activity. Emphasis relied on the functional relevance for the Hugin neuropeptide concerning feeding behavior and taste processing.

We show that motor neurons comprising the larval feeding movements are located in the subesophageal zone (SEZ) of the larval central nervous system (CNS) and that the CPG driving neural activity of the motor neurons is located in the same brain area. Serotonergic neurons located in the nearby area of feeding related motor neurons project through the enteric nervous system to the gut. Functional analysis of these neurons revealed that brain derived serotonin plays a functional role in modulating foregut motility and we suggest that this serotonergic cluster consisting of four neurons is part of a brain-gut pathway functionally analogous to the mammalian vagus nerve. Manipulating the activity of other central neural populations expressing neuropeptides or neurotransmitters revealed that the different neural populations regulate all or distinct motor subprograms for feeding. Serotonergic neurons acted as general activator of all analyzed motor programs. Dopaminergic neurons and neurons expressing the Hugin neuropeptide inhibited specifically the motor pattern of the antennal nerve, whose efferent motor output is most dedicated to food intake by generating contractions of the cibarial dilator muscles (CDM).

The detailed analysis of the 20 Hugin neurons revealed that a subset of 16 cells (Hugin$^{0.8}$) is responsible for the inhibition of food intake and wandering like behavior from an appetitive food source. The remaining four Hugin neurons (Hugin^{VNC}) were responsible for an increase in locomotive motor programs. Taken together, activation of the 20 Hugin neurons in the larval CNS leads to regulation of two mutually exclusive behaviors, inhibition of feeding and induction of locomotion. Having been proposed as gustatory interneurons earlier, we suggested that Hugin neurons act as bitter gustatory interneurons in the larval brain. This was verified by classical two-choice experiments, in which ablation of Hugin neurons resulted in animals no longer showing appropriate aversion to bitter substrates. With the generation of a specific Gal4 line, that exclusively labels eight Hugin neurons (Hugin^{PC}), projecting to the protocerebrum, it was possible to pinpoint observed effects of the Hugin neurons like feeding inhibition, wandering like behavior and impairment of bitter taste processing to these neurons. Using a new method of calcium imaging, called CaMPARI (<u>C</u>alcium <u>M</u>odulated <u>P</u>hotoactivatable <u>R</u>atiometric <u>I</u>ntegrator), we could show that the Hugin^{PC} neurons are

selectively activated when larvae taste bitter substances. Furthermore, artificial activation of neurons expressing the bitter receptor GR66a led to rhythmic calcium activity in the Hugin^{PC} neurons. We suggest that the Hugin^{PC} neurons act as second order interneurons for bitter taste in *Drosophila* larvae. The mammalian homolog of Hugin is Neuromedin U (NMU). Pleiotropic roles have been assigned to this neuropeptide in regulating core biological processes like feeding and locomotion. Therefore, the new findings about the role of the Hugin neuropeptide might serve to gain insights into functional aspects of NMU regarding a role in taste processing.

Zusammenfassung

Die Regulation der Nahrungsaufnahme durch zentrale neuronale Schaltkreise ist überlebenswichtig für jeden Organismus. Hierarchisch organisierte Motorsysteme sind verantwortlich für die adäquate Ausführung von Fressbewegungen und können in verschiedene Kontrolleinheiten unterteilt werden. Höhere Hirnzentren regulieren die Aktivität von zentralen Mustergeneratoren (ZMG), welche ihrerseits die Aktivität von Motoneuronen steuern. Die Motoneurone innervieren Muskeln, deren koordinierte Kontraktionen zum finalen Verhaltensprogramm führen. Der Fokus dieser Arbeit lag in der Analyse von regulatorischen Elementen der Nahrungsaufnahme in Larven der Taufliege *Drosophila melanogaster*. Die Motoneurone, welche für die Bewegungen der Nahrungsaufnahme verantwortlich sind, sollten identifiziert und zentrale Neuronenpopulationen, welche die Motoneurone modulieren, näher untersucht werden. Hauptaugenmerk der hier vorgestellten wissenschaftlichen Arbeit lag auf dem Neuropeptid Hugin für das eine funktionelle Relevanz bei der Modulation der Nahrungsaufnahme, sowie eine Rolle bei der zentralen Geschmacksverarbeitung erarbeitet werden sollte.

In dieser Arbeit wurde gezeigt, dass sich die für die Nahrungsaufnahme verantwortlichen Motoneurone im suboesophagealen Ganglion (SOG) des larvalen zentralen Nervensystems (ZNS) befinden. Der zentrale Mustergenerator, dem die Aktivität der Motoneurone zugrunde liegt konnte ebenfalls im SOG lokalisiert werden. Serotonerge Neurone, welche sich in räumlicher Nähe zu den für die Nahrungsaufnahme relevanten Motoneuronen liegen, projizieren durch das enterische Nervensystem zum Darm. Eine funktionelle Untersuchung dieser Neurone konnte zeigen, das Serotonin, welches im Gehirn produziert wird, eine Rolle bei der Vorderdarmbewegung spielt. Wir schlagen vor, dass diese identifizierten vier serotonergen Neurone Teil eines Gehirn-Darm Signalsystems sind, welche funktionell analog zum Vagus-Nerv bei Säugetieren agiert. Die Manipulation anderer zentraler Neuronenpopulationen, welche Neuropeptide oder Neurotransmitter ausschütten, ergab, dass bestimmte Neuronenpopulation alle oder spezifische Motorsubprogramme der Nahrungsaufnahme modulieren. Serotonerge Neurone agierten in dieser Studie als genereller Aktivator aller untersuchten Motorprogramme. Dopaminerge Neurone und Neurone, welche das Neuropeptid Hugin freisetzen inhibierten spezifisch die Aktivität des Antennalnervs, dessen efferente Motoreinheiten exklusiv der Nahrungsaufnahme durch Kontraktion der cibarialen Dilatormuskulatur (CDM) dienen.

Die detaillierte Untersuchung der 20 Hugin Neurone konnte zeigen, dass 16 dieser Neurone (Hugin$^{0.8}$) verantwortlich für die Inhibition der Nahrungsaufnahme sind, als auch für das aktive Verlassen einer appetitiven Futterquelle. Die verbleibenden vier Hugin Neurone (Hugin^{VNC}), welche zum ventralen Nervensystem der Larve projizieren, waren für eine Erhöhung des Motorprogramms für die Fortbewegung verantwortlich. Zusammenfassend wurde gezeigt, dass die Aktivität der Hugin Neurone im ZNS zwei gegensätzliche exklusive

Verhaltensweisen steuert: Inhibition der Nahrungsaufnahme und Zunahme von Lokomotion. Hugin Neurone wurden schon früher als gustatorische Interneurone bezeichnet, die möglicherweise an der Geschmacksverarbeitung von Bitterstoffen beteiligt sind. Der Beweis erfolgte durch Ablation der Hugin Neurone. Die Ablation führte zu einem veränderten Entscheidungsverhalten bei Larven, die nun bittere Substrate nicht mehr adäquat vermieden. Durch die Verwendung einer spezifischen GAL4 Linie, welche nur in den acht Hugin Neuronen exprimiert wird, die zum Protocerebrum der Larven projizieren (Hugin^{PC} Neurone), konnte die Anzahl der für diesen Effekt verantwortlichen Neurone genau bestimmt werden. Manipulation der Hugin^{PC} Neurone führte zu den gleichen Phänotypen, die auftreten, wenn alle Hugin Neurone aktiviert oder inaktiviert werden, nämlich Inhibition der Nahrungsaufnahme, verstärktes Wanderverhalten und beeinträchtigte Verarbeitung des Bittergeschmacks. Durch die Anwendung einer neuen Methode zur Messung der Kalzium Aktivität in Neuronen (CaMPARI), konnten wir zeigen, dass die Hugin^{PC} Neurone selektiv durch bitter schmeckende Substanzen aktiviert werden. Eine künstliche Aktivierung von Neuronen, die den Bitter-Rezeptor GR66a exprimieren, führte zu rhythmischer Kalzium abhängiger Aktivität der huginPC Neurone. Zusammenfassend konnten wir zeigen, dass die Hugin^{PC} Neurone als gustatorische Interneurone für die Verarbeitung von Bittergeschmack dienen.

Für das Säugetier-Homolog von Hugin - das Neuropeptid Neuromedin U (NMU) - wurden verschiedene Funktionen in physiologischen Prozessen wie der Regulation der Nahrungsaufnahme und Lokomotion identifiziert. Eine Funktion bei der Geschmacksverarbeitung wurde bisher jedoch nicht beschrieben. Somit könnten die hier gewonnenen Erkenntnisse über die Funktion der Hugin Neurone genutzt werden um weitere funktionelle Aspekte von NMU hinsichtlich einer Rolle bei der Geschmacksverarbeitung in Säugern zu untersuchen.

Table of Contents

List of Figures

1   General Introduction

In neurobiology one of the most fundamental questions to date is how the brain controls certain behaviors and why we choose these behaviors over others. How important it is for us to understand brain function is demonstrated by the huge investments of initiatives like BRAIN (Brain Research through Advancing Innovative Neurotechnologies®, USA) or the Human Brain Project (Europe). These aim to accelerate the development and application of innovative technologies to show how individual cells and complex neural circuits interact in both time and space (BRAIN) or to accumulate scientific knowledge about the brain and simulate brain functions in computerbased models (Human Brain Project).

The central regulation of feeding and its dysregulation represent an important aspect of research since progress in this scientific area facilitates the establishment of new methods and therapies for emerging society diseases like diabetes and obesity [FRIEDMAN & HALAAS, 1998; HARROLD ET AL., 2012; MEISTER, 2007]. To be able to design drugs that specifically target the source of dysfunction, it is necessary to precisely understand the mechanisms how the neural system operates and orchestrates activity to achieve the appropriate behavior.

In this thesis, the central neural control of feeding and taste processing in the brain was investigated using larvae of the fruit fly *Drosophila melanogaster* as a model organism for deconstructing neural networks underlying feeding behavior. *Drosophila* serves as a genetic model organism for more than 100 years. Since 1910 with the discovery of the *white* gene by Thomas Hunt Morgan, *Drosophila melanogaster* has greatly contributed to the field of genetics [MORGAN, 1910]. Researchers like Nüsslein-Volhard and Wieschaus paved the way for the genetic research on embryonic development [NÜSSLEIN-VOLHARD & WIESCHAUS, 1980]. Work on the Notch signaling pathway, being important for neurogenesis and differentiation of neurons, was based on findings in *Drosophila* research from 1915 till the cloning of the mammalian Notch in the 90`s [ELLISEN ET AL., 1991]. Notch is highly conserved between invertebrates and vertebrates with functional similarities in vivo [BRAY, 2006; MORGAN & BRIDGES, 1916]. With the technical advance over the last 30 years the genetically developed tools offered the possibility to turn *Drosophila* into one of the most powerful model organisms in neuroscience. *Drosophila* research elucidated functional key aspects in biological processes like circadian rhythm, learning and memory, chemosensory processing, synaptic transmission [BELLEN ET AL., 2010]. Nowadays *Drosophila* serves in addition to the existing mouse models as model for neural diseases like Parkinson or Alzheimer [FEANY & BENDER, 2000; PRÜßING ET AL., 2013]. One of the holy grails in todays neuroscience is the

dissection of sensorimotor circuits to understand how external cues and internal states of the organism are integrated and processed by the central nervous system and ultimately affect the motor output driving the final behavior.

The following introductory chapters will provide the basic and current knowledge about the neural basis of feeding regulation and taste processing in mammals and flies. This comparison seems to be tough at a first glance, but indeed conservation of both biological processes exists and thus allows to use *Drosophila*, adult and larval stages, to gain insight into the basic biological computation of sensorimotor behaviors in the brain [RAJAN & PERRIMON, 2013; YARMOLINSKY ET AL., 2009].

1.1 Regulation of Feeding

The physiological act of food intake and swallowing is a complex motor event in humans and is primarily investigated in animal models. Although the muscle contractions from oral to pharyngeal muscles are influenced by sensory and higher brain center inputs, the sequence of contractions is not altered. This is one example for the existence of a central pattern generator (CPG) for feeding in humans [ERTEKIN & AYDOGDU, 2003].

A CPG is defined as neural circuit that produces a rhythmic motor pattern. This happens in the absence of any sensory or descending inputs that provide timing information [MARDER & BUCHER, 2001]. Behaviors like walking, breathing, flying, swimming and feeding are regulated by the activity of CPG networks [BÄSSLER & BÜSCHGES, 1998; KATZ & FROST, 1995; SILLAR, 1993; STRAUB & BENJAMIN, 2001; VON EULER, 1983; WILSON, 1961]. The work on vertebrate and invertebrate animal models over the past 40 years provided detailed insights into the structure, function and network dynamics of CPG`s [DELCOMYN, 1980; GRILLNER & ZANGGER, 1979; SELVERSTON, 2010]. One of the most detailed analyzed neural networks that is driven by a CPG is the crustacean stomatogastric ganglion (STG). The pyloric and gastric CPG of the STG represent the best understood neural circuits related to feeding [SILLAR, 1993]. Locomotor CPGs have been studied in lamprey [COHEN, 1987] and the decerebrated cat [GRILLNER & ZANGGER, 1979], as well as in the stick insect [BÄSSLER & BÜSCHGES, 1998]. Investigations in these models have led to great knowledge about the function of neural network dynamics. Less is known about cellular details of CPGs for feeding in the central nervous system.

In addition to the intrinsic properties of oscillating neural networks every nervous system is subject to neuromodulation. Neuromodulators which act as hormones, namely neuropeptides or neurotransmitters shape and reconfigure neural circuits and thereby specify their function to give rise to the appropriate behavior [MARDER, 2012].

1.1.1 Motor Control of Swallowing

Mammals

To swallow food is one of the most natural and crucial behaviors animals, including humans, display in order to survive. The physiological nature of swallowing, due to its complexity, has received less attention than other motor activities like locomotion or respiration [ERTEKIN & AYDOGDU, 2003].

The physiological act of swallowing, also called deglutition, is mainly structured into three phases: the oral phase, the pharyngeal phase (oropharyngeal phase) and the esophageal phase. The oral phase of swallowing is considered as being voluntarily and depends on taste, environment, hunger, motivation and consciousness. Several functions are involved in this stage like movement of the tongue, pressing the bolus (chewed food or liquid) to the hard palate and initiation of movement of the bolus to the posterior part of the tongue and oropharynx. Further movements of lip and cheek muscles prevent the escape of the solid food (**Figure 1.1 a and b**). The pharyngeal phase describes all motor events like laryngeal elevation for airway protection or positioning of the larynx anterosuperiorly under the tongue (**Figure 1.1 c**). The tongue then pushes the bolus throughout the pharynx into the esophagus and a set of pharyngeal constrictor muscles clears the material from the pharynx into the esophagus (**Figure 1.1 d**). The upper esophageal sphincter (UES) consists of the inferior pharyngeal muscles and the cricopharyngeal muscle and represents the functional border to the esophageal phase of swallowing (**Figure 1.1 e**). The UES is tonically contracted (closed), but relaxed during swallowing. This relaxation of the UES during swallowing is thought to undergo neural inhibition from the medulla in the brainstem during swallowing [ERTEKIN & AYDOGDU, 2003].

The esophageal phase of swallowing describes the passage of food from the UES to the lower esophageal sphincter (LES). Similar to the UES, the LES is also contracted to prevent regurgitation from the stomach, when no food is swallowed. The peristaltic movements of the esophagus transport the food bolus to the stomach via the LES [MATSUO & PALMER, 2009].

The swallowing musculature is innervated by five cranial nerves. Cranial nerve V innervates muscles for mastication and bolus propulsion, cranial nerve VII (facial) innervates lips to prevent spilling out food during swallowing. Cranial nerves IX (glossopharyngeal) and X (vagus) innervate the stylopharyngeus muscle that elevates and pulls the larynx to aid in relaxation of the cricopharyngeal muscle (upper esophageal sphincter). The vagus nerve innervates muscles involved in the esophageal phase of swallowing. The cranial nerve XII (hypoglossal) innervates muscles of the tongue [MATSUO & PALMER, 2009].

The sequential neural activity of the cranial nerves leads to the sequential contractions of swallowing muscles (**Figure 1.1 f**).
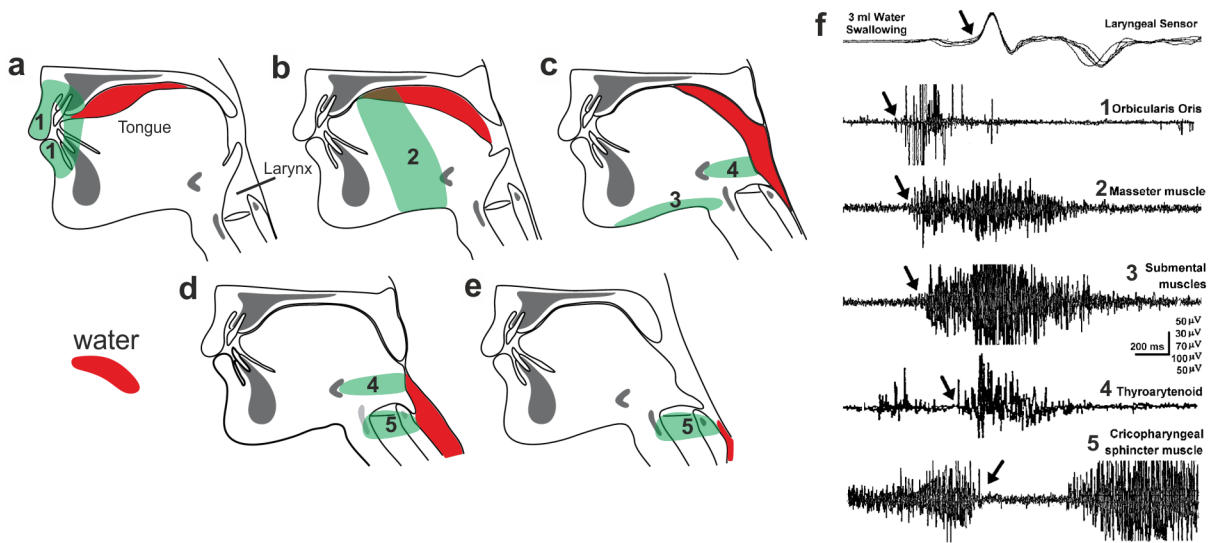

Figure 1.1: Physiology of Swallowing

> **a**) Part of the oral phase of swallowing. The bolus (food or liquid) is held by the tongue and lip muscles (e.g. orbicularis oris, 1) this prevents spillage. **b**) Bolus is processed from oral cavity to pharynx. Muscles of tongue and cheeks (masseter muscle, 2) are involved. **c**) Part of the pharyngeal phase of swallowing. The bolus is transported to the esophagus. Muscles involved are submental muscles and thyroarytenoid, 3 and 4. **d**) Begin of esophageal phase of swallowing. The UES opens and the bolus is transported to the esophagus (cricopharyngeal muscle, 5). **e**) After passage of the bolus, the cricopharyngeal muscle returns to contracted state and closes the UES. **f**) Electrophysiological recordings from the sequential activity of muscles involved in the different swallowing phases. Numbers in front of the muscles correspond to the number indicated in a-e. a-e are adapted and modified from Matsuo & Palmer, 2009. F is adapted and modified from Ertekin & Aydogdu, 2003. UES, upper esophageal sphincter.

Motor neurons driving the sequential contractions of feeding related muscles are located in the nucleus tractus solitarius (NTS) and the reticular formation surrounding the nucleus ambiguus in the brainstem. Neurons in the NTS are active during the oropharyngeal or esophageal phase and are thought to be part of the swallowing CPG [JEAN, 2001]. Those neurons extent their efferent fibers through a branch of the vagus nerve to innervate posterior portions of the tongue muscles. The vagus nerve is also known to harbor taste afferents and sensory fibers from the gastrointestinal tract, thereby playing a predominant role in the regulation of feeding and taste processing [TRAVAGLI ET AL., 2006].

Drosophila

Drosophila larvae represent an ideal model system for the investigation of neural circuits underlying the execution of feeding movements. Due to its limited behavioral repertoire, which consists of 84% feeding, 12% locomotion and 4% other behaviors [GREEN ET AL., 1983], the larva displays feeding behavior throughout most of its developmental time. The investigation of feeding in adult stages of *Drosophila* is more complex, since they are discontinuous feeders and prestarvation before experiments is necessary to ensure robust feeding behavior. In order to be able to elucidate specific aspects of feeding, anatomical and functional knowledge serves as prerequisite. In the last years much progress has been made to turn *Drosophila* into a powerful model organism to investigate basic principles of feeding regulation and taste processing.

Most of the previous studies investigating feeding behavior in flies monitored the final behavioral outcome, like measuring ingested food [EDGECOMB ET AL., 1994; JA ET AL., 2007]. In *Drosophila* larvae food intake was measured as frequency of mouth hook contractions [WU ET AL., 2005], although mouth hooks additionally serve to facilitate locomotion. More recently identification of GABAergic interneurons in adult flies that impose direct feeding restraint [POOL ET AL., 2014a] or motor neurons being involved in the motor control of the feeding circuit [GORDON & SCOTT, 2009; MANZO ET AL., 2012] expanded our knowledge about feeding motor control in the *Drosophila* brain. In larval and adult stages of *Drosophila* the motor neurons innervating pharyngeal muscles are located in the subesophageal zone (SEZ), formerly known as subesophageal ganglion [GORDON & SCOTT, 2009; TISSOT ET AL., 1998]. In other insects motor circuits for chewing and foregut contractions can be localized in the SEZ [GRISS, 1990] and/or in the frontal ganglion (FG) [AYALI, 2004; MILES & BOOKER, 1994, 1998].

The behavioral sequence of feeding in *Drosophila* larvae consists of foraging to the food source and elevation of the mouth hooks. Subsequently the feeding apparatus is moved into the food substrate and mouth hooks are moved downwards to shovel food to the mouth opening. Food is pumped into the pharynx by contraction of cibarial dilator muscles (CDM) and subsequently transported through to the esophagus and proventriculus. The ingested food is further processed in the midgut (**Figure 1.2 a-b**) [SCHOOFS ET AL., 2010; ZINKE ET AL., 1999].

Recently the existence of a CPG for feeding in *Drosophila* larvae was shown [SCHOOFS ET AL., 2010]. A detailed description of the underlying anatomical and morphological components of the larval feeding system was established. Three pharyngeal nerves leave the larval central nervous system (CNS) to innervate specific sets of muscles, whose alternating contractions represent this larval feeding cycle (**Figure 1.2 c**). The maxillary nerve

(MN) innervates bilaterally the muscles involved in up and downward movements of the mouth hooks, called the mouth hook elevator and depressor (MHE and MHD). Apart from shoveling food to the oral cavity the mouth hooks facilitate locomotion by hooking into the substrate during forward movement. The prothoracic accessory nerve (PaN) innervates two dorsal protractor muscles (Pro$_{do}$A and B) realizing head tilting movements into the food substrate. The antennal nerve (AN) innervates the CDM, whose contraction leads to a volume increase of the cibarium, a structure comparable to the oral cavity in mammals. This movement in turn generates negative pressure for sucking food into the pharynx. Electrophysiological measurements of all three nerves on isolated central nervous systems describe the motor pattern sequence that leads to a fictive feeding cycle (**Figure 1.2 d**) [SCHOOFS ET AL., 2010]. Their rhythmic alternating neural activity occurs in defined phase relation to ensure the effective sequence of muscle contractions for food intake behavior (**Figure 1.2 e**). In blowfly larvae it was be shown that the CDMs are not simultaneously active, but follow the principle of sequential activity, to facilitate food transport within the cibarium [SCHOOFS & SPIEß, 2007] (**Figure 1.2 f**). This step of the larval feeding behavior shares the functional similarities to the oral and pharyngeal phase in mammals as depicted earlier. Thus, motor activity within the AN is exclusively dedicated to food intake behavior. Although the existence of a feeding CPG was demonstrated and the nerve activity underlying feeding movements was monitored, the responsible motor neurons for these muscle movements to generate a feeding cycle in *Drosophila* larvae have not yet been identified.
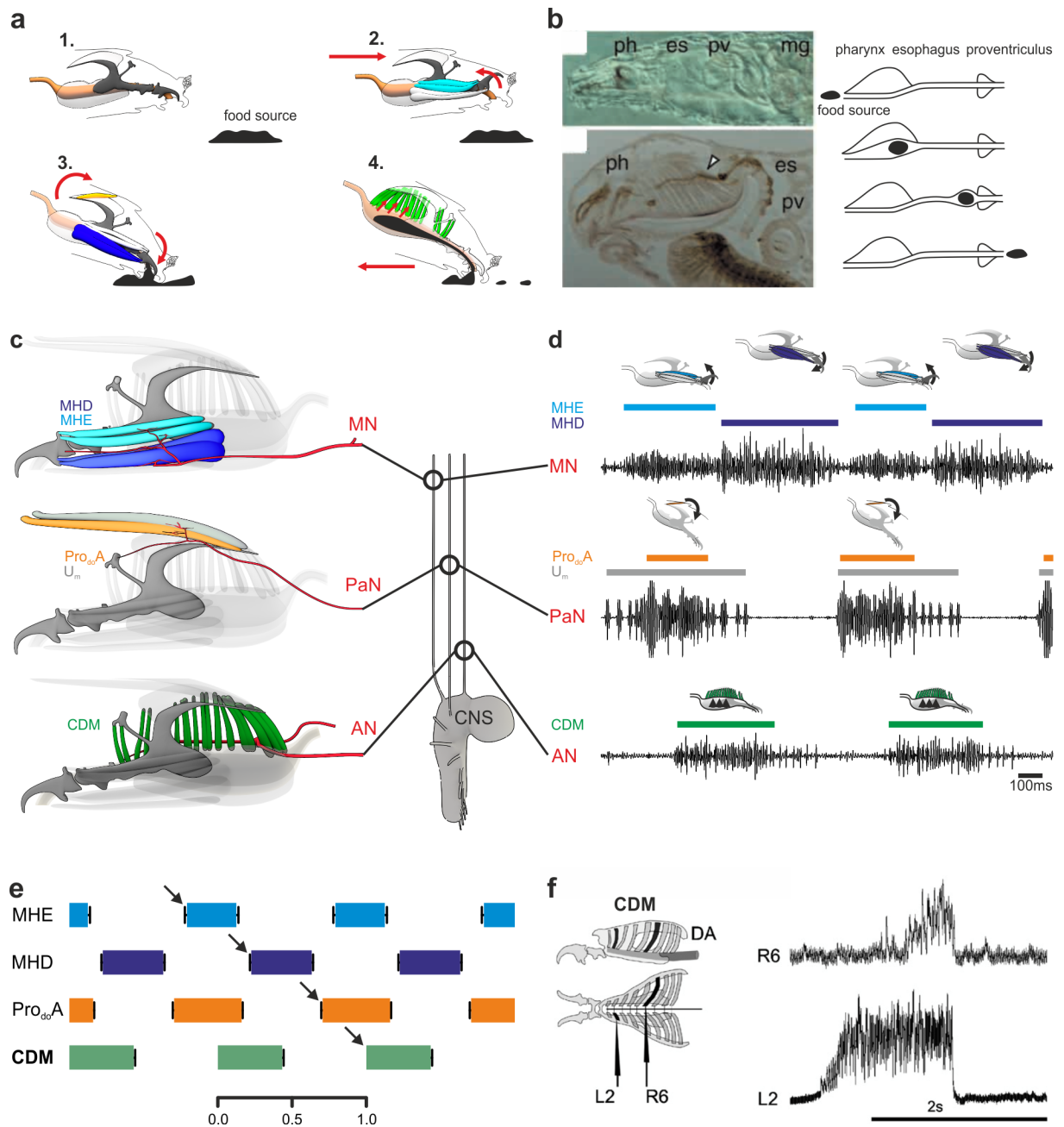
Figure 1.2: Physiology of Food Intake in *Drosophila* Larvae

a) Feeding related movements of *Drosophila* larvae. Larva is in the nearby area of a food source (black) (1.) and forages to it with elevation of the mouth hooks (2.). The feeding apparatus is tilted and mouth hooks shovel food to the mouth opening (3.). Increase of the cibarial lumen leads to negative pressure and food sucked into pharynx (4.). **b**) After entering the pharynx (ph) food is further processed via the esophagus (es) to the proventriculus (pv) and subsequently digested in the midgut (mg). Adapted and modified from [ZINKE ET AL., 1999]. **c**) Muscle groups involved in feeding related movements. Mouth hook depressor and -elevator (MHD and MHE, respectively) are innervated by the maxillary nerve (MN). Dorsal protractor muscle A (Pro$_{do}$A) is innervated by the prothoracic accessory nerve (PaN). The cibarial dilator muscles (CDM) are innervated by the antennal nerve (AN). CNS, central nervous system. **d-e**) Extracellular recordings of all three pharyngeal nerves give rise to a sequentially phase related neural activity and the motor pattern for "fictive feeding". shown in [SCHOOFS ET AL., 2010], recordings are courtesy of Dr. Andreas Schoofs. **f**) Within the group of CDM, sequential rhythmic muscle activity can be observed. DA, dorsal arms. Taken from [SCHOOFS & SPIEß, 2007].

1.1.2 Neuromodulation

"Neuromodulators play a key role in adjusting animal behavior based on environmental cues and internal needs… the basic challenge in food intake is to maintain energetic homeostasis by balancing food consumption with energy expenditure" [POOL & SCOTT, 2014b]. In isolated CNS, CPGs for feeding produce a basic rhythmic output. In intact animals this rhythm is modulated by intrinsic and extrinsic cues. Extrinsic cues are environmental factors detected by sense organs to adapt behavior to visual, mechanical, olfactory or gustatory inputs. Organs like stomach, gut, liver or adipose tissue release intrinsic cues to report internal state and to tune feeding habits. Neuromodulators like peptides, transmitters or biogenic amines are capable of modulating food intake and other behaviors [MARDER ET AL., 2014]. The effects of neuromodulators influencing behavioral outcome is well conserved among animals [RAJAN & PERRIMON, 2013; THOMAS ET AL., 2015].

Certain brain regions implicated to be important for feeding and taste processing show functionally and evolutionary similarities between mammals and flies. The hypothalamus, a brain area important for feeding and stress related behaviors in mammals, is comparable to the insect protocerebral pars intercerebralis (PI) and pars lateralis (PL). For the pituitary gland similarities to the ring gland (RG) ,the major neuroendocrine organ in *Drosophila*, [HARTENSTEIN, 2006] was shown. Further, a brain region in mammals within the medulla in the brainstem is called nucleus tractus solitarius (NTS) and represents the first relay center for sensory information [YAMAMOTO, 2008]. The functional and morphological homolog in *Drosophila* is the SEZ serving sensory integration and relaying information to higher brain centers [COLOMB & STOCKER, 2007]. Apart from brain areas representing functional homologies in both species, also neuropeptidergic circuits are conserved.

In the following chapter specific examples of such neuromodulatory circuits will illustrate the complexity of neuromodulation in the light of food intake decisions in mammals and *Drosophila*. The homologous function of Neuromedin U (NMU) and Hugin will be introduced in separate chapters (1.2 and 1.3).

Mammals

To control food intake and prevent overconsumption the brain has to integrate numerous signals in order to evaluate the energy demands of the body and to initiate the relevant behavioral actions [HARROLD ET AL., 2012]. Signals for appropriate feeding regulation are manifold like peripheral receptors in the gut or metabolic changes in liver. This information is sent via vagal afferents to the NTS in the brainstem. Signals can also derive from receptors within the brain, which detect circulating levels of nutrients in the periphery or substances like glucose or neurotransmitters. These cross the blood brain barrier and act directly on the CNS changing neurochemically the activity at key regulatory sites [BLUNDELL, 1991; HALFORD & BLUNDELL, 2000].

The main feeding regulatory site within the vertebrate brain is the hypothalamus where release of distinct neuropeptides has been shown to play a key role in feeding [ELMQUIST ET AL., 1999; HOEBEL & TEITELBAUM, 1962; SOHN ET AL., 2013]. Neuropeptides modulating feeding behavior have been categorized in either being orexigenic, promoting food intake, or anorexigenic, inhibiting food intake. Orexigenic neuropeptides in the CNS are Agouti related peptide (AGRP), Neuropeptide Y (NPY) and GABA, Melanin concentrating hormone (MCH) and orexins. Peripheral orexigenic peptides are mainly produced by feeding related organs like stomach, gut, fat tissue and liver. Being transported to the brain they deliver information about the current status of energy metabolism and internal homeostasis. Examples are Galanin or Ghrelin produced in stomach and gut.

Anorexigenic peptides in the CNS are Corticotropin releasing hormone (CRH), Pro-opiomelanocortin (POMC), Oxytocin or Neuromedin U (NMU). Leptin and Insulin are the most investigated peripheral satiety factors known today. They are released by white adipose tissue and pancreatic islet cells, respectively. Furthermore, release of Cholecystokinin (CCK) from the gut is a potent peripheral signal that downregulates feeding and is thought to act as satiety signal. Also the neurotransmitters gamma amino butyric acid (GABA) and serotonin (5-HT) act as anorexigenic transmitters within the CNS.

Since the discovery of Leptin [FRIEDMAN & HALAAS, 1998; Y. ZHANG ET AL., 1994], a cytokine released from white adipose tissue to induce satiety, research in the field of feeding regulation experienced a renaissance. Recent technological progress made it possible to deconstruct the neural pathways underlying central feeding regulation. It was shown that peripheral signals like Leptin or CCK activate or inhibit distinct areas in the brain to modulate food intake. These areas include the NTS and the arcuate nucleus (ARC), a region within the hypothalamus strongly involved in appetite regulation. For Leptin it is known, that it can bind via the Leptin receptor to AGRP or POMC neurons in the ARC, inhibiting the neural activity of AGRP neurons, while enhancing the activity of POMC neurons [COWLEY ET AL., 2001;

SCHWARTZ ET AL., 1997]. POMC neurons release α-Melanocyte stimulating hormone (α-MSH) to bind to and activate Melanocortin receptors in the para ventricular nucleus of the hypothalamus (PVN). Whereas POMC neurons have been shown to downregulate feeding, AGRP neurons are activated by weight loss and actively inhibit POMC neurons through GABAergic input. Projections of both neural populations, POMC and AGRP, target the PVN. Next order neurons then project to the NTS, which is the first processing center for taste and satiety [MORTON ET AL., 2014]. This is just one example of peptidergic modulation of feeding. It has also been shown, that neurotransmitters are involved in signaling satiety. On the one hand GABA signaling, as previously mentioned, takes place in AGRP neurons to promote feeding through inhibition of POMC neurons and tonical inhibition of Calcitonin gene related peptide (CGRP) neurons in the parabrachial nucleus (PBN) [WU ET AL., 2009, 2012], which when activated trigger anorexia. On the other hand serotonin and glutamate have been implicated to play a pivotal role in signaling of satiety via POMC neurons in the ventromedial hypothalamic nucleus (VMN) (**Figure 1.3**) [MORTON ET AL., 2014].

A different neural network to control food intake is involved in the acquisition of a conditioned taste aversion (CTA). CTA is established when the taste of a novel food source is followed by gastrointestinal malaise. Responsible for this feeding suppression is the neuropeptide Calcitonin gene related peptide (CGRP). Neurons expressing CGRP are localized in the PBN and are activated by LPS (lipopolysaccharides from bacteria) or the toxic substance lithium chloride. These substances lead to the activity of CGRP neurons which in turn might regulate downstream neural circuits in the amygdala, where visceral discomfort and sensory taste signals converge [CARTER ET AL., 2013, 2015].

Taken together multiple neuropeptides and neurotransmitters act in concert to maintain energy homeostasis and metabolism together with emergency systems that prevent us from intake of harmful and toxic food. Most of these findings were obtained using pharmacological approaches to assess the overall function of a certain peptide or transmitter. Genetically more tractable animal models like mouse, rat or *Drosophila* will facilitate our understanding of how specific brain circuits act together to form the appropriate behavioral outcome. In *Drosophila*, homologous peptides to the mammalian system have been identified, which make it an ideal model to investigate the principles of feeding regulation. The following chapter will summarize the current knowledge of feeding regulatory elements in *Drosophila*.
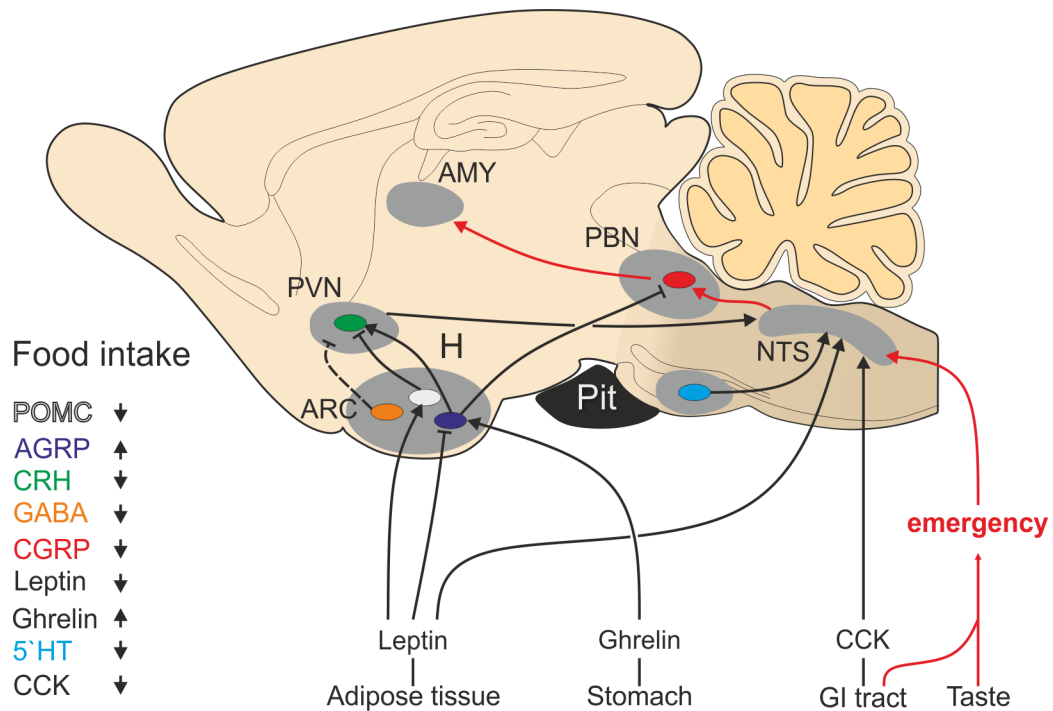
Figure 1.3: Neuromodulation of Food Intake in the Mammalian CNS

Neuromodulatory pathways in the central nervous system (CNS) are defined by the neural activity of neuropeptides and neurotransmitter acting on next order neurons to up- or downregulate feeding (arrows on the left). POMC, Pro-opiomelanocortin neurons; AGRP, Agouti related protein; CRH, Corticotropin-releasing hormone; GABA, gamma amino butyric acid; CGRP, Calcitonin gene-related peptide; 5-HT, serotonin; CCK, Cholecystokinin; AMY, amygdala; PBN, parabrachial nucleus; NTS, nucleus tractus solitarius; Pit, pituitary gland; ARC, arcuate nucleus; PVN, paraventricular nucleus; H, hypothalamus. Arrows represent activation, bar headed lines represent inactivation (in scheme). Information for drawing scheme from [MORTON ET AL., 2014].

Drosophila

Adult and larval stages of *Drosophila* have numerically a much simpler central nervous system, which offers the possibility to study the function of conserved neuropeptides down to the cellular level. *Drosophila* neuropeptides were shown to act on different subprograms of feeding behavior (**Figure 1.4**). Like NPY in mammals, its homolog Neuropeptide F (NPF) promotes food intake in *Drosophila* [BROWN ET AL., 1999; WU ET AL., 2003]. Ablation of NPF neurons leads to deficits in foraging behavior and decreased motivation to feed after fasting. This is in line with findings in the mammalian system, where NPY knockout mice also showed reduced refeeding after fasting [SEGAL-LIEBERMAN ET AL., 2003]. This effect observed in *Drosophila* was not due to an alteration of the basic feeding motor program, but to an altered motivation to feed as also shown in mammals [FLOOD & MORLEY, 1991]. In contrast to peptides that promote feeding, CCK released from the gut is known to be a potent satiety signal in mammals [STRADER & WOODS, 2005]. The *Drosophila* homolog Drosulfakinin

(DSK) [NICHOLS ET AL., 1988] was recently investigated to unravel its role in satiety [SÖDERBERG ET AL., 2012]. DSK immunoreactivity was present in various central neuronal populations of the adult and larval stage of *Drosophila*, in contrast to the peripherally released mammalian homolog. Three DSK positive neurons displayed colocalization with *Drosophila* Insulin like peptide (DILP) producing neurons. Decreasing DSK content only in these three neurons resulted in increased feeding in adults and larvae as well as affecting food choice behavior. Further knockdown of either peptide, DILP or DSK, affected transcript levels of the other, indicating that in *Drosophila* DSK and DILPs act in concert to modulate food intake.

Adipokinetic hormone (AKH) is the *Drosophila* homolog of mammalian Glucagon. As in mammals it was shown that AKH activates glycogen phosphorylase and mobilizes carbohydrates (trehalose) in the fat body [GRÖNKE ET AL., 2007; KIM & RULIFSON, 2004]. AKH positive cells are found exclusively in the corpora cardiaca (CC), a portion of the ring gland, which is the major neuroendocrine organ of *Drosophila*. AKH signaling has been shown to be important for metabolic balance and glucose homeostasis. Mutation of the *akh* gene leads to an obese phenotype in adult flies. This phenotype is not caused by hyperphagic (overconsummatory) behavior, but instead is due to the inability to mobilize fat stores and conversion into carbohydrates [BHARUCHA ET AL., 2008]. It was postulated, that hyperglycemic effects of AKH act antagonistically to the activity of DILP to fine tune systemic energy requirements [KIM & RULIFSON, 2004].

Insulin is known to act as a general regulator of glucose homeostasis [WOODS ET AL., 1998] and as adiposity signal to reduce food intake when confronted with excess of carbohydrates in mammals. In *Drosophila* larvae it was shown, that pan-neuronal overexpression of DILP2 leads to a reduction in food intake [WU ET AL., 2005], whereas ablation of insulin producing cells (IPCs) leads to developmental delay in early larval stages and increased circulating sugars in the hemolymph displaying a diabetes like phenotype [RULIFSON ET AL., 2002]. The neuropeptide Leucokinin (LK) has been described as a diuretic hormone in *Drosophila* being involved in ion transport and fluid secretion in Malpighian tubules. It has been proposed that LK and vertebrate Tachykinin share similar pathways based on homology of their receptors [RADFORD, 2002]. Activity of LK neurons regulates meal size in adult *Drosophila*. Silencing neuronal function of LK neurons led to an strong overconsumption of fluid food in adult flies by prolonging a single meal and reducing the meal frequency for compensation [AL-ANZI ET AL., 2010].

Despite the above-mentioned homologous roles of peptidergic modulation of feeding and metabolism other neuropeptides and -transmitters in *Drosophila* have been shown to modulate specific aspects of feeding behavior. Corazonin (CRZ) has been implicated in

promoting food consumption, while Allatostatin A directly inhibits starvation induced feeding in adults [HERGARDEN ET AL., 2012]. Small neuropeptide F (sNPF) promotes food consumption as well as foraging behavior [LEE ET AL., 2004; 2008].
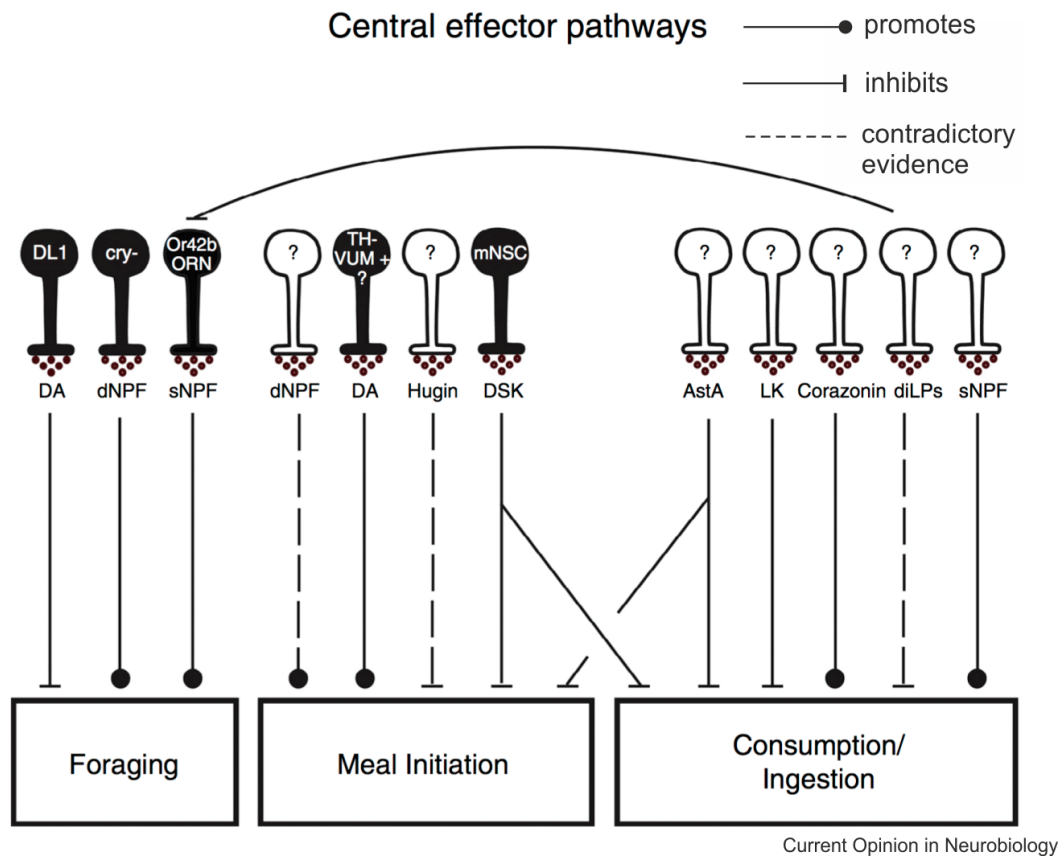
Figure 1.4: Neuromodulation of Feeding in *Drosophila*

Neuromodulators are involved in the regulation of one ore more feeding behavior subprograms. DA, Dopamine; LK, Leucokinin; DSK, Drosulfakinin; cry- dNPF, cryptochrome negative NPF neurons; AstA, Allatostatin A; dilPs, *Drosophila* insulin like peptides; sNPF, Short neuropeptide F. Adapted and modified from [POOL & SCOTT, 2014b].

A controversial role of feeding regulation can be attributed to the biogenic amine dopamine (DA) acting as a neurotransmitter in the CNS. On the single cell level certain dopaminergic populations in the brain act differently in the modulation of feeding. It has been shown that the release of dopamine in the SEZ acts on primary sensory neurons via the Dopamine receptor DopECR expressed in sugar sensory neurons to control the gain of responsiveness by enhancing sugar evoked calcium influx [INAGAKI ET AL., 2012]. A second study identified the dopaminergic TH-VUM neuron located in the ventromedial portion of the SEZ as a potent initiator of the proboscis extension reflex in adult *Drosophila.* Activation of this neuron leads to enhanced meal initiation. Furthermore, the endogenous activity of the neuron showed an increase in neuronal firing with prolonged starvation time [MARELLA ET AL., 2012]. In

Drosophila larvae a study revealed activation of all dopaminergic neurons inhibits food intake and that three neurons of DL1 cluster, which is located in the lateral protocerebrum act via activity of the GCN2 kinase as a sensor of amino acid imbalanced food [BJORDAL ET AL., 2014]. A second major neurotransmitter involved in feeding in the *Drosophila* CNS is serotonin (5-HT) [GASQUE ET AL., 2013]. Actions of 5-HT include modulation of gut motility, which has recently been shown to be regulated by brain derived 5-HT in mammals [LI ET AL., 2011]. The cellular identity of serotonergic neurons involved in feeding regulation in the fly has not yet been shown.

While the distribution of neuropeptides in the CNS has been well established [PARK ET AL., 2008], there is currently a gap in knowledge of their local actions and effect on feeding motor subprograms. This is due to a lack of tools to analyze actions of neuromodulators on a cellular level. Thus, molecular biological tools in combination with the ability to monitor motor subprograms of a given behavior offer the possibility to gain insights on how the brain translates internal and external signals into meaningful behavior. Not only feeding regulation in the light of energy homeostasis, or hunger and satiety have to be considered, but also immediate environmental cues like taste and olfaction modulate the decision to either accept or reject a food for consumption.

The homology of the neuropeptides NMU-8 in mammals and Hugin in *Drosophila* will be introduced extensively in the next chapter.

1.2   Neuromedin U

NMU-25 (25 amino acids long) and its cleavage product NMU-8 (eight amino acids long) are neuropeptides first identified in porcine spinal cord. They are capable of stimulating smooth muscle contractions of the uterus in rats. Both neuropeptides are derived from a 174 amino acid NMU precursor [LO ET AL., 1992]. Whereas NMU-8 stimulated rat uterine contractions directly, NMU-25 served for the reinforcement and prolongation of these contractions [MINAMINO ET AL., 1985a; MINAMINO ET AL., 1985b]. Over the last 30 years of research NMU has become an all-rounder (jack-of-all-trades) neuropeptide having biological functions in a variety of biological contexts. It is highly conserved throughout vertebrate species [BRIGHTON ET AL., 2004] and homologs exist in insects, like the *hugin* gene in *Drosophila melanogaster* [MELCHER ET AL., 2006]. Bioactivity of NMU is located in the last five amino acids at its C-terminus, as manipulation of this region leads to a loss of function of the peptide [HASHIMOTO ET AL., 1991]. Biological activity further requires amidation (NH2 group at the C-terminus) to functionally lead to smooth muscle contraction or to a Ca^{2+} influx in postsynaptic cells [FUNES ET AL., 2002; MINAMINO ET AL., 1985b]. The conservation throughout animal kingdom displays the anxiety of this neuropeptide and its biological importance [BRIGHTON ET AL., 2004].

NMU is expressed in different tissues to fulfill its physiological role. Immunoreactivity was found in the entire gastrointestinal tract reaching from esophagus to rectum with high expression in small intestine [AUGOOD ET AL., 1988; AUSTIN ET AL., 1995, 1994; BALLESTA ET AL., 1988]. NMU is localized in distinct brain regions in the CNS, like several nuclei of the hypothalamus, the pituitary gland (Pit, the main neurosecretory gland in mammals), the NTS (first relay center for sensory information) and spinal cord [BRIGHTON ET AL., 2004; MARTINEZ & O'DRISCOLL, 2015]. This localization pattern alone already suggests a role of NMU in feeding regulation. The presence of NMU in these brain areas was shown for rodents and humans [FUJII ET AL., 2000; HOWARD ET AL., 2000; SZEKERES ET AL., 2000] (**Figure 1.5 a**).

The functional role of NMU includes several biological processes like modulation of smooth muscle contractions, vasoconstrictive effects on veins and modulation of blood pressure and heart rate, gastric secretion, circadian rhythm, hormone release, bone remodeling, immune regulation and involvement in cancer proliferation [MARTINEZ & O'DRISCOLL, 2015]. The majority of investigations to date have concentrated on the role of NMU in stress response and feeding regulation (**Figure 1.5 b**).
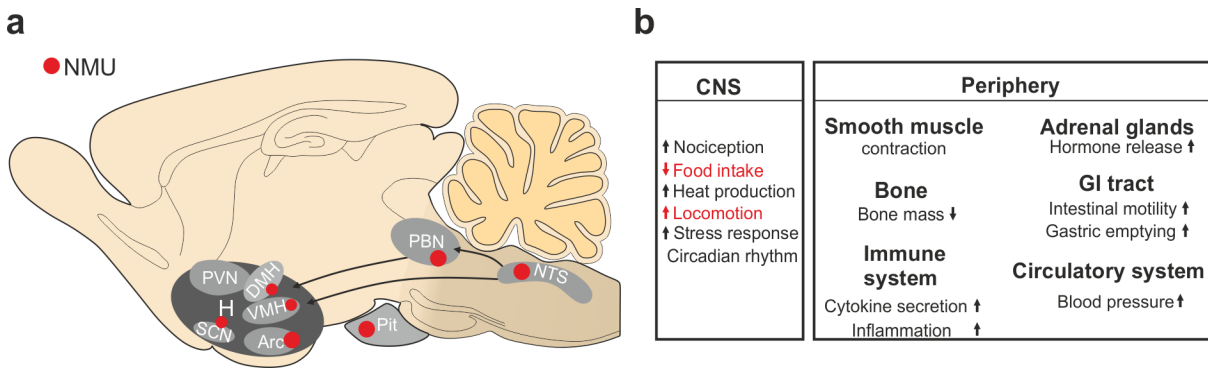
a

b

CNS	Periphery	
↑ Nociception	**Smooth muscle** contraction	**Adrenal glands** Hormone release ↑
↓ Food intake		
↑ Heat production	**Bone** Bone mass ↓	**GI tract** Intestinal motility ↑ Gastric emptying ↑
↑ Locomotion		
↑ Stress response	**Immune system** Cytokine secretion ↑ Inflammation ↑	**Circulatory system** Blood pressure ↑
Circadian rhythm		

Figure 1.5: Neuromedin U: Localization and Biological Role

a) Schematic of a mouse brain showing the localization of NMU positive neurons and fibers (red dots) in the hypothalamus (H), pituitary gland (Pit) and nuclei of the brainstem, nucleus tractus solitarius (NTS) and parabrachial nucleus (PBN). Information about localization of NMU taken from [BRIGHTON ET AL., 2004; MARTINEZ & O'DRISCOLL, 2015]. PVN, paraventricular nucleus; DMH, dorsomedial hypothalamic nucleus; Arc, arcuate nucleus; SCN, suprachiasmic nucleus. **b**) Summary of the physiological roles of NMU in different tissues of the body. GI, gastrointestinal. Information about NMU function from [MARTINEZ & O'DRISCOLL, 2015].

Stress response in mammals, especially in rodents, manifests in form of certain behavioral routines like face washing, grooming and reduction in gastric secretion and food intake [MORLEY & LEVINE, 1982]. Corticotropin releasing hormone (CRH) released from the PVN in the hypothalamus is the major hormone being responsible for this behavioral stress response [BRIGHTON ET AL., 2004]. NMU neurons known to be located in the ARC of the hypothalamus, brainstem and Pit prominently project to the PVN, where CRH neurons are located. The feeding suppressive effect of NMU is thought to be promoted by release CRH in the PVN [HANADA ET AL., 2001; JETHWA ET AL., 2006].

The most studied role of NMU is its suppressive effect on food intake. It was shown by several studies, that NMU injection into the CNS reduces food intake in rodents [BECHTOLD ET AL., 2009; HANADA ET AL., 2003; HOWARD ET AL., 2000; NAKAHARA ET AL., 2010; WREN ET AL., 2002], chicken [KAMISOYAMA ET AL., 2007], japanese quail [SHOUSHA ET AL., 2005] and goldfish [MARUYAMA ET AL., 2008]. This effect was also seen by transgenic overexpression of NMU in mice [KOWALSKI ET AL., 2005]. The opposite effect resulting in an increase of food intake [JETHWA, 2005] and obese phenotypes was shown with antibody injections for NMU and NMU knock out mice [HANADA ET AL., 2004], respectively. NMU mRNA was shown to be reduced after a period of fasting in rat, suggesting NMU itself being regulated by internal energy status of the animal [HOWARD ET AL., 2000]. The most prominent sensor in our body to regulate and stop food intake, is the satiety inducing cytokine Leptin, that acts as secreted hormone from the adipose white tissue on the central nervous system. Interactions of NMU and Leptin provide an explanation for the feeding suppressive phenotype in addition to stress signaling. The release of Leptin from adipose tissue leads to a release of NMU in the

hypothalamus and thereby reducing food intake [WREN ET AL., 2002]. Mice not being able to produce Leptin display reduced levels of NMU [HOWARD ET AL., 2000] and NMU antisera in turn reduce the effect of Leptin [JETHWA, 2005]. Thus, apart from Leptin acting on the anorectic peptide POMC, feeding suppressive effects of Leptin are partially mediated by NMU.

NMU plays a significant role in feeding regulation in the context of energy homeostasis and internal status. Most studies tackle functional implications of NMU and neuropeptides in general with pharmacological approaches. Recent efforts focus on drug therapies, which reduce or promote neuropeptide actions in order to treat diseases like obesity and cancer induced anorexia [ARGILÉS ET AL., 2010; NEUNER ET AL., 2014]. Regarding the manifold physiological roles of neuropeptides, especially as described for NMU, the site of action of a drug is critical to target its effect to the defined physiological effect of a neuropeptide. Therefore, it is important to know where to target treatment of a disease in order not to elicit side effects.

The conserved roles of neuropeptides in *Drosophila* and mammals offer this possibility, since due to its simpler nervous system the local actions of the neuropeptide can be investigated on a cellular level. As mentioned before, the gene *hugin* has been shown to be a homolog of mammalian NMU [MELCHER ET AL., 2006] and findings gathered from studies on Hugin neuropeptide in the fly might expand our knowledge of the pathways how NMU acts in mammals.

1.3 Hugin

The gene *hugin* was identified encoding the myostimulatory and ecdysis modifying neuropeptides Pyrokinin-2 (PK2) and Hugin-γ in *Drosophila*. PK2 consists of eight amino acids. Three of the five C-terminal amino acids, which are important for bioactivity of the peptide, are identical in mammalian NMU-8 [MENG ET AL., 2002]. Not only the PK2 peptide shares sequence homology, but also the two putative Hugin receptors PK2R1 (CG8784) and PK2R2 (CG8795) are highly conserved between *Drosophila* and mammalian NMU receptors NMU1R and NMU2R. PK2 was able to activate both vertebrate receptors in vitro [PARK ET AL., 2002; ROSENKILDE ET AL., 2003].

Similar to its mammalian homolog *hugin* is expressed in the CNS, in 20 neurons located in the SEZ, a region, important for feeding regulation and taste processing (**Figure 1.6 a**). A role in feeding behavior for the *hugin* gene was first described in an P-element screen, investigating feeding deficiencies [MELCHER & PANKRATZ, 2005]. In one of these lines, P(9036), the *klumpfuss* (*klu*) gene was mutated. *Drosophila* larvae containing a mutation in this gene display a severe feeding deficit and enhanced locomotor behavior, later termed as "wandering like behavior". A genome wide gene expression analysis showed, that the *hugin* gene activity was upregulated in the *klumpfuss* mutant background [MELCHER & PANKRATZ, 2005]. Subsequently this upregulation of *hugin* was also observed in another feeding deficient mutant, *pumpless* (*ppl*). Similar to downregulation of NMU upon fasting in rats [HOWARD ET AL., 2000], in situ hybridization of *hugin* could show that it is down regulated in starved *Drosophila* larvae [MELCHER & PANKRATZ, 2005]. This supports the view that both genes serve similar functions in both organisms. Using a *hugin-Gal4* driver line (HugS3-Gal4), projection targets of Hugin neurons were analyzed. Hugin dendrites projected to the protocerebrum (PC), the ring gland (RG), ventral nerve cord (VNC) and via the prothoracic accessory nerve (PaN) to the pharyngeal region. Due to their glomerular like dendrites within the SEZ near the foramen, they offer an expression pattern likely to serve the function as gustatory interneurons [MELCHER & PANKRATZ, 2005]. Glomerular like organization of gustatory processing has not yet been validated and is so far only known to exist in olfactory processing [SINGH, 1997]. Colocalization studies with promoter lines driving expression in chemosensory afferents suggested overlap with dendritic compartments of Hugin neurons within the SEZ. Specifically the chemosensory receptor GR66a identified in 2001 by Kristin Scott and colleagues [SCOTT ET AL., 2001], was shown to display dendrites in close proximity of Hugin dendrites.
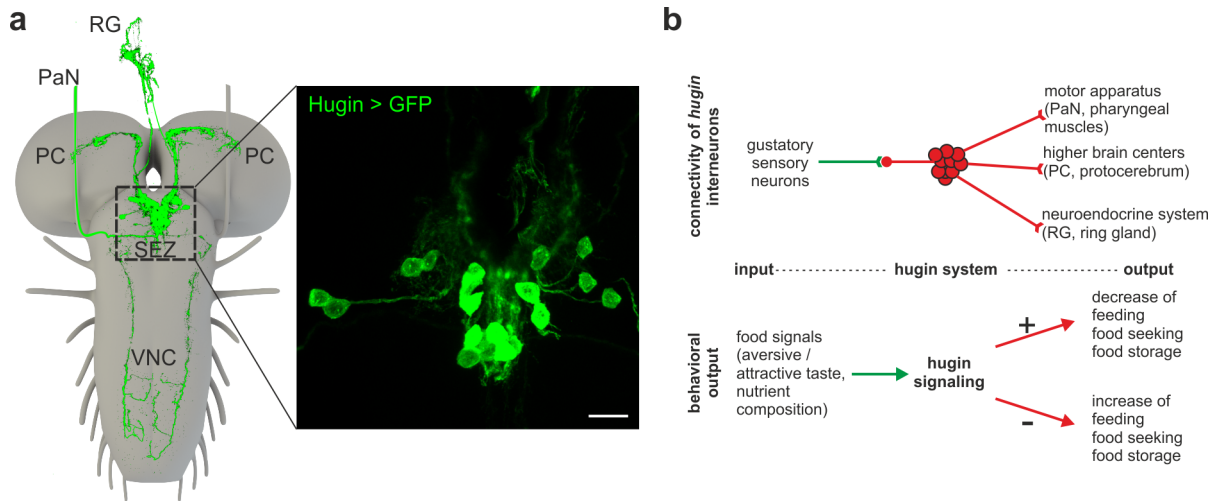
Figure 1.6: Hugin: Localization and Biological Role

a) Left: Expression pattern of the Hugin neurons in the larval CNS. Hugin neurons can be subdivided into four subclasses based on their projection targets, PC (protocerebrum), RG (ring gland), VNC (ventral nerve cord) and PaN (prothoracic accessory nerve). Right: detailed view of Hugin neuronal expression in the SEZ showing the 20 Hugin neurons. **b**) Model for the function of Hugin neuropeptide in adult and larval *Drosophila* (adapted and modified from [MELCHER & PANKRATZ, 2005]).

This receptor serves the function of bitter (caffeine) detection [WEISS ET AL., 2011]. The Hugin neurons were thought not to be olfactory projection neurons, as olfactory processes take a different route to higher brain centers [MELCHER & PANKRATZ, 2005]. The assumption of them being gustatory interneurons based on the projection to higher brain centers was strengthened by a comparison to honeybee, where SEZ neurons projecting to higher brain centers were shown to process gustatory information [SCHRÖTER & MENZEL, 2003]. Pan-neuronal misexpression of *hugin* in larvae caused defective growth and food intake. Adult flies were used to get insights into potential physiological effects by silencing Hugin neurons. Flies initiated food intake on a new food source earlier and filled their crop within much shorter time than controls, when Hugin neurons were silenced. On an aversive bitter food source these flies filled their crops faster than controls. It was suggested that a previously encountered food source does define Hugin neural activity and thereby Hugin acts as feeding regulator once a new food source is detected (**Figure 1.6 b**) [MELCHER & PANKRATZ, 2005].

Since a function for Hugin and its mammalian homolog NMU is linked to feeding regulatory behavior, a next logical step would be to further dissect the effect of Hugin in the context of feeding regulation and taste processing. This includes investigating specific roles of Hugin subclasses. In the following chapter the basic knowledge about taste processing in mammals and *Drosophila* will be introduced.

1.4   Taste Processing

Feeding can be categorized in different stages. After hunger and subsequent food search behavior the last step before the actual food intake is the decision to either ingest the food or to reject it. This decision is led by gustatory stimuli acting as final arbiter of consummatory behavior. These stimuli are represented by the five prototypical taste modalities known today: bitter, sweet, salty, umami and sour [CHANDRASHEKAR ET AL., 2006]. A certain valence can be assigned to each of the five modalities, as for examples general perception of sugar is associated with pleasant and nutritious food, whereas the taste of bitter food is associated with more toxic or even harmful substances [GLENDINNING, 1994]. Salt represents a special taste modality, since it has a bivalent function. Low amounts are perceived as pleasant, whereas high amounts of salt leads to rejection of the food [NIEWALDA ET AL., 2008]. The taste of umami can be described as protein taste and glutamate acts as being representative for this modality. It was identified in the seaweed kombu in 1909 by Kikunae Ikeda, who stated glutamate taste being uniquely different from the other four basic taste modalities and named it umami [LINDEMANN, 2002].

Mammals

Mammals detect the different taste modalities with taste receptor cells (TRCs) that are tuned to a certain taste modality. TRCs are housed in taste buds, structures that are composed of 50-100 taste receptor cells (**Figure 1.7, right panel**). The taste buds are distributed over the tongue`s surface (**Figure 1.7, middle panel**). Contrary to the common belief, every taste modality can be detected throughout the taste epithelia on the tongue, called papillae [CHANDRASHEKAR ET AL., 2006]. 16 years ago the first taste receptor was identified as a bitter receptor (T2R) [CHANDRASHEKAR ET AL., 2000], and was followed in the subsequent years with the identification of the sweet receptor (T1R2 + T1R3) [NELSON ET AL., 2001], amino acid receptor (T1R1 + T1R3) [NELSON ET AL., 2002], the sour receptor (PKD2L1) [ISHIMARU ET AL., 2006] and the salt receptor ENaC [CHANDRASHEKAR ET AL., 2010]. These receptors are expressed in the membrane of TRCs and lead to activation, once the appropriate taste molecule has bound. TRCs are synaptically connected via three cranial nerves (chorda tympani, glossopharyngeal and vagus nerve branch) to peripheral ganglia, the geniculate and the petrosal ganglion (**Figure 1.7, left panel**). Cells within the geniculate ganglion respond taste modality specifically with an increase in calcium activity and encode not only the quality but also valence of a taste in mice. Most of the neurons within this ganglion are single tuned cells responding predominantly to one taste. The minority of ganglion cells are able to

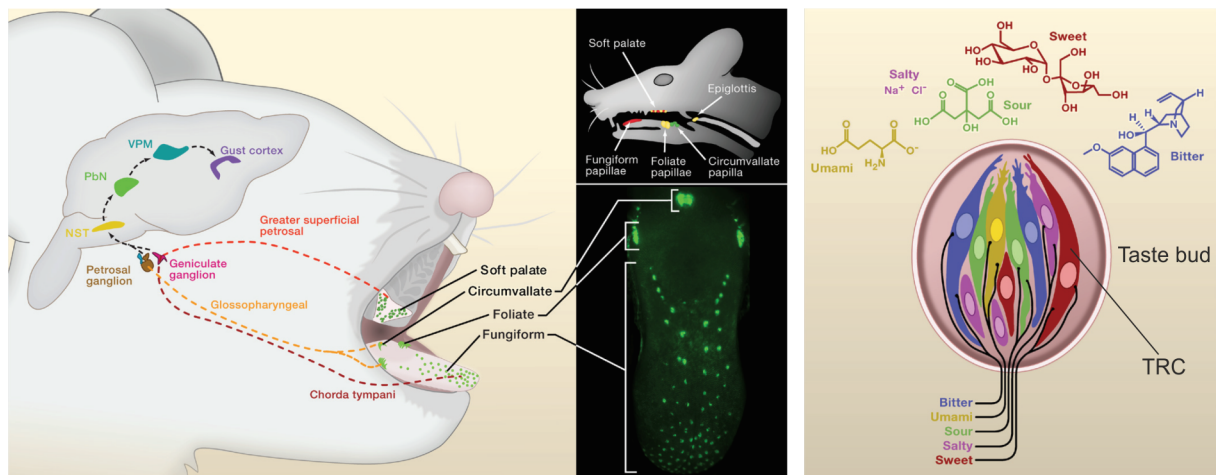respond to a bitter-sour mixture or to a lesser extent to other taste mixtures [BARRETTO ET AL., 2015].

Figure 1.7: Taste Pathways in the Mammalian Brain

Taste receptor cells responding to different taste modalities are housed in taste buds (right panel) distributed throughout the tongue in papillae (Fungiform, Foliate and Circumvallate) and the soft palate (middle panel). Afferent axons, connected to the taste receptor cells (TRCs) project via three cranial nerves (greater superficial petrosal, glossopharyngeal and chorda tympani) to peripheral ganglia (geniculate ganglion and petrosal ganglion). Taste signals further converge to the nucleus tractus solitarius (NST) and are processed via the parabrachial nucleus (PbN) and the ventral posterior nucleus (VPM) to the gustatory cortex (left panel). Figure adapted from [YARMOLINSKY ET AL., 2009].

The first taste relay center within the brain is located in the NTS [SPECTOR, 2005] in the brain stem in the medulla oblongata and all three cranial nerves project to in the rostral portion of the NTS. Recently a calcium imaging approach verified that neurons within the NTS are responding preferentially to a certain taste modality. From the NTS taste information is further processed to the PBN [DI LORENZO ET AL., 2009]. In the PBN taste information is further processed via the parvicellular part of the ventral posteromedial nucleus of the thalamus (VPM_{PC}) to the gustatory cortex (**Figure 1.7, left panel**). The PBN not only connects to thalamic structures but was also shown to connect reciprocally to the ventral forebrain, lateral hypothalamus and also amygdala, suggesting the involvement in feeding related processes and taste memory formation [CARLETON ET AL., 2010; TOKITA ET AL., 2009]. From the gustatory cortex reciprocal connections exist back to the PBN, the somatosensory cortex and the orbitofrontal cortex (OFC). This suggests also input from other sensory modalities related to food intake, like olfaction, taste, visceral afferents, somatosensation and vision [ONGUR, 2000]. In general the gustatory cortex is seen as a multisensory integration center in the brain [DE ARAUJO & SIMON, 2009] and with its dynamic feed forward and top-down circuits

gustatory pathways are important for the identification, reward evaluation and finally food intake decisions (for general review see [YAMAMOTO, 2008]). Most of the studies that identified these taste pathways were originally based on electrophysiological experiments or, more recently, calcium imaging approaches monitoring neural populations in higher brain areas like the gustatory cortex. Despite this extensive research to unravel brain mechanisms of taste processing, our knowledge about the identity of the neurons involved, in terms of the transmitters/peptides they release or their synaptic connectivity is still sparse.

One of the best known sensory pathways to date is the *Drosophila* olfactory system [COUTO ET AL., 2005; STOCKER, 2009]. Although taste processing seems to be more complex, *Drosophila* offers the ideal system to investigate the underlying neural mechanisms of feeding and taste processing, due to the genetic toolbox and fast developmental times. The following chapter will provide background about *Drosophila* research on taste processing.

Drosophila

Extensive knowledge about peripheral taste coding was gathered throughout the last 16 years, when gustatory receptor genes (GRs) were identified in *Drosophila* [CLYNE ET AL., 2000; DUNIPACE ET AL., 2001; SCOTT ET AL., 2001]. The main taste organ of adult *Drosophila* is the labellum located on the anterior proboscis that represents a functional analog to our tongue. Gustatory receptor neurons (GRNs) in sensilla located on the labellum respond to water, sugar, low salt and bitter compounds [MEUNIER ET AL., 2003]. Within the pharynx, labral sense organ (LSO), ventral and dorsal cibarial sense organs (VSCO and DSCO) are gustatory organs [VOSSHALL & STOCKER, 2007]. Similar to mammals, in *Drosophila* a taste is also not detected in one particular organ, but one taste organ houses multiple gustatory receptors detecting several different taste modalities [YARMOLINSKY ET AL., 2009]. In adult stages of *Drosophila* taste is not limited to the mouthparts and pharynx, taste sensilla can also be found on the wing margins and legs. Taste receptors on the legs in male flies serve the function to detect female pheromones [WATANABE ET AL., 2011]. Female flies possess taste receptors on their vaginal plates to detect an appropriate oviposition site to lay their eggs [STOCKER, 1994]. Other taste receptors on the legs serve as a "quality check" to decide whether to extend the proboscis to a food source or not (**Figure 1.8 a**).

The larval taste system is anatomically more simple organized than in adults. Research on dipteran larval sense organs is more than 125 years old and extensive knowledge has arisen from morphological and functional studies. Initially interpreted as light sensing organs in 1890 [LOWNE, 1890], the terminal organ (TO) and the dorsal organ (DO) are today known to be important organs for the detection of taste and smell, respectively.
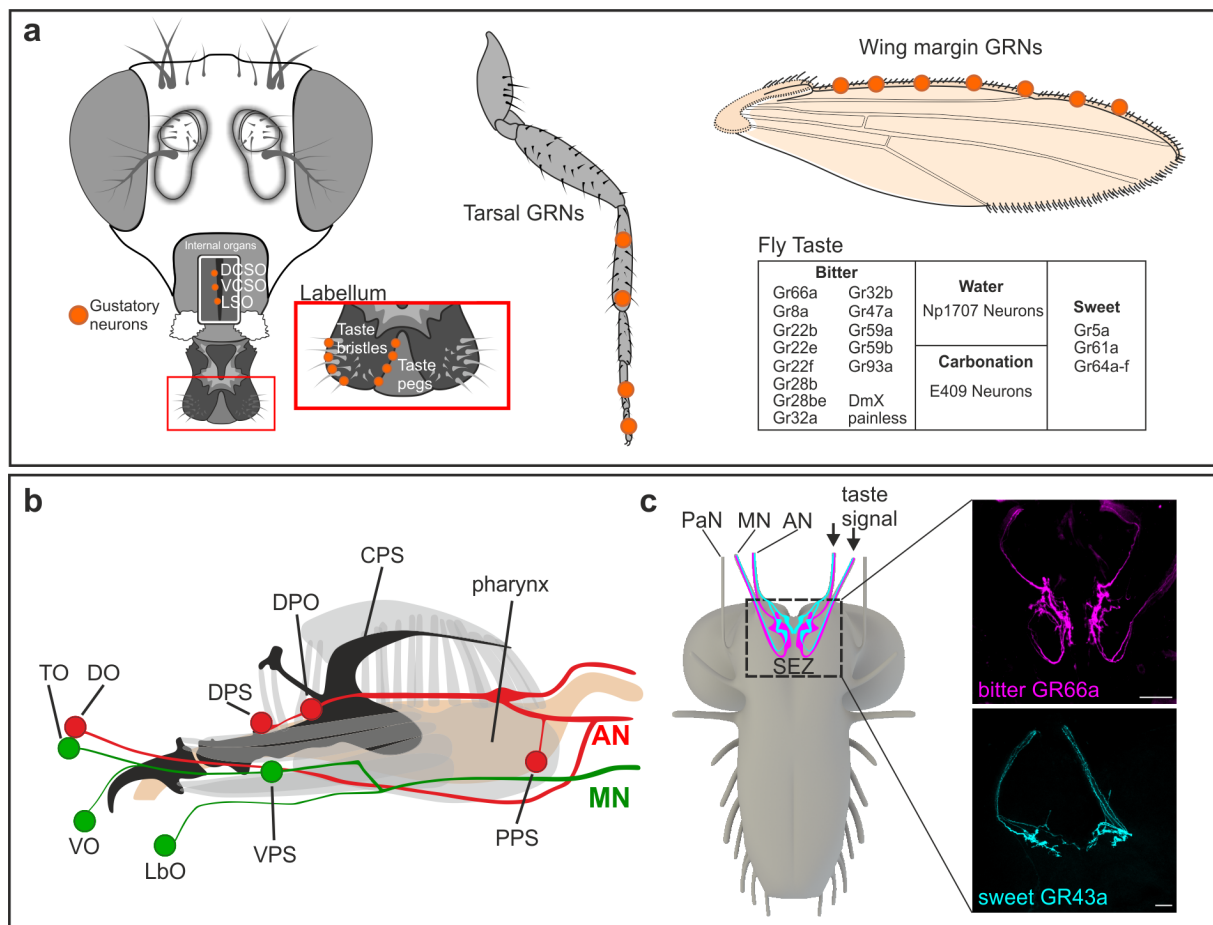
Figure 1.8: Taste Pathways in *Drosophila*

a) Gustatory receptor neurons (GRNs) are distributed on the labellum in taste bristles or taste pegs and within the pharynx in internal gustatory organs, the DCSO, VCSO and LSO. Additionally, adult flies posses GRNs on the legs and wing margins. Gustatory receptors (GRs) are expressed in GRNs and are specific for certain taste modalities like bitter and sweet. Figure adapted from [YARMOLINSKY ET AL., 2009]. DCSO, dorsal cibarial sense organ; VCSO, ventral cibarial sense organ; LSO, labral sense organ. **b)** *Drosophila* larvae possess gustatory organs located in the anterior head cuticle (TO, DO, VO and LbO) as well as internal sense organs (DPS, DPO, VPS and PPS) positioned along the pharynx. **c)** These organs harbor GRNs, which project through the antennal nerve (AN) and maxillary nerve (MN) to the subesophageal zone (SEZ), the primary taste relay center in larval and adult stages of *Drosophila*. Shown is the expression of the bitter caffeine receptor GR66a and the sweet fructose receptor GR43a. Their neuronal projections target the SEZ in the larval brain. TO, terminal organ; DO, dorsal organ; VO, ventral organ; LbO, labial organ; DPS, dorsal pharyngeal sensilla; VPS, ventral pharyngeal sensilla; DPO, dorsal pharyngeal organ; CPS, cephalo pharyngeal skeleton; PPS, posterior pharyngeal sensilla; AN, antennal nerve; MN, maxillary nerve; PaN, prothoracic accessory nerve; SEZ, subesophageal zone. Scale bars in **c)** represent 10µm.

The DO is the olfactory organ of the larvae located on the dorsal side of the anterior head cuticle, housing 21 sensilla in a dome-like structure, dedicated to detect odors [OPPLIGER ET AL., 2000]. Projections of olfactory receptor neurons arborize within the CNS in a glomerular

structure called antennal lobe. In addition, eleven neurons in the DO are thought to primarily serve a gustatory function based on anatomical studies. The terminal organ (TO) and the ventral organ (VO) are located beneath the DO and serve mainly the detection of taste. Gustatory function has also been assigned to the inner pharyngeal sense organs, the dorsal pharyngeal sensilla (DPS) and organ (DPO), the ventral pharyngeal sensilla (VPS) and the posterior pharyngeal sensilla (PPS) (**Figure 1.8 b**). Studies using behavioral paradigms and imaging approaches made it possible to investigate peripheral taste processing down to cellular level [APOSTOLOPOULOU ET AL., 2014].

Today 60 gustatory receptor genes coding for 67 receptor proteins are known [CLYNE ET AL., 2000; DUNIPACE ET AL., 2001; SCOTT ET AL., 2001]. Each sensory neuron of the respective gustatory sense organs expresses a variety of gustatory receptor genes [KWON ET AL., 2011] with gustatory function [APOSTOLOPOULOU ET AL., 2015] and ionotropic receptor genes ,recently identified [BENTON ET AL., 2009], with various functions. Of 67 Gal4 lines generated for each GR, 43 GRs are expressed in larval sense organs [KWON ET AL., 2011]. As in mammals and adult flies, bitter receptors represent the largest group among gustatory receptor genes, pointing out their important role in preventing uptake of noxious food [WEISS ET AL., 2011]. While the receptors for bitter taste [MOON ET AL., 2006] and sweet taste [DAHANUKAR ET AL., 2007] are well studied, the specific receptors for sour, protein and high salt taste have not yet been identified. The gustatory receptor GR5a and the six GR64 receptors (GR64a-f) are needed to detect all common sugars like trehalose, glucose, fructose and saccharose to display attraction to sweet tastants [DAHANUKAR ET AL., 2007] (**Figure 1.8 a**). However, larvae lack expression of the sugar receptors GR5a and GR64a-f [COLOMB ET AL., 2007]. But recently a fructose receptor (GR43a) was found to be expressed in pharyngeal organs and the brain and is now thought to act as main sugar receptor in larvae [MISHRA ET AL., 2013].

Bitter taste is detected by a variety of GR`s, whereas GR66a and GR33a together are expressed in all bitter sensory neurons acting presumably as bitter co-receptors for functional bitter taste detection [WEISS ET AL., 2011]. In total 12 bitter sensory neurons co-express the bitter receptors GR66a and GR33a, which are distributed in the TO and the pharyngeal sense organs DPS, VPS and PPS [KWON ET AL., 2011]. Interestingly activity of one neuron in the TO is sufficient to alter quinine dependent aversive behavior, shown by loss- and gain-of-function experiments [APOSTOLOPOULOU ET AL., 2014]. Also neural activity of GR33a expressing neurons is required for this behavior [APOSTOLOPOULOU ET AL., 2014; EL-KEREDY ET AL., 2012]. When flies are confronted with sugar solution containing bitter compounds, food intake decreased [FRENCH ET AL., 2015]. This exemplifies that bitter taste represents an aversive stimulus for flies and that bitter taste overrides the attractive taste of sugar in order

to guarantee that the taste of potential harmful or toxic bitter food cannot be masked by sweet attractive food.

A common target area of gustatory neurons in the CNS is the SEZ. It represents the first relay center for taste [COLOMB ET AL., 2007; KWON ET AL., 2011; THORNE ET AL., 2004] (**Figure 1.8 c**). Although the peripheral taste system has been studied to great detail in larval and adult stages of *Drosophila*, very little is known about taste integration in the CNS. To date only two neurons in the SEZ have been identified to be second order neurons for sweet taste in adult stages of *Drosophila* [KAIN & DAHANUKAR, 2015; MIYAZAKI ET AL., 2015]. Broad areas important for taste integration are the SEZ and the higher brain centers like mushroom bodies and pars intercerebralis [HARRIS ET AL., 2015; KIRKHART & SCOTT, 2015]. This is in line with findings in the mammalian system, where taste is being processed in the nucleus tractus solitarius (NTS), the first taste relay center in mammals. Further processing takes place in higher brain centers like the thalamus, gustatory cortex and hypothalamus, an area important for feeding regulation [CARLETON ET AL., 2010] and functionally comparable to the PI and pars lateralis (PL) in *Drosophila* [HARTENSTEIN, 2006]. Bitter and sweet taste has been shown to activate separated neural clusters in these brain regions, but the molecular identity of released neurotransmitters or peptides is still unknown [HARRIS ET AL., 2015]. In *Drosophila* larvae, no second order gustatory neurons have been identified yet. Promising candidates for acting as second order gustatory neurons are the Hugin neurons [COLOMB ET AL., 2007; MELCHER & PANKRATZ, 2005]. In order to understand taste processing not only in the periphery, but also the integrative pathways in the brain, it is necessary to unravel the identity of second order taste neurons and subsequently their downstream targets to get an idea of taste processing. Punishment and reward pathways in higher brain centers, mainly in the mushroom bodies, rely to a huge extent on taste processing in larvae [SCHLEYER ET AL., 2015]. One of the main neurotransmitters involved is dopamine acting as reward signal [ROHWEDDER ET AL., 2016]. It is important to anatomically and functionally link the peripheral sensory system to higher brain centers via gustatory interneurons to understand taste processing, not only in flies.

1.5   Tools for the Investigation of Neural Circuits

With the sequencing of the *Drosophila* genome in 2000 [ADAMS ET AL., 2000] and the invention of the Gal4/UAS expression system [BRAND & PERRIMON, 1993] it is today possible to activate, silence, ablate or overexpress molecular factors in the neurons of interest to study their functions in intact and semi intact adults and larvae. The Gal4/UAS system is used for targeted gene expression to analyze gene function and to express an effector or reporter in specific neurons in the brain or tissues in the whole animal [DUFFY, 2002]. Gal4 is a transcription factor derived from yeast that specifically binds to an upstream activating sequence (UAS) to transactivate downstream genes (**Figure 1.9 a**). Today thousands of Gal4 driver lines are available in stock centers (Bloomington stock center, VDRC) being specific for certain populations of neurons or even single neurons in the brain. Together with the vast number of established effector or reporter lines to visualize or manipulate neurons, this system provides a powerful armada for deconstructing neurobiological processes.

One of the first tools to transiently manipulate neurons was introduced in 2001. The gene *shibire* encodes for the protein Dynamin, which is essential for synaptic vesicle recycling. Misexpression of a mutant form, *shibire^{TS}*, is able to block synaptic vesicle recycling in neurons of interest upon a temperature shift over 29°C. This enables the researcher to silence the neural activity of neurons by inhibiting the recycling of vesicles containing neurotransmitters [KITAMOTO, 2001] (**Figure 1.9 b**). A second transient thermogenetic effector implies the usage of the endogenous temperature and voltage sensitive cation channel dTrpA1. Expression of dTrpA1 in neurons leads to an excitation when temperature is shifted over 27°C. Above this restrictive temperature the cation channel dTrpA1 in the cell membrane opens and leads to a permanent depolarization of the membrane potentials resulting in constant neural activity [HAMADA ET AL., 2008; PULVER ET AL., 2009] (**Figure 1.9 c**). In addition to thermogenetic tools the first optogenetic tools were introduced to the fly community in 2003. Channelrhodopsin is derived from the green alga *Chlamydomonas reinhardtii* and is involved in the generation of photocurrents and thereby phototaxis. When expressed in neurons Channelrhodopsin 2 (ChR2) leads to activation upon illumination with blue light [NAGEL ET AL., 2003; SCHROLL ET AL., 2006] (**Figure 1.9 d**). This light-inducible neural activator was used, for instance, to study the larval neuromuscular junction [HORNSTEIN ET AL., 2009; PULVER ET AL., 2009]. In contrast another optogenetic tool, Halorhodopsin, is a light gated chloride pump activated by orange light, originally identified in *Halobacterium halobium* [LANYI, 1986]. Once activated Cl⁻ ions are pumped into the cell leading to a hyperpolarization and thereby to neuronal inhibition [INADA ET AL., 2011] (**Figure 1.9 d**).

The classical approach of monitoring neural activity is electrophysiology. By recording the neural activity extracellularly or intracellularly it is possible to monitor afferent and efferent neural signals to and from the CNS (**Figure 1.9 e**). Another approach to measure neural activity is the use of genetically encoded calcium reporters, called GCaMPs [NAKAI ET AL., 2001] (**Figure 1.9 f**). Every action potential of a cell generates an influx of extracellular calcium [CALLEWAERT ET AL., 1996]. A genetically expressed calcium reporter in the cell of interest shows enhanced fluorescence when calcium enters the cell. A recently developed method for calcium imaging enables the researcher to investigate neural activity in intact animals. The calcium integrator CaMPARI (Calcium Modulated Photoactivatable Ratiometric Integrator) has the properties of GCaMPs, but based on an EOS protein green fluorescence switches permanently to red fluorescence in the presence of calcium (neural activity) and UV light (**Figure 1.9 g**). UV light exposure to the animal can be controlled by the investigator, enabling the timed monitoring of neural activity in a cell [FOSQUE ET AL., 2015].

Neuroanatomy represents the prerequisite for interpretation of neurophysiological data. Without knowing if a nerve innervates a certain muscle, or a neuron projects through a nerve it is not possible to interpret biological functions of the nerve activity. A classical method for labeling neurons or identify neurons that project through a nerve in the CNS are dye backfills. A neural tracer (in this thesis tetramethyl rhodamine D, TMR-D) is applied to a lesioned nerve. After a certain incubation time, it is possible to follow the fluorescence of the diffused dye within the nerve to identify neurons located in the CNS. Photoactivatable GFP (PaGFP) represents a genetic method for neural tracing [PATTERSON ET AL., 2002]. When expressed in neurons of interest PaGFP is activated in a region of interest with a 2-photon laser and displays fluorescence exclusively in the activated area. Advantage of this method is the precise fluorescent tracing of neurons and axons of interest being genetically defined by their respective driver line in *Drosophila* neurons (**Figure 1.9 h**).

a Promotor GAL4   UAS-gene X

male   female

F1:
genomic promotor — GAL4 → GAL4 ⬤⬤⬤⬤⬤ UAS → gene X

tissue specific expression of GAL4   transcriptional activation of gene X

b Inhibition (UAS-shibire^TS)

presynaptic

shibire^TS

18°C   32°C

ON   OFF

postsynaptic

c Activation (UAS-dTrpA1)

cations

depolarization

dTrpA1   32°C   depolarization

presynaptic   dTrpA1   18°C   postsynaptic

d Activation (UAS-ChR2)   Inhibition (UAS-eNpHR)

blue light (470nm)   yellow light (590nm)

K^+   extracellular   extracellular

intracellular   intracellular

Na^+   Cl^-

depolarization   hyperpolarization

e Extracellular Nerve Recording

AN

1 s

Intracellular Muscle Recording

CDM   10mV   1 s

f GCaMP (inactive)   GCaMP (active)

cpEGFP   Ca^{2+}   cpEGFP

M13   M13 CaM

CaM

inactive   active

Ca^{2+}

Axons   Axons

g CaMPARI

EOS   high Ca^{2+}   EOS

405nm UV light

M13   M13 CaM

CaM

low   high
neural activity

h PaGFP

PaGFP dark state   820nm   PaGFP bright state

t1 pre-activation   t2 post-activation   t3   t4

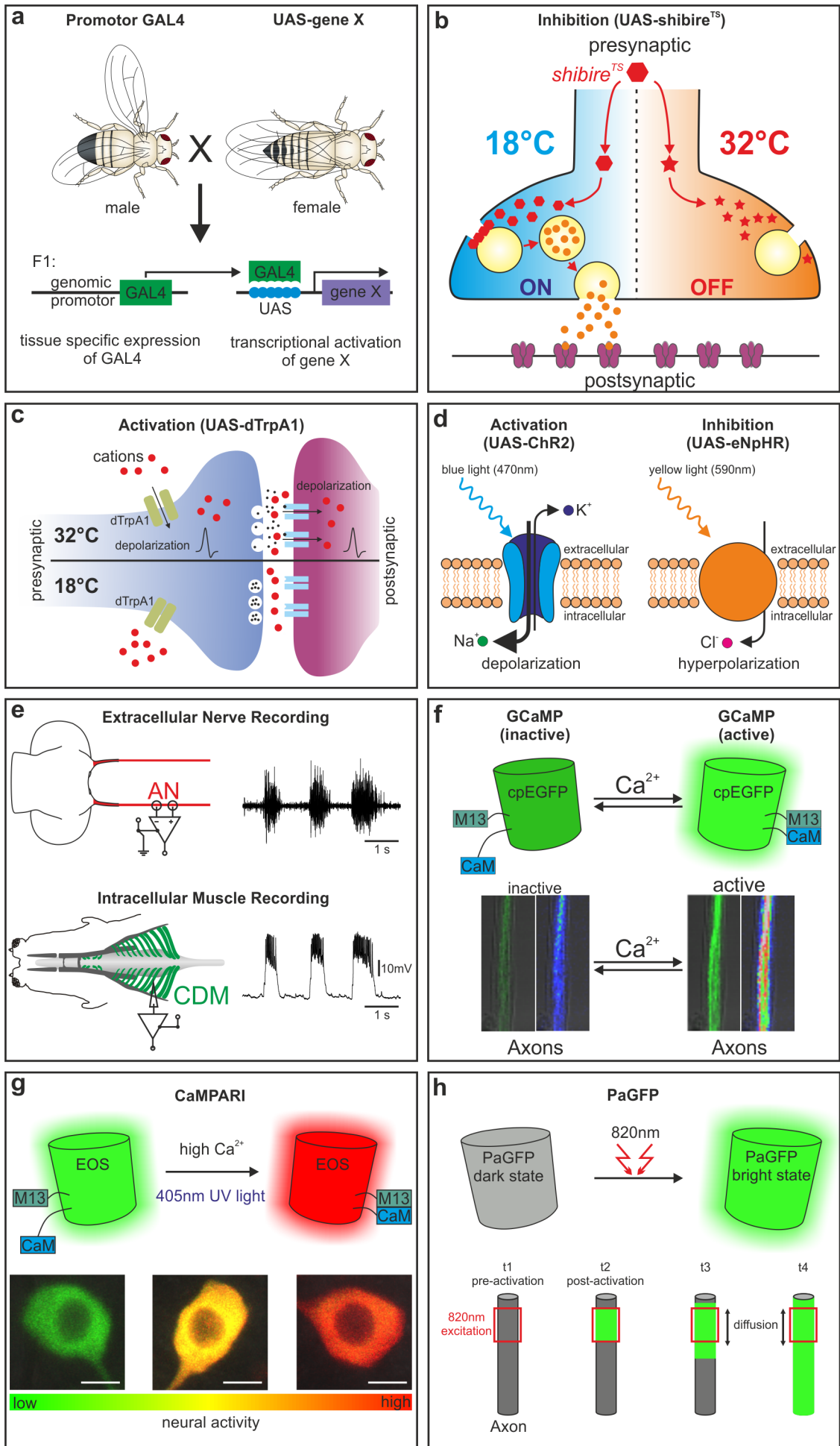820nm excitation   diffusion

Axon

Figure 1.9: The Genetic Toolbox for Manipulating and Monitoring Neural Activity

a) Scheme of the Gal4/UAS binary expression system (adapted from [BRAND & PERRIMON, 1993]) . **b)** Expression of shibire[TS] in neurons leads to block of synaptic vesicle recycling, subsequently to depletion of synaptic vesicles and thereby to stop of transmission of neurotransmitters in the synaptic cleft at temperatures above 29°C. Adapted from [KASUYA, 2009]. **c)** Expression of dTrpA1 in neurons leads to influx of cations into the cell and thereby to a depolarization upon temperatures above 27°C. **d)** Depolarization of neurons by the blue light gated cation channel Channelrhodopsin 2 and hyperpolarization of neurons by the yellow light gated chloride pump Halorhodopsin (eNpHR). (Adapted with permission of Macmillan Publishers Ltd: [NPG] [ZHANG ET AL., 2007], copyright (2007). **e)** Extracellular nerve recording from the antennal nerve (AN) in *Drosophila* larvae displays rhythmic neural activity in the isolated CNS, intracellular recording of a cibarial dilator muscle (CDM) displays rhythmic postsynaptic potentials correlating with the neural activity of the AN (recordings provided by Dr. Andreas Schoofs). **f)** GCaMP, reversible enhancement of green fluorescence of the cpEGFP upon binding of calcium to Calmodulin (CAM) and the resulting interaction of the M13 fragment of myosin light chain kinase. Information about function from [NAKAI ET AL., 2001]. Fluorescent pictures show *Drosophila* larval motor axons expressing GCaMP6s [CHEN ET AL., 2013],(own data) **g)** CaMPARI, mEOS protein photoconverts from green to red fluorescence upon simultaneous presence of calcium and UV light exposure of the tissue. information for scheme from [FOSQUE ET AL., 2015]. Fluorescent pictures show neurons expressing CaMPARI with low calcium activity, intermediate activity and high activity (own data). Scale bars: 5µm. **h)** Photoactivatable GFP (PaFGP) in dark state enhance fluorescence to a bright state upon activation with a two-photon laser tuned to 820nm. The activated GFP diffuses along axons and in neurons enabling fluorescent tracing of neural processes. Information for excitation from [LAI ET AL., 2012].

Methods of transiently activating/inhibiting neurons of interest and simultaneously monitoring neuronal populations with calcium indicators represent the today`s state of the art techniques to gather insights into neural circuit function. GCaMPs, CaMPARI, Channelrhodopsin and PaGFP are tools available also for other model organisms, like mouse and zebrafish [CHEN ET AL., 2013; FOSQUE ET AL., 2015; PETER ET AL., 2013; UMEDA ET AL., 2013; ZHAO ET AL., 2011]. This points to the fact that the pure ease of genetic accessibility of *Drosophila* is no longer the only reason to investigate neural circuit function in the fly. The numerically simple nervous system and the ability to manipulate and monitor neurons down to the single cell level make *Drosophila* the number one choice model organism for many neuroscientists.

1.6   Aims of the Thesis

Taste processing and feeding regulation in animals are crucial biological processes in order to survive. Larvae of *Drosophila melanogaster* represent the ideal model organism to investigate both processes. Its fast life cycle, genetic accessibility and numerical simplicity of the central nervous system make it possible to facilitate our understanding of general neurobiological questions. In the past, the peripheral chemosensory system in larvae was studied in great detail and feeding regulatory elements, which describe the peripheral innervation of feeding relevant muscles and functions of pharyngeal nerves underlying the actions of feeding CPG were investigated. Yet, motor neurons in the CNS responsible for the different feeding movements have not yet been identified in *Drosophila* larvae. In addition, feeding regulatory networks of neurotransmitters and -peptides have been investigated using whole animals and gross behavioral paradigms. The control of specific aspects of the feeding motor programs modulated by upstream neuronal populations has not yet been addressed in sufficient detail.

Further, despite the extensive knowledge of peripheral coding of taste in mammals and adult or larval stages of *Drosophila*, information about second order neurons relaying taste information is limited. Molecular identity in terms of neurotransmitters or -peptides released by second order taste neurons is actually not known in any organism.

Aim of this thesis was to broaden the understanding of the feeding regulatory mechanisms by identification of feeding relevant motor neurons using a combination of imaging, behavioral and electrophysiological tools. Artificial activation and simultaneous electrophysiological monitoring of pharyngeal nerve activity should be used to analyze feeding regulatory neuronal populations, like serotonin and Hugin positive neurons. Additionally the function of Hugin neurons as gustatory interneurons were to be analyzed in detail by artificial activation and ablation. Furthermore, the new CaMPARI technique was to be established to measure neural activity in intact animals by calcium imaging.

2   Localization of Motor Neurons and Central Pattern Generators for Motor Patterns Underlying Feeding Behavior in *Drosophila* Larvae

2.1   Introduction

To be able to interact with our environment we require the information about our surrounding, provided by our sense organs, the ability to process this information and translate it into meaningful behavior. For every interaction with the environment we use muscles, whether it is for simple behaviors like breathing and walking or for complex behaviors like the interaction among individuals (speech in humans) or feeding. Rhythmic stereotyped movements are under control of central patterns generators (CPGs) located in the nervous system. CPGs are defined as neuronal ensembles with the intrinsic property of rhythmic activity that subsequently drives the final movement [DELCOMYN, 1980]. Fundamental insights into the existence and nature of CPGs derived from work on locust flight [WILSON, 1961], on feeding motor control in the stomatogastric ganglion of crustaceans [MARDER & BUCHER, 2001] and on the feeding network in aplysia [BAXTER & BYRNE, 2006; KABOTYANSKI ET AL., 2000]. In all these invertebrate animals, isolated neural structures were capable of producing rhythmic motor output. Investigations of these rhythmic oscillating networks were carried out in invertebrate and vertebrate model organisms in the past decades. Classical lesion experiments on cat spinal cord [GRILLNER & ZANGGER, 1979] or the locomotor system in lampreys and stick insects [BÄSSLER & BÜSCHGES, 1998; COHEN, 1987] facilitated our understanding of the execution of basic motor programs. Such a rhythmic motor output generated without intrinsic or extrinsic sensory input was termed fictive behavior [MARDER & BUCHER, 2001].

Recently the existence of a CPG for feeding in *Drosophila* larvae was established and the fictive feeding motor sequence could be narrowed down to the sequential rhythmic motor activity of three major pharyngeal nerves [SCHOOFS ET AL., 2010]. 1) The antennal nerve (AN), which innervates the cibarial dilator muscles to drive pharyngeal pumping; 2) the maxillary nerve (MN), which innervates the mouth hook musculature, driving mouth hook movements, which are important for feeding and locomotion; 3) the prothoracic accessory nerve (PaN), which innervates the dorsal protractor muscles, driving head tilting movements, which realize episodic rhythmic feeding movements into the substrate (**Figure 1.2 c and d**).

This publication provides essential knowledge for understanding the fictive feeding motor network in *Drosophila,* feeding related movements and localization of the CPGs underlying feeding.

2.1.1 Statement of Contribution

Figure	Experiment	Author
1A-D	Peripheral innervation of glutamatergic axons onto feeding related muscles	Sebastian Hückesfeld
2A-D	Identification of feeding related motor neurons using PaGFP	Sebastian Hückesfeld
3A-D	Comparison of calcium signal and electrophysiological recording of three pharyngeal nerves	Sebastian Hückesfeld Andreas Schoofs Philipp Schlegel
3E, F	CNS calcium imaging of Motor neurons for pharyngeal pumping	Sebastian Hückesfeld
4A-D	Nerve lesion experiments to physiologically investigate the innervation of the CDM	Andreas Schoofs
4E-I	Anatomical proof for bilateral innervation of the CDM by one CDM motor neuron	Sebastian Hückesfeld
5A-D	Activation and inactivation of feeding related motor neurons	Sebastian Hückesfeld
6A-D	Lesion experiments for the localization of the CPG for feeding related movements in the CNS	Andreas Schoofs
S1A-C	Identification of feeding related motor neurons using retrograde dye backfills	Sebastian Hückesfeld
S2A-D	Example for CNS lesions with simultaneous extracellular nerve recordings	Andreas Schoofs

The author Anton Miroschnikow contributed reagents and established the setup for the food intake assay.

2.2   Publication

Hückesfeld, S., Schoofs, A., Schlegel, P., … Pankratz, M. J. (2015)

Localization of Motor Neurons and Central Pattern Generators for Motor Patterns Underlying Feeding Behavior in *Drosophila* Larvae

PLOS ONE, *10*(8), e0135011.

PLOS | ONE

RESEARCH ARTICLE

Localization of Motor Neurons and Central Pattern Generators for Motor Patterns Underlying Feeding Behavior in *Drosophila* Larvae

Sebastian Hückesfeld, Andreas Schoofs, Philipp Schlegel, Anton Miroschnikow, Michael J. Pankratz*

LIMES-Institute, University of Bonn, 53115, Bonn, Germany

* pankratz@uni-bonn.de

Abstract

Motor systems can be functionally organized into effector organs (muscles and glands), the motor neurons, central pattern generators (CPG) and higher control centers of the brain. Using genetic and electrophysiological methods, we have begun to deconstruct the motor system driving *Drosophila* larval feeding behavior into its component parts. In this paper, we identify distinct clusters of motor neurons that execute head tilting, mouth hook movements, and pharyngeal pumping during larval feeding. This basic anatomical scaffold enabled the use of calcium-imaging to monitor the neural activity of motor neurons within the central nervous system (CNS) that drive food intake. Simultaneous nerve- and muscle-recordings demonstrate that the motor neurons innervate the cibarial dilator musculature (CDM) ipsi- and contra-laterally. By classical lesion experiments we localize a set of CPGs generating the neuronal pattern underlying feeding movements to the subesophageal zone (SEZ). Lesioning of higher brain centers decelerated all feeding-related motor patterns, whereas lesioning of ventral nerve cord (VNC) only affected the motor rhythm underlying pharyngeal pumping. These findings provide a basis for progressing upstream of the motor neurons to identify higher regulatory components of the feeding motor system.

Introduction

Spatial and temporal execution of motor programs reflects the behavior of an organism, which results from the processing of external and internal information by the central nervous system. The most basic components of complex behaviors consist of repetitive, stereotyped movements, like breathing [1], walking, swimming, chewing, swallowing and crawling. Such stereotypical movements are often driven by CPGs, a network of neurons which has the intrinsic capability to produce a rhythmic neural activity that drives the final movement [2]. Our fundamental knowledge on the function of CPGs in the generation of rhythmic behavior derives from work in vertebrate and invertebrate model organisms over the last 40 years [3,4], like

locomotion in lampreys, cats and stick insects [5–9] or the gastric mill/pyloric filter rhythm from the crustacean stomatogastric nervous system (STG)[10]. Strongest evidence for a CPG driving rhythmic behavior derived from studies in which isolated CNS were shown to be capable of generating motor patterns in the absence of extrinsic sensory input [11]. Such motor patterns, which are not fine tuned by external or internal signals, would reflect the basic components of a given behavior in the intact organism, have been termed fictive behavior [10].

Feeding behavior of *Drosophila melanogaster* larvae offers a unique opportunity to investigate the molecular and cellular basis of neuronal substrate that underlies rhythmic motor behaviors. The rhythmic feeding movements of the *Drosophila* larva have been broadly described [12–15], while the gross anatomy of the appropriate musculature and innervating nerves has been described in different Diptera larval species [16,17]. Fictive feeding behavior in *Drosophila* larva was also recently established, based on the motor patterns recorded from three pharyngeal nerves innervating the feeding related musculature [17].

Building on these studies, in which morphological and physiological analyses focused mainly on the periphery, we have been utilizing genetic and imaging tools [18,19] to investigate neural circuits underlying feeding behavior within the CNS of *Drosophila* larva. In a recent study, we have identified numerous populations of central neurons that modulate feeding motor programs [20]. In this study, we characterize the activity and the anatomy of distinct sets of glutamatergic neurons that comprise the motor neurons for food intake and feeding-related movements (i.e., pharyngeal, mouth hook and head movements). We show that CPGs for fictive feeding are located in the SEZ, and that the brain hemispheres are necessary to maintain appropriate motor patterns underlying feeding.

Results

Feeding muscles and nerves

The muscles responsible for larval feeding cycle are innervated by three major pharyngeal nerves (Fig 1A; [17]). Pharyngeal pumping is mediated by the CDM, which is innervated by the antennal nerve (AN); mouth hook movements are mediated by mouth hook elevator (MHE) and mouth hook depressor (MHD) muscles, which are innervated by the maxillary nerve (MN); and head tilting is mediated by the dorsal protractor muscles A and B ($Pro_{do}A$ and $Pro_{do}B$) that attach the head skeleton to the body wall, and are innervated by the prothoracic accessory nerve (PaN) [17]. We first wanted to determine the innervation patterns of the motor neuron axons onto the various muscles involved in the feeding movements. For this we used a Gal-4 driver line (OK371) that drove target gene expression in nearly all glutamatergic neurons of CNS, including the motor neurons [21], and MHC-tauGFP line (myosin heavy chain) to visualize the muscles [22].

The glutamatergic axons projecting through the AN fuse near the posterior end of the CDM at the frontal nerve junction (FNJ), from which the frontal nerve (FN) extends anteriorly in between the CDM (Fig 1B). Small neurites extend out from the axons onto the muscles. For the MN, neuromuscular junction could be visualized at the MHD and MHE muscles (Fig 1C). Innervation of the PaN onto $Pro_{do}A$ and $Pro_{do}B$ muscles is shown in Fig 1D. These results show that glutamatergic axons innervate the muscles involved in feeding. This is in accordance to previous studies showing that motor neurons in the VNC are also glutamatergic [21].

Identification of glutamatergic neurons innervating the feeding muscles

We next wanted to identify the motor neurons for all three pharyngeal nerves within the CNS. Our strategy was to use photoactivatable GFP (PaGFP) assisted circuit mapping with a two-photon laser [23,24], using OK371-Gal4 driving UAS-mCD8::mRFP;UAS-PaGFP(A206K). A
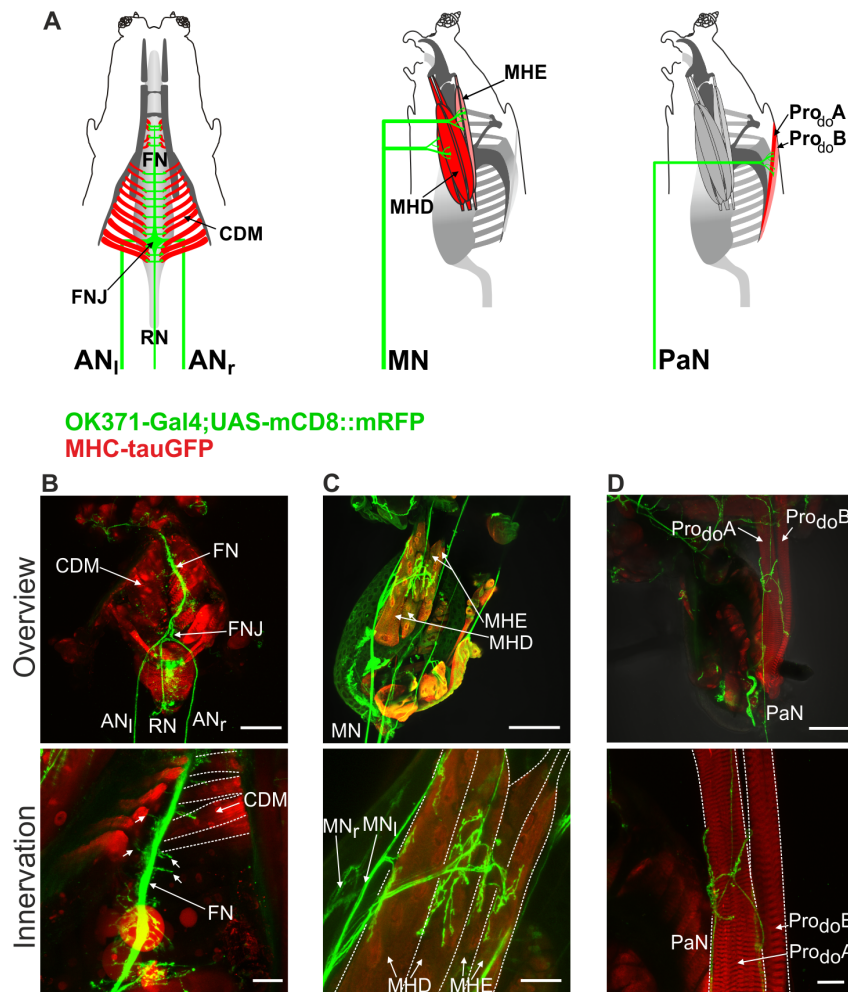
Fig 1. Peripheral innervation of glutamatergic axons onto feeding related muscles. A, Schematics of the innervation of antennal nerve (AN_l = left, AN_r = right) onto the cibarial dilator musculature (CDM), maxillary nerve (MN) onto mouth hook elevator (MHE) and mouth hook depressor (MHD) and prothoracic accessory nerve (PaN) onto prothoracic dorsal muscle A and B (Pro_{do} A/B). **B-D**, Overview of immunohistochemical staining of the larval CPS (genotype: OK371-Gal4/MHC-tauGFP;UAS-mCD8::mRFP/+) and innervation of the glutamatergic axons onto the muscles (top panels); Zoom of the neuromuscular junction of AN (fused to FN at the CDM), MN and PaN (**B,C,D**, respectively, bottom panels). FN, frontal nerve; FNJ, frontal nerve junction; RN, recurrent nerve. Scale bars: B,C,D upper panel: 100µm; B lower panel: 50µm; C,D lower panel: 25µm.

doi:10.1371/journal.pone.0135011.g001

small area of a pharyngeal nerve was activated and the diffusing GFP signal was traced back to the CNS. Somata in the SEZ, which showed enhanced green fluorescence after activation of the nerve, were subsequently photoactivated in order to increase fluorescence. This was performed for each of the three pharyngeal nerves (Fig 2).

Activation of PaGFP in the AN resulted in labeling of a tight cluster of up to 11 cells in the dorsal SEZ just lateral to the foramen (10.3 ± 0.95 cells, n = 10, Fig 2A), with dendritic arborizations in the anterior midline of the SEZ. This observation was further confirmed by retrograde nerve fillings with tetramethyrhodamine-dextran (Tmr-D) of the AN, which resulted in

OK371-Gal4/+;UAS-mCD8::mRFP/UASPaGFP(A206K)
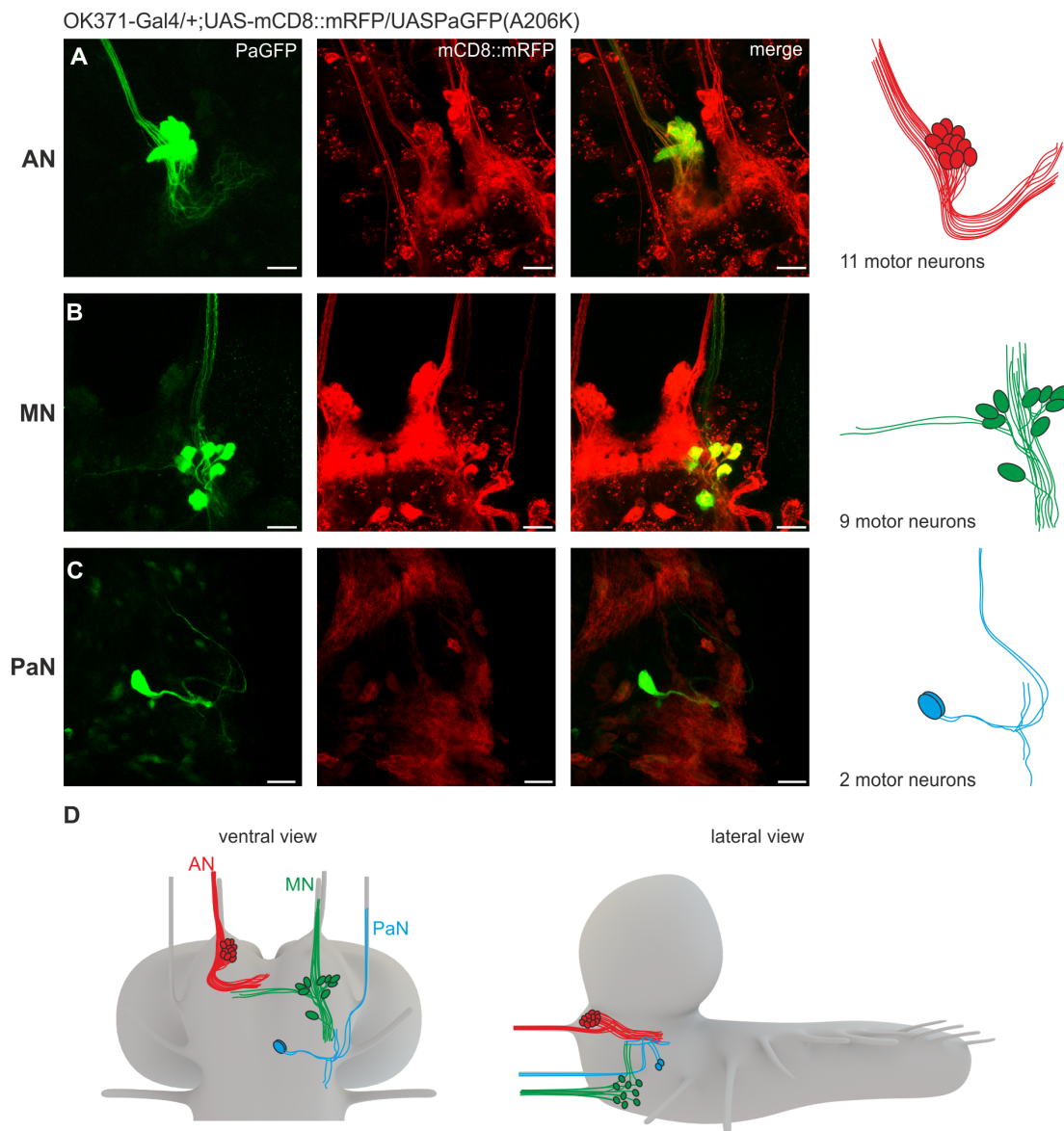
Fig 2. Anatomical identification of feeding related motor neurons using PaGFP. A, Glutamatergic neurons projecting through the antennal nerve (AN) visualized by activation of PaGFP (genotype: OK371-Gal4/UAS-mCD8::mRFP;UAS-PaGFP(A206K/+). Up to 11 motor neurons could be identified for the AN. Left = PaGFP, middle = mRFP, right = merge. **B**, Glutamatergic neurons projecting through the maxillary nerve (MN). Up to 9 motor neurons could be identified. **C**, Glutamatergic neurons projecting through the prothoracic accessory nerve (PaN). Two motor neurons could be identified. **D**, Schematic overview (ventral and lateral) of the identified glutamatergic neurons in the subesophageal zone (SEZ) projecting through the AN, MN and PaN. Scale bars: 20µm.

doi:10.1371/journal.pone.0135011.g002

labelling of the CDM motor neuron cluster (colocalization with OK371-Gal4 driving UAS-G-CamP6s). Up to two additional cells were labelled by Tmr-D, which did not colocalize with cells marked by OK371-Gal4 (S1A Fig and S1 File)(see Discussion for what these extra labelled cells could represent).

Activation of PaGFP in the MN resulted in labeling of a more loosely organized cluster with up to 9 cells at the ventro-lateral border of the SEZ (8.25 ± 0.7 cells, n = 8, Fig 2B). Several of the neurons projecting through the MN showed dendritic arborizations in the midline of the SEZ near the dendritic fields of the neurons labelled by the AN. Retrograde filling of the MN showed that 9 glutamatergic neurons were projecting out of the CNS via the MN (S1B Fig and S2 File).

Activation of PaGFP in the PaN resulted in the labeling of two cells located in medial SEZ (2 cells, n = 15, Fig 2C). Dye filling labelled additional two non glutamatergic cells projecting out of the CNS via the PaN (S1C Fig and S3 File)(see Discussion). Schematics of the relative locations of glutamatergic motor neurons in the CNS are shown in Fig 2D.

Imaging rhythmic activity of pharyngeal nerves

If the identified glutamatergic neurons comprise the motor neurons driving the different movements of feeding behavior, they should also be rhythmically active. We first asked whether the axons were rhythmically active, thus reflecting the motor pattern recorded from the pharyngeal nerves. Calcium indicators can be utilized to measure neuronal activity as a complement to electrophysiological methods, since action potentials and the induced synaptic transmissions generate large and rapid cytoplasmic $[Ca^{2+}]$-transients. Therefore, we expressed the genetically encoded calcium indicator GCaMP3 [25] in glutamatergic neurons using the OK371 driver line, and measured the neuronal activity of the three pharyngeal nerves (Fig 3A). In all cases, calcium imaging analysis revealed spontaneous, rhythmic activity (Fig 3B).

Comparison of bursting activity from extracellular recordings and calcium-imaging data (Fig 3C) revealed close temporal correlation of the rhythmic motor patterns observed in the AN, MN and PaN (performed Mann-Whitney-Rank-Sum-Test revealed no significant differences; Fig 3D). Taken together, calcium imaging analysis showed that the glutamatergic motor neurons display rhythmic activity, in correlation with the rhythmic motor output recorded extracellularly from the respective nerves.

We next wanted to determine the neural activity of the previously identified neurons, focusing on the CDM motor neurons that project through the AN. By expressing a modified version of the previously described calcium indicator (GCaMP6s [26], for enhancement of the signal to noise ratio), we observed temporal correlation of calcium activity between the AN, the two clusters of CDM motor neurons and their dendritic arborizations in the SEZ (Fig 3E and 3F). These results suggested that these clusters house the somata of glutamatergic motor neurons that extend through the AN to innervate the CDM. Furthermore the calcium imaging results provide a rhythmic blueprint for larval pharyngeal pumping in the CNS.

AN targets both ipsi- and contra-lateral muscle systems

Of the three nerves, the AN is the most dedicated to feeding behavior since it innervates the muscles that drive pharyngeal pumping. This nerve is also anatomically distinct, since it fuses together at the FNJ and projects as a single fiber, the FN, in between the muscle palisades (see Fig 1A). This is in contrast to either MN or PaN, both of which end in a bilateral fashion on either side of the pharynx. This led us to ask whether each AN (or axons in the AN) innervates CDM on both sides.

Therefore, we performed a series of lesion experiments together with simultaneous recordings from both nerves (extracellularly) and muscles (intracellularly) (see Fig 4A for experimental scheme); this setup thus represents a quadruple recording. In the unimpaired state (Fig 4B), both ANs show a simultaneous motor pattern that temporally correlates with the postsynaptic potentials (PSPs) in the CDM recordings. After completion of the first lesion on the right AN
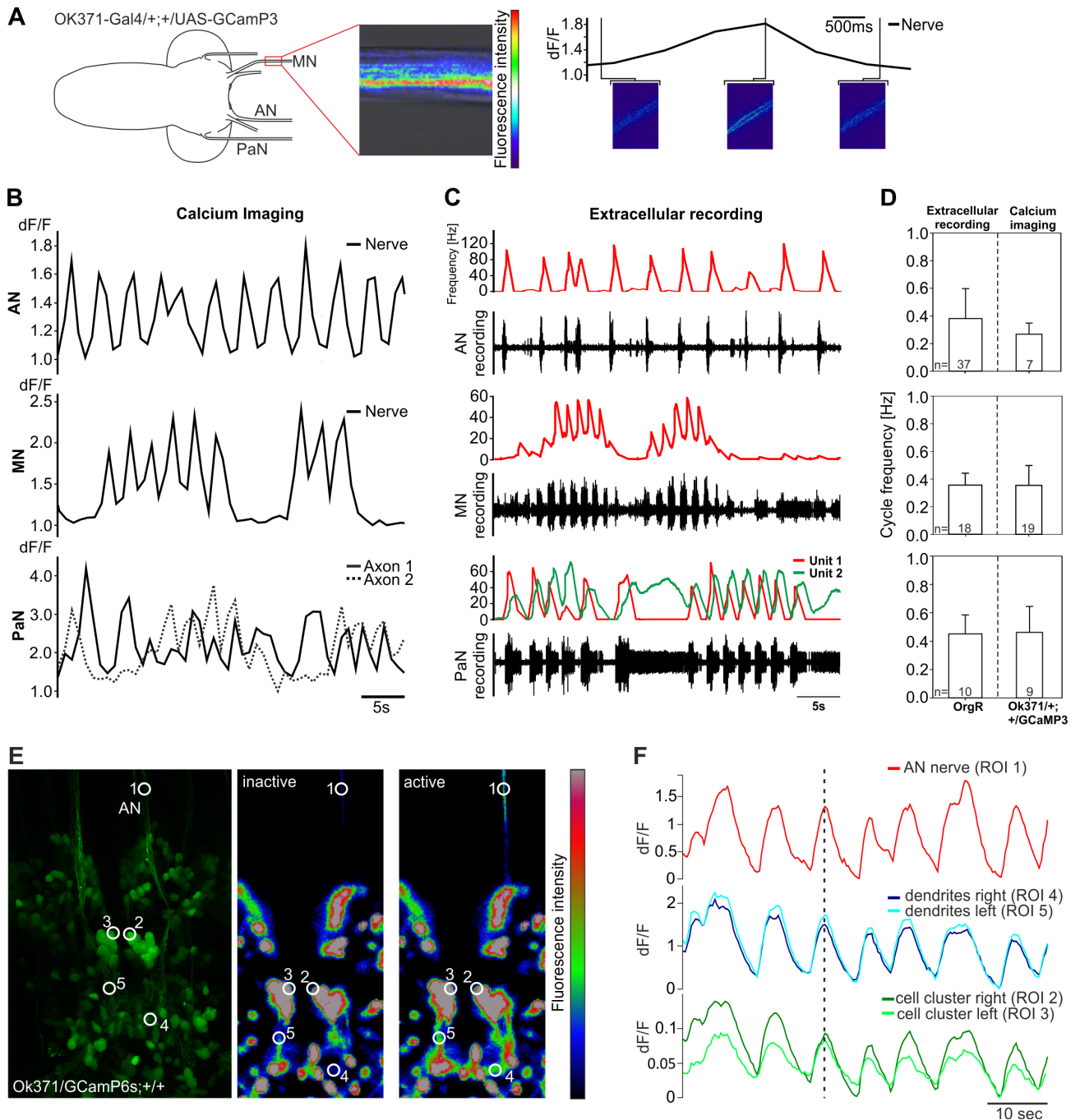
Fig 3. Comparison between calcium activity and extracellular recordings from AN, MN and PaN. A, Experimental setup for calcium imaging of the three pharyngeal nerves. Here shown for the MN. **B**, Calcium transients and **C**, extracellular recordings for all three pharyngeal nerves (AN, MN and PaN). Note the temporal correlation similarities between optogenetic and electrophysiological data. **D**, Quantitative comparison of measured cycle frequencies in all three nerves show no significant difference. **E**, left panel = maximum projection of the SEZ region in larvae with the genotype OK371-Gal4/UAS-GCaMP6s; +/+, middle/right panel = location of AN, motor neurons and dendritic arborizations being inactive/active. White circles showing regions of interest (ROI) used for measurements shown in F. **F**, Calcium activity from AN on one side temporally correlates to the activity of AN motor neurons and their dendritic fields on ipsi- and contralateral sides. AN, antennal nerve; MN, maxillary nerve; PaN, prothoracic accessory nerve. dF/F = change of fluorescence intensity over baseline fluorescence.

doi:10.1371/journal.pone.0135011.g003
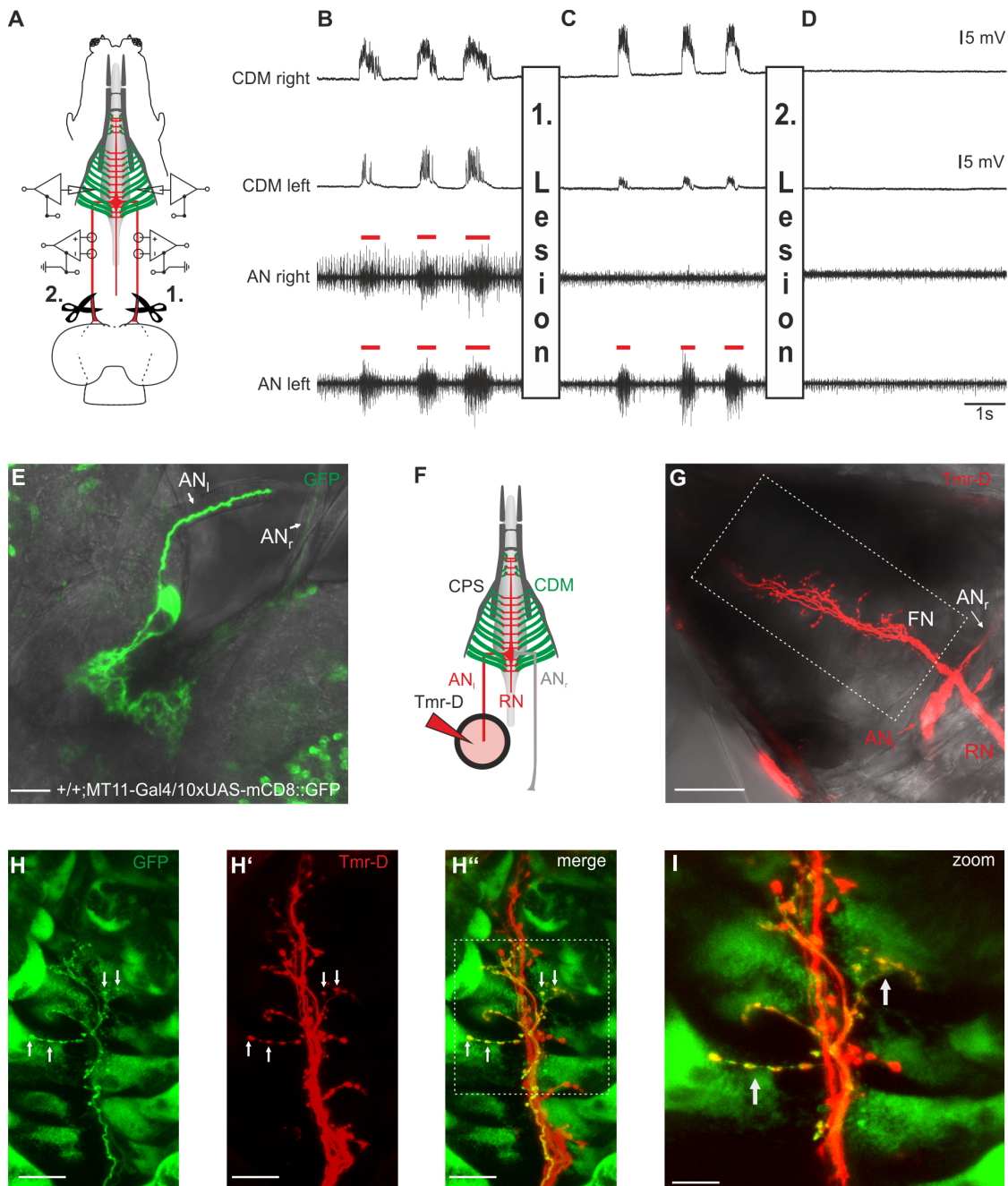
Fig 4. Motor neurons for pharyngeal pumping innervate the cibarial dilator musculature (CDM) ipsi- and contra-laterally. A, Simultaneous antennal nerve (AN) and cibarial dilator muscle (CDM) recordings of left and right side of the larval body of an OregonR larva. **B,** Under unimpaired conditions, AN motor pattern (red bars) of the left and right side is synchronous, and shows temporal correlation with the evoked postsynaptic potentials (PSPs) of the left and right CDM. **C,** Lesion of the right AN (1. Lesion) between the CNS and recording site results in abolishment of the corresponding AN motor pattern, whereas the PSPs on both sides of the CDM persist. Note that the diminished amplitude of the PSPs in the left CDM recording is caused by displacement of the glass electrode due to the lesion. **D,** Subsequent lesion of the left AN (2. Lesion) eliminated additionally the AN motor pattern on the left side and resulted in total disappearance of the PSP in left and right CDM. **E**, One CDM motorneuron (left side) strongly labelled in a larvae expressing 10xUAS-mCD8::GFP driven by MT11-Gal4. **F**, Schematic of the setup used for anterograde filling of the AN with tetramethylrhodamine-Dextran (Tmr-D). **G**, Tmr-D filled left AN

Feeding Related Motor Neurons in *Drosophila* Larvae

shows axons with bilateral innervation of the CDM. **H-H"**, Colocalization of the Tmr-D labelled FN and one Axon of MT11-Gal4 driving 10xUAS-mCD8::GFP showing bilateral innervation of the CDM by one CDM motor neuron. **I**, Magnified region of the FN (marked in H" by white dotted box). Scalebars: E: 20µm,G: 50µm, H-H": 20µm, I:10µm.

doi:10.1371/journal.pone.0135011.g004

(see 1.in Fig 4A), no neural activity is detectable in the right AN, whereas the motor pattern in the left AN still persists, as expected. Remarkably, however, both left and right CDM show series of PSPs which are elicited by the motor pattern of the remaining left AN (Fig 4C). As a control, a second lesion was performed by cutting the left AN (both ANs are now cut), which abolished its motor pattern and the muscle activity in both CDMs (Fig 4D). These observations indicate that the CDM motor neurons on one side of the CNS innervate the muscles ipsi- and contra-laterally. Subsequently we used the published MT11-Gal4 line, which drives expression in one CDM motor neuron per side in the larval CNS [27]. In larvae carrying MT11-Gal4 driving 10xUAS-mCD8::GFP we observed that GFP expression strength varies in individual larvae (Fig 4E). We used this advantage to use a CNS which shows strong GFP expression in one CDM motor neuron and subsequently backfilled the AN nerve with tetramethylrhodamine-Dextran (Tmr-D) to visualize the potential bilateral innervation of the CDM (Fig 4F and 4G). By labelling exclusively the left AN, we could see a bilateral innervation onto the CDM muscles by the visualized axons. Colocalization with the MT11-Gal4 line driving 10xUAS-mCD8::GFP shows that one CDM motoneuron projects onto both, the ipsi- and contralateral side of the CDM (Fig 4H–4I).

Manipulation of glutamatergic motor neuronal activity

The line OK371-Gal4 labels a large population of motor neurons, if not all, and neuronal activation using this line results in a tonic excitation pattern of AN and other pharyngeal nerves [20]. Since this Gal4-line also marks the feeding motor neurons, inhibiting OK371-Gal4 labelled neurons should lead to a decrease in food intake and an inhibition of muscle contraction. Therefore, we expressed shibire^TS in glutamatergic neurons (OK371-Gal4 drives UAS-shibire^TS), which blocks synaptic transmission upon shifting to restrictive temperature, and performed food intake assays as well as recording extracellularly from the AN and intracellularly from the CDM (Fig 5A–5C). We focused on the AN/CDM pair since it was technically more feasible to perform double recordings from the nerve and the innervated muscles.

Inhibiting glutamatergic neurons completely eliminated food intake (Fig 5A and 5B). This was similar to what was observed when these neurons are activated through TrpA1 (OK371-Gal4 driving UAS-TrpA1) (Fig 5B; [20]). Since this inactivation through shibire^TS and the activation through TrpA1 target a large population of glutamatergic neurons, we also performed simultaneous nerve (AN) and muscle (CDM) recordings. Inactivation through shibire^TS by temperature shift to 40°C near the CPS did not affect the motor pattern of the AN. By contrast, CDM recordings showed no post-synaptic potentials as a response to AN motor output (Fig 5C), indicating that the motor neurons for pharyngeal pumping are inactivated by shibire^TS. Only a few single post-synaptic potentials with decreased peak topeak amplitude were detectable upon blocking the synaptic transmission by shibire^TS. Therefore shibire^TS is able to block synaptic transmission in glutamatergic motor neurons projecting through the AN, which leads to physiological and behavioral alterations. These results were further confirmed by using light instead of temperature as manipulators of neuronal activity. Fig 5D shows that channelrhodopsin (UAS-ChR2(H134R)) mediated activation of glutamatergic neurons results in tonic excitation, whereas inhibition by halorhodopsin (UAS-eNpHR) leads to suppression of neural activity.

Feeding Related Motor Neurons in *Drosophila* Larvae
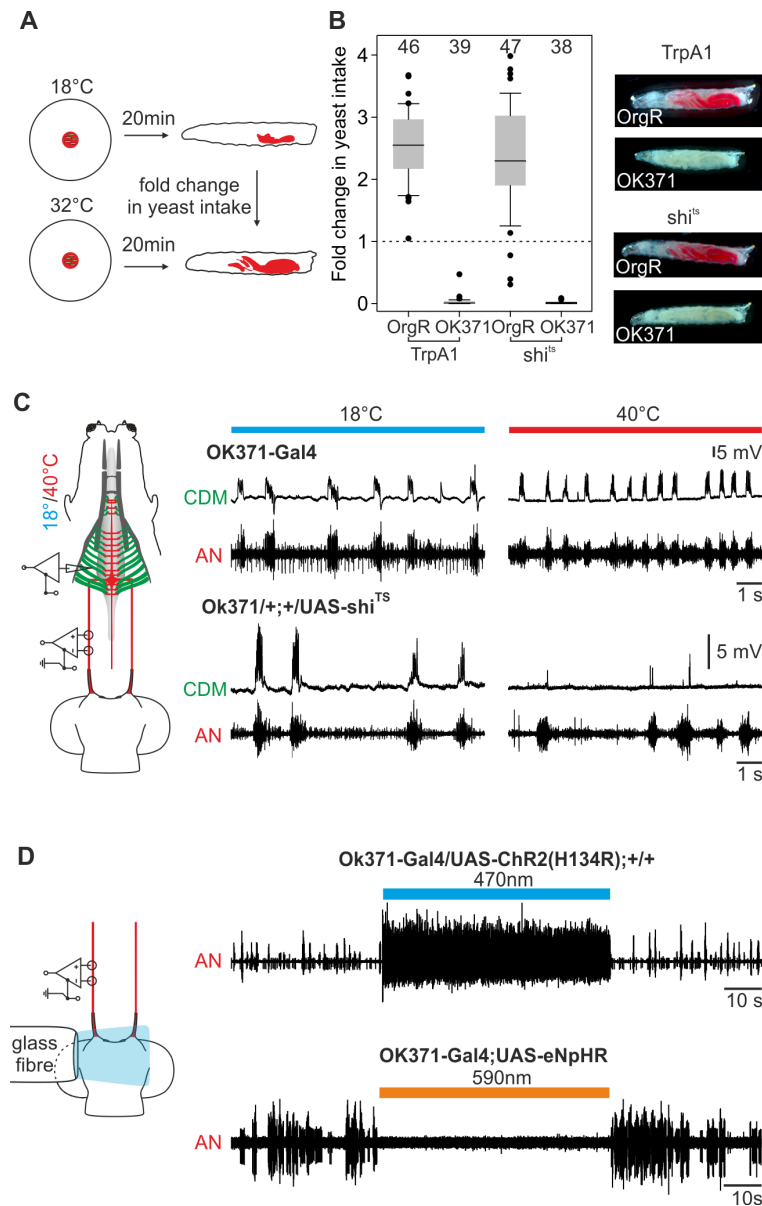
Fig 5. Activation and inactivation of feeding related motor neurons leads to decline in feeding. A, Experimental setup: yeast intake of larvae at 18°C and 32°C (% of larval body stained with red yeast) was determined after 20min of TrpA1-activation and shi^TS-inactivation. **B**, Fold change in yeast intake; in both cases no dyed food could be observed in experimental larvae. **C**, Inactivation by shi^TS of glutamatergic neurons results in decline of cibarial dilator muscle (CDM) postsynaptic potentials (PSP), but not in the antennal nerve (AN) motor pattern. **D**, Activation of glutamatergic neurons via channelrhodopsin (UAS-ChR2 (H134R)) or inhibition via halorhodopsin (UAS-eNpHR) resulted in direct tonic excitation or complete inhibition of the AN motor pattern.

doi:10.1371/journal.pone.0135011.g005

CPG for feeding motor patterns is located in the SEZ

After having characterized the activity and anatomy of the motor neurons, we next wanted to determine where the feeding CPG was localized. To this end, we caused lesions to the isolated CNS preparation and simultaneously recorded the motor pattern (Fig 6A). This was done individually for the AN, the MN and the PaN. Lesion of the VNC did not affect the maintenance of AN, MN and PaN motor patterns (Fig 6B, 1. Lesion); however, it did result in increased cycle frequency of the AN motor pattern, whereas the motor pattern for MN and PaN were unaffected (Fig 6B, right graphs). These findings indicate that in the unimpaired state the VNC inputs can decelerate the AN motor pattern.

In the second lesion, both brain hemispheres were removed from the residual CNS. The remaining isolated SEZ was capable of generating rhythmic motor patterns in all three nerves. These data support the view that for all three motor patterns the CPG is located in the SEZ of the larval CNS. However, rhythm analysis of the patterns showed a severe decrease in cycle frequency of all motor patterns (Fig 6B, 2. Lesion), pointing to the importance of higher brain center inputs for adequate modulation of the CPG. The third lesion, in which the isolated SEZ was bisected along the longitudinal body axis, resulted in long lasting tonic activity of the neuronal units in all nerves (Fig 6B, 3. Lesion). Example of lesions performed for extracellular recordings is shown for the AN in S2 Fig. Taken together the lesion experiments indicate that the CPGs for feeding rhythm generation are localized in the SEZ (Fig 6D).

Discussion

Feeding motor neurons in the SEZ

Fundamental component of any motor system are the motor neurons that innervate the effector muscles. Our findings fill a crucial gap in knowledge by characterizing the motor neurons of the *Drosophila* larval feeding motor system. Cell bodies of the glutamatergic neurons that project through the three major pharyngeal nerves form spatially distinct clusters in the SEZ. Glutamatergic neurons projecting through the AN (which innervates the pharyngeal muscles) form a tight cluster of up to 11 cells. Additional cells, which do not colocalize with glutamatergic cells labelled by the OK371-Gal4 line could be visualized with retrograde filling of the AN. These are likely serotonergic cells, which are located close to the CDM motor neuron cluster as previously shown [28,29]. Neurons projecting through the MN (innervates the mouth hook muscles) form a more loosely organized cluster of 9 cells colocalizing with OK371-Gal4. No additional cells were labelled using retrograde fillings of the nerve. This indicates that neurons projecting out of the CNS via the MN are exclusively glutamatergic. Some of these may correspond to those identified by dye filling or lacZ enhancer trap staining of one of the pharyngeal nerves [27,30]. For the PaN (innervates muscles enabling head tilting), two glutamatergic neurons were found. Two additional neurons were labelled using retrograde filling. These neurons correspond to the two Hugin positive neurons on each side of the CNS that project out of the PaN. This is also consistent with two neuronal motor units described for PaN nerve recordings [17].

The identification of the motor neurons also enabled the monitoring of neuronal activity by calcium imaging analysis for one of these, the AN. This revealed that the rhythmic activity of the glutamatergic axonal projections and the rhythmic activity of the corresponding cell clusters in the SEZ are coincident. In addition, correlation of calcium imaging with electrophysiological recordings provides strong indication that the rhythmically active cells represent the respective motor neurons innervating the feeding muscles. A further notable feature of the AN is that its motor neurons innervate the CDM both ipsi- and contra-laterally. This might assure
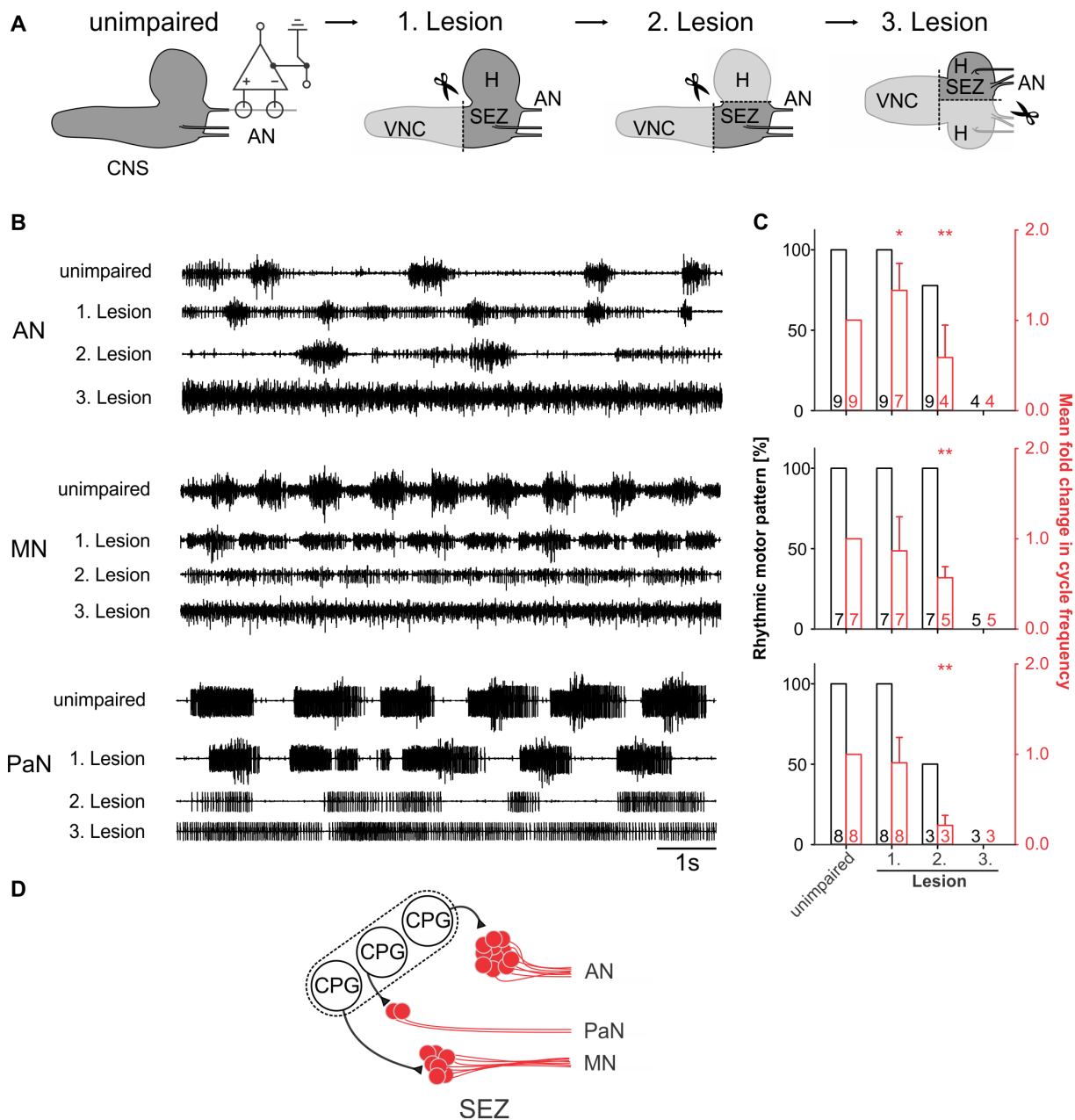
Fig 6. Central pattern generators (CPGs) of feeding-related motor patterns are localized to the subesophageal zone (SEZ). A, Starting with the intact central nervous system (CNS, unimpaired), antennal (AN), maxillary (MN) and prothoracic accessory nerve (PaN) motor patterns were individually recorded while successively lesioning the ventral nerve cord (VNC, 1. Lesion), brain hemispheres (H, 2. Lesion) and finally bisecting the SEZ (3. Lesion) of OregonR larvae. **B,** Single nerve recordings of AN, MN and PaN under unimpaired conditions, after consecutive removal of the VNC, hemisphere (H) and bisection of the SEZ. Note that the lesion of the VNC has minor effects on the rhythmic motor patterns, whereas removing the H severely impaired the motor patterns of AN, MN and PaN. Bisection of the residual SEZ results in tonic motor activity. **C**, Bar plots represent the percentage of the nerve recordings showing rhythmic motor activity (black) and the fold change in cycle frequency of the motor patterns (red) in the unimpaired state and after the successive lesions (n = number of experiments). **D,** Schematic drawing of the potential functional organization of CPG(s) driving the feeding related motor patterns in the SEZ. SEZ: subesophageal zone.

doi:10.1371/journal.pone.0135011.g006

that the bilateral parts of the CDM operate in unison, a feature that would facilitate food intake.

Feeding CPGs

A core element of behavior is built up of stereotypical repetitive movements controlled by CPGs which are embedded into a complex network of higher order neural circuits [31]. The cellular components that comprise a CPG have been characterized only in a few cases. For invertebrates, this includes the stomatogastric nervous system in crabs [32], food intake in *Lymnaea* [33], and locomotion in leech [34,35]. For vertebrates, only single components of CPGs have been described functionally [36,37].

In *Drosophila*, previous investigations showed, using surgical and genetic techniques, that neuronal circuits for the generation of larval crawling behavior are located in thoracic and abdominal segments of the CNS [38]. Furthermore they were able to show that crawling behavior is partially maintained directly after lesion of the brain hemispheres and SEZ and showed no difference in forward or backward peristaltic waves after several minutes. Although we do not know the cellular composition of the feeding CPGs, our lesion experiments demonstrate that they are localized in the SEZ and that for maintenance of a basic feeding rhythmic activity the brain hemispheres and the VNC are not necessary. Interestingly, generation of the rhythmic pattern requires interaction between the left and right side of the SEZ, since bisection of the SEZ leads to tonic firing of all three nerves. This result points to several possibilities, e.g., that interaction between both halves of the SEZ is essential for proper functioning of feeding CPG, that the lesion has injured the CPG and/or motor neurons in the SEZ. Future efforts will be aimed towards identifying specific Gal-4 lines targeting the different pharyngeal motor neurons and specific components of the feeding CPG, that will allow genetic manipulations of the brain hemispheres and the SEZ alone. The current study provides a foundation for further elucidation of the neural network underlying feeding in *Drosophila* larvae. Our identification of the motor neurons responsible for feeding movements will facilitate the identification of upstream cellular elements that comprise the CPGs and higher modulatory centers in the larval CNS.

Materials and Methods

Fly lines

Following lines were used: OK371-Gal4 (genotype w^{1118};OK371-Gal4;+, Bloomington #26160) for targeting glutamatergic neurons, MHC-tauGFP [22] as a muscle reporter line, MT11-Gal4 (genotype w;+;P{GawB}MT11)(Bloomington #37295), UAS-mCD8::mRFP (genotype y,w; UAS-mCD8::mRFP;+, Bloomington #27398 and y,w;+;UAS-mCD8::mRFP) (Bloomington #27399 (3rd Chr.)),10xUAS-mCD8::GFP(genotype w;+;10xUAS-mCD8::GFP)(Bloomington #32184) UAS-TrpA1 (genotype w;UAS-TrpA1;+) (Bloomington #26263), UAS-shi^{TS} (w;+; UAS-shi^{TS} [39]), UAS-ChR2(H134R) (w;UAS-ChR2(H134R);+, Bloomington #28995), UAS-eNpHR (w;+;UAS-eNpHR::YFP, Bloomington #41752 gift from Leslie Griffith), UAS-PaGFP (A206K) (w;+;UAS-PaGFP(A206K), gift from A.S. Chiang [40]), UAS-GCamP3 (genotype w;+;UAS-GCamP3, Bloomington #32236), UAS-GCamP6s (genotype w^{1118};UAS-GCamP6s;+, Bloomington #42746), OregonR (genotype +/w;+/UAS-TrpA1;+/+). For PaGFP experiments genotype was y,w/w;UAS-mCD8::mRFP; UAS-PaGFP(A206K).

Fly care

Flies and larvae were kept on 25°C under 12h light/dark conditions unless otherwise stated. 4h egg collections were made on apple juice agar plates containing a spot of yeast-water paste. After 48h, larvae were transferred into food vials containing lab standard fly food. All larvae used for the experiments were 98 +/- 2 h old. Only feeding larvae were used for the experiments.

For experiments with OK371-Gal4 driving either UAS-H134R-ChR2 or UAS-eNpHR.YFP, larvae were transferred after 48h into food vials containing additionally 100µM all-trans retinal (ATR). Food vials were darkened with surrounding aluminum foil to prevent ATR degradation.

Electrophysiology

Extracellular recordings of pharyngeal nerves (AN, MN and PaN) and intracellular recordings of the CDM were performed as previously described in [20]. In brief, for extracellular recordings of pharyngeal nerves, each nerve was electrically isolated using a petroleum jelly pool surrounding the nerve placed on a piece of Parafilm. Silver wire electrodes were used for measuring with differential recordings motor output of the deafferented nerve. A preamplifier (Model MA103, Ansgar Büschges group electronics lab) connected to a four-channel amplifier/signal conditioner (Model MA 102, Ansgar Büschges group electronics lab) was used. All recorded signals were amplified (amplification factor: 5000) and filtered (bandpass: 0.1–3 kHz). Recordings were sampled at 20 kHz. Data was acquired with Micro3 1401 or Power 1401 mk2 A/D board (Cambridge Electronic Design) and Spike2 software (Cambridge ElectronicDesign). Intracellular muscle recordings of the CDM were recorded using glass microelectrodes filled with 3 M KCl solution (tip resistance: 20–30 MΩ) connected to an intracellular amplifier (BRAMP-01R, npi electronic GmbH). All recordings were digitally sampled by a Power 1401 mk2 A/D board (Cambridge Electronic Design) at 20 kHz. Data was acquired with Spike2 software (Cambridge Electronic Design).

Temperature stimulation

Application of temperature shifts to the CNS was accomplished using a custom built temperature stimulator as described earlier in [20]. For shibire[TS] experiments (Fig 5C) the temperature stimulator was placed near the cephalopharyngeal skeleton (CPS) and heated up to 40°C to reach the permissive temperature at the CDM.

Light stimulation

Mounted ultra-bright blue (470nm)/orange (590nm) LEDs (M470L2 and M590L2, Thorlabs) with collimated lenses and heat sink were used in experiments with UAS-ChR2(H134R) or UAS-eNpHR. LEDs were positioned in a custom built holder, supplemented with an optical multimode fiber (AFS200/220Y Thorlabs). Distal end of the optical fiber was placed directly over the ventral side of the CNS. LEDs were controlled by a LED controller unit (LEDBB1 Thorlabs) and light stimuli were delivered using A/D board (CED). All light stimuli were applied using highest intensity of the controller at 1mA. The optical fiber had a length of approx. 90cm with a transmission efficiency of >99.8%/m. Experiments were performed under dark conditions.

Immunohistochemistry

For the staining of peripheral anatomy (Fig 1) a line with the genotype OK371-Gal4;UAS-mCD8::mRFP was used and crossed into MHC-tauGFP line. Dissection protocol for extracellular recordings was used, leaving all three pharyngeal nerves and projections intact. Remaining cuticle surrounding the CPS was removed. The sample of remaining CNS, CPS and nerves of interest was stained using anti-chicken-GFP (1:500, Abcam plc) and anti-mouse-mRFP (1:500) as primary antibodies. In brief, samples were fixed for 60min in 4% PFA and the washed with 0.5 PBT (2x10min, 2x15min, 2x30min), then tissue was blocked using 0.5 PBT containing 5% goat-serum for 60min. Primary antibody was added and incubated overnight at 4°C. Samples were washed the next day with 0.1 PBT (2x10min, 2x15min, 2x30min) and 60min blocked with 0.1 PBT containing 5% goat serum. Secondary antibodies (anti-mouse-Cy3, 1:250 Jackson ImmunoResearch and anti-chicken-Alexa488, 1:250 Invitrogen) were added and the samples were incubated at 4°C overnight. After washing the samples the next day, they were immediately scanned using a Laser scanning microscope (Zeiss LSM 780) equipped with a Zeiss LCI "Plan-Neofluar" 25x/0.8 Imm Korr DIC M27 objective and a Zeiss "PlanNeofluar" 10x/0.3 objective.

Antero-/Retrograde nerve fillings

Larvae were dissected as described for extracellular recordings. A jelly pool was used to isolate the nerve of interest. Saline level was lowered until the fluids inside and outside the jelly pool were separated from each other. The nerve was cut within the jelly pool and saline was replaced with tetramethylrhodamine-dextran solution (Tmr-D) (Life Technologies, 3000MW anionic at 10mg/ml in distilled water). The preparations were stored at room temperature for 3 hr. After uptake of the dye, preparations were fixed in 4% paraformaldehyde (PFA) for 40 min, washed in PBS and mounted in Mowiol. The CNS was scanned the following day using a Laser scanning microscope (Zeiss LSM 780) equipped with a Zeiss LCI "Plan-Neofluar" 25x/0.8 Imm Korr DIC M27 objective. For colocalization with glutamatergic neurons we used larvae with the genotype OK371-Gal4/+;UAS-GCamP6s/+. Using GCamP6s for scanning the CNS had the advantage that the strong fluorescent signal was evenly distributed throughout the cells and their dendritic arborizations.

After verification of expression of the CDM motor neurons in the CNS of larvae (+/+; MT11-Gal4/10xUAS-mCD8::GFP), anterograde fillings of the left AN were done using the same procedure as described for retrograde dye filling.

Photoactivation of PaGFP

The CNS, CPS and attached pharyngeal nerves of larvae with the genotype OK371-Gal4/UAS-mCD8::mRFP;UAS-PaGFP(A206K)/+ were placed with ventral side down onto a Poly-L-lysine (Sigma Aldrich) coated cover slide and mounted upside down in Ringer solution. Images were acquired using a laser scanning microscope (Zeiss LSM 780) with a Zeiss LCI "Plan-Neofluar" 25x/0.8 Imm Korr DIC M27 objective. To photoactivate the GFP we used a Ti:Sapphire Chameleon Ultra II Laser (Coherent) tuned to 820nm. Laser power was set to 8% for activation of the GFP in nerves. Bleach period of 8s was sufficient to activate the GFP in axons of the nerves. This was repeated two times at different areas of the nerve. Following settings were used: image size at 161.31x161.31µm, resolution at 256x256, pixel dwell 2µs, speed 11 and region of interest (ROI) size at 140µm.

After successful activation of GFP in the nerve, low GFP signal in somas in the SEZ were visible. Those were subsequently activated using the same protocol, adjusting ROI sizes to somata. This procedure was done for AN, MN and PaN. Z-stacks were acquired using 488nm laser and

PLOS | ONE   Feeding Related Motor Neurons in *Drosophila* Larvae

Calcium imaging

Third instar feeding larvae with the genotype OK371-Gal4/+;UAS-GCamP3/+ (Fig 3A and 3B) or OK371-Gal4/UAS-GCamP6s;+/+ (Fig 3E and 3F) were used for calcium imaging experiments.

Neural activity of the three pharyngeal nerves was studied using semi intact preparations as described above consisting of CNS, CPS and the nerves. Calcium imaging was performed with Laser scanning microscope (Zeiss LSM 780) equipped with ZEISS LCI "Plan-Neofluar" 25x/0.8 Imm Korr DIC M27 objective dipped into the saline solution (Fig 3A and 3B). In Fig 3E and 3F CNS with nerves and CPS was placed ventral side down onto a polylysine coated cover slide and imaged upside down to visualize somata and dendritic arborizations in the SEZ (scan speed: 347.7ms). For excitation an argon laser with a wavelength of 488 nm was used. Fluorescence was collected using photomultiplier tubes after filtering using the MBS 488/561/633 emission filter. Images were acquired using Zen. Data were analyzed using the software Zen 2011 (Zeiss) and Spike2.

Feeding assay

Feeding assay was performed as previously described in [20]. In brief, 5 larvae were starved for 30min on water soaked filter paper and then placed onto a drop of yeast-water-paste in the middle of an apple-juice-agar plate. The plates were placed on either 18°C or 32°C in an incubator for 20min. Afterwards larvae were washed in hot water (60°C) and pictures were taken using an Axiocam. Values were calculated as percentage of larval body stained red for each temperature and the fold change in yeast intake was calculated. For experiments with shibire[TS], 32°C experiments were performed following 1h incubation at 32°C to ensure that the storage of synaptic vesicles are emptied.

Lesion experiments

In the lesion experiments the typical semi-intact preparation of third instar larvae was used (see section: Electrophysiology; for details: [20]). Lesion of nerves and parts of CNS (VNC, brain hemispheres and SEZ) were ablated by a micro-dissecting scissor (Fine Science Tools). For the successive lesions of different brain regions, extracellular recording of the AN was started five minutes after the ablation.

Data analysis

Processing of electrophysiological recordings was performed with a modified script of Spike2 software (provided by Cambridge Electronic Design). Statistical analysis of the electrophysiological data was accomplished using SigmaPlot (Version 12.0). For significance test we used Mann-Whitney Rank Sum Test (* $p \leq 0.05$, ** $p \leq 0.01$ and *** $p \leq 0.001$).

Food intake analysis was performed as described in [20] using a custom script in Fiji for analysis. Calcium imaging data was processed in Zen2009 and Spike2 software.

Supporting Information

S1 Fig. Anatomical identification of feeding related motor neurons using retrograde dye filling of pharyngeal nerves. Glutamatergic cells and dendrites were visualized using

OK371-Gal4 driving UAS-GCamP6s (GCamP6s used for scanning due to very high signal quality in live scans). Each pharyngeal nerve was filled with tetramethylrhodamine-dextran (Tmr-D) for 3h, subsequently fixed in PFA and directly scanned. **A**, Retrograde filling of the antennal nerve (AN) revealed up to 14 neurons labelled by Tmr-D and up to 11 colocalized with OK371-Gal4 driving UAS-GCamP6s. **B**, Retrograde filling of the maxillary nerve (MN) revealed 9 neurons labelled by Tmr-D and all colocalized with OK371-Gal4 driving UAS-G-CamP6s.**C**, Retrograde filling of the prothoracic accessory nerve (PaN) revealed 4 labelled neurons by Tmr-D, 2 neurons colocalized with OK371-Gal4 driving UAS-GCamP6s. Scale bars: most left panels: 50μm, magnified regions: 20μm.
(TIF)

S2 Fig. Motor patterns of the antennal nerve (AN) and subsequent applied lesions during extracellular recording. Starting with the intact central nervous system (CNS, unimpaired), the antennal nerve (AN) motor pattern was recorded while successively lesioning the ventral nerve cord (VNC, 1. Lesion), brain hemispheres (H, 2. Lesion) and finally bisecting the subesophageal zone (SEZ) (3. Lesion). **A,** Single nerve recording of AN in unimpaired conditions. **B,** Removal of the VNC leads to acceleration of the AN motor pattern (recording trace). Imaginal discs of the prothoracic nerve (ProN) served as landmark for the lesion. **C**, Removal of the brain hemispheres (H) leads to slight deceleration of the AN motor rhythm. Optic stalks (OS) served as residual tissue for grabbing the hemispheres with forceps to ensure more precise lesion. **D,** Bisection of the residual SEZ leads to tonic activity in the AN motor pattern and abolishment of rhythmic activity of the motor neurons. Remaining imaginal discs of ProN and Mesothoracic nerve (MeN) served as landmarks for proper lesions.
(TIF)

S1 File. Retrograde filling of the AN. The AN was filled with tetramethyrhodamine-dextran (Tmr-D) in larvae with the genotype OK371-Gal4/UAS-GCamP6s;+/+. Apart from cells colocalizing with the OK371-Gal4 expression pattern, up to two additional cells were labelled by Tmr-D. These might be serotonergic cells, which form a cluster of four neurons leaving the CNS via the AN (reference for the SE0 cluster) and whose cell bodies lie in the same area as the CDM motor neurons described here.
(AVI)

S2 File. Retrograde filling of the MN. The MN was filled with tetramethyrhodamine-dextran (Tmr-D) in larvae with the genotype OK371-Gal4/UAS-GCamP6s;+/+. All cells labelled bey Tmr-D colocalized with glutamatergic cells.
(AVI)

S3 File. Retrograde filling of the PaN. The MN was filled with tetramethyrhodamine-dextran (Tmr-D) in larvae with the genotype OK371-Gal4/UAS-GCamP6s;+/+. Two neurons colocalized with glutamatergic neurons. Two additionals neurons were labelled by Tmr-D. The additional cells likely correspond to the previously published hugin positive neurons leaving the CNS via the PaN.
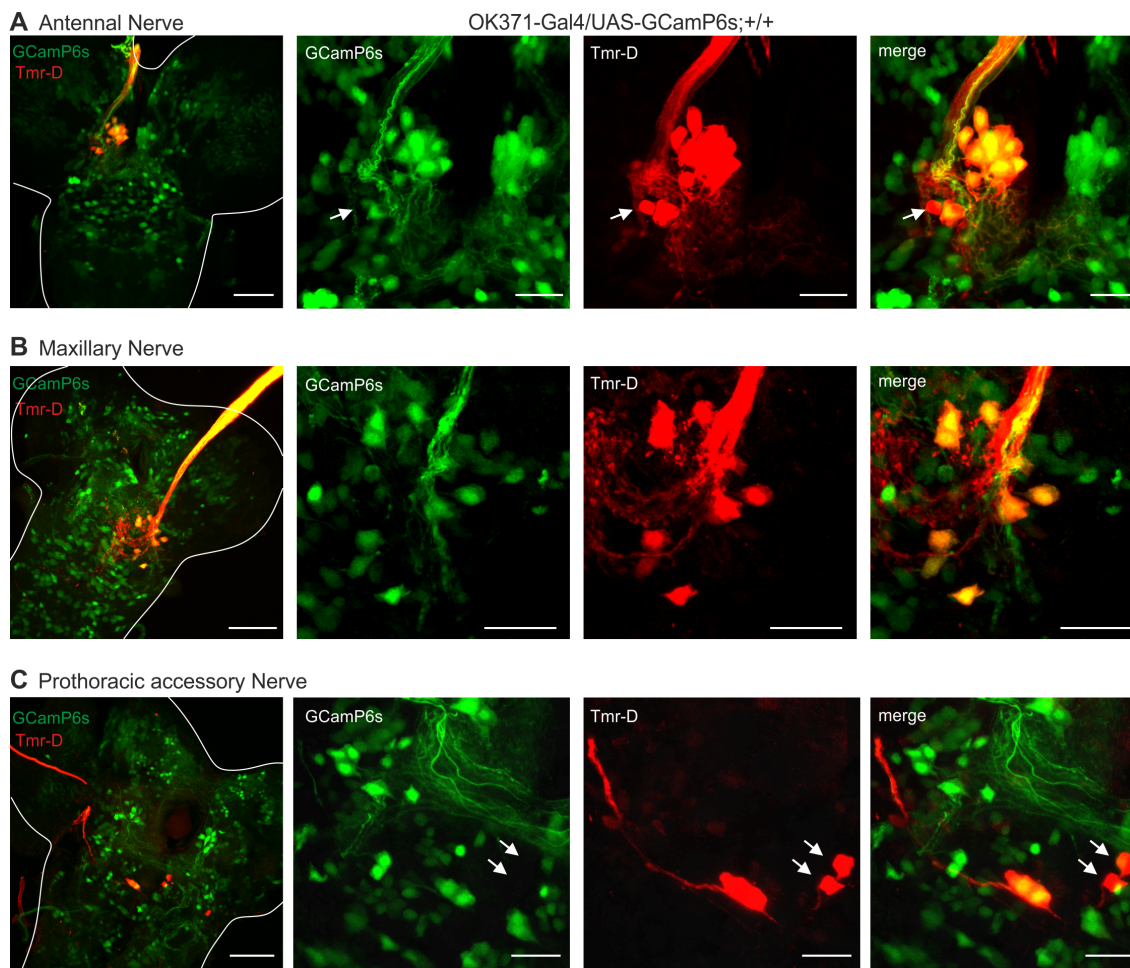(AVI)

Author Contributions

Conceived and designed the experiments: SH AS MJP. Performed the experiments: SH AS. Analyzed the data: SH AS PS. Contributed reagents/materials/analysis tools: SH AS PS AM. Wrote the paper: SH AS MJP.

References

1. Feldman JL, Smith JC (1989) Cellular mechanisms underlying modulation of breathing pattern in mammals. Ann New York Acad Sci 563: 114–130.

2. Delcomyn F (1980) Neural basis of rhythmic behavior in animals. Science 210: 492–498. PMID: 7423199

3. Grillner S (2006) Biological pattern generation: the cellular and computational logic of networks in motion. Neuron 52: 751–766. PMID: 17145498

4. Selverston AI (2010) Invertebrate central pattern generator circuits. Philos Trans R Soc Lond B Biol Sci 365: 2329–2345. doi: 10.1098/rstb.2009.0270 PMID: 20603355

5. Cohen AH (1987) Intersegmental coordinating system of the lamprey central pattern generator for locomotion. J Comp Physiol A 160: 181–193.

6. Grillner S; Wallen P; Brodin L; Lansner A (1991) Neuronal network generating locomotor behavior in lamprey: circuitry, transmitters, membrane properties, and simulation. Annu Rev Neurosci 14: 169–199. PMID: 1674412

7. Hinsey J, Ranson S, Dixon H (1930) Responses elicited by stimulation of the mesencephalic tegmentum in the cat. Arch Neurol Psychiatry 24(5): 966–977.

8. Grillner S, Zangger P (1979) On the central generation of locomotion in the low spinal cat. Exp Brain Res 34: 241–261. PMID: 421750

9. Baessler U, Bueschges A (1998) Pattern generation for stick insect walking movements—multisensory control of a locomotor program. Brain Res Rev 27: 65–88. PMID: 9639677

10. Marder E, Bucher D (2001) Central pattern generators and the control of rhythmic movements. Curr Biol 11: R986–R996. PMID: 11728329

11. Wilson DM (1961) The central nervous control of flight in a locust. J Exp Biol 38: 471–490.

12. Sokolowski MB (1982) *Drosophila* Larval Foraging Behavior: Digging. Anim Behav 30: 1252–1261.

13. Gorczyca MG, Budnik V, White K, Wu CF (1991) Dual muscarinic and nicotinic action on a motor programm in *Drosophila*. J Neurobiol 22: 391–404. PMID: 1679841

14. Zinke I, Kirchner C, Chao LC, Tetzlaff MT, Pankratz MJ (1999) Suppression of food intake and growth by amino acids in *Drosophila*: the role of pumpless, a fat body expressed gene with homology to vertebrate glycine cleavage system. Development 126: 5275–5284. PMID: 10556053

15. Wu Q, Wen T, Lee G, Park JH, Cai HN, Shen P (2003) Developmental control of foraging and social behavior by the *Drosophila* neuropeptide Y-like system. Neuron 39: 147–161. PMID: 12848939

16. Schoofs A, Niederegger S, Spiess R (2009) From behavior to fictive feeding: anatomy, innervation and activation pattern of pharyngeal muscles of *Calliphora vicina* 3rd instar larvae. J Insect Physiol 55: 218–230. doi: 10.1016/j.jinsphys.2008.11.011 PMID: 19100742

17. Schoofs A, Niederegger S, van Ooyen A, Heinzel H-G, Spiess R (2010) The brain can eat: establishing the existence of a central pattern generator for feeding in third instar larvae of *Drosophila virilis* and *Drosophila melanogaster*. J Insect Physiol 56: 695–705. doi: 10.1016/j.jinsphys.2009.12.008 PMID: 20074578

18. Olsen SR, Wilson RI (2008) Cracking neural ciruits in a tiny brain: new approach for understanding the neural circuits of *Drosophila*. Trends Neurosci 31: 512–520. doi: 10.1016/j.tins.2008.07.006 PMID: 18775572

19. Simpson JH (2009) Mapping and manipulating neural circuits in the fly brain. Adv Genet 65: 79–143. doi: 10.1016/S0065-2660(09)65003-3 PMID: 19615532

20. Schoofs A, Hückesfeld S, Schlegel P, Miroschnikow A, Peters M, Zeymer M, et al. (2014) Selection of motor programs for suppressing food intake and inducing locomotion in the *Drosophila* brain. PLoS Biol 12: e1001893. doi: 10.1371/journal.pbio.1001893 PMID: 24960360

21. Mahr A, Aberle H (2006) The expression pattern of the *Drosophila* vesicular glutamate transporter: a marker protein for motoneurons and glutamatergic centers in the brain. Gene Expr Patterns 6: 299–309. PMID: 16378756

22. Chen EH, Olson EN (2001) Antisocial, an intracellular adaptor protein, is required for myoblast fusion in *Drosophila*. Dev Cell 1: 705–715. PMID: 11709190
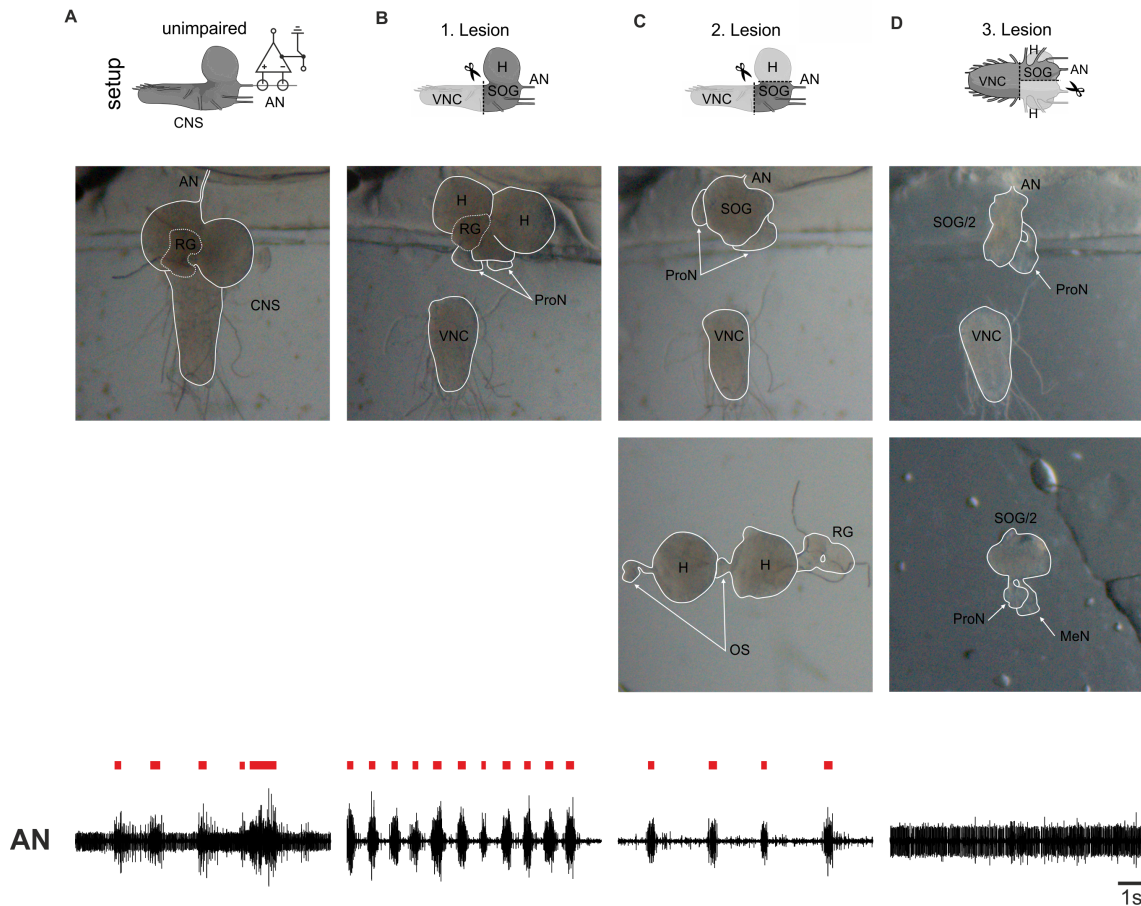
23. Datta SR, Vasconcelos ML, Ruta V, Luo S, Wong A, Demir E, et al. (2008) The *Drosophila* pheromone cVA activates a sexually dimorphic neural circuit. Nature 452: 473–477. doi: 10.1038/nature06808 PMID: 18305480

24. Ruta V, Datta SR, Vasconcelos ML, Freeland J, Looger LL, et al. (2010) A dimorphic pheromone circuit in *Drosophila* from sensory input to descending output. Nature 468: 686–690. doi: 10.1038/nature09554 PMID: 21124455

25. Tian L, Hires SA, Mao T, Huber D, Chiappe M, Chalasani SH, et al. (2009) Imaging neural activity in worms, flies and mice with improved GCaMP calcium indicators. Nat Methods 6 (12): 875–884. doi: 10.1038/nmeth.1398 PMID: 19898485

26. Chen T-W, Wardill TJ, Sun Y, Pulver SR, Renninger SL, Baohan A, et al. (2013) Ultrasensitive fluorescent proteins for imaging neuronal activity. Nature 499: 295–300. doi: 10.1038/nature12354 PMID: 23868258

27. Tissot M, Gendre N, Stocker RF (1998) *Drosophila* P[Gal4] lines reveal that motor neurons involved in feeding persist through metamorphosis. J Neurobiol 37: 237–250. PMID: 9805270

28. Schoofs A, Hückesfeld S, Surendran S, Pankratz MJ (2014) Serotonergic pathways in the *Drosophila* larval enteric nervous system. J Insect Physiol 69: 118–125. doi: 10.1016/j.jinsphys.2014.05.022 PMID: 24907674

29. Huser A, Rohwedder A, Apostolopoulou A A, Widmann A, Pfitzenmaier JE, Maiolo EM, et al. (2012) The serotonergic central nervous system of the *Drosophila* larva: anatomy and behavioral function. PLoS One 7: e47518. doi: 10.1371/journal.pone.0047518 PMID: 23082175

30. Spieß R, Schoofs A, Heinzel HG (2008) Anatomy of the stomatogastric nervous system associated with the foregut in *Drosophila melanogaster* and *Calliphora vicina* third instar larvae. J Morphol 269: 272–282. PMID: 17960761

31. Harris-Warrick R (1988) Chemical modulation of central pattern generators. In: Cohen A.H., Rossignol S., and Grillner S., eds. Neural Control of Rhythmic Movements. Cohen A, Rossigno S, Grillner S, editors New York: John Wiley & Sons. 285–331 p.

32. Marder E, Bucher D (2007) Understanding circuit dynamics using the stomatogastric nervous system of lobsters and crabs. Annu Rev Physiol 69: 291–316. PMID: 17009928

33. Benjamin PR, Rose RM (1979) Central generation of bursting in the feeding system of the snail, *Lymnaea stagnalis*. J Exp Biol 80: 93–118. PMID: 227979

34. Friesen WO (1989) Neuronal control of leech swimming movements. J Comp Physiol A 208: 205–215.

35. Brodfuehrer PD, Debski EA, O'Gara BA, Friesen WO (1995) Neuronal control of leech swimming. J Neurobiol 27: 403–418. PMID: 7673898

36. Hattox A, Li Y, Keller A (2003) Serotonin regulates rhythmic whisking. Neuron 39: 343–352. PMID: 12873389

37. Goulding M (2009) Circuits controlling vertebrate locomotion: moving in a new direction. Nat Rev Neurosci 10: 507–518. doi: 10.1038/nrn2608 PMID: 19543221

38. Berni J, Pulver SR, Griffith LC, Bate M (2012) Autonomous circuitry for substrate exploration in freely moving *Drosophila* larvae. Curr Biol 22: 1861–1870. doi: 10.1016/j.cub.2012.07.048 PMID: 22940472

39. Kitamoto T (2001) Conditional modification of behavior in *Drosophila* by targeted expression of a temperature-sensitive shibire allele in defined neurons. J Neurobiol 47: 81–92. PMID: 11291099

40. Lin H-H, Chu L-A, Fu T-F, Dickson BJ, Chiang A-S (2013) Parallel neural pathways mediate CO2 avoidance responses in *Drosophila*. Science (80-) 340: 1338–1341.

Supplemental information of Hückesfeld et al., PLOS ONE (2015)

S1 Fig. Anatomical identification of feeding related motor neurons using retrograde dye filling of pharyngeal nerves

Glutamatergic cells and dendrites were visualized using OK371-Gal4 driving UAS-GCaMP6s (GCaMP6s used for scanning due to very high signal quality in live scans). Each pharyngeal nerve was filled with tetramethylrhodamine-dextran (Tmr-D) for 3h, subsequently fixed in PFA and directly scanned. **A**, Retrograde filling of the antennal nerve (AN) revealed up to 14 neurons labelled by Tmr-D and up to 11 colocalized with OK371-Gal4 driving UAS-GCaMP6s. **B**, Retrograde filling of the maxillary nerve (MN) revealed 9 neurons labelled by Tmr-D and all colocalized with OK371-Gal4 driving UAS-GCaMP6s.**C**, Retrograde filling of the prothoracic accessory nerve (PaN) revealed 4 labelled neurons by Tmr-D, 2 neurons colocalized with OK371-Gal4 driving UAS-GCaMP6s. Scale bars: most left panels: 50µm, magnified regions: 20µm.

S2 Fig. Motor patterns of the antennal nerve (AN) and subsequent applied lesions during extracellular recording

Starting with the intact central nervous system (CNS, unimpaired), the antennal nerve (AN) motor pattern was recorded while successively lesioning the ventral nerve cord (VNC, 1. Lesion), brain hemispheres (H, 2. Lesion) and finally bisecting the subesophageal zone (SEZ) (3. Lesion). **A,** Single nerve recording of AN in unimpaired conditions. **B**, Removal of the VNC leads to acceleration of the AN motor pattern (recording trace). Imaginal discs of the prothoracic nerve (ProN) served as landmark for the lesion. **C**, Removal of the brain hemispheres (H) leads to slight deceleration of the AN motor rhythm. Optic stalks (OS) served as residual tissue for grabbing the hemispheres with forceps to ensure more precise lesion. **D,** Bisection of the residual SEZ leads to tonic activity in the AN motor pattern and abolishment of rhythmic activity of the motor neurons. Remaining imaginal discs of ProN and Mesothoracic nerve (MeN) served as landmarks for proper lesions.

Supplemental video files S1 File - S3 File can be found at:

http://www.ncbi.nlm.nih.gov/pmc/articles/PMC4529123/

2.3   Summary

Goal of this study was to identify the neuronal substrate in the CNS comprising the motor neurons and innervated muscle groups for execution of feeding relevant movements in *Drosophila* larvae. Three pharyngeal nerves were shown to innervate these muscle groups. The AN innervates the CDM, which upon rhythmic contractions leads to pharyngeal pumping and therefore food intake. The MN innervates the mouth hook muscles MHD and MHE. Its neural activity generates up- and down movements of the mouth hooks, which is necessary for shoveling food to the mouth opening and for facilitation of forward locomotion. The PaN innervates the dorsal protractor muscles A and B (Pro$_{do}$A/B), which realize the protraction of the cephalo-pharyngeal skeleton (CPS) and anterior segments into the substrate by their contraction [SCHOOFS ET AL., 2010]. Detailed innervation of these muscles by the respective nerves could be visualized by a muscle reporter line (MHC-tauGFP) and simultaneous expression of a red fluorescent protein (mRFP) in glutamatergic neurons (OK371>mRFP), including all motor neurons.

To identify the feeding relevant motor neurons two strategies were used: 1) PaGFP was expressed in the glutamatergic neurons to activate a small area of the AN, MN and PaN with a two-photon laser. The PaGFP signal was traced back into the CNS. Distinct clusters of glutamatergic neurons for each of the previously mentioned nerves were visualized. A tight cluster of eleven glutamatergic neurons in the anterior SEZ, which showed dense arborizations near the midline of the SEZ could be identified projecting through the AN. For the MN, a more loosely organized cluster of nine neurons could be identified and for the PaN two neurons could be identified. 2) The second approach to identify neurons projecting through these nerves was classical retrograde dye backfills with tetramethyl-rhodamine (Tmr-D). The diffusing dye could be visualized in the CNS and labeled all neurons projecting from the CNS through the three pharyngeal nerves. Two additional cells could be visualized in the AN, which probably correspond to previously published serotonergic neurons located in the same area in the CNS [SCHOOFS ET AL., 2014a]. No additional cells occurred in dye backfills of the MN. In addition to the glutamatergic neurons leaving the PaN, two neurons at the midline of the SEZ did not colocalize with glutamatergic cells. These likely correspond to previously identified Hugin positive neurons [BADER ET AL., 2007].

From previous studies it has been shown by electrophysiological methods that motor units of the three pharyngeal nerves are rhythmically active [SCHOOFS ET AL., 2010]. Here, the rhythmic activity of axons in the nerves was monitored using the calcium based indicator GCaMP3. Calcium imaging with GCaMP6s furthermore enabled the activity measurement of the glutamatergic AN cell cluster and its dendritic arborizations in the SEZ using GCaMP6s.The calcium activity of axons of all three nerves corresponded to the

electrophysiologically measured motor rhythms. It was concluded that fluorescence imaging is sufficient to monitor the fictive feeding rhythms generated by the three pharyngeal nerves. The calcium activity measurements of the AN cell cluster and the nerve axons represent a rhythmic blueprint for fictive feeding in the CNS.

Since the right and left AN were shown to fuse at the frontal nerve junction (FNJ) near the posterior end of the CPS to proceed in one single fiber, the frontal nerve (FN), the question was whether one side of the CDM is innervated by the ipsilateral AN or both. Classic lesions of the left or right AN could show that one AN innervates both sides of the CDM. This was undermined by dye filling of the left AN by Tmr-D and fluorescent labeling of one CDM motor neuron. Using the previously published *MT11* driver line, it was shown that a single CDM motor neuron not only innervates multiple muscles of the CDM on one side, but also innervates the CDM on the contralateral side, which may facilitate the effectiveness of synchronous pharyngeal pumping movements.

Manipulating the activity of glutamatergic neurons with thermogenetic (Shibire^{TS} or TrpA1) or optogenetic (ChR2 or eNpHR) neuronal effectors showed direct effects on feeding in intact and semi-intact larvae. Activation and inactivation of the glutamatergic motor neurons led to abolishment of food intake in intact larvae. This is caused by tonic excitation of the feeding relevant motor neurons upon constant activation (shown with ChR2) or complete suppression of neural activity in the motor neurons shown with Shibire^{TS} or halorhodopsin (eNpHR).

Since stereotyped movements, like pharyngeal pumping, are driven by a CPG, localization of this rhythm-generating network in the CNS was further analyzed. Lesion experiments demonstrated that the isolated SEZ is capable of producing a rhythmic motor output for pharyngeal pumping in the AN. Thus, it was possible to localize the CPG network for feeding to the SEZ.

Taken together we could identify a set of glutamatergic motor neurons in the SEZ of larvae, which drive feeding related movements like pharyngeal pumping, mouth hook movements and head tilting. Additionally we could proof that coordinated rhythmic activity arises from a CPG network located in the SEZ.

3   Serotonergic Pathways in the *Drosophila* Larval Enteric Nervous System

3.1   Introduction

Apart from the central control of feeding relevant muscles to coordinate food intake, the movements of esophagus and gut have to be controlled to ensure efficient nutrient digestion. This is realized by a part of the peripheral nervous system, the enteric nervous system (ENS). It connects the central nervous system with the esophagus and the gut. In mammals, information flow is bidirectionally through the vagus nerve from the CNS to the ENS (efferent) and vice versa (afferent). Sensory afferents from the gut enable the CNS to monitor gut content or quality for regulation of food intake, whereas efferent processes to the gut ensure modulation of gut motility. The innervation and modulation of the gut through the ENS has been shown to be conserved between vertebrates and invertebrates [COPENHAVER, 2007].

The anatomy and physiological function of the ENS in dipteran larvae was investigated in detail earlier [SCHOOFS & SPIEß, 2007]. The CNS is connected with the proventriculus and the foregut via the bilateral ANs to the frontal nerve junction (FNJ), the recurrent nerve (RN), the hypocerebral ganglion (HCG) and the proventricular nerve with associated proventricular ganglion (PVG). In *Drosophila* the frontal ganglion lacks neuronal cell bodies [SPIEß ET AL., 2008], which in other insect species were shown to be motor neurons controlling the muscular system of the foregut [AYALI, 2004; MILES & BOOKER, 1998] and neurons for modulating gut motility. In *Drosophila* these neurons seem to be located in the CNS [SPIEß ET AL., 2008] and were to be further analyzed in this study. Just recently the motor neurons for feeding related movements were identified to be located in the SEZ of *Drosophila* larvae [SEE CHAPTER 2].

In mammals it is known that the main portion of serotonin is synthesized in the gut (TPH1) and less from neuronal serotonergic cells (TPH2). In terms of gut motility it could be shown, that the enteric neuronal synthesized serotonin is important for the modulation of gut motility and that mucosal (gut derived) serotonin has no or little effect on gut motility [LI ET AL., 2011]. Among modulatory neurons of the ENS, serotonergic neurons have been implicated to play an important role in modulating gut motility in invertebrates [COOPER & HE, 1994; HERNÁDI ET AL., 1998; LUFFY & DORN, 1991].

In this study a functional role of the neurotransmitter serotonin in modulating gut movements in *Drosophila* larvae was to be investigated.

3.1.1 Statement of Contribution

Figure	experiment	author
1A-C	Immunohistochemical analysis of serotonergic projections in the larval CNS	Sebastian Hückesfeld
1D-F	Immunohistochemical analysis of serotonin expression in the SEZ area	Sandy Surendran
2A, C-G, I, J	Expression analysis of serotonergic projections in the enteric nervous system and schematics	Andreas Schoofs
2B	Overview of the serotonergic expression in the enteric nervous system	Sebastian Hückesfeld
2H	Expression analysis of serotonergic projections in the midgut	Sandya Surendran
3A, B	Extracellular double recordings from AN-RN and AN-NCS	Andreas Schoofs
3C	Extracellular double recordings from AN-PVN	Andreas Schoofs, Sebastian Hückesfeld
4A-D	Calcium imaging analysis of SEA axons	Sebastian Hückesfeld
5A-B	Behavioral video analysis of ENS structures	Andreas Schoofs
6	Comparative model of the ENS in human and *Drosophila*	Andreas Schoofs

3.2   Publication

Schoofs, A., Hückesfeld, S., Surendran, S., & Pankratz, M. J. (2014)

Serotonergic Pathways in the *Drosophila* Larval Enteric Nervous System

Journal of Insect Physiology, *69*, 118–125.

Contents lists available at ScienceDirect

Journal of Insect Physiology

journal homepage: www.elsevier.com/locate/jinsphys

Serotonergic pathways in the *Drosophila* larval enteric nervous system

Andreas Schoofs *, Sebastian Hückesfeld, Sandya Surendran, Michael J. Pankratz *

Department of Molecular Brain Physiology, LIMES Institute, University of Bonn, Carl Troll Str. 31, 53115 Bonn, Germany

ARTICLE INFO

ABSTRACT

The enteric nervous system is critical for coordinating diverse feeding-related behaviors and metabolism. We have characterized a cluster of four serotonergic neurons in *Drosophila* larval brain: cell bodies are located in the subesophageal ganglion (SOG) whose neuronal processes project into the enteric nervous system. Electrophysiological, calcium imaging and behavioral analyses indicate a functional role of these neurons in modulating foregut motility. We suggest that the axonal projections of this serotonergic cluster may be part of a brain–gut neural pathway that is functionally analogous to the vertebrate vagus nerve.

© 2014 The Authors. Published by Elsevier Ltd. This is an open access article under the CC BY-NC-SA license (http://creativecommons.org/licenses/by-nc-sa/3.0/).

1. Introduction

Feeding requires coordination of different parts of the body. In many invertebrates and vertebrates, a distinct part of the peripheral nervous system, the enteric nervous system (ENS), exists to regulate specific phases of feeding (Gershon, 2008; Penzlin, 1985; Selverston and Moulins, 1987). In insects, the nerves comprising the ENS were shown to interconnect the central nervous system (CNS), neuroendocrine organs and foregut structures (Kirby et al., 1984; Willey, 1961). Physiologically the ENS has been shown to be important for a wide range of feeding and metabolic related processes (Penzlin, 1985). What has been generally lacking in these studies, however, is the cellular resolution and the projection patterns of identified neurons that comprise the ENS.

Genetic tools available in *Drosophila melanogaster* provide an opportunity to complement and extend the analysis of the ENS at a cellular and axonal level. Genetic approaches have already been used in the analysis of ENS and foregut development during embryogenesis (Gonzalez-Gaitan and Jäckle, 1995; Pankratz and Hoch, 1995). Subsequently, the basic neuroanatomy of the ENS in association with the foregut structures have been characterized in the Diptera larva (Spieß et al., 2008). The *Drosophila* larval ENS shows similar overall structure as other insects. The ENS is connected to the CNS through the antennal nerve (AN). The bilateral AN fuses with the frontal nerve junction via the frontal connectives, which bifurcates into the anteriorly projecting frontal nerve (FN) and the posteriorly projecting recurrent nerve (or nervus

recurrens, RN). The FN innervates the pharyngeal muscles, whereas the RN innervates the esophagus. The RN is connected to the proventricular nerve (PVN) by the hypocerebral ganglion (HCG), from which a separate nerve (NCS: nervi cardiostomatogastrici) branches out to innervate the ring gland (RG). One notable difference between *Drosophila* larval ENS and most other insect studied is that *Drosophila* larva lack a frontal ganglion (FG). Instead, it is replaced by a nerve junction devoid of neurons, and the motor neurons that are located in FG in most insects are presumably found in the brain (Spieß et al., 2008). The most posterior component of the ENS is the proventricular ganglion (PVG), which innervates the proventriculus (PV), a valve-like organ which gates the passage of food from the esophagus to the midgut.

Here we identify a cluster of four serotonergic cells that innervates all the major target organs of the ENS, including the pharynx, esophagus, proventriculus and the ring gland. Their cell bodies are located in the brain and send their axons through all the nerves of the ENS. Calcium imaging and electrophysiological studies suggest their role in regulating gut movement.

2. Materials and methods

2.1. Flies

The following Gal4 driver and UAS effector lines were used: TRH-Gal4 (Alekseyenko et al., 2010), UAS-dTrpA1 (Bloomington #26263), UAS-eYFP (Bloomington #6659), UAS-H134R-ChR2-mCherry (Bloomington #28995), UAS-GCaMP3 attp2 (Bloomington #32236) and UAS-10X-mCD8-GFP (Bloomington #32184). In control experiments OregonR (wildtype) was used. For ChR2 experiments a stable homozygous line of TRH-Gal4 and UAS-H134R-ChR2-mCherry was generated.

* Corresponding authors. Tel.: +49 (0)228 73 62755; fax: +49 (0)228 73 62641 (A. Schoofs). Tel.: +49 (0)228 73 62740; fax: +49 (0)228 73 62641 (M.J. Pankratz).
E-mail addresses: schoofs@uni-bonn.de (A. Schoofs), pankratz@uni-bonn.de (M.J. Pankratz).

Adult flies and larvae were reared on standard fly-food and kept at 25 °C. 4 h egg collections were made on apple juice-agar plates with yeast-water paste. After 48 h, hatched larvae were transferred into vials containing standard fly food. For ChR2 experiments, 48 h old larvae were transferred into vials with standard fly-food containing 100 μM all-trans retinal (ATR). Vials with retinal were darkened with aluminum foil to protect the retinal from degradation. After additional 48 h, larvae were used for experiments.

All experiments were performed with third instar larvae 98 ± 2 h AEL (after egg laying).

2.2. Immunohistochemistry

Dissected larval brains of third instar larvae were fixed in paraformaldehyde (4%). For the antibody staining of TRH > 10X-mCD8-GFP, a FITC conjugated goat anti-GFP antibody (1:500, Abcam plc) was used. The simultaneous antibody staining of serotonin, primary antibody was rabbit anti-5'HT (1:1000, Sigma–Aldrich) and secondary antibody was anti-rabbit Alexa568 (1:200, Invitrogen).

For immunofluorescence staining of serotonin and elav, we used third instar larvae of OregonR (wildtype). The primary antibodies were rabbit anti-5'HT (1:1000, Sigma–Aldrich) and rat anti-elav (1:500, DSHB). Secondary antibody was anti-rabbit Alexa488 (1:200, Invitrogen) and anti-rat Alexa568 (1:200, Invitrogen). Nuclei were counter stained with DAPI. Labeled larval brains were mounted in Moviol. Imaging was carried out using Laser Scanning Microscope (ZEISS LSM780). The obtained images were arranged using Zen LE and Corel DrawX5 (for detailed staining procedures see (Bader et al., 2007)).

2.3. Fluorescence microscopy

All images were obtained by using a confocal microscope Zeiss LSM 780. Images were acquired using Zen 2011 (Zeiss).

2.4. Calcium imaging

For calcium imaging the genotype: TRH > GCaMP3 was used. Neural activity of neurons in the CNS was studied in isolated CNS of third instar larvae. Calcium imaging was performed with a Laser Scanning Microscope (ZEISS LSM780) using a ZEISS LCI "Plan-Neofluar" 25×/0.8 Imm Korr DIC M27 objective dipped into the saline solution. For excitation an argon laser with a wavelength of 488 nm was used. Images were acquired using Zen 2011 (Zeiss). Data was analyzed using custom made script for Fiji (ImageJ).

2.5. Electrophysiology

For the electrophysiological experiments, a reduced semi-intact preparations were made of TRH-Gal4/TRH-Gal4; UAS-H134R-ChR2-mCherry/UAS-H134R-ChR2-mCherry larva consisting of the CNS, cephalopharyngeal skeleton (CPS), antennal nerve and the enteric nervous system with the innervation targets (ring gland and proventriculus). Detailed description of the dissection has been described earlier (Schoofs et al., 2010). All dissections and
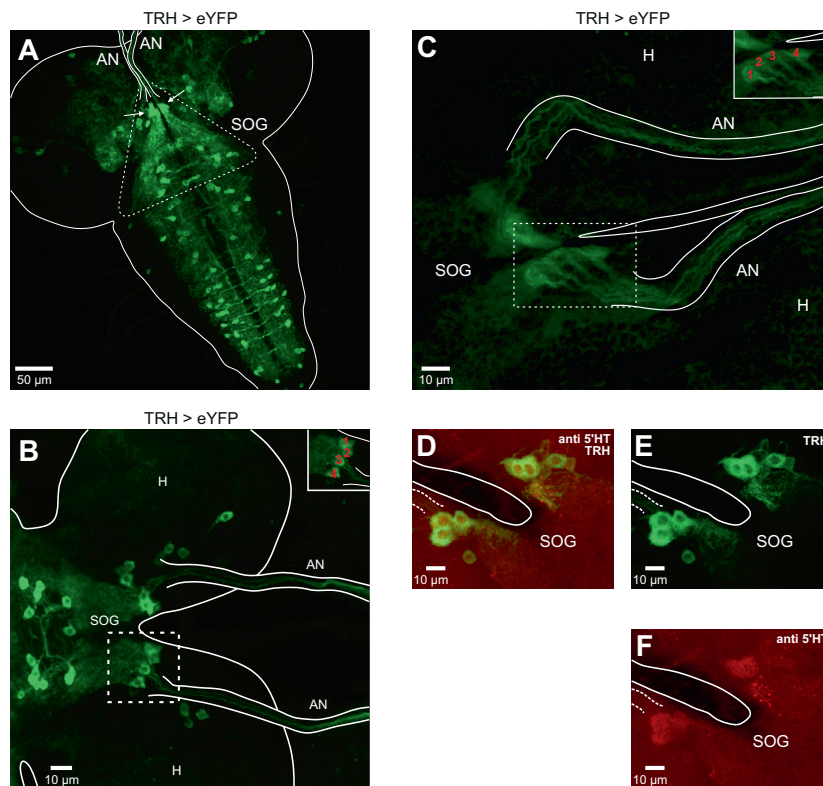
Fig. 1. Four serotonergic neurons projecting through antennal nerve. (A) Overview of larval CNS (third instar) showing the expression pattern TRH > eYFP, SOG marked by dashed lines, arrows indicate the serotonergic cell cluster, (B and C) images of the larval subesophageal ganglion (TRH > eYFP) revealing a cluster four cells whose axons project through the antennal nerve; inlaid image shows the four cells by red numbers in the SOG region marked by dashed box, (D–F) 5'HT antibody staining of TRH > eYFP: fluorescence expression driven by TRH-Gal4 (E), cells (3–4) and arborizations labeled by 5'HT antibody (F), merge of E and F (D). *Abbr.:* AN, antennal nerve; H, brain hemispheres; SOG, subesophageal ganglion.

experiments were performed in saline solution composed of (in mM): 140 NaCl, 3 KCl, 2 CaCl$_2$, 4 MgCl$_2$, 10 sucrose and 5 HEPES (Rohrbough and Broadie, 2002). Neural activity was measured by *en passant* extracellular recording of the respective nerves with a preamplifier connected to a four channel amplifier/signal conditioner (Model MA 102/103; Ansgar Büschges group electronics lab, University of Cologne). For *en passant* extracellular recording, the nerve was insulated with a surrounding petroleum jelly border on a piece of Parafilm. Recording electrodes were made of silver wire (diameter: 25–125 μm, Goodfellow). All recorded signals were amplified (amplification factor: 5000) and filtered (bandpass: 0.1–3 kHz). The recordings were sampled at 20 kHz. Data was acquired with Micro3 1401 or Power 1401 mk2 A/D board (Cambridge Electronic Design) and Spike2 software (Cambridge Electronic Design). Analysis of the double recordings was performed with the Spike2 analysis tools.
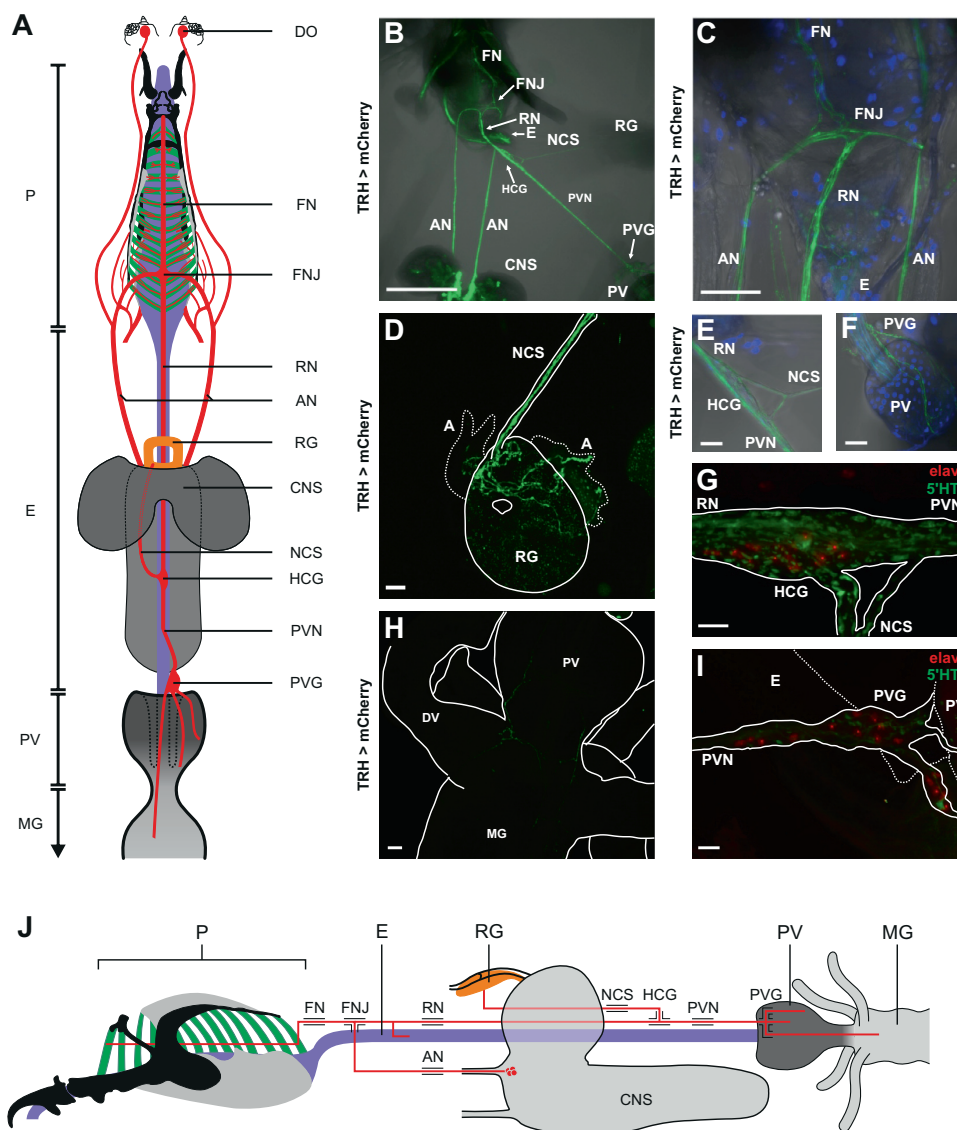
Fig. 2. Serotonergic projection of the enteric nervous system. (A) Schematic drawing of the larval enteric nervous system and associated foregut and midgut structures, (B) overview of a dissected third instar larva showing the fluorescence expression driven by TRH-Gal4 in the enteric nervous system, (C) magnification of the posterior portion of the pharynx and anterior part of esophagus; note that axons of the antennal nerve cross the frontal nerve junction and project to frontal nerve and recurrent nerve, (D) innervation of the ring gland via nervus cardio stomatogastricus; note the projections on the ring gland and aorta, (E) focus on hypocerebral ganglion; the projections pass the hypocerebral ganglion to proventricular nerve and nervus cardio stomatogastricus, (F) focus on the proventricular ganglion; note the arborization on the proventriculus which extend into the midgut (H), (G) double antibody staining of elav and 5′HT indicating neurons in the hypocerebral ganglion (14–15 somata, n = 3) and a 5′HT positive neural plexus, (I) double antibody staining of elav and 5′HT revealing neurons in the proventricular ganglion (9–13 somata, n = 3) and 5′HT positive projections onto the proventriculus, (J) schematic drawing 5′HT positive somata which send out projections through the enteric nervous system and larval endocrine organ. *Abbr.:* AN, antennal nerve; A, aorta; CNS, central nervous system; DO, dorsal organ; E, esophagus; FN, frontal nerve; FNJ, frontal nerve junction; HCG, hypocerebral ganglion; MG, midgut; NCS, nervi cardiostomatogastrici; P, pharynx; PV, proventriculus; PVG, proventricular ganglion; PVN, proventricular nerve; RG, ring gland; RN, recurrent nerve (Scale bars: B – 200 μm; F, H – 50 μm; D, E – 20 μm G, I – 10 μm).

For the light stimulation during extracellular recordings, a mounted ultrabright blue LED with collimated lens and heatsink with a wavelength of 470 nm (M470L2, Thorlabs) was used for all ChR2-experiments. LED was regulated via the A/D board which was connected to voltage-controlled LED power supply (LEDD1B, Thorlabs). LED was mounted on a custom built LED holder. Optical multimode fiber (AFS200/220Y, Thorlabs) was placed into the LED holder in front of the LED. Distal end of the optical fiber was then placed directly over the ventral side of CNS. Timing of the stimulus was given through stimulus protocols in Spike2 software. All stimuli were applied with the highest intensity (1 mA). Optical fiber had a length of approx. 90 cm with a transmission efficiency of >99.8%/m. All experiments with ChR2 were done in dark conditions.

2.6. Behavioral experiments

Movements of the esophagus, proventriculus and midgut were studied in semi-intact larvae. The preparation consisted of the CNS and associated enteric nervous system, CPS, foregut and midgut. Thermal stimulation was applied directly to the CNS of TRH > dTrpA1 and OrgeonR (control) crossed to UAS-dTrpA1 or TRH-Gal4.

For the temperature stimulation, a custom-made stimulator consisted of a silver wire (diameter: 4 mm) which was attached to a Peltier element by thermally conductive adhesive. Peltier element was driven by a voltage-regulated power supply (VSP 2405, Voltcraft) connected to an A/D board. End of the thermal stimulator was filed to a tip and insulated with nail polish. Applied temperature was measured by digital thermometer (GMH 3210, Greisinger electronic). Sensor for the thermometer was placed 5 mm from the tip of the thermal stimulator. Before the experiments the thermal stimulator was calibrated to ensure constant thermal stimuli to the CNS. Temperature signals were acquired with the A/D board. Thermal stimulator was regulated by a script-based feedback loop via the A/D-board.

Consecutive videos of 5 min at 18 °C and 5 min at 32 °C were recorded using a digital camera (Quickcam 9000 Pro, Logitech) mounted on a binocular (Stemi 2000-CS, Zeiss). Movements of esophagus, proventriculus and midgut were counted at 18 °C and 32 °C. The measurements were performed using the software ImageJ (Fiji). All behavioral experiments were tested for significance with the Mann–Whitney-Rank-Sum-test ($^*p \leqslant 0.05$, $^{**}p \leqslant 0.01$, $^{***}p \leqslant 0.001$).

3. Results and discussion

3.1. Four central serotonergic neurons innervate the entire enteric nervous system

During our analysis on the role of the central neurons in regulating *Drosophila* larval feeding behavior (Schoofs et al., 2014; accepted for publication), we noticed that a small cluster of serotonergic cells located in the subesophageal ganglion (SOG) sent their axons out to the periphery through the AN (Fig. 1). This was visualized by using TRH-Gal4 line to drive expression of eYFP ($n = 10$, Fig. 1A–C). The soma of these four serotonergic cells are located near the point where AN extends out from the CNS (Fig. 1B and C). Staining with antibodies to serotonin revealed three to four labeled cells ($n = 3$, Fig. 1D–F).

The projections from these cells extend throughout the ENS (Fig. 2A and B). They project anteriorly to the pharyngeal muscles as part of the FN, as well as posteriorly along the esophagus as part of the RN (Fig. 2C). Branching of the projections at the HCG can also be seen (Fig. 2E), as well as its innervation of the ring gland via the NCS (Fig. 2D) and proventriculus via the PVN (Fig. 2F). The
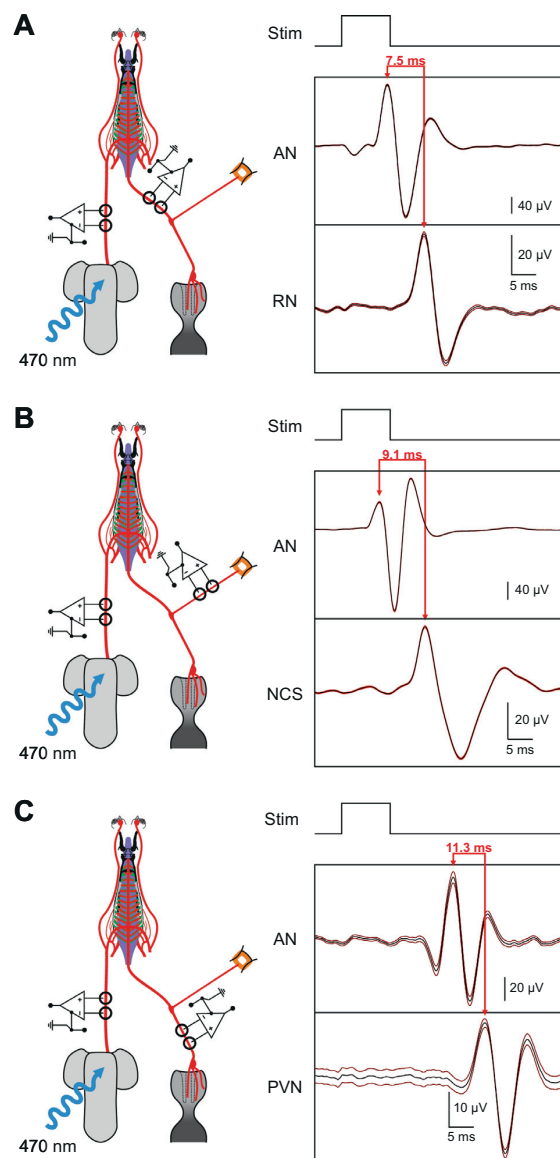
Fig. 3. Double recordings of larva expressing ChR2 driven by TRH-Gal4. (A) Double recording of the antennal nerve and recurrent nerve (experimental setup left panel), waveform average of the spikes evoked by a 10 ms light stimuli of 470 nm wavelength in the antennal nerve and recurrent nerve (right panel) which showed a temporal correlation (mean delay: 7.5 ms ± 0.8 (Std.Dev.), $n = 141$; 4 experiments), (B) double recording of the antennal nerve and nervi cardiostomatogastrici (experimental setup left), waveform average of the spikes evoked by a 10 ms light stimuli of 470 nm wavelength in the antennal nerve and nervi cardiostomatogastrici (right panel) which showed a temporal correlation (mean delay: 9.1 ms ± 0.8 (Std.Dev.), $n = 316$; 7 experiments), (C) double recording of the antennal nerve and proventricular nerve (experimental setup left), waveform average of the spikes evoked by a 10 ms light stimuli of 470 nm wavelength in the antennal nerve and proventricular nerve (right panel) which indicated a temporal correlation (mean delay: 11.3 ms ± 2.2 (Std.Dev.), $n = 171$; 4 experiments). *Abbr.:* AN, antennal nerve; NCS, nervi cardiostomatagastrici; PVN, proventricular nerve; RN, recurrent nerve.

projection ends at the anterior region of the midgut (Fig. 2H). We could not detect any serotonergic positive cell bodies within HCG or PVG (Fig. 2G and I; based on stainings with antibody to serotonin and additionally elav, which labels post-mitotic neurons, we counted approximately 14–15 cells in the HCG, and 9–13 cells in the PVG; $n = 3$ in both cases). These results indicated that the
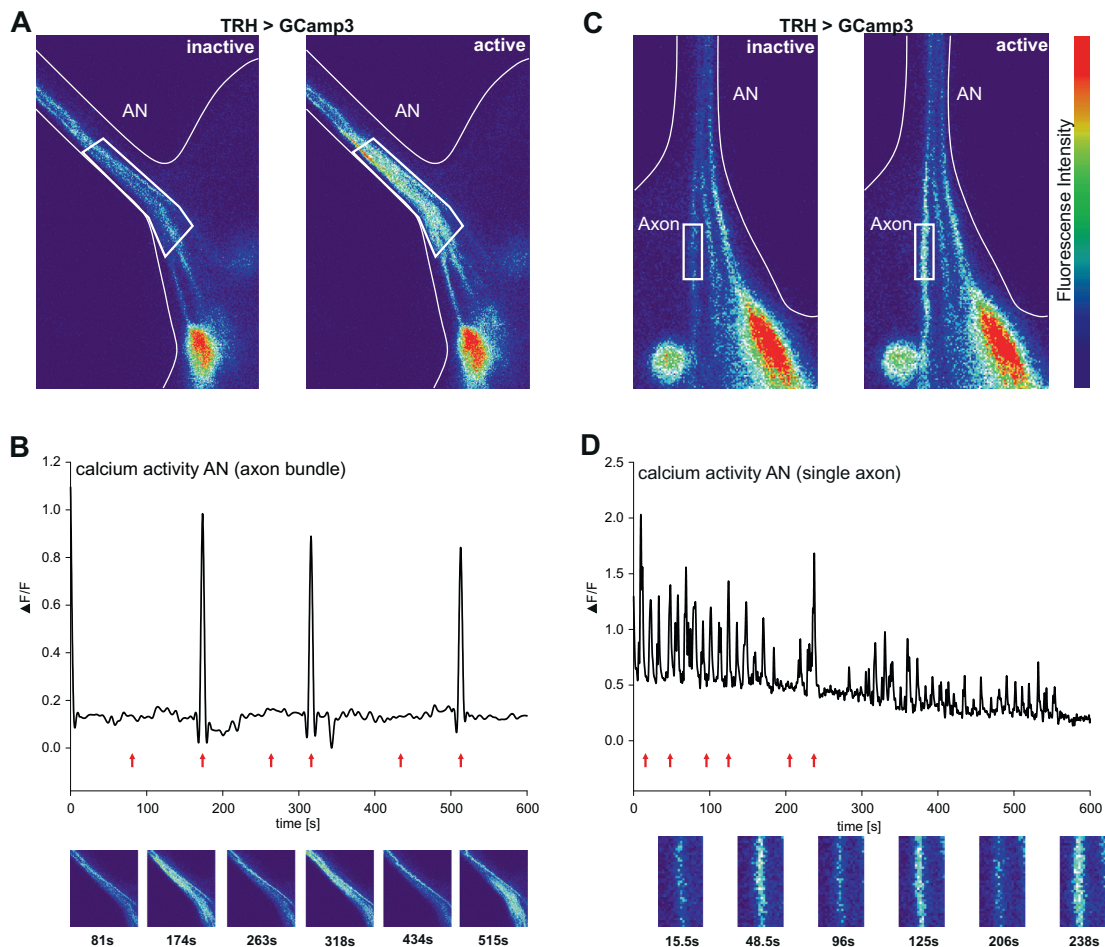
Fig. 4. GCamp analysis of TRH positive projections leaving the CNS via the antennal nerve. (A, C) Thermal color representation of calcium activity in projections of TRH positive neurons leaving the CNS via the AN in inactive (left) and active (right) state. Region of interest is marked as rectangular field. The activity of the whole axon bundle is shown in (A). The activity of a single axon is shown in (C). (B, D) Fluorescence change plotted as delta *F/F* in a 600 s time period. Red arrows mark the time points seen in the pictures below. Analysis of the axon bundle is shown in (B), whereas the analysis of a single axon is shown in (D). *Abbr.:* AN, antennal nerve. (For interpretation of the references to color in this figure legend, the reader is referred to the web version of this article.)

serotonergic projections within the entire ENS derive from the cluster of four cells located in the brain. (See Fig. 2J for scheme).

3.2. Electrophysiological analysis of serotonergic pathways in the ENS

Based on the anatomical analysis, we next investigated whether the different branches of the serotonergic projections from the CNS were functionally connected. The experimental strategy was to activate the central serotonergic neurons and perform double extracellular recordings from the different branches. Therefore, we performed double recordings of AN and RN (Fig. 3A), AN and NCS (Fig. 3B) and AN and PVN (Fig. 3C). For technical reasons, we could not record from the frontal nerve. Neuronal activation was achieved with light after expressing Channelrhodopsin (ChR) in the serotonergic cells (Nagel et al., 2003; Pulver et al., 2009; Schroll et al., 2006). We could detect a neuronal unit in the recordings for all cases (Fig. 3). The unit could be temporally correlated with the onset of the light stimulus, supporting the view that the serotonergic axons of the AN are functionally connected to those of RN, NCS and PVN (Fig. 3).

3.3. Calcium imaging of serotonergic AN axons

We then wanted to monitor the activity of these neurons using the genetically encoded calcium indicator, GCaMP3 (Tian et al., 2009). Therefore, we expressed GCaMP3 in serotonergic cells and recorded from the axons of the AN (Fig. 4). To quantify the recordings, we measured the $\Delta F/F$-peak frequency. Due to the low temporal resolution of the GCaMP3, a detected peak can reflect one action potential or up to series of action potentials. Two types of activity patterns were observed, a slower acting (Fig. 4A and B) and a faster acting (Fig. 4C and D). However, these patterns were not observed in the majority of the larvae. Only 16 out of 34 GCaMP3-recordings exhibited activity patterns. The slow acting pattern showed $\Delta F/F$-peak frequency range of 0.003–0.028 Hz (occurred in 24% of the total recordings), whereas the fast acting pattern had a $\Delta F/F$-peak frequency range of 0.04–0.15 Hz (detected in 18% of the total recordings). As the recordings are performed over a maximum time span of about 10 min, the low frequency may reflect a slower acting signal that modulates post-ingestive movements.
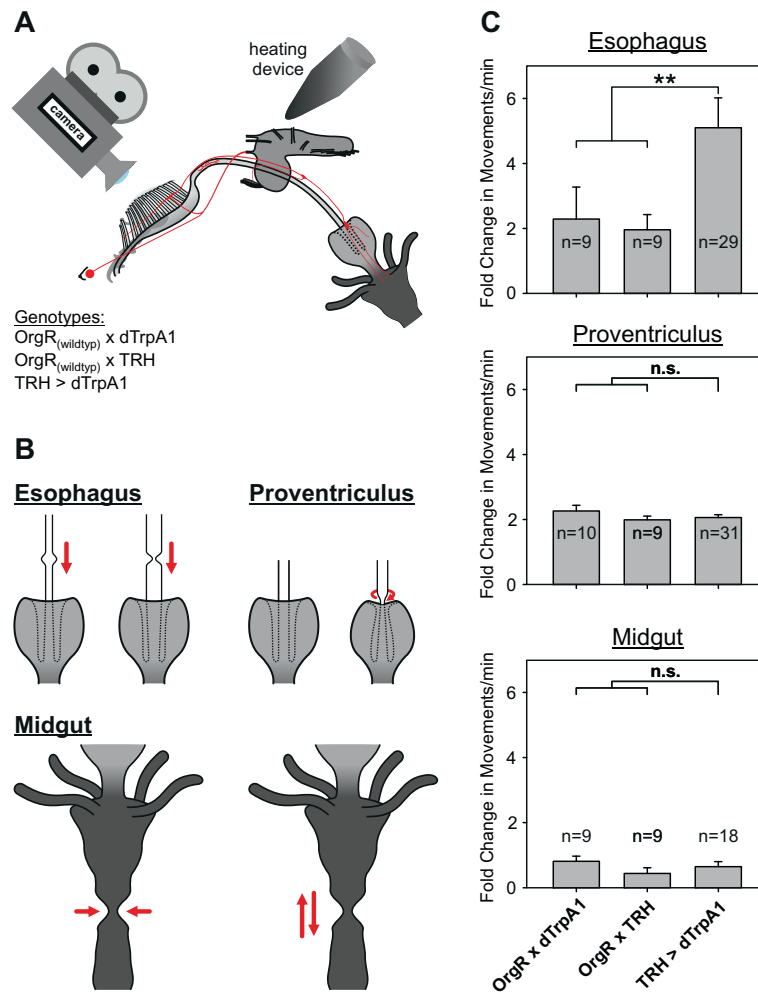
Fig. 5. Activation of central serotonergic neurons affects esophagus and proventriculus movements. (A) Experimental setup: semi-intact larvae of OregonR crossed with TRH/dTrpA1 and TRH > dTrpA1 with exposed foregut and midgut were video-recorded to monitor the movements of the esophagus, proventriculus and midgut at 18 °C and 32 °C, note temperature stimulus was applied to CNS, (B) esophagus showed local extension and local contraction propagating from anterior to posterior; proventriculus showed ring-like contraction restricted to the anterior part; midgut showed local squeezing and bidirectional peristaltic waves. (C) Bar graph represents the fold change in movements/min between 18 °C and 32 °C for OregonR crossed with TRH/dTrpA1 and TRH > dTrpA1, result exhibit a significant increase of the esophagus movements during TrpA-induced activation of central serotonergic neurons, but not of the proventriculus and midgut.

3.4. Central serotonergic regulation of esophagus movements

To determine if serotonergic neurons in the CNS, in particular the four cell cluster projecting within the ENS, modulated post-ingestive movements associated with passage of food through the esophagus and the proventriculus, we activated these central serotonergic neurons and monitored the movements of three different gut structures: esophagus, proventriculus and midgut.

For this, we used the temperature dependent dTrpA1 activation (Pulver et al., 2009) of serotonergic neurons (Fig. 5A). Via the Gal4-UAS system we directed the expression of dTrpA1 to the central serotonergic system. This temperature- and voltage-gated channel induces a cation influx at a restrictive temperature of above 27 °C, which can be used to remotely activate specific neuronal circuits. In our experiments we measured the fold change in foregut and midgut movements per min between 18 °C (inactivated dTrpA1 state) and 32 °C (activated dTrpA1 state).

The esophagus showed two types of peristaltic waves which propagate from anterior to posterior: (1) a circular, local relaxation traveling over the contracted esophagus and (2) a local contraction propagating over the relaxed esophagus. For the proventriculus, we observed a ring-like contraction at the anterior portion of the proventriculus. The study of the midgut revealed three types of movements: local contraction ("squeezing") and peristaltic waves from posterior to anterior/anterior to posterior (Fig. 5B). The control strains OrgR crossed to TRH-Gal4 and dTrpA1 showed an increase in esophagus and proventriculus movements whereas the midgut was not affected. Normally in *Drosophila*, dTrpA1 is expressed in subset of neurons involved in regulating thermotaxis (Hamada et al., 2008) which presumably caused this endogenous temperature effect on the foregut structures.

In the motility study of the foregut, we detected a significant increase in movements of the esophagus but no difference was seen for the proventriculus. Additionally, we investigated the midgut upon activation of central serotonergic neurons; no significant effect on midgut motility was observed (Fig. 5C).

Taken together, our anatomical and physiological analyses suggest that a four-cell cluster of serotonergic cells in the brain

Human: **Drosophila:**

Fig. 6. Innervation pattern of the human vagus nerve and *Drosophila* antennal nerve. Schematic showing the innervation pattern of the vagus nerve in humans and of the antennal nerve in *Drosophila* larva.
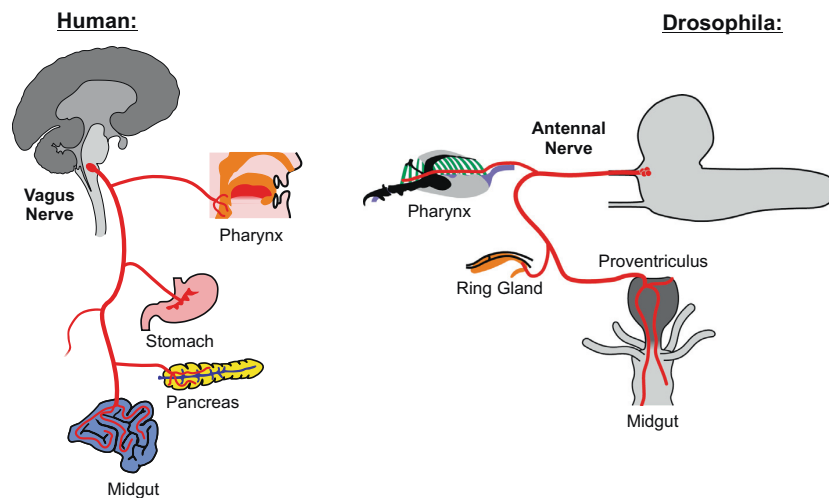
innervates the entire ENS and may be involved in coordinating motor and endocrine activities of the foregut.

3.5. Brain–gut neural pathways

Our results indicate that the four-serotonergic neurons play a special role by acting as a conduit through which the brain communicates with the gut. At this point, we cannot exclude the possibility that other serotonergic neurons within the CNS participate in the modulation of post-ingestive movements. The uniqueness of these cells can be seen in the context of the different serotonergic neurons that have been analyzed in previous studies (Huser et al., 2012; Neckameyer, 2010; Vallés and White, 1988): of all the serotonergic neurons in the brain, this cluster is the only one that leaves the CNS and extends into the gut. Furthermore, we consistently observed only two of the four axons showing rhythmic activity in the calcium imaging studies, suggesting that there may be further functional subdivision within this cluster (we have termed these neurons as SEA neurons, for serotonergic-antennal; some of these may correspond to the SE0 neurons of Huser et al., 2012). Based on the innervation of the ring gland by the SEA neurons, a possible function is in regulating hormonal release in response to nutrient or digestive cues. These neurons may also be analogous to the "SNS neurons" (satellite nervous neurons) in the locust (Schachtner and Bräunig, 1993), which are serotonergic neurons in the SOG that project out into the periphery.

In vertebrates, there is a major nerve that also connects the brain to the gut, namely the vagus nerve (Travagli et al., 2006). The vagus nerve projects from the brainstem to innervate the pharynx, the stomach and the midgut. It also innervates the pancreas. In *Drosophila*, the nerves that extend from the brain to the periphery have different names (AN, FN, RN, NCS and PVN); however, the projections of the SEA cluster of serotonergic neurons illustrate that there is a direct projection from the brain to the different foregut structures. Thus, the projections of the AN to the gut may be functionally analogous to the vagus nerve of vertebrates (Fig. 6).

Acknowledgments

References

Alekseyenko, O.V., Lee, C., Kravitz, E.A., 2010. Targeted manipulation of serotonergic neurotransmission affects the escalation of aggression in adult male *Drosophila melanogaster*. PLoS One 5, e10806.

Bader, R., Colomb, J., Pankratz, B., Schröck, A., Stocker, R.F., Pankratz, M.J., 2007. Genetic dissection of neural circuit anatomy underlying feeding behavior in *Drosophila*: distinct classes of hugin-expressing neurons. J. Comp. Neurol. 856, 848–856.

Gershon, M.D., 2008. Functional Anatomy of the Enteric Nervous System. In: Holschneider, A.M., Puri, Prem (Eds.), Hirschsprung's Disease and Allied Disorders. Springer Berlin Heidelberg, pp. 21–49. http://dx.doi.org/10.1007/978-3-540-33935-9_3.

Gonzalez-Gaitan, M., Jäckle, H., 1995. Invagination centers within the *Drosophila* stomatogastric nervous system anlage are positioned by Notch-mediated signaling which is spatially controlled through wingless. Development 121, 2313–2325.

Hamada, F.N., Rosenzweig, M., Kang, K., Pulver, S.R., Ghezzi, A., Jegla, T.J., Garrity, P.A., 2008. An internal thermal sensor controlling temperature preference in *Drosophila*. Nature 454, 217–222.

Huser, A., Rohwedder, A., Apostolopoulou, A., Widmann, A., Pfitzenmaier, J.E., Maiolo, E.M., Selcho, M., Pauls, D., von Essen, A., Gupta, T., Sprecher, S.G., Birman, S., Riemensperger, T., Stocker, R.F., Thum, A.S., 2012. The serotonergic central nervous system of the *Drosophila* larva: anatomy and behavioral function. PLoS One 7, e47518.

Kirby, P., Beck, R., Clarke, K.U., 1984. The stomatogastric nervous system of the house cricket *Acheta domesticus* L. I. The anatomy of the system and the innervation of the gut. J. Morphol. 180, 81–103.

Nagel, G., Szellas, T., Huhn, W., Kateriya, S., Adeishvili, N., Berthold, P., Ollig, D., Hegemann, P., Bamberg, E., 2003. Channelrhodopsin-2, a directly light-gated cation-selective membrane channel. Proc. Natl. Acad. Sci. USA 100, 13940–13945.

Neckameyer, W.S., 2010. A trophic role for serotonin in the development of a simple feeding circuit. Dev. Neurosci. 32, 217–237.

Pankratz, M.J., Hoch, M., 1995. Control of epithelial morphogenesis by cell signaling and integrin molecules in the *Drosophila* foregut. Development 121, 1885–1898.

Penzlin, H., 1985. Stomatogastric nervous system. In: Kerkut, G.A., Gilbert, L.I. (Eds.), Compr. Insect Physiol. Biochem. Pharmacol., vol. 5, Oxford, UK: Pergamon, pp. 371–406.

Pulver, S.R., Pashkovski, S.L., Hornstein, N.J., Garrity, P.A., Griffith, L.C., 2009. Temporal dynamics of neuronal activation by channelrhodopsin-2 and TRPA1 determine behavioral output in *Drosophila* larvae. J. Neurophysiol. 101, 3075–3088.

Rohrbough, J., Broadie, K., 2002. Electrophysiological analysis of synaptic transmission in central neurons of *Drosophila* larvae. J. Neurophysiol. 88, 847–860.

Schachtner, J., Bräunig, P., 1993. The activity pattern of identified neurosecretory cells during feeding behaviour in the locust. J. Exp. Biol. 185, 287–303.

Schoofs, A., Niederegger, S., van Ooyen, A., Heinzel, H.-G., Spieß, R., 2010. The brain can eat: establishing the existence of a central pattern generator for feeding in third instar larvae of *Drosophila virilis* and *Drosophila melanogaster*. J. Insect Physiol. 56, 695–705.

Schoofs, A., Hückesfeld, S., Schlegel, P., Miroschnikow, A., Peters, M., Zeymer, M., Spieß, R., Chiang, A.S., Pankratz, M.J., 2014. Selection of motor programs for suppressing food intake and inducing locomotion in the *Drosophila* brain. PLoS Biol. (Accepted for publication).

Schroll, C., Riemensperger, T., Bucher, D., Ehmer, J., Völler, T., Erbguth, K., Gerber, B., Hendel, T., Nagel, G., Buchner, E., Fiala, A., 2006. Light-induced activation of distinct modulatory neurons triggers appetitive or aversive learning in *Drosophila* larvae. Curr. Biol. 16, 1741–1747.

Selverston, A.I., Moulins, M., 1987. The Crustacean Stomatogastric System. Springer-Verlag, Berlin Heidelberg.

Spieß, R., Schoofs, A., Heinzel, H.G., 2008. Anatomy of the stomatogastric nervous system associated with the foregut in *Drosophila melanogaster* and *Calliphora vicina* third instar larvae. J. Morphol. 269, 272–282.

Tian, L., Hires, S.A., Mao, T., Huber, D., Chiappe, M., Chalasani, S.H., Petreanu, L., Akerboom, J., McKinney, S.A., Schreiter, E.R., Bargmann, C.I., Jayaraman, V., Svoboda, K., Looger, L.L., 2009. Imaging neural activity in worms, flies and mice with improved GCaMP calcium indicators. Nat. Methods 6 (12), 875–884.

Travagli, R.A., Hermann, G.E., Browning, K.N., Rogers, R.C., 2006. Brainstem circuits regulating gastric function. Annu. Rev. Physiol. 68, 279–305.

Vallés, A., White, K., 1988. Serotonin containing neurons in *Drosophila melanogaster*: development and distribution. J. Comp. Neurol. 268, 414–428.

Willey, R.B., 1961. The morphology of the stomodeal nervous system in *Periplaneta americana* (L.) and other *Blattaria*. J. Morphol. 108, 219–261.

3.3   Summary

The ENS is part of the peripheral nervous system and regulates the motility of the digestive tract. In mammals, the ENS is comprised by the vagus nerve that connects the brain with organs like esophagus, stomach, gut and spleen. The vagus nerve has been implicated to act like a second brain, since it serves as main information route from the CNS to the stomach and gut and transmits internal metabolic signals from gut and stomach to the NTS in the CNS [TRAVAGLI ET AL., 2006]. The ENS has analogous function throughout animal kingdom [GERSHON, 2008; PENZLIN, 1985; SELVERSTON & MOULINS, 1987]. In insects, the ENS consists of neural projections leaving the CNS fusing into the frontal ganglion projecting via the HCG down to the PVG, which in turn innervates the proventriculus and the gut. The frontal ganglion in insects is known to harbor motor neurons for feeding and modulatory neurons that affect gut motility and thereby modulate digestive functions [MILES & BOOKER, 1994, 1998].

In *Drosophila,* the frontal ganglion harbors no neurons according to [SPIEß ET AL., 2008]. In this study we identified a distinct set of four serotonergic neurons in the SEZ using a driver line for serotonergic neurons (TRH-Gal4) together with immunohistochemical staining of serotonin. These neurons leave the CNS via the AN and project through the FNJ to the frontal nerve (FN), HCG and the PVG to innervate all major targets of the ENS, namely the pharynx, esophagus, proventriculus, midgut and ring gland. Serotonergic innervation of the proventriculus and midgut implies a modulatory role for serotonin in the digestive system. This is in line with findings of a previous study describing serotonergic fibers innervating the proventriculus and midgut [NECKAMEYER & BHATT, 2012]. Serotonergic cell bodies were not detected in the HCG or PVG, indicating that the projections on proventriculus and midgut are derived from the serotonergic SEZ neurons, termed SEA neurons (serotonergic antennal neurons). Using an optogentic approach to activate serotonergic neurons in the CNS with Channelrhodopsin it was possible to interprete action potential propagation with extracellular double nerve recordings in different parts of the ENS (AN, RN, NCS and PVN). Optogenetically activated SEA neurons showed time correlation of measured action potentials in all nerve branches of the ENS. The activity of the SEA neurons was further examined using the calcium indicator GCaMP3, which was expressed in serotonergic neurons of the CNS. This analysis revealed that two kinds of activity pattern exist within the described four-cell cluster, a fast and a slow acting calcium activity.

To determine whether neural serotonergic neurons are associated with fore- and midgut function a behavioral experiment was conducted. Fore- and midgut structures (esophagus,

proventriculus and midgut) were video taped in semi intact larvae, when serotonergic neurons in the CNS were artificially activated using the temperature sensitive cation channel dTrpA1. Whereas proventriculus and midgut movement were not altered upon activation of serotonergic neurons, the esophagus showed a significant increase in movement frequency. This demonstrated that central serotonergic neurons are capable of modulating foregut movements in *Drosophila* larvae. Due to this findings together with the described analysis of serotonergic projections, it was postulated that the AN and the vagus nerve are functional analogs.

4 Selection of Motor Programs for Suppressing Food Intake and Inducing Locomotion in the *Drosophila* Brain

4.1 Introduction

Rhythmic behaviors, like feeding, have long been the basis for neuroscientists to investigate the neuronal principles of brain circuits. Oscillatory networks of neurons, which are responsible for these rhythmically executed behaviors are central pattern generators (CPGs). By definition a CPG is a oscillatory neural circuit that is able to produce the fictive behavior in the absence of intrinsic and extrinsic cues, which can be observed in semi intact preparations of isolated nervous tissues [MARDER & BUCHER, 2001]. This has been shown in the case of the decerebrated cat in vertebrate locomotion [GRILLNER & ZANGGER, 1979] or feeding regulation in the STG of invertebrate models [SELVERSTON, 2010].

Over the past 40 years, studies on feeding related CPGs underlying rhythmic movements have provided valuable insights on how modulation of these circuits affects the fictive behavior. Neurotransmitters, e.g. serotonin, and peptides, e.g. FMRFamide are capable of modulating feeding CPG`s in the crustacean stomatogastric ganglion (STG) [MARDER, 2012] and in buccal feeding circuits of snails, like *Lymnea* [STRAUB & BENJAMIN, 2001] or *Helisoma* [MURPHY, 2001]. These studies mainly relied on pharmacological experiments and therefore could only study the general actions of modulators without cellular precision in the CNS.

Drosophila is a continuous feeder in the larval stage. It serves as the ideal model organism to investigate modulation of feeding rhythm by the CNS. Recently, the existence of a CPG for feeding was verified using electrophysiological tools [SCHOOFS ET AL., 2010]. We identified motor neurons, which are responsible for these fictive feeding motor patterns [SEE CHAPTER 2: HÜCKESFELD ET AL., 2015 and SCHOOFS ET AL., 2010]. The identification of neuropeptide and neurotransmitter encoding genes in *Drosophila* and *C. elegans* (nematode) in conjunction with the establishment of genetic tools to cell type specific manipulate their expression levels via the Gal4/UAS system, led to the facilitating knowledge of modulatory neurons that affect behavior [BARGMANN, 2012].

A role for modulatory actions on food intake of adult and larval stages of *Drosophila* was shown for various neuropeptides over the past years. Thus, peptides like Allatostatin A (AstA) [HERGARDEN ET AL., 2012], LK [AL-ANZI ET AL., 2010], DSK [SÖDERBERG ET AL., 2012] and Hugin-derived peptides [MELCHER & PANKRATZ, 2005] have been implicated to play a

role as inhibitory neuromodulators of feeding behavior and foraging. In contrast sNPF (Lee et al., 2004), CRZ [HERGARDEN ET AL., 2012] and NPF [WU ET AL., 2003] have been shown to promote feeding. Controversial roles for biogenic amines have been investigated, with Dopamine (DA) being able to inhibit foraging or promote meal initiation in adult flies [POOL & SCOTT, 2014b]. The role of peptides and transmitters in feeding was primarily assessed with behavioral paradigms leading to general modulation of feeding, for example whether the animals ate more or less than control animals.

Goal of this study was the identification of neuropeptides and neurotransmitters involved in the modulation of certain feeding motor subprograms in *Drosophila* larvae. A combination of electrophysiological measurements and behavioral paradigms was used, in order to monitor feeding motor programs and behavior. Emphasis should lie on the neurotransmitter serotonin and the neuropeptide Hugin, which was implicated earlier to be involved in feeding regulation [MELCHER & PANKRATZ, 2005].

4.1.1 Statement of Contribution

Figure	Experiment	Author
1A-C	AN, MN and PaN recordings of larvae in which certain neurotransmitters or peptides were artificially activated	Andreas Schoofs Sebastian Hückesfeld Philipp Schlegel
2A	Food intake assays with larvae in which certain neurotransmitters or peptides were artificially activated	Philipp Schlegel
2B	Video monitoring of CDM contractions	Philipp Schlegel Andreas Schoofs
3A-D	Analysis of feeding behavior in larvae with activated Hugin neurons in the CNS	Anton Miroschnikow Sebastian Hückesfeld
4A-H	Intracellular double recordings of the CDM and M6 muscles	Anton Miroschnikow Andreas Schoofs
5A, C	Efficiency test of *hugin* RNAi and analysis of food intake in larvae with knocked down *hugin* in the CNS	Sebastian Hückesfeld
5B	Electrophysiological recordings of the AN and M6 in larvae with activated Hugin neurons and knocked down *hugin*	Andreas Schoofs Sebastian Hückesfeld Anton Miroschnikow
6A-C'	Expression pattern analysis in Hug0.8-Gal4 line and Hugin antibody staining	Marc Peters
6D-F'	Expression pattern analysis in HugVNC-Gal4 line and Hugin antibody staining	Anton Miroschnikow
6G	Schematic of *hugin* promotor constructs	Sebastian Hückesfeld
6H, I	Behavior analysis of larvae using different *hugin* promoter lines	Anton Miroschnikow Sebastian Hückesfeld

Figure	Experiment	Author
7A-C	AN recordings in larvae with genotypes Hug0.8>dTrpA1 and HugVNC>dTrpA1, control	Sebastian Hückesfeld Andreas Schoofs
7D-I	Intracellular recordings of M6 and CDM in larvae with genotypes HugS3>dTrpA1, Hug0.8>dTrpA1, HugVNC>dTrpA1 and control	Anton Miroschnikow Andreas Schoofs
8A-C	Classical CNS lesion experiments while activating Hugin neurons in HugS3>dTrpA1 larvae	Andreas Schoofs
9A, B	Model for the selection of motor programs	Andreas Schoofs Sebastian Hückesfeld Philipp Schlegel
S1	Calibration curve of the thermo stimulator	Anton Miroschnikow
S2	Expanded food intake screen of neurotransmitter and peptides	Philipp Schlegel Malou Zeymer
S3A-C'	Expression pattern analysis in HugS3-Gal4 line and Hugin antibody staining	Marc Peters
S4	AN recordings of larvae expressing tubGal80ts;NaChBac in Hugin neurons and control	Andreas Schoofs
S5A, C	Intracellular recordings of CDM and M6 in larvae where Hugin neural activity is silenced (UAS-shi^{TS})	Andreas Schoofs
S5B	Extracellular recordings of the AN in larvae where Hugin neurons are ablated with UAS-rpr;;hid or their function is blocked with UAS-Kir2.1	Andreas Schoofs Sebastian Hückesfeld
S6	Analysis of feeding behavior in larvae expressing UAS-shi^{TS} in Hugin neurons upon different feeding conditions	Sebastian Hückesfeld
S7	Efficiency test on *hugin* RNAi lines (UAS-HugRNAi and TRiP.JF03122) using Hugin antibody staining	Sebastian Hückesfeld
S8	Hugin antibody staining in Hug0.8>rpr;;hid larvae	Marc Peters
S9	Intracellular recordings of M6 in larvae with the genotypes HugS3>dTrpA1 and TRH>dTrpA1, control	Andreas Schoofs Anton Miroschnikow
S9	Recordings of AN in larvae with genotypes HugS3>dTrpA1 and TRH>dTrpA1, control	Andreas Schoofs Sebastian Hückesfeld

The authors Roland Spieß and Ann-Shyn Chiang contributed reagents and comments to the manuscript.

4.2   Publication

Schoofs, A., Hückesfeld, S., Schlegel, P., … Pankratz, M. J. (2014)

Selection of Motor Programs for Suppressing Food Intake and Inducing Locomotion in the *Drosophila* Brain

PLoS Biology, *12*(6), e1001893.

Selection of Motor Programs for Suppressing Food Intake and Inducing Locomotion in the *Drosophila* Brain

Andreas Schoofs[1], **Sebastian Hückesfeld**[1], **Philipp Schlegel**[1], **Anton Miroschnikow**[1], **Marc Peters**[1], **Malou Zeymer**[1], **Roland Spieβ**[2], **Ann-Shyn Chiang**[3], **Michael J. Pankratz**[1]*

1 Molecular Brain Physiology and Behavior, LIMES-Institute, University of Bonn, Germany, **2** Department of Forensic Entomology, Institute of Legal Medicine, Jena University Hospital, Germany, **3** Brain Research Center, National Tsing Hua University, Taiwan

Abstract

Central mechanisms by which specific motor programs are selected to achieve meaningful behaviors are not well understood. Using electrophysiological recordings from pharyngeal nerves upon central activation of neurotransmitter-expressing cells, we show that distinct neuronal ensembles can regulate different feeding motor programs. In behavioral and electrophysiological experiments, activation of 20 neurons in the brain expressing the neuropeptide hugin, a homolog of mammalian neuromedin U, simultaneously suppressed the motor program for food intake while inducing the motor program for locomotion. Decreasing hugin neuropeptide levels in the neurons by RNAi prevented this action. Reducing the level of hugin neuronal activity alone did not have any effect on feeding or locomotion motor programs. Furthermore, use of promoter-specific constructs that labeled subsets of hugin neurons demonstrated that initiation of locomotion can be separated from modulation of its motor pattern. These results provide insights into a neural mechanism of how opposing motor programs can be selected in order to coordinate feeding and locomotive behaviors.

Introduction

The recruitment of appropriate motor programs to changing environmental conditions is an essential aspect of animal behavior [1]. The nervous system of invertebrates and vertebrates includes a broad variety of motor programs with neuronal circuits having the intrinsic property to generate rhythmic motor output, termed central pattern generators (CPGs). These motor programs underlie the spatial and temporal activation of specific muscle groups that characterize movements like chewing, swallowing, walking, breathing, and locomotion [2,3]. The mechanisms by which a specific motor program is selected from a repertoire of potential motor programs are not well understood.

In vertebrates, the motor system for locomotion has been extensively studied with various methods including pharmacological, electrophysiological, and more recently genetic tools [4–9]. Isolated spinal cord preparations have been used to demonstrate the existence of locomotive CPGs in the mammalian spinal cord [10,11]. The neural networks comprising the motor programs and the motor neurons for the single limbs are located in the spinal cord, and the motor network of a limb can be divided into motor subprograms and sets of motor neurons for each joint of a limb. These spinal–cortical networks are activated via reticulospinal neurons by command centers in the mesencephalon and diencephalon, which in turn are controlled by neuronal structures in basal ganglia [1,12]. Neurotransmitters such as serotonin, for example, have been shown to be necessary to induce motor patterns in isolated brainstem–spinal preparations [13,14]. Specific neurotransmitter-expressing cells that are involved in regulating the speed of locomotion have also been identified by genetic tools in lamprey, zebrafish, and mouse [15–19]. Currently, little is known about the cellular circuits in the brainstem or descending cortical pathways which regulate the locomotion CPGs in the spinal cord [20].

In addition to the highly conserved locomotor motor behaviors, those related to feeding are critical for growth and survival. These encompass movements involving the whole body for searching and getting access to food sources, local parts of the body for actual food intake, as well as organ-specific movements for post-ingestive phases of feeding. In invertebrates, the rhythmic nature of swallowing and food transport has been utilized as a model to study the structure of CPGs that generate oscillating motor patterns [3,21], as well as providing insights into the physiological parameters that drive feeding behavior [22–25]. This has also been the case in mammalian systems, where the discovery of leptin provided a major nucleation point for analyzing how peripheral signals influence central circuits that regulate food intake behavior and energy homeostasis [26,27]. Simpler genetic systems such as

80   4 Schoofs A., Hückesfeld S. et al. Plos Biology (2014)

Selection of Motor Programs in *Drosophila*

Author Summary

In the animal kingdom, two of the most essential behaviors are locomotion and feeding. The motor programs underlying these behaviors are controlled by higher-order circuits in the central nervous system. However, how an organism selects a particular motor program based on inputs from the information-processing higher brain centers to generate an adaptable behavior is not well understood. Here, we analyze the behavior of *Drosophila* larvae after activating a small cluster of neurons in the brain and show that the animals simultaneously stop eating and start moving. These neurons express the neuropeptide hugin, which is homologous to the mammalian neuromedins. We show that the reduction of food intake depends on hugin and that the cluster of hugin neurons is functionally divided into distinct subgroups that both accelerate the motor program for locomotion and decelerate the motor program for feeding. We propose that hugin neurons represent a control system between the higher brain circuits that process information and those that execute motor programs.

Drosophila and *Caenorhabditis elegans* are increasingly being used to study the genes and neural circuits that control feeding and feeding-related processes. These studies include the identification of the first gene involved in food search behavior [28], metabolic genes that influence feeding, as well as numerous neuropeptide- and neurotransmitter-encoding genes, to name a few [29–32].

Studies in *Drosophila* have, to date, focused mostly on analyzing feeding behavior in response to chemosensory or metabolic cues [33–39].These studies have used sophisticated genetic tools to manipulate specific neuronal populations in the brain [40,41], but what has lagged behind is a high resolution readout of such manipulations on motor programs. Most have used behavioral paradigms as readout assays, for example extension of the proboscis towards a food source, measurement of food ingested, the direction a fly takes in two-choice food assays. Although providing valuable information, these approaches determine the summation of many motor programs, and it is difficult to deconstruct the distinct motor programs that produce the observed behavioral output. In addition, most of the feeding behavior assays are performed in response to sensory stimuli, and it is not possible to distinguish which step in the sensorimotor pathway is primarily being affected. Thus, it is not surprising that, in comparison with chemosensory circuits [42–44], much less is known about the motor circuits that underlie feeding behavior.

Recently, an electrophysiological approach was used in semi-intact preparations to monitor the rhythmic motor patterns that comprise the *Drosophila* larval feeding cycle [45]. These analyses led to the identification of three motor patterns derived from three distinct nerves that innervate the feeding apparatus and which together comprise larval feeding behavior: motor output of antennal nerve (AN) results in pharyngeal pumping, motor output of maxillary nerve (MN) drives mouth hook movements, and that of prothoracic accessory nerve (PaN) causes head tilting movements [45]. In addition to providing higher resolution dissection of feeding motor patterns, this approach also overcomes an important issue relevant for studying motor circuits in general: it eliminates external inputs provided by a wide variety of sensory organs, as well as by internal peripheral tissues that can affect feeding responses, such as the gut, fat body, or the oenocytes [46–48]. The approach provides an opportunity to combine molecular genetics with electrophysiology in order to study how the central nervous system (CNS) selects and executes motor programs.

In this study, we used behavioral, genetic, imaging, and electrophysiological approaches to study central mechanisms that modulate feeding-related behaviors. We first identified neurotransmitter and neuropeptide clusters that modulate subsets of motor programs for feeding. This revealed that a small neuronal cluster can oppositely regulate feeding and locomotive motor programs. The cells of this cluster express the gene *hugin*, which encodes a neuropeptide homolog to mammalian neuromedin U and which was previously proposed as being involved in food intake and food search behaviors [23,49]. Increased neuromedin U signaling in mammals has been shown to suppress feeding and increase locomotion [50,51]. We show here that activation of hugin neurons suppresses the motor program for feeding and simultaneously initiates the motor program for locomotion. Our results provide a model for how selection of coordinately regulated motor programs can be brought about through activation of a single cluster of neurons in the brain.

Results

Electrophysiological Analysis of Central Neurons that Alter Feeding Motor Patterns

We previously characterized the major muscles and the nerves driving the movements that underlie feeding behavior [45,47]: AN, MN, and the PaN (see also Figure 1A). Our next goal in characterizing the feeding motor system was to identify central components of the motor hierarchy that could modulate the motor pattern recorded from the three pharyngeal nerves. The strategy was to activate specific neurotransmitter- and neuropeptide-expressing neurons in an inducible manner, and assay their effect on motor programs of feeding-related behavior (Figure 1). Directing the expression of the temperature-sensitive cation channel dTrpA1 [52] via the Gal4-UAS system enabled us to characterize the effect of activating distinct neuronal populations in a temporally controlled manner (Figure S1). We initially prescreened 11 lines, representing major neurotransmitter and selected neuropeptide lines, by a food intake assay (Figure S2); those that showed significant effect on food intake were taken for electrophysiological as well as additional feeding analysis. Five lines selected for this study were those labeling glutamatergic (Glu), cholinergic (ACh), serotonergic (5-HT), dopaminergic (DA), and hugin (Hug) neurons. The effect of temperature-induced activation of neuronal populations on the motor patterns was then monitored with single extracellular recordings of the three pharyngeal nerves (AN, MN, and the PaN) to distinguish neuronal populations that would affect the feeding motor pattern either globally or as just a subset (Figure 1). We then compared the changes in cycle frequency, which is a crucial feature of rhythmic behavior: classical studies on crustacean stomatogastric nervous systems revealed that all known modulatory inputs affect the cycle frequency of pyloric motor rhythm by altering the endogenous properties of at least one component of the CPG [3].

Neuronal activation of the Glu population resulted in a reversible state of tonic excitation in the motor patterns of all three pharyngeal nerves (Figure 1B). This was expected since the Gal-4 driver line (OK371) drives target gene expression in nearly all Glu neurons of the CNS that comprise the motor neurons [53]. Activating the ACh neurons showed a significant increase in cycle frequency of all motor patterns; in some instances the pattern approached the tonic excitation seen for Glu neurons. Activation of 5-HT neurons also caused an increase in cycle frequency; the effect on the 5-HT neurons stood out because of the remarkable
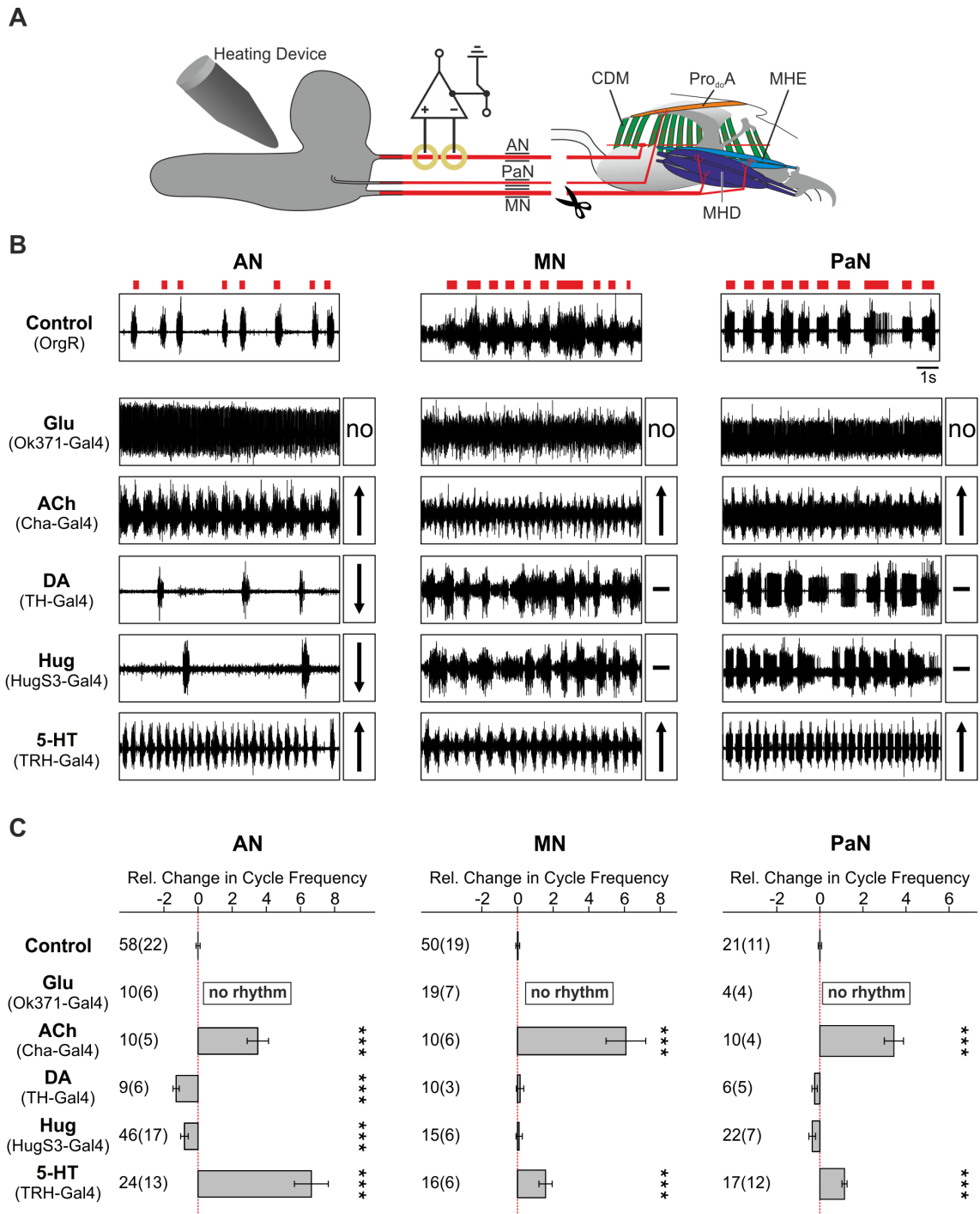
Figure 1. Identification of neuronal networks modulating motor patterns using Gal4-directed thermo-sensitive UAS-dTrpA1 expression. (A) Experimental setup for AN, MN, and PaN recordings at the deafferented CNS; dTrpA1 was activated by a Peltier-driven heating device. (B) Single extracellular recordings of AN, MN, and PaN revealed differential alteration of feeding-related motor patterns by dTrpA1 activation. Red blocks on top of the control recordings denote motor output. For the experimental recordings, an up arrow ($\uparrow$) indicates significant acceleration of motor pattern, down arrow ($\downarrow$) indicates significant deceleration of motor pattern and a dash (–) indicates no significant difference in the motor pattern (exception: Glu (Ok371-Gal4 showed no rhythmic motor pattern by dTrpA1 activation [no]). (C) Statistical data from AN, MN, and PaN motor patterns quantified as relative change in cycle frequency (mean $\pm$ standard error). Significance was tested by Mann-Whitney Rank Sum Test (***$p \leq 0.001$). 5-HT, serotonin; ACh, acetylcholine; DA, dopamine; Glu, glutamate; Hug, hugin neuropeptide; MHD, mouth hook depressor; MHE, mouth hook elevator; Pro$_{do}$A, dorsal protractor A.

doi:10.1371/journal.pbio.1001893.g001

regularity of the accelerated motor pattern in all three pharyngeal nerves. By contrast, activation of DA and Hug neurons decreased rhythm frequency. Moreover, these showed differential effect on the feeding motor patterns: only the AN motor pattern was affected, and not the MN or the PaN. (Figure 1B). These results indicated that certain neuronal classes affected all, whereas others affected only a subset, of the feeding motor programs.

Food intake studies further confirmed the roles of these neurones in feeding behavior. A short-term yeast intake assay was used in order to minimize longer-acting peripheral influence on the feeding response (Figure 2A). Four neuronal populations significantly decreased yeast intake: Glu, ACh, DA, and Hug neurons. Only one increased yeast intake: 5-HT (Figure 2A). Contraction of the cibarial dilator muscles (CDM), which is due to the AN motor program, is the movement most dedicated to food intake per se as compared to those driven by MN or PaN motor programs. Contractions of CDM presumably generate a negative pressure, resulting in ingestion of liquidized food: 'pharyngeal pumping'. Thus, we also performed video-based monitoring of the CDM contractions in semi-intact larvae to see how this particular movement could be correlated with the electrophysiology and food intake data (CDM tracking, Figure 2B). There is indeed a good correlation between the CDM contraction pattern and the AN recordings, which may explain the food intake results. For Glu, the tonic-like excitation resulted in convulsive contractions of the CDM, leading to essentially no food intake. For ACh, the CDM relaxed incompletely between successive contractions, causing less effective pharyngeal pumping, which likely accounts for the decreased food intake despite increased pumping rate. For DA and Hug, the frequency of the contraction was reduced (Figure 2B); the effect was more drastic for Hug, as seen by the strength of each contraction. The decreased food intake in both cases is as expected. For 5-HT, there was a rapid increase in the rate of CDM contractions, consistent with the increase in AN recording cycle frequency and food intake.

The combined electrophysiological and behavioral analyses opened up several avenues to pursue, as all the lines revealed interesting features relating to selection and modulation of motor patterns. For example, the unique finding that the serotonergic line, when activated, was the only one of 11 lines tested which resulted in increased food intake. The dopaminergic and hugin lines were interesting since they affected only a subset of the motor
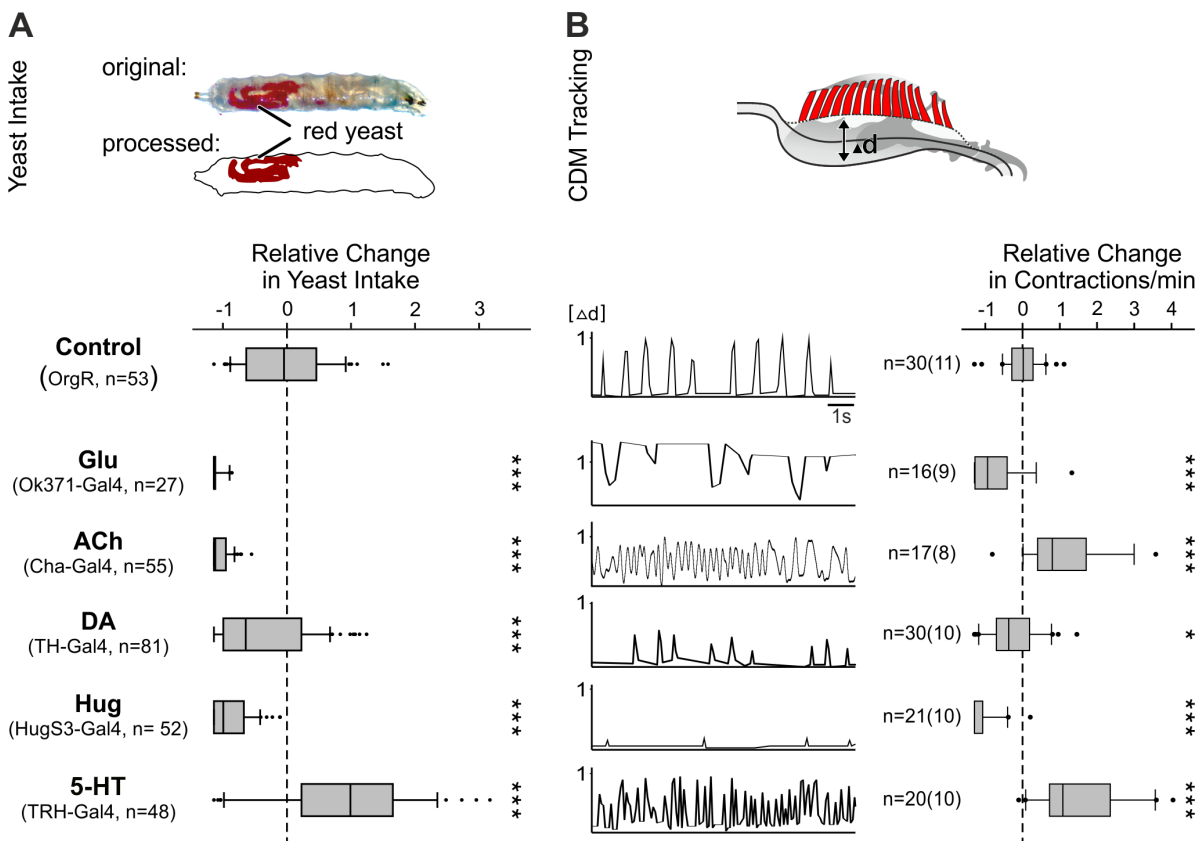
Figure 2. Effect on yeast intake and CDM contractions by Gal4-directed dTrpA1-mediated activation of neuronal networks. (A) Experimental setup: yeast intake of larvae (% of body stained) was determined after 20 min of dTrpA1 activation (upper picture). All tested Gal4-lines showed a decreased relative change in yeast intake except 5-HT (TRH-Gal4) line, which showed an increase (lower panel; Mann-Whitney Rank Sum Test: ***p≤0.001). (B) CDM contractions were tracked by measuring the length difference of pharyngeal lumen (Δd) at 32°C relative to the maximal contractions at 18°C (upper picture). Tracking of the CDM contractions correspond to deduced muscle activity based on the AN recordings (lower left panel). CDM contractions were quantified as relative change in contractions/min (lower right panel). Significance was tested by Mann-Whitney Rank Sum Test (*p≤0.05, ***p≤0.001). 5-HT, serotonin; ACh, acetylcholine; DA, dopamine; Glu, glutamate; Hug, hugin neuropeptide.
doi:10.1371/journal.pbio.1001893.g002

programs (i.e., the AN, but not MN or PaN motor programs), thus demonstrating a specificity in recruitment of different motor programs that comprise the feeding system. For the current study, we decided to focus on the hugin neuronal cluster for one critical reason, namely the relative simplicity of the expression pattern generated by the HugS3-Gal4 line in both numerical and spatial terms. Previous studies showed that this line drives reporter gene expression precisely in 20 cells, all tightly clustered in the subesophageal ganglion (SOG) [49] (Figure S3), and send projections to the ventral nerve cord and the protocerebrum, which is the higher brain center.

Activation of Neurons Expressing Hugin Neuropeptide Suppresses Feeding and Increases Wandering-like Behavior

We first wanted to verify the effect of hugin on the feeding motor system using an independent method to activate neurons. Thus, we used NaChBac and recorded the AN motor pattern [54,55]. The recordings showed a significant suppression of AN motor activity, further strengthening the view that hugin neurons suppress feeding motor patterns (Figure S4). We also wanted to perform the converse experiment by inhibiting hugin neuronal activity through the use of temperature-sensitive shibire (shibire^ts), which blocks synaptic transmission [56]. However, we did not observe any difference in the frequency of the AN motor pattern (Figure S5A). This indicated that activating hugin neurons suppresses AN motor activity, but inhibiting them does not increase it. We do not think this is due to the normal larval feeding motor system operating at a maximal level (since larvae are

continuous feeders), since we can in fact observe an increase in motor activity when serotonergic neurons are activated. Instead, we believe that this reveals insights into the mechanism by which hugin neurons function in modulating the feeding motor system (see Discussion). Consistent with this view, ablating the hugin cells (by expressing reaper-hid to induce apoptosis [57]) or inhibiting the neuronal activity using Kir2.1 also had no effect on the AN motor pattern (Figure S5B).

Based on these observations, we next wanted to analyze the alterations in feeding behavior when hugin neurons were activated in more detail. Specifically, we wanted to determine if the suppressed food intake was accompanied by alterations in a food-related locomotory behavior, namely the wandering-like behavior. This is a behavior that is observed in certain mutant larvae which are defective in food intake, where they move away from the food source and wander about the surrounding area [47–49]. Indeed, in addition to suppression of food intake, a significant wandering-like behavior is also observed when hugin neurons are activated (Figure 3).

Due to the alteration in locomotive behavior, we next asked if the activity of the abdominal segmental muscles that underlie locomotion were affected by activating the hugin neurons. The *Drosophila* larval neuromuscular junctions of the ventral longitudinal muscle (M6 and M7) are well established and have provided valuable insight into synapse function and muscle membrane excitability [58,59]. The rhythmic motor outputs recorded from abdominal muscle M6 are representative for locomotory patterns generated by the larval CNS and likely reflect crawling behavior [60,61]. We therefore monitored the activity of the abdominal muscle M6 by intracellular recordings (Figure 4A). Interestingly,
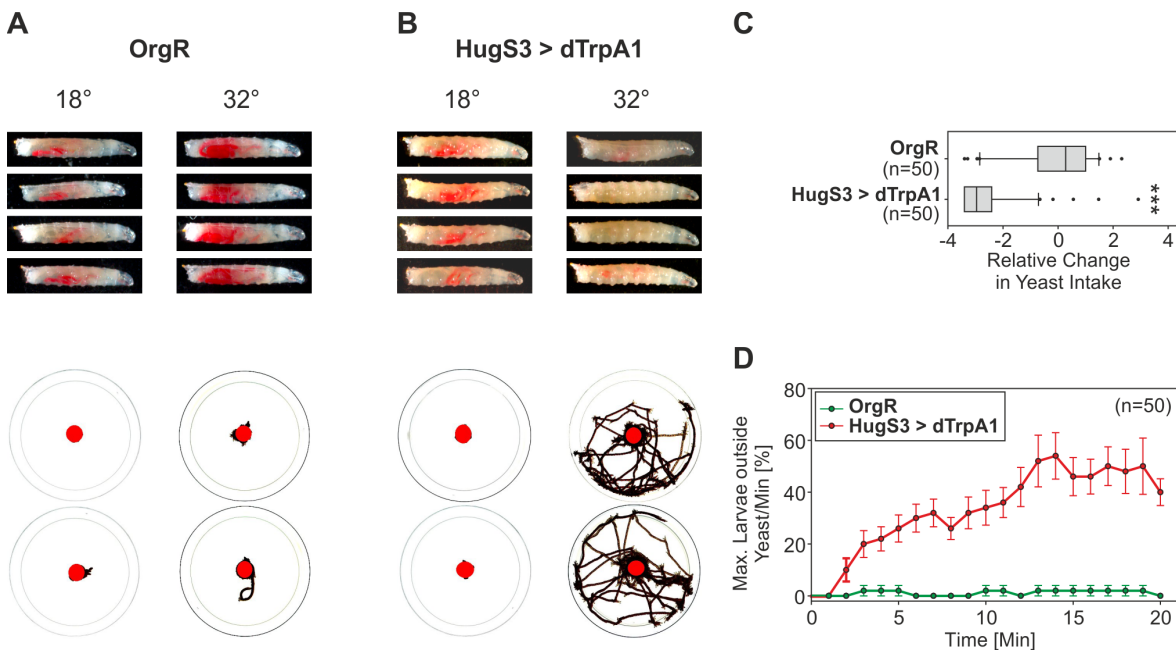
Figure 3. Behavioral consequence of dTrpA1-induced activation of hugin neurons on yeast intake and wandering-like behavior. (A–B) Photographs of OrgR (A) and HugS3>dTrpA1 (B) larvae (upper panel) and crawling tracks (lower panel) after 20 min at 18°C (no dTrpA1 activation) and 32°C (dTrpA1 activation), displaying the yeast intake and wandering-like behavior. Compared with OrgR, HugS3>dTrpA1 larvae showed reduced yeast intake and increased wandering-like behavior. (C) Activation of the hugin neurons by dTrpA1 significantly reduced the relative change in yeast intake compared with OrgR. Data is presented as a box plot (Mann-Whitney Rank Sum Test: ***p≤0.001). (D) Analysis of the locomotory activity showing that HugS3>dTrpA1 had a significantly increased wandering-like behavior (max. larvae outside the yeast/min [%]) relative to OrgR on the restrictive temperature (32°C).
doi:10.1371/journal.pbio.1001893.g003
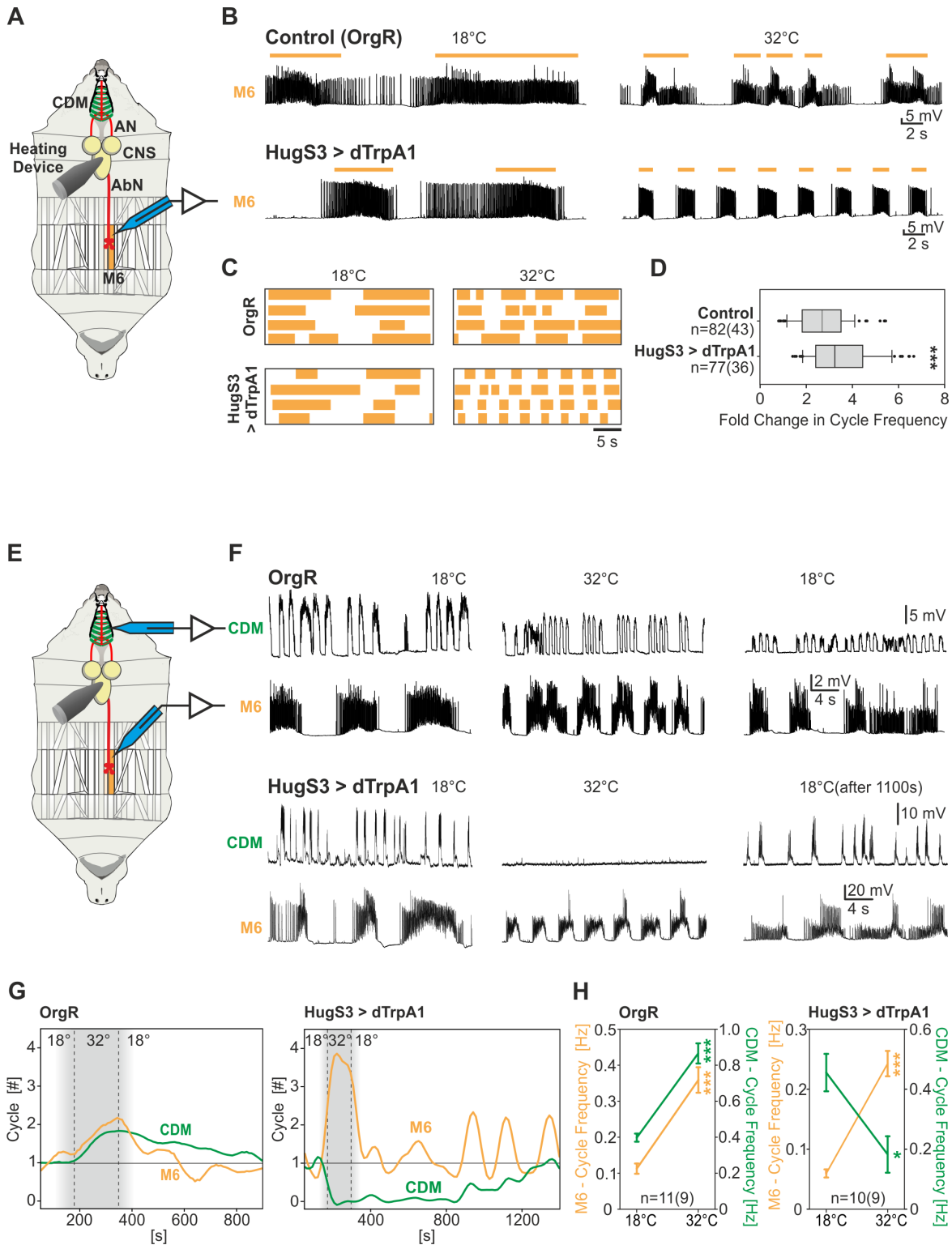
Figure 4. Hugin neurons have opposite effects on the motor patterns underlying feeding and locomotion behavior. (A) Single intracellular muscle recording of M6 (experimental setup). (B) Representative muscle recordings of OrgR and HugS3>dTrpA1 at 18°C (before dTrpA1 activation) and 32°C (during dTrpA1 activation); activation of the hugin neurons leads to an acceleration of the M6 motor pattern (colored bars

indicate bursts of PSPs). (C) Increased acceleration effect of dTrpA1 induced activation of the hugin neurons on the motor pattern (indicated by colored bars) for individual muscle recordings. (D) Activation of the hugin neurons significantly increased cycle frequency (presented as box plot) of the M6 motor pattern (Mann-Whitney Rank Sum Test: ***p≤0.001). (E) Double intracellular muscle recording of the CDM and M6 (experimental setup). (F) Representative CDM/M6 recordings of OrgR and HugS3>dTrpA1 at 18°C (before dTrpA1 activation), at 32°C (during dTrpA1 activation), and after shift down to 18°C. Note the opposite effect on the CDM and M6 motor patterns at 32°C. (G) Temporal progression of CDM and M6 motor activity for OrgR- and HugS3>dTrpA1 recordings (F) upon temperature stimulation. The graph shows the number of cycles per bin (bin size: 20 s) over the recording. (H) Temperature shift from 18°C to 32°C increased the cycle frequency of the CDM and M6 motor pattern of OrgR in the same manner, whereas in the case of HugS3>dTrpA1 the CDM cycle frequency decreased and the M6 cycle frequency increased (symbols indicate the mean, whiskers indicate the standard error). Significance was tested by Mann-Whitney Rank Sum Test (*p≤0.05, ***p≤0.001). AbN, abdominal nerve.
doi:10.1371/journal.pbio.1001893.g004

we observed an accelerating effect on abdominal muscle contraction pattern upon activation of the hugin neurons (Figure 4B–D). We note at this point that we also recorded the M6 muscle motor pattern when shibire[ts] was used to silence hugin neurons, but as with the pharyngeal motor pattern above, no effect was observed (Figure S5C).

We then asked if pharyngeal pumping and abdominal activity could be coordinately regulated. Therefore, we performed double intracellular recordings of the CDM and the abdominal muscle M6 (Figure 4E). Remarkably, hugin neuron activation resulted in a concomitant decrease in feeding and increase in locomotion motor program: the post-synaptic potentials (PSPs) of CDM are completely suppressed, whereas those of abdominal muscle (M6) persist and the motor pattern increased in cycle frequency (Figure 4F–H). In wild type situations, an increase in temperature results in the usually observed temperature effect where both activities are increased (Figure 4H). It is well established that temperature has a profound effect on intrinsic network properties that influence the setting of rhythm frequencies in the CNS of invertebrates and vertebrates [62,63]. In HugS3>dTrpA1, the increased abdominal motor activity is accompanied by a concomitant decrease in CDM motor activity. These results indicated that hugin neurons can modulate two opposite motor programs simultaneously: the feeding program and the locomotory program. Consistent with the previous results, shibire[ts] also had no effect on the CDM motor pattern recordings (Figure S5A) and the underlying feeding behavior (Figure S6).

Hugin Neuropeptide Is Required to Suppress the Feeding Motor Program

Since the results described above indicated that activation of the hugin neurons leads to suppression of feeding, we next wanted to determine if the hugin neuropeptide is required for this suppression. The strategy was to decrease hugin neuropeptide levels in the hugin neurons through RNA interference (RNAi) and see if activating the hugin neurons would still result in suppression of feeding behavior. First we determined the effectiveness of several RNAi lines to decrease hugin neuropeptide levels (Figure 5A; Figure S7). We chose two independent constructs that were effective in reducing hugin neuropeptide levels (HugRNAi1A and Hug-TriPJF03122).

Animals which only expressed the *hugin* RNAi gene construct did not show any alterations in the feeding phenotype, in line with the results, described in the previous section, showing that inhibiting or ablating hugin neurons also had no effect (Figure S5). However, if hugin neurons were activated with dTrpA1 in animals expressing the HugRNAi construct, the suppression of AN motor pattern was no longer observed (Figure 5B, top panel). Similar results were observed with food intake and wandering-like behavior. In both cases, the HugRNAi lines significantly prevented the hugin neurons from exerting their suppressive effect (Figure 5C). Interestingly, the increase in cycle frequency of M6 motor pattern was not affected—that is, activating the hugin neurons still resulted in increased cycle frequency (Figure 5B, bottom panel). Thus, the induction of wandering-like behavior can be decoupled from modulation of the locomotory motor program. Taken together, these results show that

hugin neuropeptide is required for modulating food intake but not for the locomotion motor program; it is also required for initiating wandering-like behavior.

Distinct Cells of the Hugin Cluster Modulate Speed of Abdominal Muscle Contraction

The hugin neuronal cluster comprises just 20 cells, whose soma are all located in the SOG. Earlier work showed that the hugin neurons form four distinct subclasses, each having different projection targets [23,49]. One subclass sends projections down the entire length of the ventral nerve cord (VNC) [64], suggesting a possible role in locomotion. To explore this, we made several deletion constructs of the hugin cis-regulatory region in order to see if the different subclasses were under the control of separable enhancers. In one construct (Hug0.8) there was a complete absence of expression in the four hugin cells that project to the VNC (Figure 6A–C; G), whereas the other 16 neurons were present. Furthermore, using this promoter element in cell ablation experiments resulted in the loss of the 16 cells, whereas the four hugin VNC neurons remained (Figure S8), demonstrating the specificity of this promoter element. To analyze the behavioral consequence, we carried out both food-intake and wandering-like locomotion assays. The 16-cell construct (Hug0.8), in which the VNC projections were missing, could still suppress food ingestion as well as induce wandering-like behavior (Figure 6H,I).

We then performed the converse experiment: to determine the function of the 4-cell hugin cluster that projects to the VNC. We therefore made a promoter construct from a region that was deleted in Hug0.8 construct relative to the HugS3 construct. This line drove target gene expression in precisely the four hugin cells that project down the VNC (Figure 6D–F, G). dTrpA1 activation of this 4-cell VNC cluster had no effect on food intake or wandering-like behavior (Figure 6 H,I).

Next we measured cycle frequency of the AN motor pattern after dTrpA1 activation of these two nonoverlapping neuronal clusters. The hugin-0.8 line suppressed the AN motor pattern, whereas the VNC-line could not (Figure 7A–C), supporting the food intake data. However, when M6 abdominal muscle recordings were performed, we observed the acceleration of the motor pattern with the 4-cell element but not with the 16-cell element (Figure 7D–F). Similar results were obtained when we performed simultaneous double recordings from CDM (for pharyngeal pumping) and M6 abdominal muscles (Figure 7 G–I).

Taken together, these results indicated that food intake (motor program for pharyngeal pumping) and initiation of wandering-like behavior can be decoupled from modulation of the speed of abdominal muscle contraction. The 4-cell hugin VNC cluster can thus regulate locomotion speed separately from pharyngeal pumping. Therefore, although activation of the entire 20-cell hugin cluster coordinately suppresses feeding and enhances locomotion speed, the two motor programs are under the control of distinct hugin neuronal subclasses. Both the suppression of food intake and the induction of wandering-like behavior are performed by the 16-cell cluster, whereas the 4-cell VNC cluster is required to increase the cycle frequency of the locomotor motor pattern.
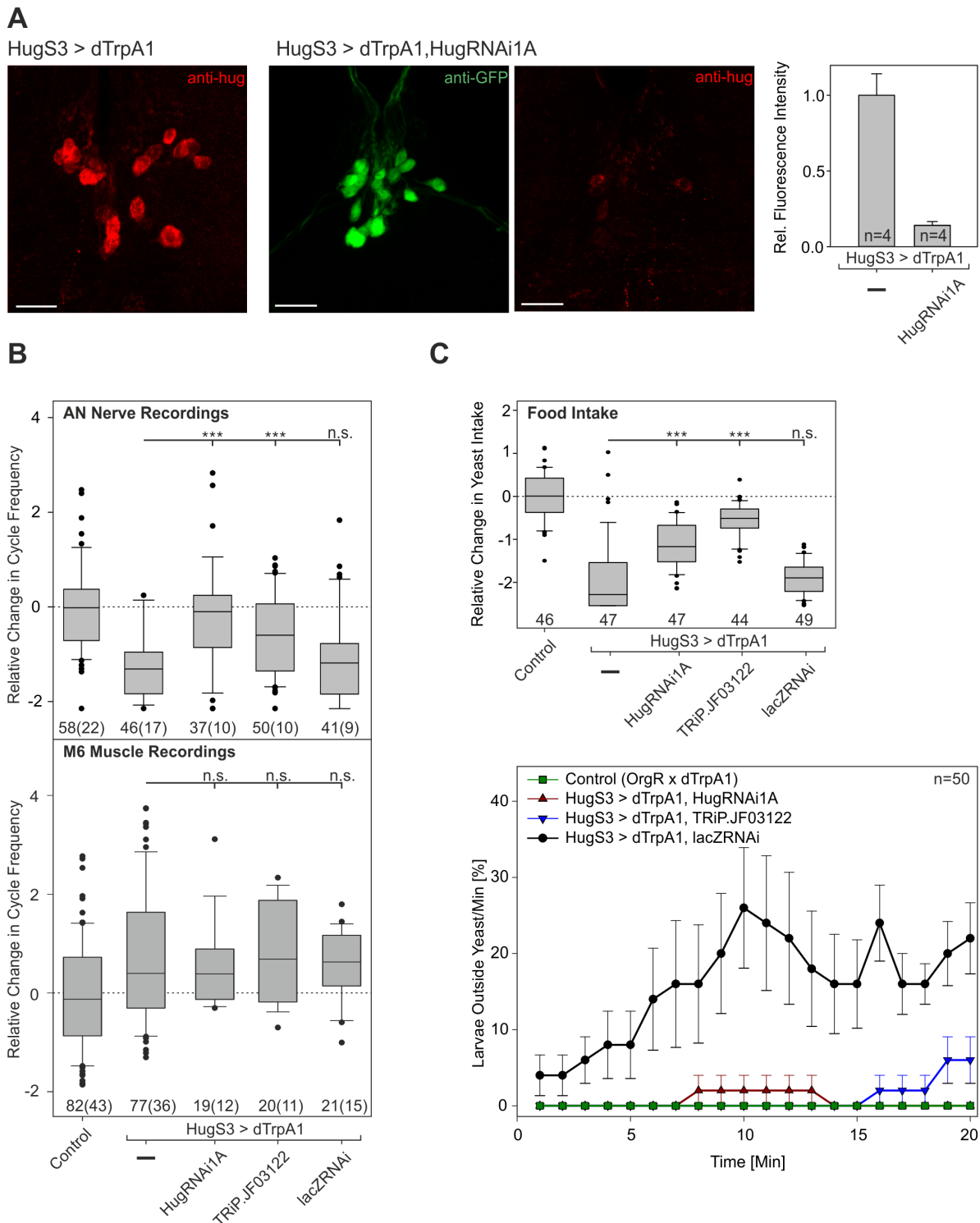
Figure 5. Analysis of hugin neuropeptide function in feeding and locomotion by *hugin* RNAi. (A) Antibody staining of CNS from HugS3>dTrpA1 larva with hugin antibody (left panel). Double staining of CNS from HugS3>dTrpA1,HugRNAi1A larva (middle two panels); this *hugin* RNAi construct also expresses GFP (scale bar: 20 µm). Fluorescence intensity analysis of hugin antibody staining indicates significant decrease of hugin neuropeptide for HugS3>dTrpA1,HugRNAi1A compared with HugS3>dTrpA1 (antibody staining of all genotypes is shown in Figure S7). LacZRNAi serves as control RNAi construct. (B) Analysis of AN motor pattern was quantified as relative change in cycle frequency (upper panel). Recordings

revealed that HugS3>dTrpA1,HugRNAi1A showed a complete, and HugS3>dTrpA1,TRiP.JF03122 a partial, rescue by the RNAi on the motor output most dedicated to food ingestion. Analysis of M6 muscle recording results (lower panel) is presented as relative change in cycle frequency). HugS3>dTrpA1,HugRNAi1A and HugS3>dTrpA1,TRiP.JF03122 showed a significant difference compared with the control and no significant difference to the HugS3>dTrpA1. In contrast to AN motor pattern and wandering-like behavior, the effect of HugS3>dTrpA1 on motor pattern of muscle M6 could not be rescued by the knock down of the hugin neuropeptide (see text for discussion, Mann-Whitney Rank Sum Test: n.s., nonsignificant; ***p≤0.001). (C) Analysis of food intake behavior (upper panel). Results are presented as relative change in yeast intake. HugS3>dTrpA1,HugRNAi1A and HugS3>dTrpA1,TRiP.JF03122 showed a significant difference to control and HugS3>dTrpA1, indicating partial rescue by two independent RNAi constructs. Analysis of locomotor activity is presented as larvae outside the yeast/min at 32°C (during dTrpA1 activation) over a time period of 20 min (lower panel). Knock down of hugin neuropeptide in the two *hugin* RNAi harboring animals prevented induction of wandering-like behavior; the effect is similar to Control (OrgR, OrgR x dTrpA1), and significantly different to HugS3>dTrpA1,lacZRNAi (Mann-Whitney Rank Sum Test: n.s., nonsignificant; ***p≤0.001).
doi:10.1371/journal.pbio.1001893.g005

The Protocerebrum Is Required for Suppression of the AN Motor Pattern

The above results indicated that the 16 cell hugin cluster mediates the suppressive effect of hugin neurons on the AN motor pattern. These comprise three different subclasses of hugin neurons [49,64]: two of these have projections which leave the CNS and target the periphery (to the pharynx, and the ring gland), and one has projections to the protocerebrum. In an effort to start addressing the issue of whether the protocerebrum is required for hugin function in modulating feeding motor pattern, we used a
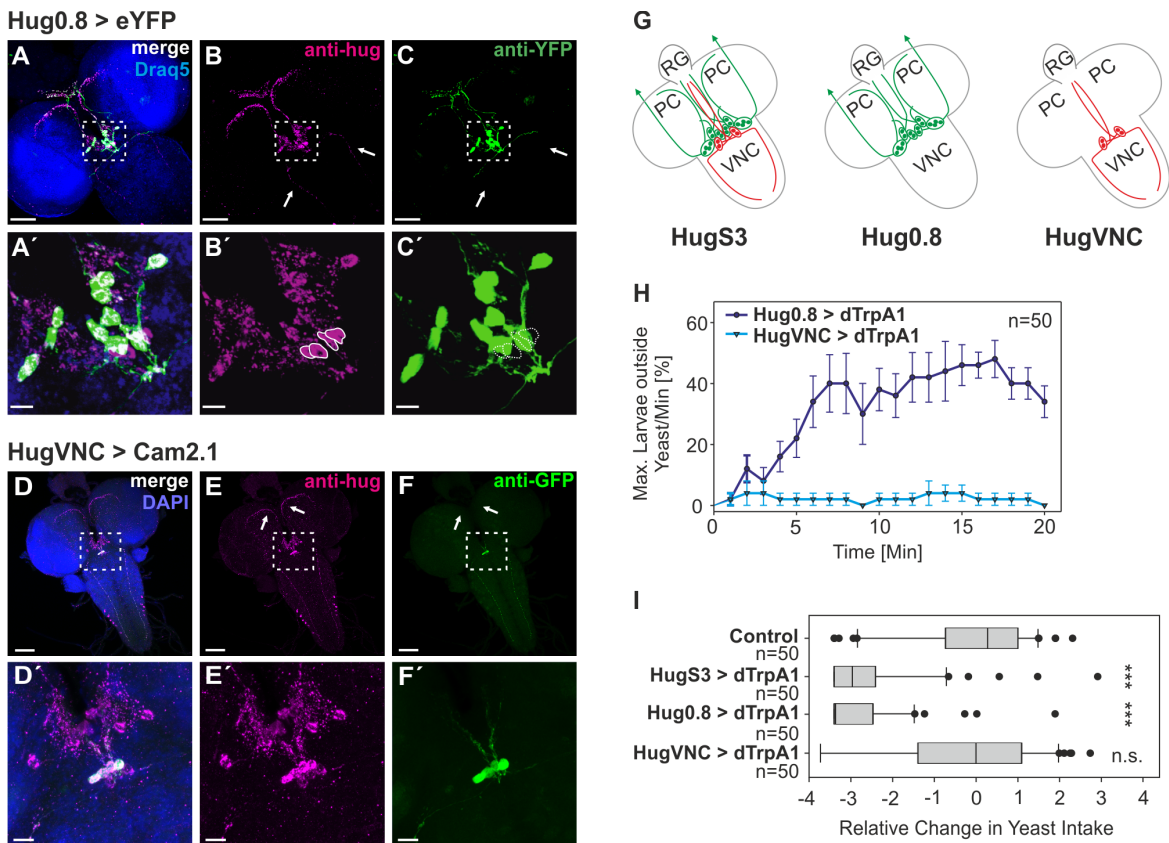
Figure 6. Effect of different subclasses of hugin neurons on the motor pattern underlying feeding and locomotion behavior. (A–C) Double antibody staining of Hug0.8: fluorescence expression driven by Hug0.8-Gal4 (C). Cell bodies and aborizations labelled by hugin antibody (B); merge of B and C (A). (A′–C′) Magnification of labeled somata in the SOG (magnified region indicated by dashed box in the original image (A–C)). Hug0.8 lacks the four hugin cells (marked in B′ and C′) which project to the VNC (indicated by arrows in B and C). (D–F) Double antibody staining of HugVNC: fluorescence expression driven by HugVNC-Gal4 (F). Cell bodies and aborizations labelled by hugin antibody (E); merge of E and F (D). (D′–F′) Magnification of labeled somata in the SOG (magnified region indicated by dashed box in the original image (D–F)). Only the four cells that project to the VNC are labelled. Arrows mark the missing projections to protocerebrum (A–F: 50 µm, A′–F′: 10 µm). (G) Schematic summary of the three different hugin promoter constructs. HugS3 drives target gene expression in all 20 hugin cells; Hug0.8 lacks the four cells that project to the VNC; HugVNC drives expression only in the four cells that project to the VNC. (H) At activating temperature (32°C), HugVNC>dTrpA1 animals displayed no wandering-like behavior whereas Hug0.8>dTrpA1 animals displayed increased wandering-like behavior similar to HugS3>dTrpA1 (see Figure 3D). Locomotor activity was measured as max. larvae outside the yeast/min [%]. (I) Relative change in yeast intake after 20 min of dTrpA1 activation. Control (OrgR), HugS3>dTrpA1, Hug0.8>dTrpA1, and HugVNC>dTrpA1 animals were measured for food intake after 20 min of dTrpA1 activation (32°C). In comparison with the control, HugS3>dTrpA1 and Hug0.8>dTrpA1 showed a significant decrease in food intake (Mann-Whitney Rank Sum Test: n.s., nonsignificant; ***p≤0.001).
doi:10.1371/journal.pbio.1001893.g006
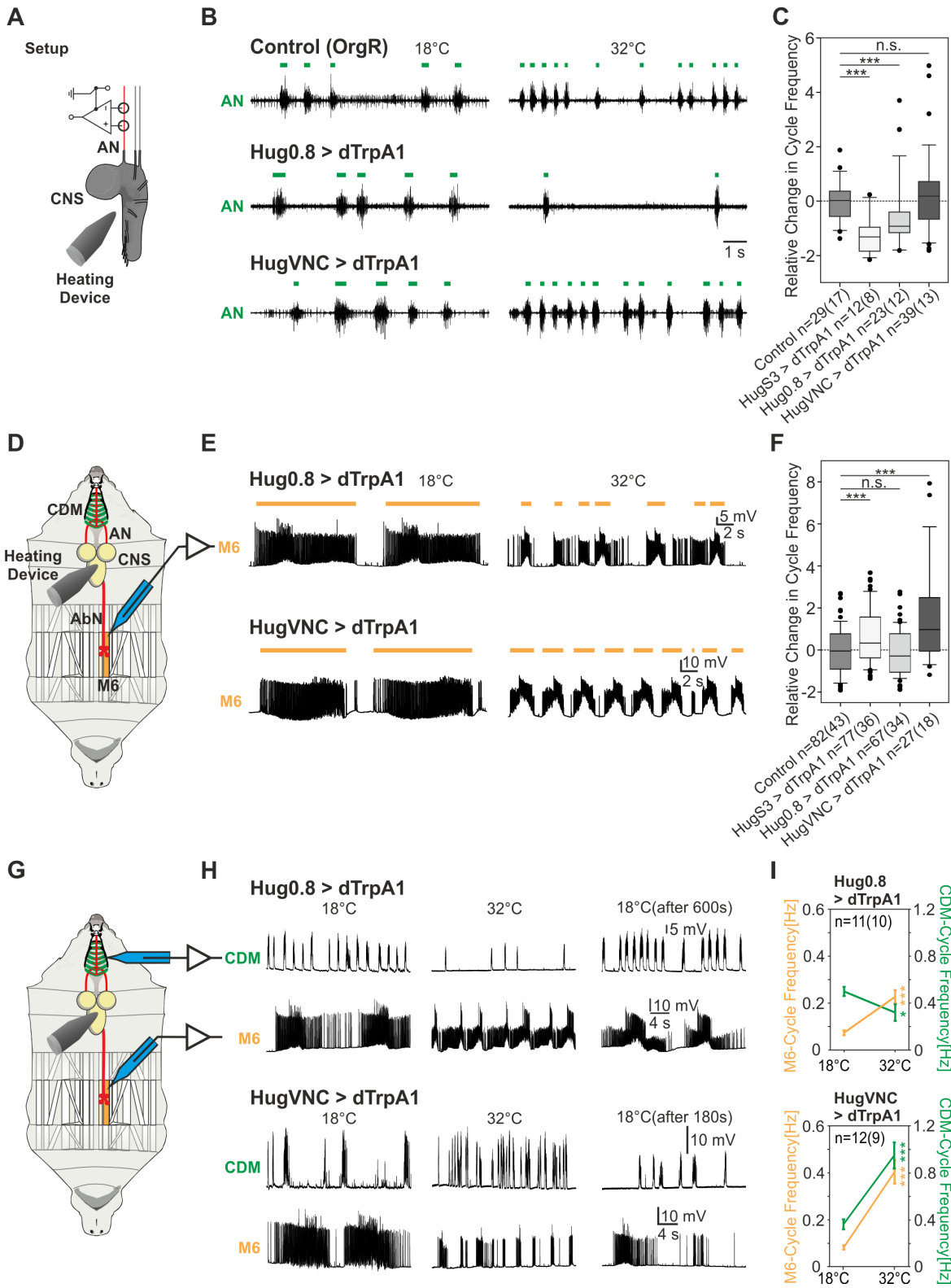
Figure 7. Effect of different subclasses of hugin neurons on the motor pattern underlying feeding and locomotion behavior. (A) Experimental setup of AN recording for dTrpA1 activation. (B) Representative AN recordings of control (OrgR), Hug0.8>dTrpA1, and HugVNC>dTrpA1 at 18°C (before dTrpA1 activation) and 32°C (during dTrpA1 activation). Activation of dTrpA1 in Hug0.8-Gal4 significantly decreased the cycle frequency of the AN-motor pattern, but not in HugVNC-Gal4 (colored bars indicate the motor pattern). (C) Relative change in cycle frequency of the AN-motor pattern by dTrpA1 activation in control, HugS3>dTrpA1, Hug0.8>dTrpA1, and HugVNC>dTrpA1, illustrated as box plots (Mann-Whitney Rank Sum Test: n.s., nonsignificant; ***p≤0.001). The effect of 20-cell hugin cluster on the CDM motor pattern was verified by a second genetic tool to activate neurons (tubGal80^{ts}; NaChBac; for details see Figure S4). (D) Experimental setup of abdominal muscle M6 recordings. (E) Representative M6 recordings of Hug0.8>dTrpA1 and HugVNC>dTrpA1 showing the motor patterns (colored bars) at 18°C (before dTrpA1 activation) and 32°C (during dTrpA1 activation). (F) Analysis of M6 motor pattern revealed a significant increase (Mann-Whitney Rank Sum Test: n.s., nonsignificant; ***p≤0.001) in relative change in cycle frequency (presented as box plot) by dTrpA1 activation for HugVNC, similar to HugS3. (G) Double intracellular muscle recording of the CDM and M6 (experimental setup). (H) Representative CDM/M6 recordings of Hug0.8>dTrpA1 and HugVNC>dTrpA1 at 18°C (before dTrpA1 activation), at 32°C (during dTrpA1 activation) and after shift down to 18°C. Hug0.8>dTrpA1 affected only the CDM motor pattern and HugVNC>dTrpA1 only the M6 motor pattern at 32°C. (I) Temperature shift from 18° to 32°C decreased the cycle frequency of Hug0.8>dTrpA1 for the CDM but not M6 motor pattern, which was comparable to OrgR (see Figure 4). For HugVNC>dTrpA1 the CDM cycle frequency increased as in OrgR, M6 cycle frequency increased (symbols indicate the mean, whiskers indicate the standard error, Mann-Whitney Rank Sum Test: *p≤0.05; ***p≤0.001).
doi:10.1371/journal.pbio.1001893.g007

classical lesion approach in combination with dTrpA1 activation. The experimental strategy was to make lesions to the isolated CNS preparation and record the AN motor pattern upon dTrpA1 activation of hugin neurons (Figure 8).

At 18°C, when dTrpA1 is not activated, lesioning the VNC or the brain hemispheres (H) still resulted in a rhythmic motor pattern from the AN (Figure 8, 18°C), although there were some noticeable variations relative to the pattern generated by an intact

CNS. Upon dTrpA1 activation, the suppression of AN motor pattern was still observed when the VNC was lesioned (Figure 8B). However, when the hemispheres were lesioned, we no longer observed this suppression (Figure 8C). These results suggested that the protocerebrum is required for hugin neuronal function in suppressing the AN motor pattern underlying pharyngeal pumping. Furthermore, these results demonstrate that the CPG for the AN motor pattern is located in the SOG.
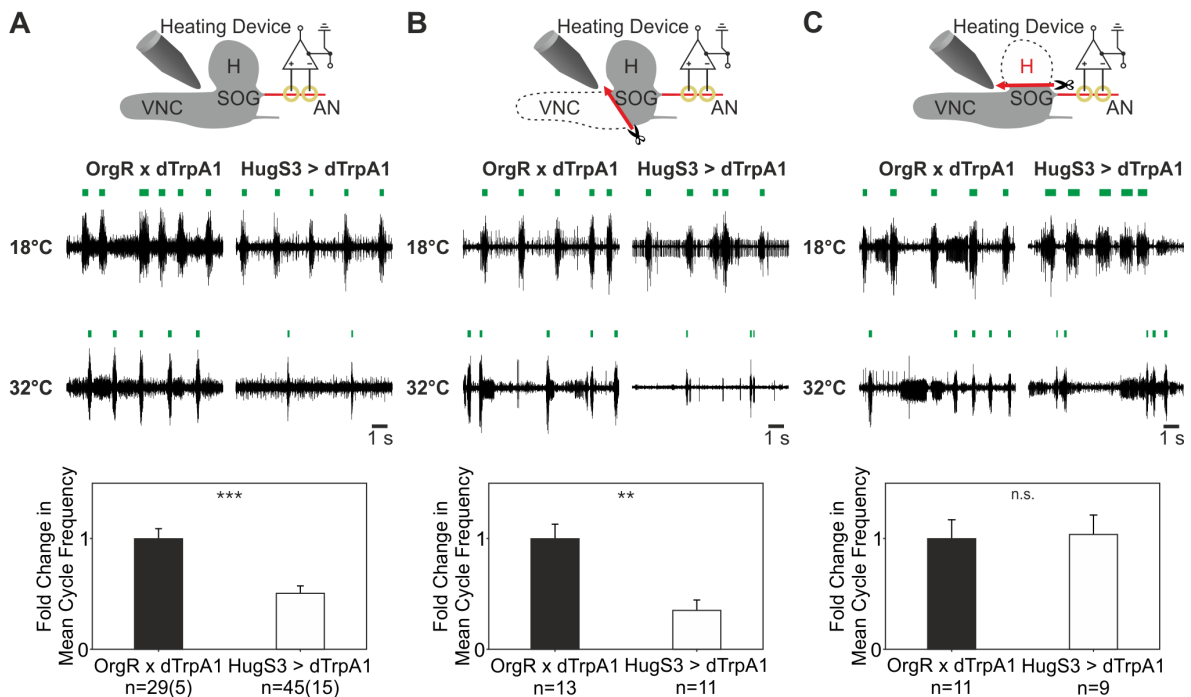
Figure 8. Lesion experiments of OrgR>dTrpA1 and HugS3>dTrpA1. (A) AN recording of the intact CNS (experimental setup, upper panel). At 18°C, OrgR×dTrpA1 and HugS3>dTrpA1 show a rhythmic motor output. At 32°C (dTrpA1 activation), the motor pattern of HugS3>dTrpA1 is decelerated (middle recordings). Analysis of the AN motor pattern during dTrpA1 activation of both genotypes quantified as fold change in mean cycle frequency (lower panel). (B) AN recording after removal of VNC (experimental setup, upper panel). Representative AN recording of OrgR×dTrpA1 and HugS3>dTrpA1 at 18°C and 32°C (dTrpA1 activation). During dTrpA1 activation, the deceleration of motor pattern effected by HugS3>dTrpA1 was still observed after removing the VNC (middle recordings). Analysis of the AN motor pattern during dTrpA1 activation of both genotypes quantified as fold change in mean cycle frequency (lower panel). (C) AN recording after removal of the brain hemispheres (experimental setup, upper panel). In HugS3>dTrpA1, lesion of the brain hemispheres resulted in no deceleration of the AN motor pattern during dTrpA1 activation (representative AN recordings of both genotypes; middle recordings). Analysis of the AN motor pattern during dTrpA1 activation of both genotypes quantified as fold change in mean cycle frequency (lower panel: Mann-Whitney Rank Sum Test: n.s, nonsignificant; **p≤0.01, ***p≤0.001).
doi:10.1371/journal.pbio.1001893.g008

90   4 Schoofs A., Hückesfeld S. et al. Plos Biology (2014)

Selection of Motor Programs in *Drosophila*

Figure 9. Model for the selection of motor programs. (A) Illustration of effect of neuronal populations on different motor programs. Hugin neurons affect a subset (pharyngeal pumping), whereas serotonergic neurons affect all feeding motor patterns (head tilting, mouth hook movement, and pharyngeal pumping). Hugin neurons also regulate in an opposite manner the motor program for segmental contraction, whereas serotonergic neurons affect segmental contraction in the same manner as the feeding motor pattern. (B) Activation of the 20-cell hugin cluster simultaneously suppresses feeding and initiates locomotion motor programs (see text for details). 5-HT, serotonergic neurons.
doi:10.1371/journal.pbio.1001893.g009

Discussion

Action Selection of Motor Programs for Different Behavioral Modules

Behavioral modules can be seen to be composed of distinct motor programs that are differentially recruited based on adaptive needs [1]. These can be cooperative or antagonistic, and the right combinations must be selected in order to bring about the required behavior. For feeding, this requires motor programs that allow actual ingestion of food as well as those locomotor programs involved in food search or food avoidance behaviors. This implies that animals must distinguish motor programs that run serially or in parallel, and those that are essentially mutually exclusive. In humans for example, feeding normally requires arm movements to bring the food to the mouth, followed by biting and chewing, and finally swallowing; but the act of swallowing can occur in the absence of the earlier movements; conversely, similar arm movements to those made during eating can be observed during running. Within a given motor program there are additional levels of modulation—for example, the speed with which a given movement is made.

The behavioral module that comprises *Drosophila* larval feeding is also composed of distinct motor programs, as shown by motor patterns of three pharyngeal nerves, the AN, MN, and the PaN [45]. Our electrophysiology screen reveals distinct populations of central neurons that can regulate motor patterns in a different manner. Some, such as serotonergic neurons, affect all three motor programs; others, like hugin neurons, act on a subset. These differences can be viewed as having varying degrees of functional overlap. Pharyngeal pumping (due to the AN motor program) is the movement most dedicated to food intake; at the other end of the functional spectrum, the segmental longitudinal muscle contractions would be most dedicated to locomotion. Mouth hook and head tilt movements (due to MN and PaN motor programs, respectively) are likely involved in both feeding and locomotion. These motor programs can be separately regulated and recruited

for different behavioral modules. Such mechanisms have been demonstrated at the CPG level in other invertebrates, where the same neurons can be used in different CPGs [21,65].

For both feeding and locomotion, the cellular identities of the CPGs remain largely unknown. Previous studies have demonstrated the existence of feeding CPG(s) in the *Drosophila* larval CNS [45]. We have now localized one of these, the AN motor pattern underlying pharyngeal pumping, to the SOG by lesion experiments. Spieβ et al. [66] has provided evidence that the motor neurons of the AN are also located in the SOG. Although the lesioning of VNC or brain hemisphere can still generate a rhythmic motor pattern, it is not identical to that generated when both are present, indicating that inputs from the VNC and brain hemispheres have a modulatory effect on the pharyngeal pumping CPG. Our results on feeding are complementary to earlier findings on the motor program for locomotion. Forward crawling of *Drosophila* larvae is composed of repetitive wave-like contractions of the segmental body wall musculature from posterior to anterior [67]. Several studies indicated that the neural networks of the crawling motor program (CPGs for crawling) are located in the thoracic and abdominal segments of the central nervous system [60,68], and genetic manipulations showed that the brain hemispheres and the SOG are not required to produce a rhythmic motor pattern in the VNC and crawling behavior, although the rhythmic motor pattern is required for directed movements in response to chemosensory cues [68].

In this context, a major issue is that of cellular specificity: which of the cells targeted by these neurotransmitter Gal4 lines are responsible for the observed effects on the feeding and locomotor program? For example, serotonin is expressed in about 84 cells in the larval CNS: ~56 in the VNC, ~8 in the SOG, and ~20 in the protocerebrum [69]. As mentioned above, the activation of the serotonergic cells results in an increased cycle frequency of all three motor programs; it also enhances the locomotion program in the VNC (see Figure S9, Figure 9A). However, we do not know

which of the serotonergic cells contribute to which of these programs. In addition, different groups of serotonergic cells may have different, even opposite functions, and it may be that the promoting effect dominates when all groups become activated. The various sparse lines and intersectional strategies to narrow down the types of cells being manipulated will be valuable in addressing this issue. This can be combined with the ability to record, from isolated CNS, both feeding and locomotor motor patterns, permitting the identification of central neurons that coordinate the motor programs underlying different behavioral modules.

Neuropeptide Modulation of Mutually Exclusive Actions

A striking finding from our study is the fact that activating a small cluster of 20 neurons in the SOG, all expressing the neuropeptide hugin, leads to a simultaneous suppression of a motor program for feeding and induction of one for locomotion. This is observed both at the behavioral and electrophysiological level. Thus, the hugin cluster can regulate two essentially competing programs since larvae, as with most animals, do not feed and move at the same time. A notable feature of the hugin neuronal cluster is that we have not been able to observe any difference to the control situation when hugin neuronal activity is decreased. For both pharyngeal pumping and wandering-like behavior, it is only when the hugin neurons are activated that we see a modulatory effect. Similarly, the increase in the frequency of M6 abdominal muscle contraction is observed only under activation of hugin neurons. We believe these observations provide insights into the mechanism by which the hugin neurons act. This can be illustrated in terms of how a brake and gas pedal function to coordinate two mutually exclusive operations of a car. Activating hugin neurons decreases feeding, but inhibiting them does not increase feeding: applying a brake causes deceleration, but removing it does not cause acceleration. Similarly, activating the hugin neurons enhance abdominal muscle contraction, but their inhibition does not slow down contraction: stepping on the gas pedal increases speed, but taking it off does not actively decrease speed. This scenario can be used to explain the requirement of hugin neuropeptide in our RNAi experiments. Lowering the level of hugin neuropeptide in activated hugin neurons no longer affected the motor patterns underlying food intake and locomotion, indicating that hugin neuropeptide is necessary for the hugin neurons to suppress feeding and induce wandering-like behavior.

It is of interest to note that hugin neuropeptide does not seem to be required for speeding up the motor program for locomotion. This could be because of the residual quantity of hugin neuropeptide or to some compensation mechanism; more likely, the accelerating effect is due to a different neurotransmitter. At this point, we do not know which classical neurotransmitters are expressed in the hugin cells. In mammals, it has been shown that serotonergic and cholinergic systems influence the speed of motor neuron firing in the spinal cord that underlies locomotion [6,10]. Furthermore, our results show that modulation of the speed of locomotion motor program can be decoupled with the initiation of wandering-like behavior. The decision to both stop feeding and to move out of the food is mediated by a separate cluster of 16 hugin cells, eight of which project to the protocerebrum. A possible scenario is that the cells which adjust the speed of locomotion are recruited during or after the selection of motor programs for suppressing food intake and initiating wandering-like behavior.

Neural Substrate of Action Selection: the Protocerebrum–SOG Corridor

In many vertebrates, the center for swallowing is thought to be localized in the brainstem [70–72]. The cranial nerves that innervate muscles involved in chewing and swallowing descend from the brainstem. The neuronal components are much less understood relative to the spinal cord, although identifying the specific brain areas that regulate food intake is a focus of intense study in the mouse [73]. In *Drosophila*, the larval SOG occupies a central position within the CNS to integrate information on feeding and locomotion, as it connects the VNC with the brain hemispheres. The pharyngeal nerves that innervate the feeding musculature originate from the SOG, and gustatory sensory neurons send projections to the SOG [43,45]. The brainstem in vertebrates is analogously positioned, being located at the junction between the brain and the spinal cord, and the cranial nerves that innervate the pharynx originate from this part of the CNS [74], suggesting that the SOG could represent an analogous structure to the vertebrate brainstem.

It has recently been postulated that the insect central complex might play an analogous role to the basal ganglia [75–77]. Although a canonical central complex has not yet been identified in the *Drosophila* larval brain, a functional analogue is probably located in the protocerebrum. The neuroanatomy of the hugin neurons, especially exemplified by the projection pattern that connects the SOG to the protocerebrum, suggests that the SOG/protocerebrum corridor encompassing the hugin neuronal projections may play an important role in action selection of motor programs underlying feeding and locomotion (Figure 9B). The hugin projections to the protocerebrum and the connections to the gustatory cells and the insulin-producing cells [49,78], would process external and internal sensory cues, and determine which motor programs modulating feeding and locomotion are selected.

A major future challenge will be to determine how the different neuronal components of the feeding motor hierarchy are interconnected. One essential effort will be to analyze the receptor for the hugin neuropeptides. Two putative receptors have already been identified and it would be necessary to determine the cells that express the receptors [79,80]. Another effort will be to localize the classical neurotransmitters that may be expressed in the different hugin cells. Complementary to these would be to exploit the high-resolution connectivity mapping of the larval CNS that is currently being done through serial EM reconstructions [81], as has been done in the classic work for *C. elegans* [82]. Working on a small brain with its limited behavioral repertoire may thus lead to a functional map superimposed on the connectome of the larval motor system.

Materials and Methods

Flies

The following Gal4 driver and UAS effector lines were used: OK371-Gal4 (Bloomington #26160), Cha-Gal4 (Bloomington #6798), GAD-Gal4 [83], TRH-Gal4 [84], TH-Gal4 (Bloomington #8848), DDC-Gal4 (Bloomington #8849), TDC2-GaL4 (Bloomington #9313), DILP2-Gal4 [85], HugS3-Gal4 [49], NPF-Gal4 (Bloomington #25682), sNPF-Gal4 (Kyoto DGRC #113901 (NP6301)), UAS-dTrpA1 (Bloomington #26263), UAS-eYFP (Bloomington #6659), UAS-mCD8-mRFP (Bloomington #27398), 10×UAS-mCD8-GFP (Bloomington #32184), UAS-LacZRNAi (a gift from M. Jünger), UAS-shibire^{ts} (a gift from A. Thum), and UAS-TRiP.JF03122 (Bloomington#28705). Stable homozygous lines of tubulin-Gal80^{ts} and UAS-NaChBac (a gift from R. Jackson (Tufts University)) and of tubulin-Gal80^{ts} (Bloomington #7108) and UAS-eYFP (Bloomington #6660) as control for NaChBac experiments were used. For control experiments OregonR (wild type) or w^{1118} was used.

92 4 Schoofs A., Hückesfeld S. et al. Plos Biology (2014)

Selection of Motor Programs in *Drosophila*

Adult flies and larvae were reared on standard fly food and kept at 25°C unless otherwise stated. All experiments were performed with third instar larvae 98±2 h AEL (after egg laying). Four hours egg collections were made on apple juice-agar plates with yeast-water paste. After 48 h, larvae were transferred into vials containing standard fly food. For experiments with shibire[ts] larvae were raised at 18°C to avoid temperature-induced developmental defects [56]. Experiments were performed with third instar larvae 8 days old. In the experiments using tubulin-Gal80[ts] and UAS-NaChBac/UAS-eYFP larvae were raised on 18°C for 7 days and were transferred on 30°C for 8–12 h prior to the experiment to induce the expression of the NaChBac/eYFP.

Generation of Transgenic hug0.8-Gal4 and hugVNC-Gal4 Line

For Hug0.8-Gal4 line, a 793 bp hugin promoter fragment was amplified by primer1: CATTGACATTGCCCCCCATT and primer2: GGGACAACTGATGCCAGC, subcloned into TOPO TA pCRII vector (Invitrogen), digested with BamHI and NotI and ligated into the pCasperAUG-Gal4-X vector (Addgene plasmid 8378, [86]). The construct was injected into w[1118] (Bloomington#3605). For HugVNC-Gal4, a 403 bp hugin promoter fragment was amplified by primer1: ATCGCAGTGCTCA-CAATCTG and primer2: GTGGGGCATCCTGTTTAATG from wild type DNA and subcloned into TOPO TA pCRII vector. A BamHI/NotI digestion product was ligated into pENTR4 Gateway Entry vector (Invitrogen) and cloned into the destination vector pBPGUw (Addgene plasmid 17575), [87], by using LR Clonase II enzyme mix (Invitrogen). Transgenic lines were generated using standard methods for PhiC31 integrase-mediated genomic integration into y,w; P{CaryP}attP2 (BestGene Inc, USA).

Electrophysiology

Reduced semi-intact preparations were made of third instar larva consisting of the CNS, CPS, and associated pharyngeal nerves and muscles. Detailed description of the dissection has been described earlier [45]. All dissections and experiments were performed in saline solution composed of (in mM): 140 NaCl, 3 KCl, 2 CaCl$_2$, 4 MgCl$_2$, 10 sucrose, and 5 HEPES [88].

For *en passant* extracellular recording, the nerve was insulated with a surrounding petroleum jelly border on a piece of Parafilm. Recording electrodes were made of silver wire (diameter: 25–125 μm, Goodfellow). Motor output was measured by differential recordings of the deafferented nerve with a preamplifier connected to a four-channel amplifier/signal conditioner (Model MA 102/103; Ansgar Büschges group electronics lab). All recorded signals were amplified (amplification factor: 5000) and filtered (bandpass: 0.1–3 kHz). The recordings were sampled at 20 kHz. Data was acquired with Micro3 1401 or Power 1401 mk2 A/D board (Cambridge Electronic Design) and Spike2 software (Cambridge Electronic Design).

For intracellular muscle recordings, semi-intact CDM/M6 preparations of third instar larvae were used. PSPs of the muscle M6 of 4th abdominal segment and CDM were recorded using glass microelectrodes filled with 3 M KCl solution (tip resistance: 20–30 MΩ) connected to an intracellular amplifier (BRAMP-01R, npi electronic GmbH). All recordings were digitally sampled by a Micro3 1401 or Power 1401 mk2 A/D board (Cambridge Electronic Design) at 20 kHz. Data was acquired with Spike2 software (Cambridge Electronic Design).

For analysis, data pairs of successive 60 s or 120 s recording-sections under unstimulated and stimulated conditions were analyzed. Processing of the electrophysiological recordings was performed with a modified script of Spike2 (provided by Cambrigde

Electronic Design). For a pair of successive recording-sections, fold change in cycle frequency was calculated. The dTrpA1-experiments revealed an endogenous temperature effect which could mask the impact of dTrpA1-activated GAL4-driver lines on the rhythmic motor output. Due to this, the mean fold change in cycle frequency of the respective control experiments was subtracted for each data point, termed relative change in cycle frequency.

Temperature Stimulation

For dTrpA1-experiments (nerve/muscle recording and CDM tracking) thermal stimuli were applied to the dorsal side of CNS. The custom-made stimulator consisted of a silver wire (diameter: 4 mm) attached to a Peltier element with thermally conductive adhesive. Peltier element was driven by a voltage-regulated power supply (VSP 2405, Voltcraft) connected to an A/D board. The end of the thermal stimulator was filed to a tip and insulated with nail polish. Applied temperature was measured by digital thermometer (GMH 3210, Greisinger electronic). The sensor for the thermometer was placed 5 mm from the tip (for temperature calibration see Figure S1). Temperature signals were acquired with the A/D board. The thermal stimulator was regulated by a script-based feedback loop via the A/D-board.

Behavioral Assay

For measurement of yeast ingestion, larvae were first washed and then starved in a Petri dish lined with tap water-moistened tissue for 30 min on RT. Afterwards they were transferred on colored yeast (colored with crimson red powder) on pre-warmed (30 min at 32°C) apple juice-agar plates and incubated for 20 min at 32°C. Afterwards the larvae were removed from the yeast and placed in 65°C hot water. For analysis larvae were photographed using a digital camera (Axiocam ICc 1, Zeiss) mounted on a binocular (Stemi 2000-CS, Zeiss). For each individual, the amount of yeast ingested was calculated as area of the alimentary tract stained by colored yeast divided by body surface area using the software ImageJ (Fiji). Data on the feeding assay is represented as percentage of ingested yeast relative to the body surface.

For simultaneous investigation of feeding and wandering-like behavior, five larvae were placed on a pre-heated/-cooled apple juice agar plate (18°C or 32°C). 20 min videos at 18°C and 32°C were acquired using a digital camera (Quickcam 9000 Pro, Logitech) and the software VirtualDub. The measurement of yeast ingestion was performed as listed in the previous paragraph. The locomotion data was analyzed using the tracking software MTrack2 (Fiji). Analysis of larvae leaving the yeast spot was carried out using a custom-made macro for ImageJ (Fiji).

Monitoring CDM Activity

CDM contractions were studied in semi-intact larvae. The preparation consisted of the CNS, the abdominal body wall, and the feeding apparatus (CPS including associated muscles). Thermal stimulation was applied directly to the CNS. Consecutive videos of 60 s at 18°C and 60 s at 32°C were recorded using a digital camera (Axiocam ICc 1, Zeiss) mounted on a binocular (Stemi 2000-CS, Zeiss). CDM contractions were tracked by measuring the length-difference of pharyngeal lumen (Δd) over time relative to the maximal contractions at 18°C. The measurements were performed using the software ImageJ (Fiji).

Immunohistochemistry

Dissected larval brains were fixed in paraformaldehyde (4%). For the antibody staining of hug-eYFP, primary antibody was rabbit-antiGFP (1:500, Abcam plc) and the secondary antibody

was rabbit-antiGFP Cy2 (1:200, Dianova GmbH). The antibody staining of HugVNC>Cam2.1 was performed with chicken anti-GFP (1:500, Abcam plc) and as secondary antibody anti-chicken Alexa488 (1:200, Invitrogen) was used. Antibody staining of hugin was performed with guinea pig anti-Hugin (1:200, Pankratz laboratory; for hug0.8>rpr/hid) or rabbit anti-Hugin (1:500, Pankratz laboratory; hug0.8>eYFP). Antibody stainings for RNAi experiments were done using rabbit anti-Hugin (1:500).Secondary antibodies were: anti-rabbit Cy3, anti-guinea pig Cy3 (1:200, Jackson ImmunoResearch), and mouse anti-GFP (1:500, Sigma-Aldrich). Nuclei were counter stained with DAPI or Draq5. Labeled larval brains were mounted in Mowiol. Imaging was carried out using Laser Scanning Microscope (ZEISS LSM780). The obtained images were arranged using Zen LE and Photoshop CS5 (Adobe) (for detailed staining procedures see [64]).

Fluorescence Microscopy

All images were obtained by using a confocal microscope Zeiss LSM 780; non-specific background fluorescence of the in vivo images was reduced by the Median Filter of the Zeiss Zen Software.

Cloning of *Hugin* RNAi Construct

Hugin cDNA PCR fragment flanked by a *Bam*HI and a *Kpn*I restriction sites was cloned into *pHIBS* vector [89] (primer sequences GGATCCGTTCCATTCGATCGTCCGAC and GGTACCGTGGCACTGGCCTTCTGG). The 394 bp hugin fragment represents bases 41 to 434 of 1033 bp hugin full length cDNA (flybase.org). A 478 bp *Sal*I/*Kpn*I fragment of hugin-*HIBS* was then cloned into *Xho*I/*Kpn*I cut *pUdsGFP* [89]. Next a 407 bp *Bam*HI/*Eco*RI fragment of hugin-*HIBS* was cloned into the *Eco*RI/*Bgl*II cut hugin-*pUdsGFP*. The *pUdsGFP* plasmid harboring two hugin fragments in opposite orientation was used for standard germline transformation [90]. The line used in the text is referred to as HugRNAi1A.

Lesion Experiments

For the lesion experiments we used the standard reduced semi-intact preparations of third instar larvae as mentioned above (see Electrophysiology). VNC or brain hemispheres were removed by a microdissecting scissor (Fine Science Tools). Five minutes after the lesion of the neuronal tissue, extracellular recording of antennal nerve was started. Thermal stimuli were applied by the above described protocol for temperature stimulation. Consecutive 60 s sections of the AN motor output at 18°C and 32°C were analyzed. The cycle frequency of AN motor pattern at 18°C showed no significant difference between OrgR×dTrpA1 and HugS3>dTrpA1 for each lesion. Therefore the data is presented as fold change in cycle frequency of AN motor pattern between both genotypes at 32°C (during dTrpA1 activation) for each experiment.

Data Analysis

All electrophysiological and behavioral experiments were tested for significance with the Mann-Whitney-Rank-Sum-test (*$p \leq 0.05$, **$p \leq 0.01$, ***$p \leq 0.001$).

Supporting Information

Figure S1   (A) Experimental set up of heating device calibration. (B) Calibration curve of the heating device (x-axis – $T_{heat\ element}$ [°C], y-axis – $T_{environment}$ [°C]). At $T_{heat\ element}$ 18°C the measured $T_{environment}$ was 19.8+/−0.48°C and at $T_{heat\ element}$ 32°C the measured $T_{environment}$ was 26.9+/−0.3°C.
(TIF)

Figure S2   (A) Experimental setup: yeast intake of larvae [% of body stained] was determined after 20 min of dTrpA1-activation. The following major neurotransmitter systems were used for the initial screening: glutamatergic (Glu), cholinergic (ACh), GABAergic (GABA), serotonergic (5-HT), dopaminergic (DA), combined serotonergic/dopaminergic (5-HT/DA) and combined octopaminergic/tyraminergic (OA/TYR) neuronal populations. We also tested four neuropeptide genes shown in earlier studies to be involved in some aspect of feeding response: *Drosophila* insulin-like peptide (Dilp), hugin (Hug), neuropeptide F (NPF) and short NPF (sNPF) (see Materials and Methods for the respective Gal4-lines). (B) Statistical data of yeast intake screen for all tested Gal4-lines is represented as box plots. Crosses were categorized based on their effect on larval food intake (Mann-Whitney Rank Sum Test: *$p \leq 0.05$, **$p \leq 0.01$, ***$p \leq 0.001$).
(TIF)

Figure S3   (A–C) Antibody staining of HugS3>10×GFP expression pattern in the CNS; Magnification (A′–C) of hugin cell cluster (20 cells) in the SOG (A: scale bar: 50 μm; A′: scale bar: 10 μm). Schematic summary of the projection pattern HugS3-Gal4 line in the larval CNS (right side). Target region of the projections are: PC, RG, SOG, VNC and periphery via PaN. Abbr.: CNS – central nervous system; PaN – prothoracic accessory nerve; PC – protocerebrum; RG – ring gland; SOG – subesophageal ganglion; VNC – ventral nerve cord.
(TIF)

Figure S4   (A) Experimental set up of AN recordings at the isolated CNS. Larvae of both genotypes were 166+/−2 h old (raised on 18°C) and kept for at least 8–12 h on 30°C before recording. (B) Original AN recordings of HugS3>tubGal80^{ts};eYFP and HugS3>tubGal80^{ts};NaChBac (colored boxes represent the CDM activity). (C) Box plot of the cycle frequency [Hz] of HugS3>tubGal80^{ts};eYFP (mean (std. dev.): 0.423 (+/−0.121); number of larvae (number of experiments): 29(10)) and HugS3>tubGal80^{ts};NaChBac (mean (std. dev.): 0.196 (+/−0.192); number of larvae (number of experiments): 30(10)). HugS3>tubGal80^{ts};NaChBac was significant different to HugS3>tubGal80^{ts};eYFP (p-value$\leq$ 0.001). Abbr.: AN – antennal nerve; CDM – cibarial dilator muscle; CNS – central nervous system.
(TIF)

Figure S5   (A) Motor pattern recorded from CDM (presented as box plot for OrgR, OrgR>shi^{ts}, HugS3>shi^{ts}). CDM motor patterns showed no significant difference in fold change of cycle frequency between OrgR, OrgR>shi^{ts}, HugS3>shi^{ts} (performed Mann-Whitney Rank Sum Test (n.s. – not significant)). (B) Left side: Experimental setup for the nerve recordings of HugS3>rpr/hid (upper panel) and HugS3>Kir2.1 (lower panel). Right side: Graph shows the cycle frequency of the AN motor pattern after ablation of the hugin neurons by the apoptotic factors rpr and hid and during inhibition of hugin neurons using Kir2.1 (lower panel). Compared to the control (OrgR) inhibiting and ablating the hugin neurons showed no significant difference (performed Mann-Whitney Rank Sum Test (n.s. – not significant)). (C) Motor pattern recorded from M6 (presented as box plot for OrgR, OrgR>shi^{ts}, HugS3>shi^{ts}). M6 motor output showed no significant difference in fold change of cycle frequency between OrgR, OrgR>shi^{ts}, HugS3>shi^{ts} (performed Mann-Whitney Rank Sum Test (n.s. – not significant)).
(TIF)

Figure S6   (A,B) Statistical analysis of food intake and wandering-like behavior assay of OrgR×shi^{ts} compared to HugS3>shi^{ts} under starved (A) and fed (B) conditions. The graph (left) shows the

intake of yeast (area of the alimentary tract stained by colored yeast divided by body surface area) after 20 min at 32°C. Graph (right) illustrates the statistical data of the wandering-like behavior of OrgR×shi[ts] compared to HugS3>shi[ts] measured as larvae outside the yeast/min [%] over a time period of 20 min. In both nutritional conditions HugS3>shi[ts] showed no significant difference in food intake and wandering-like behavior relative to OrgR×shi[ts] at 32°C.
(TIF)

Figure S7 Hugin antibody staining of the genotypes: OrgR> dTrpA1, HugS3>dTrpA1, HugS3>dTrpA1, HugRNAi1A and HugS3>dTrpA1, TRiP.JF03122. Images show the subesophageal ganglion of the larval CNS as indicated in the schematic drawing (left side, scale bar: 20 µm).
(TIF)

Figure S8 (A) Hugin antibody staining of hug0.8>rpr/hid showing four remaining cells in the SOG that project to the VNC (A, scale bar: 50 µm; A′, scale bar: 10 µm).
(TIF)

Figure S9 Graphs show the relative change in cycle frequency of M6- and CDM-motor pattern of HugS3>dTrpA1 and TRH>

dTrpA1 compared to the control lines (Mann-Whitney Rank Sum Test: *p≤0.05, **p≤0.01, ***p≤0.001).
(TIF)

Author Contributions

The author(s) have made the following declarations about their contributions: Conceived and designed the experiments: AS SH PS AM MP MJP. Performed the experiments: AS SH PS AM MP MZ. Analyzed the data: AS SH PS AM MP MZ MJP. Contributed reagents/materials/ analysis tools: RS ASC. Wrote the paper: AS MJP.

References

1. Grillner S, Hellgren J, Ménard A, Saitoh K, Wikström MA (2005) Mechanisms for selection of basic motor programs—roles for the striatum and pallidum. Trends Neurosci 28: 364–370.
2. Delcomyn F (1980) Neural basis of rhythmic behavior in animals. Science 210: 492–498.
3. Harris-Warwick RM, Marder E, Selverston AI, Moulins M (1992) Dynamic biological networks: the stomatogastric nervous system. Cambridge (Massachusetts): The MIT Press.
4. Grillner S (2003) The motor infrastructure: from ion channels to neuronal networks. Nat Rev Neurosci 4: 573–586.
5. Grillner S (2006) Biological pattern generation: the cellular and computational logic of networks in motion. Neuron 52: 751–766.
6. Grillner S, Jessell TM (2009) Measured motion: searching for simplicity in spinal locomotor networks. Curr Opin Neurobiol 19: 572–586.
7. Goulding M (2009) Circuits controlling vertebrate locomotion: moving in a new direction. Nat Rev Neurosci 10: 507–518.
8. Kiehn O, Kullander K (2004) Central pattern generators deciphered by molecular genetics. Neuron 41: 317–321.
9. Büschges A, Scholz H, El Manira A (2011) New moves in motor control. Curr Biol 21: R513–R524.
10. Kiehn O (2011) Development and functional organization of spinal locomotor circuits. Curr Opin Neurobiol 21: 100–109.
11. Whelan PJ (2010) Shining light into the black box of spinal locomotor networks. Philos Trans R Soc Lond B Biol Sci 365: 2383–2395.
12. Takakusaki K, Saitoh K, Harada H, Kashiwayanagi M (2004) Role of basal ganglia-brainstem pathways in the control of motor behaviors. Neurosci Res 50: 137–151.
13. Cazalets J, Borde M, Clarac F (1995) Localization and organization of the central pattern generator for hindlimb locomotion in newborn rat. J Neurosci 15 (7): 4943–4951.
14. Jiang Z, Carlin KP, Brownstone RM (1999) An in vitro functionally mature mouse spinal cord preparation for the study of spinal motor networks. Brain Res 816: 493–499.
15. Gosgnach S, Lanuza GM, Butt SJB, Saueressig H, Zhang Y, et al. (2006) V1 spinal neurons regulate the speed of vertebrate locomotor outputs. Nature 440: 215–219.
16. Miles GB, Hartley R, Todd AJ, Brownstone RM (2007) Spinal cholinergic interneurons regulate the excitability of motoneurons during locomotion. Proc Natl Acad Sci U S A 104: 2448–2453.
17. Smetana R, Juvin L, Dubuc R, Alford S (2010) A parallel cholinergic brainstem pathway for enhancing locomotor drive. Nat Neurosci 13: 731–738.
18. Wyart C, Del Bene F, Warp E, Scott EK, Trauner D, et al. (2009) Optogenetic dissection of a behavioural module in the vertebrate spinal cord. Nature 461: 407–410.
19. Zagoraiou L, Akay T, Martin JF, Brownstone RM, Jessell TM, et al. (2009) A cluster of cholinergic premotor interneurons modulates mouse locomotor activity. Neuron 64: 645–662.
20. Miri A, Azim E, Jessell TM (2013) Edging toward entelechy in motor control. Neuron 80: 827–834.
21. Marder E, Bucher D (2007) Understanding circuit dynamics using the stomatogastric nervous system of lobsters and crabs. Annu Rev Physiol 69: 291–316.
22. Hirayama K, Catanho M, Brown JW, Gillette R (2012) A core circuit module for cost/benefit decision. Front Neurosci 6: 123.
23. Melcher C, Bader R, Pankratz MJ (2007) Amino acids, taste circuits, and feeding behavior in *Drosophila*: towards understanding the psychology of feeding in flies and man. J Endocrinol 192: 467–472.
24. Palmer CR, Kristan WB (2011) Contextual modulation of behavioral choice. Curr Opin Neurobiol 21: 520–526.
25. Taghert PH, Nitabach MN (2012) Peptide neuromodulation in invertebrate model systems. Neuron 76: 82–97.
26. Belgardt BF, Brüning JC (2010) CNS leptin and insulin action in the control of energy homeostasis. Ann N Y Acad Sci 1212: 97–113.
27. Oury F, Karsenty G (2011) Towards a serotonin-dependent leptin roadmap in the brain. Trends Endocrinol Metab 22: 382–387.
28. Sokolowski MB (1980) Foraging strategies of *Drosophila melanogaster*: a chromosomal analysis. Behav Genet 10: 291–302.
29. Avery L, Horvitz HR (1989) Pharyngeal pumping continues after laser killing of the pharyngeal nervous system of *C. elegans*. Neuron 3: 473–485.
30. Avery L (1993) The Genetics of Feeding in *Caenorhabditis elegans*. Genetics 133: 897–917.
31. Sokolowski MB (2001) *Drosophila*: genetics meets behaviour. Nat Rev Genet 2: 879–890.
32. Avery L, You YJ (2012) *C. elegans* feeding. WormBook: 1–23.
33. Buch S, Pankratz MJ (2009) Making metabolic decisions in *Drosophila*. Fly (Austin) 3: 74–77.
34. Flood TF, Iguchi S, Gorczyca M, White B, Ito K, et al. (2013) A single pair of interneurons commands the *Drosophila* feeding motor program. Nature 499: 83–87.
35. Gordon MD, Scott K (2009) Motor control in a *Drosophila* taste circuit. Neuron 61: 373–384.
36. Hergarden AC, Tayler TD, Anderson DJ (2012) Allatostatin-A neurons inhibit feeding behavior in adult *Drosophila*. Proc Natl Acad Sci U S A 109: 3967–3972.
37. Manzo A, Silies M, Gohl DM, Scott K (2012) Motor neurons controlling fluid ingestion in *Drosophila*. Proc Natl Acad Sci U S A 109: 6307–6312.
38. Marella S, Mann K, Scott K (2012) Dopaminergic modulation of sucrose acceptance behavior in *Drosophila*. Neuron 73: 941–950.
39. Mann K, Gordon MD, Scott K (2013) A pair of interneurons influences the choice between feeding and locomotion in *Drosophila*. Neuron 79: 754–765.
40. Olsen SR, Wilson RI (2008) Cracking neural ciruits in a tiny brain: new approach for understanding the neural circuits of *Drosophila*. Trends Neurosci 31: 512–520.
41. Simpson JH (2009) Mapping and manipulating neural circuits in the fly brain. Adv Genet 65: 79–143.
42. Scott K (2005) Taste recognition: food for thought. Neuron 48: 455–464.
43. Vosshall LB, Stocker RF (2007) Molecular architecture of smell and taste in *Drosophila*. Annu Rev Neurosci 30: 505–533.
44. Su C-Y, Menuz K, Carlson JR (2009) Olfactory perception: receptors, cells, and circuits. Cell 139: 45–59.

45. Schoofs A, Niederegger S, van Ooyen A, Heinzel H-G, Spiess R (2010) The brain can eat: establishing the existence of a central pattern generator for feeding in third instar larvae of *Drosophila virilis* and *Drosophila melanogaster*. J Insect Physiol 56: 695–705.

46. Sarov-Blat L, So WV, Liu L, Rosbash M (2000) The *Drosophila* takeout gene is a novel molecular link between circadian rhythms and feeding behavior. Cell 101: 647–656.

47. Zinke I, Kirchner C, Chao LC, Tetzlaff MT, Pankratz MJ (1999) Suppression of food intake and growth by amino acids in *Drosophila*: the role of pumpless, a fat body expressed gene with homology to vertebrate glycine cleavage system. Development 126: 5275–5284.

48. Gutierrez E, Wiggins D, Fielding B, Gould AP (2007) Specialized hepatocyte-like cells regulate *Drosophila* lipid metabolism. Nature 445: 275–280.

49. Melcher C, Pankratz MJ (2005) Candidate gustatory interneurons modulating feeding behavior in the *Drosophila* brain. PLoS Biol 3: e305.

50. Nakazato M, Hanada R, Murakami N, Date Y, Mondal MS, et al. (2000) Central effects of neuromedin U in the regulation of energy homeostasis. Biochem Biophys Res Commun 277: 191–194.

51. Nixon JF, Kotz CM, Novak CM, Billington CJ, Teske JA (2012) Neuropeptides Controlling Energy Balance: Orexins and Neuromedins. Handb Exp Pharmacol 209: 77–109.

52. Hamada FN, Rosenzweig M, Kang K, Pulver SR, Ghezzi A, et al. (2008) An internal thermal sensor controlling temperature preference in *Drosophila*. Nature 454: 217–222.

53. Mahr A, Aberle H (2006) The expression pattern of the *Drosophila* vesicular glutamate transporter: a marker protein for motoneurons and glutamatergic centers in the brain. Gene Expr Patterns 6: 299–309.

54. Luan H, Lemon WC, Peabody NC, Pohl JB, Zelensky PK, et al. (2006) Functional dissection of a neuronal network required for cuticle tanning and wing expansion in *Drosophila*. J Neurosci 26: 573–584.

55. Nitabach MN, Wu Y, Sheeba V, Lemon WC, Strumbos J, et al. (2006) Electrical hyperexcitation of lateral ventral pacemaker neurons desynchronizes down-stream circadian oscillators in the fly circadian circuit and induces multiple behavioral periods. J Neurosci 26: 479–489.

56. Kitamoto T (2001) Conditional modification of behavior in *Drosophila* by targeted expression of a temperature-sensitive shibire allele in defined neurons. J Neurobiol 47: 81–92.

57. Buch S, Melcher C, Bauer M, Katzenberger J, Pankratz MJ (2008) Opposing effects of dietary protein and sugar regulate a transcriptional target of *Drosophila* insulin-like peptide signaling. Cell Metab 7: 321–332.

58. Ataman B, Ashley J, Gorczyca M, Ramachandran P, Fouquet W, et al. (2008) Rapid activity-dependent modifications in synaptic structure and function require bidirectional Wnt signaling. Neuron 57: 705–718.

59. Jan LY, Jan YN (1976) Properties of the larval neuromuscular junction in *Drosophila melanogaster*. J Physiol 262: 189–214.

60. Cattaert D, Birman S (2001) Blockade of the central generator of locomotor rhythm by noncompetitive NMDA receptor antagonists in *Drosophila* larvae. J Neurobiol 48: 58–73.

61. Barclay JW, Atwood HL, Robertson RM (2002) Impairment of central pattern generation in *Drosophila* cysteine string protein mutants. J Comp Physiol A 188: 71–78.

62. Calabrese RL (1998) Cellular, synaptic, network, and modulatory mechanisms involved in rhythm generation. Curr Opin Neurobiol 8: 710–717.

63. Marder E, Calabrese RL (1996) Principles of rhythmic motor pattern generation. Physiol Rev 76: 687–717.

64. Bader R, Colomb J, Pankratz B, Schröck A, Stocker RF, et al. (2007) Genetic dissection of neural circuit anatomy underlying feeding behavior in *Drosophila*: distinct classes of hugin- expressing neurons. J Comp Neurol 856: 848–856.

65. Kristan WB (2008) Neuronal decision-making circuits. Curr Biol 18: R928–32.

66. Spieß R, Schoofs A, Heinzel HG (2008) Anatomy of the stomatogastric nervous system associated with the foregut in *Drosophila melanogaster* and *Calliphora vicina* third instar larvae. J Morphol 269: 272–282.

67. Lahiri S, Shen K, Klein M, Tang A, Kane E, et al. (2011) Two alternating motor programs drive navigation in *Drosophila* larva. PLoS One 6: e23180.

68. Berni J, Pulver SR, Griffith LC, Bate M (2012) Autonomous circuitry for substrate exploration in freely moving *Drosophila* larvae. Curr Biol 22: 1861–1870.

69. Vallés AM, White K (1986) Development of serotonin-containing neurons in *Drosophila* mutants unable to synthesize serotonin. J Neurosci 6: 1482–1491.

70. Miller AJ (1993) The search for the central swallowing pathway: the quest for clarity. Dysphagia 8: 185–194.

71. Jean A (2001) Brain stem control of swallowing: neuronal network and cellular mechanisms. Physiol Rev 81: 929–969.

72. Bieger D, Neuhuber W (2006) Neural circuits and mediators regulating swallowing in the brainstem. Gastrointest Motil Online. doi: 10.1038/gimo74

73. Williams KW, Elmquist JK (2012) From neuroanatomy to behavior: central integration of peripheral signals regulating feeding behavior. Nat Neurosci 15: 1350–1355.

74. Shepherd GM (1994) Neurobiology. 3rd Edition. New York (NY): Oxford University Press Inc.

75. Strausfeld NJ, Hirth F (2013) Deep homology of arthropod central complex and vertebrate basal ganglia. Science 340: 157–161.

76. Stephenson-Jones M, Samuelsson E, Ericsson J, Robertson B, Grillner S (2011) Evolutionary conservation of the basal ganglia as a common vertebrate mechanism for action selection. Curr Biol 21: 1081–1091.

77. Wessnitzer J, Webb B (2006) Multimodal sensory integration in insects—towards insect brain control architectures. Bioinspir Biomim 1: 63–75.

78. Bader R, Sarraf-Zadeh L, Peters M, Moderau N, Stocker H, et al. (2013) The IGFBP7 homolog Imp-L2 promotes insulin signaling in distinct neurons of the *Drosophila* brain. J Cell Sci 126: 2571–2576.

79. Rosenkilde C, Cazzamali G, Williamson M, Hauser F, Søndergaard L, et al. (2003) Molecular cloning, functional expression, and gene silencing of two *Drosophila* receptors for the *Drosophila* neuropeptide pyrokinin-2. Biochem Biophys Res Commun 309: 485–494.

80. Park Y, Kim Y-J, Adams ME (2002) Identification of G protein-coupled receptors for *Drosophila* PRXamide peptides, CCAP, corazonin, and AKH supports a theory of ligand-receptor coevolution. Proc Natl Acad Sci U S A 99: 11423–11428.

81. Cardona A, Saalfeld S, Preibisch S, Schmid B, Cheng A, et al. (2010) An integrated micro- and macroarchitectural analysis of the *Drosophila* brain by computer-assisted serial section electron microscopy. PLoS Biol 8: e1000502.

82. White JG, Southgate E, Thomson JN, Brenner S (1986) The structure of the nervous system of the nematode *Caenorhabditis elegans*. Philos Trans R Soc London B 314: 1–340.

83. Ng M, Roorda RD, Lima SQ, Zemelman B V, Morcillo P, et al. (2002) Transmission of olfactory information between three populations of neurons in the antennal lobe of the fly. Neuron 36: 463–474.

84. Alekseyenko O V, Lee C, Kravitz EA (2010) Targeted manipulation of serotonergic neurotransmission affects the escalation of aggression in adult male *Drosophila melanogaster*. PLoS One 5: e10806.

85. Rulifson EJ, Kim SK, Nusse R (2002) Ablation of insulin-producing neurons in flies: growth and diabetic phenotypes. Science 296: 1118–1120.

86. Vosshall LB, Wong a M, Axel R (2000) An olfactory sensory map in the fly brain. Cell 102: 147–159.

87. Pfeiffer BD, Jenett A, Hammonds AS, Ngo T-TB, Misra S, et al. (2008) Tools for neuroanatomy and neurogenetics in *Drosophila*. Proc Natl Acad Sci U S A 105: 9715–9720.

88. Rohrbough J, Broadie K (2002) Electrophysiological analysis of synaptic transmission in central neurons of *Drosophila* larvae. J Neurophysiol 88: 847–860.

89. Nagel AC, Maier D, Preiss A (2002) Green fluorescent protein as a convenient and versatile marker for studies on functional genomics in *Drosophila*. Dev Genes Evol 212: 93–98.

90. Rubin GM, Spradling AC (1982) Genetic transformation of *Drosophila* with transposable element vectors. Science 218: 348–353.

Supplemental information of Schoofs A., Hückesfeld S. et al., Plos Biology (2014)

A

B

C

calibration

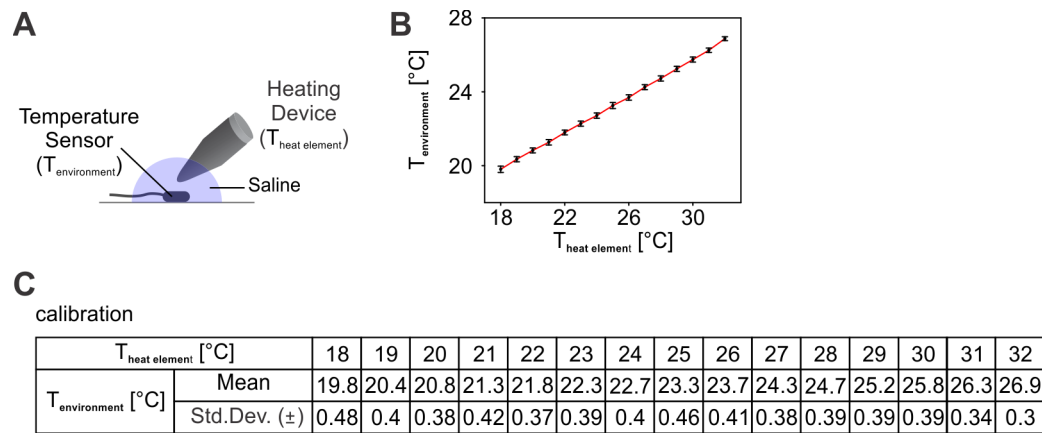| $T_{heat element}$ [°C]		18	19	20	21	22	23	24	25	26	27	28	29	30	31	32
$T_{environment}$ [°C]	Mean	19.8	20.4	20.8	21.3	21.8	22.3	22.7	23.3	23.7	24.3	24.7	25.2	25.8	26.3	26.9
	Std.Dev. (±)	0.48	0.4	0.38	0.42	0.37	0.39	0.4	0.46	0.41	0.38	0.39	0.39	0.39	0.34	0.3

Figure S1:

(A) Experimental set up of heating device calibration. (B) Calibration curve of the heating device (x-axis – $T_{heat element}$ [°C], y-axis – $T_{environment}$ [°C]). At $T_{heat element}$ 18°C the measured $T_{environment}$ was 19.8+/−0.48°C and at $T_{heat element}$ 32°C the measured $T_{environment}$ was 26.9+/−0.3°C.

A

Experimental Setup

Original:

Processed:

Red Yeast

B
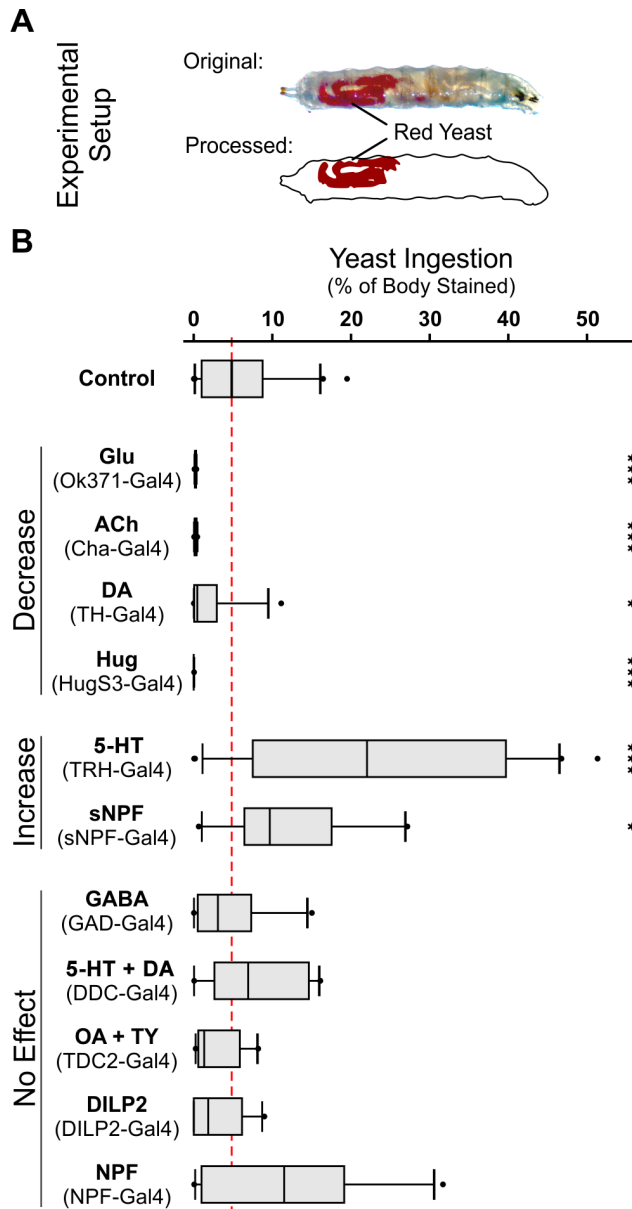
Yeast Ingestion [% of Body Stained]						
	Control	**Glu** (Ok371-Gal4)	**ACh** (Cha-Gal4)	**DA** (TH-Gal4)	**Hug** (HugS3-Gal4)	**5-HT** (TRH-Gal4)
N	21	11	10	11	10	22
Mean	6.1	0.2	0.4	1.9	0.0	22.7
Std.Dev. (±)	5.8	0.0	0.1	3.3	0.0	16.5
p-Value	—	≦0.001	≦0.001	0.015	≦0.001	≦0.001

Yeast ingestion [% of body stained]						
	sNPF (sNPF-Gal4)	**GABA** (Gad-Gal4)	**5-HT/DA** (DDC-Gal4)	**OA/TY** (TDC2-Gal4)	**DILP2** (Dilp2-Gal4)	**NPF** (NPF-Gal4)
N	10	10	10	10	10	12
Mean	11.8	4.2	7.7	2.9	3.0	11.8
Std.Dev. (±)	8.5	4.8	5.9	1.0	3.2	10.8
p-Value	0.04	0.375	0.486	0.245	0.15	0.197

Figure S2:

(A)Experimental setup: yeast intake of larvae [% of body stained] was determined after 20 min of dTrpA1-activation. The following major neurotransmitter systems were used for the initial screening: glutamatergic (Glu), cholinergic (ACh), GABAergic (GABA), serotonergic (5-HT), dopaminergic (DA), combined serotonergic/dopaminergic (5-HT/DA) and combined octopaminergic/tyraminergic (OA/TYR) neuronal populations. We also tested four neuropeptide genes shown in earlier studies to be involved in some aspect of feeding response: *Drosophila* insulin-like peptide (Dilp), Hugin (Hug), neuropeptide F (NPF) and short NPF (sNPF) (see Materials and Methods for the respective Gal4-lines). (B) Statistical data of yeast intake screen for all tested Gal4-lines is represented as box plots. Crosses were categorized based on their effect on larval food intake (Mann-Whitney Rank Sum Test: *p≤0.05, **p≤0.01, ***p≤0.001).
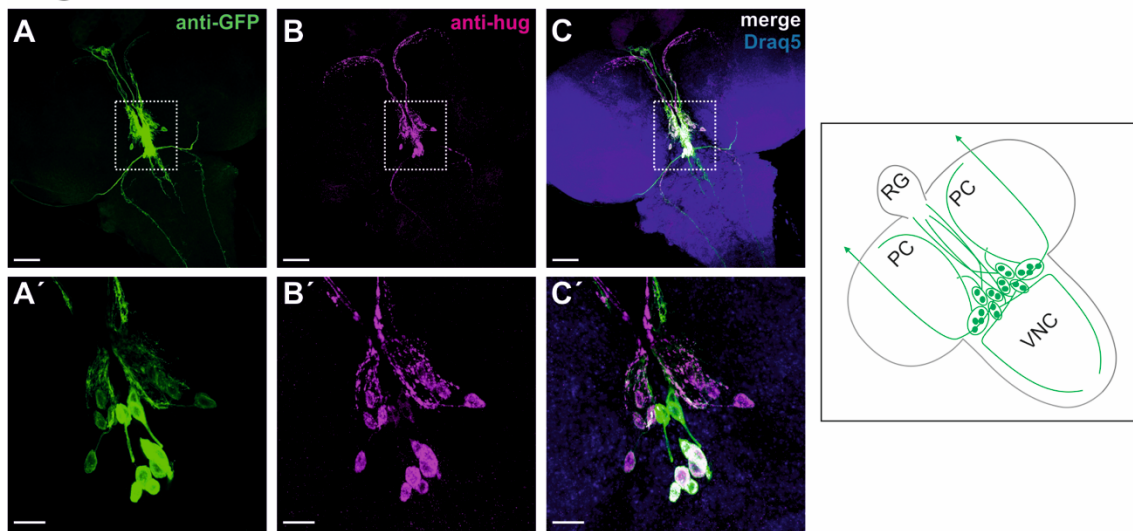
HugS3 > 10xGFP:

Figure S3:

(A–C) Antibody staining of HugS3>10×GFP expression pattern in the CNS; Magnification (A′–C) of Hugin cell cluster (20 cells) in the SOG (A: scale bar: 50 µm; A′: scale bar: 10 µm). Schematic summary of the projection pattern HugS3-Gal4 line in the larval CNS (right side). Target region of the projections are: PC, RG, SOG, VNC and periphery via PaN. Abbr.: CNS – central nervous system; PaN – prothoracic accessory nerve; PC – protocerebrum; RG – ring gland; SOG – subesophageal ganglion;
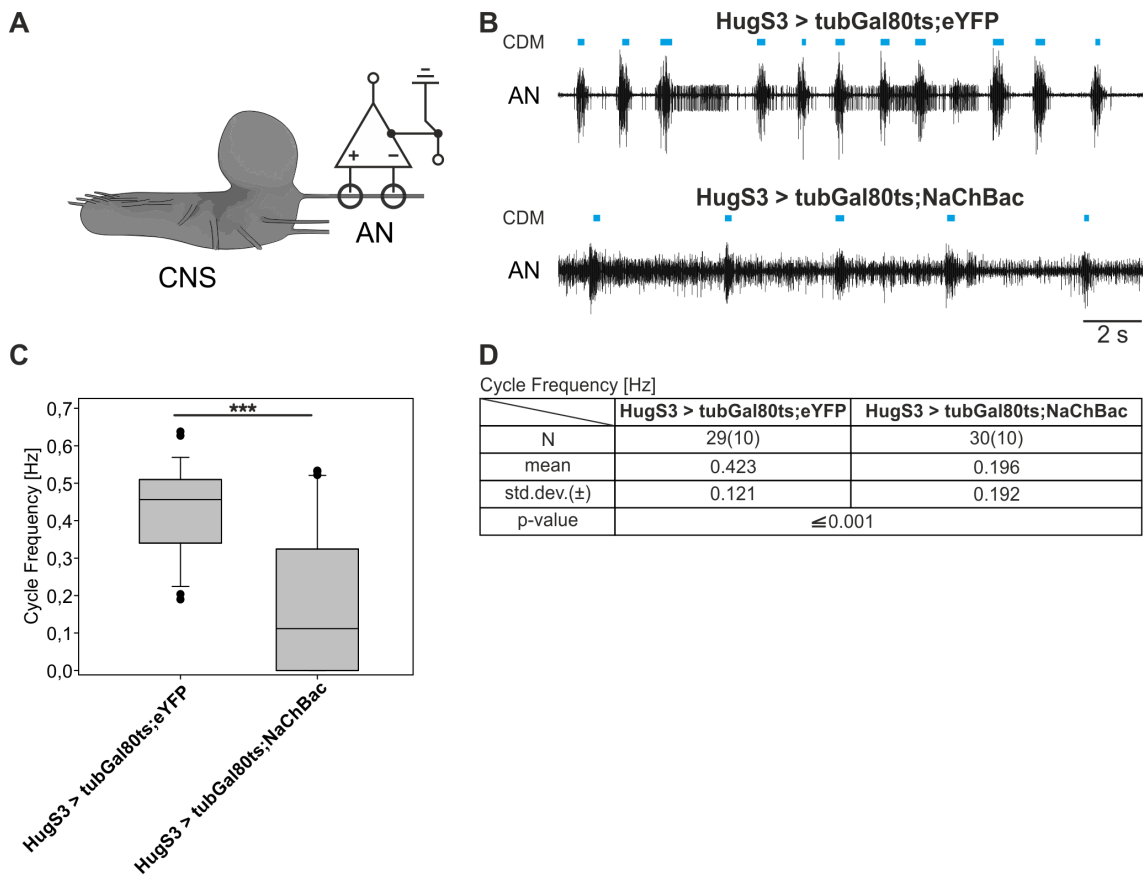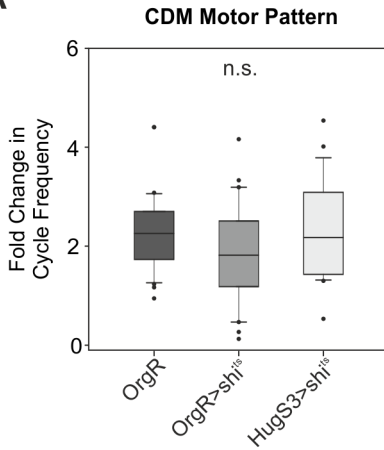
A

CNS

AN

B

HugS3 > tubGal80ts;eYFP

CDM
AN

HugS3 > tubGal80ts;NaChBac

CDM
AN

2 s

C

***

Cycle Frequency [Hz]

HugS3 > tubGal80ts;eYFP

HugS3 > tubGal80ts;NaChBac

D

Cycle Frequency [Hz]

	HugS3 > tubGal80ts;eYFP	HugS3 > tubGal80ts;NaChBac
N	29(10)	30(10)
mean	0.423	0.196
std.dev.(±)	0.121	0.192
p-value	≦0.001	

Figure S4:

(A) Experimental set up of AN recordings at the isolated CNS. Larvae of both genotypes were 166+/−2 h old (raised on 18°C) and kept for at least 8–12 h on 30°C before recording. (B) Original AN recordings of HugS3>tubGal80[ts];eYFP and HugS3>tubGal80[ts];NaChBac (colored boxes represent the CDM activity). (C) Box plot of the cycle frequency [Hz] of HugS3>tubGal80[ts];eYFP (mean (std. dev.): 0.423 (+/−0.121); number of larvae (number of experiments): 29(10)) and HugS3>tubGal80[ts];NaChBac (mean (std. dev.): 0.196 (+/−0.192); number of larvae (number of experiments): 30(10)). HugS3>tubGal80[ts];NaChBac was significant different to HugS3>tubGal80[ts];eYFP (p-value≤0.001). Abbr.: AN – antennal nerve; CDM – cibarial dilator muscle; CNS – central nervous system.
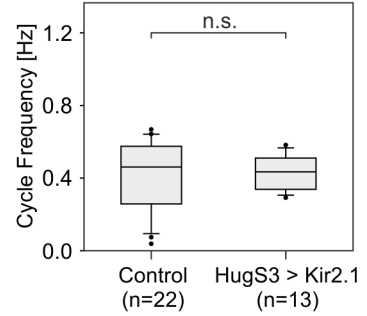
A

CDM Motor Pattern

Fold Change in Cycle Frequency (CDM)

	OrgR	OrgR > shi[ts]	HugS3 > shi[ts]
N	33(12)	39(17)	25(11)
Mean	2.559	2.056	2.44
Std.Dev.(±)	1.348	1.157	1.099
p-Value	0.081		
	↱————0.742————↱		
		0.065	

B

C

M6 Motor Pattern
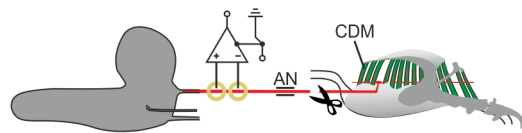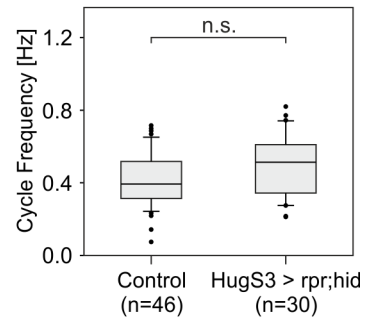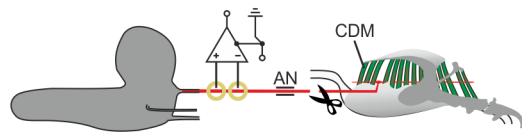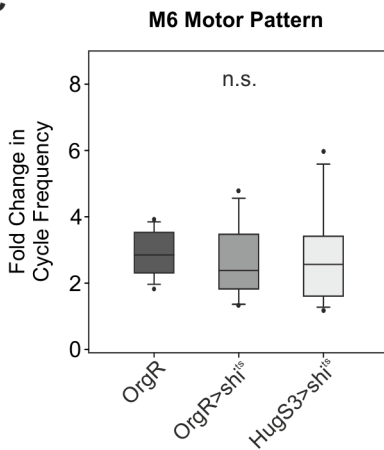
Fold Change in Cycle Frequency (M6)

	OrgR	OrgR > shi[ts]	HugS3 > shi[ts]
N	16(9)	14(9)	13(9)
Mean	2.909	2.682	2.849
Std.Dev.(±)	2.697	1.079	1.408
p-Value	0.495		
	↱————0.882————↱		
		0.732	

Figure S5:

(A)Motor pattern recorded from CDM (presented as box plot for OrgR, OrgR>shi[ts], HugS3>shi[ts]). CDM motor patterns showed no significant difference in fold change of cycle frequency between OrgR, OrgR>shi[ts], HugS3>shi[ts] (performed Mann-Whitney Rank Sum Test (n.s. – not significant)). (B) Left side: Experimental setup for the nerve recordings of HugS3>rpr/hid (upper panel) and HugS3>Kir2.1 (lower panel). Right side: Graph shows the cycle frequency of the AN motor pattern after ablation of the Hugin neurons by the apoptotic factors rpr and hid and during inhibition of Hugin neurons using Kir2.1 (lower panel). Compared to the control (OrgR) inhibiting and ablating the Hugin neurons showed no significant difference (performed Mann-Whitney Rank Sum Test (n.s. – not significant)). (C) Motor pattern recorded from M6 (presented as box plot for OrgR, OrgR>shi[ts], HugS3>shi[ts]). M6 motor output showed no significant difference in fold change of cycle frequency between OrgR, OrgR>shi[ts], HugS3>shi[ts] (performed Mann-Whitney Rank Sum Test (n.s. – not significant)).

A

B

Figure S6:

(A,B) Statistical analysis of food intake and wandering-like behavior assay of OrgR×shi[ts] compared to HugS3>shi[ts] under starved (A) and fed (B) conditions. The graph (left) shows the intake of yeast (area of the alimentary tract stained by colored yeast divided by body surface area) after 20 min at 32°C. Graph (right) illustrates the statistical data of the wandering-like behavior of OrgR×shi[ts] compared to HugS3>shi[ts] measured as larvae outside the yeast/min [%] over a time period of 20 min. In both nutritional conditions HugS3>shi[ts] showed no significant difference in food intake and wandering-like behavior relative to OrgR×shi[ts] at 32°C.

Figure S7:

Hugin antibody staining of the genotypes: OrgR>dTrpA1, HugS3>dTrpA1, HugS3>dTrpA1, HugRNAi1A and HugS3>dTrpA1, TRiP.JF03122. Images show the subesophageal ganglion of the larval CNS as indicated in the schematic drawing (left side, scale bar: 20 μm).

Figure S8:

(A) Hugin antibody staining of hug0.8>rpr/hid showing four remaining cells in the SOG that project to the VNC (A, scale bar: 50 μm; A′, scale bar: 10 μm).
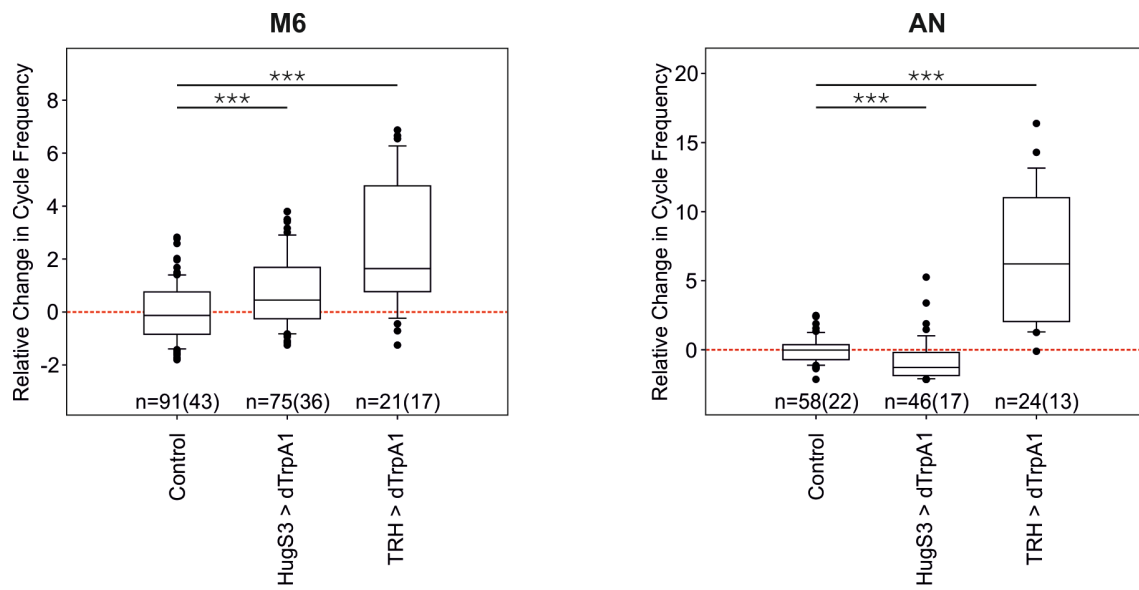
Figure S9:

Graphs show the relative change in cycle frequency of M6- and CDM-motor pattern of HugS3>dTrpA1 and TRH>dTrpA1 compared to the control lines (Mann-Whitney Rank Sum Test: *p≤0.05, **p≤0.01, ***p≤0.001).

4.3   Summary

The specific neural substrates in the CNS that contribute to alterations and adaptation of a certain behavior are still not well understood. Through artificial temperature controlled activation of neurotransmitter- and neuropeptide-expressing cells in the *Drosophila* larval CNS it was possible to screen for neural populations with modulatory effects onto different feeding motor subprograms.

It was shown that glutamatergic (Glu), cholinergic (ACh) and serotonergic neurons (TRH) enhance motor pattern output in all three pharyngeal nerves, whereas only activation of the serotonergic neural population in the brain led to an increase in food intake. Activation of Glu and ACh neural populations led to decrease of food intake, possibly due to an extent of neural activity that no longer can provide the efficient food intake related motor activity. Activation of neural populations expressing the neuropeptide Hugin or the biogenic amine dopamine led to a highly significant decrease specifically in the motor pattern of the AN and no modulation of the motor patterns in the other two pharyngeal nerves. This inhibitory effect was also observed in the food intake assay with intact larvae. A slight but significant decrease in food intake was observed for sNPF neurons, which are known to modulate the hunger response in adult flies. Other peptidergic or aminergic neural populations like GABA, the combination of serotonergic and dopaminergic neurons, octopamine and tyramine, DILP2 and NPF exhibited no significant effect in this food intake screen.

In the following experiments the study focused on the Hugin neuropeptide expressing cell cluster, which shows sparse and exclusive expression in the larval CNS. Activation of the 20 Hugin neurons not only led to a strong decrease in food intake, but also initiated a behavior in which larvae left the attractive food source, yeast. The inhibitory effect of Hugin neurons on the AN motor pattern was verified using a second method to activate neurons (NaChBac). Despite the feeding inhibitory effect upon activation of the Hugin neurons, inactivation of these neurons by either shibire[TS], ablation (induction of the expression of the apoptosis genes reaper and hid, ablation of the cells) or Kir2.1 (potassium inward rectifying channel) did not show any significant effect on feeding motor pattern of the AN. Inactivation with shibire[TS] had also no effect on the food intake or wandering like behavior. A more detailed electrophysiological analysis with intracellular double recordings of the CDM and the abdominal muscle M6 (a commonly used muscle to monitor fictive locomotion) revealed that not only the cycle frequency of the CDM decreased, but simultaneously the cycle frequency of the M6 muscle increased when Hugin neurons are activated in the CNS. Inactivation of Hugin neurons with shibire[TS] did not alter M6 cycle frequency. These results suggested that activity of the Hugin neurons oppositely regulates two mutually exclusive behaviors, feeding and locomotion.

The question arose whether the Hugin neuropeptide expressed by the Hugin neurons is responsible for these effects. Experiments with *hugin* knock down (by RNAi) verified that the Hugin neuropeptide is responsible for the effects on feeding and wandering like behavior. In contrast, M6 muscle recordings implicated that another unknown factor in the Hugin neurons might lead to an up regulation of locomotion.

The Hugin-positive neurons in the CNS are categorized into four classes by their distinct projections targets. To determine whether Hugin positive neurons of a certain class are involved in the feeding and locomotion related phenotypes Hugin promotor driver lines were made. One showed expression only in 16 Hugin positive cells (Hugin$^{0.8}$ neurons, Hug0.8-Gal4), except Hugin^{VNC} neurons, whereas the other showed expression in only the four Hugin^{VNC} neurons (HugVNC-Gal4). This paved the way to study the function of distinct Hugin subclasses. It was shown that activated Hugin$^{0.8}$ neurons exhibit the same feeding related phenotype, as observed for all 20 Hugin neurons. This was not true for activated Hugin^{VNC} neurons, which showed neither an effect on feeding nor on wandering like behavior upon activation. This observation was verified by extracellular recordings of the AN. In contrast, intracellular recordings of the CDM and M6 muscle revealed, that activated Hugin^{VNC} neurons induced an increase in M6 cycle frequency, whereas the Hugin$^{0.8}$ neurons had no effect on M6 cycle frequency. The opposite was true for the CDM activity. It could be concluded that the Hugin positive neurons not projecting to the VNC have an inhibitory effect on feeding, while the Hugin^{VNC} neurons have an excitatory effect on locomotory motor patterns.

Since the Hugin neurons project to distinct brain regions, it was determined which part of the CNS is necessary for the inhibitory effect of Hugin on feeding motor patterns using lesion experiments. Ablation of the VNC had no effect, and larvae still displayed a decline in fictive feeding motor pattern of the AN when all Hugin neurons were activated. When brain hemispheres were lesioned the suppression of the AN motor rhythm by the Hugin neurons was no longer observed, showing that the brain hemispheres are required for Hugin neural function associated with feeding.

Taken together it could be illustrated that neurotransmitters and neuropeptides show various effects on specific aspects of feeding motor subprograms of *Drosophila* larvae. Serotonin was shown to be a major upregulator of the motor patterns of all three pharyngeal nerves. The neuropeptide Hugin displayed an effect on AN and M6 motor patterns. Activation of Hugin neurons in the SEZ leads to a decrease in AN cycle frequency, while increasing cycle frequency of the motor patterns for locomotion. It was concluded that Hugin positive neurons in the *Drosophila* larval brain are potent central regulators of the selection of two mutually exclusive behaviors, feeding and locomotion, in line with physiological functions of its mammalian homolog NMU.

5   Central Relay of Bitter Taste to the Protocerebrum by Peptidergic Interneurons in the *Drosophila* Brain

This chapter of the thesis represents a manuscript submitted for publication. It was submitted on Novemebr 18, 2015 to *Nature Communications* and sent out for formal review.   On February 9, 2016 reviewer comments were sent to us and revision phase started. This manuscript represents the revised version of the follow up study of chapter 4. The current revised manuscript was resubmitted to *Nature Communications* in April 2016 and is under review.

5.1   Introduction

The sense of taste enables animals to distinguish between pleasant, nutritious food sources and harmful or even toxic food. Perceiving the flavor of the one or the other thus influences the decision to swallow or reject a given type of food. Whereas pleasant food is often associated with sweet nutritious sugars, toxic food is associated with bitter taste [BRESLIN & SPECTOR, 2008]. This general association is conserved from flies to humans. Both, mammals and flies are capable of identifying the five prototypical taste modalities bitter, sweet, salty, umami (the taste of protein) and sour. Mammals and flies are attracted by sugars and avoid bitter tasting substances [YARMOLINSKY ET AL., 2009].

It was previously shown that in *Drosophila* taste processing already takes place at the level of receptor neurons, with bitter gustatory neurons being able to suppress the activity of sugar receptors [CHU ET AL., 2014; KÖNIG ET AL., 2015]. Although detailed knowledge exists on the peripheral coding of taste in both mammals and *Drosophila*, very little is known about the cellular identity of neurons that relay taste information in the brain.

From earlier studies in *Drosophila* larvae investigating function of the Hugin neuropeptide, it was shown that Hugin positive dendritic arborizations are in close proximity to the bitter receptor GR66a expressing neurons. This could account for a possible role of Hugin neurons in bitter taste transduction [MELCHER & PANKRATZ, 2005]. Furthermore, as described in the previous chapter, activation of Hugin neurons leads to a decrease of food intake and the induction of wandering like behavior away from an appetitive food source (yeast) [SEE CHAPTER 4: SCHOOFS ET AL., 2014b], a behavior similar to avoidance phenotypes by activation of bitter receptors [MARELLA ET AL., 2006].

This led to the hypothesis, that Hugin neurons might be involved in the processing of bitter taste. In this study the role of Hugin neurons was investigated using behavioral, imaging and electrophysiological approaches to functionally link the perception of bitter taste to the Hugin neuronal cluster as a potential relay for bitter taste to the protocerebrum.

5.1.1 Statement of Contribution

Figure	Experiment	Author
1A	Colocalization analysis of Hugin and GR66a neurons	Sebastian Hückesfeld
1B	GRASP analysis of Hugin and GR66a neurons	Marc Peters
1C-F	Bitter choice assays in larvae with activated or inactivated Hugin neurons	Sebastian Hückesfeld
2A-D	Fructose and salt choice assays in larvae with activated or inactivated Hugin neurons	Sebastian Hückesfeld
3A and B	Olfaction assay in larvae with activated Hugin neurons	Sebastian Hückesfeld
4A-G	Characterization of Hugin^{PC} neurons and behavioral assays in larvae with inactivated Hugin^{PC} neurons	Sebastian Hückesfeld
5A-H	Functional analysis of the Hugin^{PC} neurons	Sebastian Hückesfeld
6	Schematic model	Sebastian Hückesfeld
supplement	Experiments for supplemental material	Sebastian Hückesfeld

5.2   Manuscript

Hückesfeld, S., Peters, M., Pankratz M.J. (XXXX)

Central Relay of Bitter Taste to the Protocerebrum by Peptidergic Interneurons in the *Drosophila* Brain

Peer reviewed, in revision at *Nature Communications*

Central relay of bitter taste to the protocerebrum by peptidergic interneurons in the *Drosophila* brain

Hückesfeld, S., Peters, M. and Pankratz, M.J.

Molecular Brain Physiology and Behavior

Life and Medical Sciences Institute (LIMES), University of Bonn

Bitter represents a taste modality associated with toxic substances and evokes aversive behavior in most animals. We show that hugin neuropeptide neurons in *Drosophila* larval brain are necessary for avoidance behavior to caffeine, and when activated, stops feeding and makes the animals refractory to gustatory cues. They project to the neurosecretory region of the protocerebrum, and functional imaging demonstrates its activation by bitter stimuli and bitter sensory receptor neurons.

Detailed knowledge exists on the anatomical distribution and function of gustatory receptors in mammals and *Drosophila*[1–5]. In *Drosophila* 60 gustatory receptor genes comprise 68 gustatory receptors[6–8], with the majority detecting bitter compounds[9]. Although gustatory receptors in *Drosophila* share no homology to mammalian taste receptors, the strategy to detect a taste molecule, process its information and the valence of aversive bitter and appetitive sweet stimuli share similarities[4]. In contrast to the extensive knowledge on the peripheral coding of taste in flies and mammals, much less is known about the central pathways that relay and translate these into meaningful behavior. Although broad regions in different parts of the brain have been shown to respond to various taste cues, there is little information on the molecular identity of specific neurons that convey different taste modalities to the higher brain centers[10,11]. Recently, secondary neurons that relay sweet taste from subesophageal zone (SEZ) to the antennal mechanosensory motor center of adult *Drosophila* were characterized[12]. Analogous secondary neurons for other taste modalities have not yet been identified.

A candidate for conveying bitter taste from the SEZ to higher brain centers are neurons that express the hugin neuropeptide[13,14], whose arborizations in *Drosophila* larvae overlap with that of bitter gustatory receptor neurons (GRNs) expressing the caffeine receptor GR66a[15–17]. In adult *Drosophila*, GR66a was shown to represent a bitter receptor for detection of caffeine[9,16,17] and inactivation of GR66a positive neurons leads to impairment of caffeine aversion[17]. In *Drosophila* larvae, artificial activation of GR66a positive neurons leads to aversive behavior[18]. Thus, hugin

neurons were good candidates for acting as a central relay for bitter information from sensory neurons. Using classical two-choice behavioral experiments, electrophysiological measurements as well as calcium imaging analysis, we now show that hugin neurons relay caffeine as well as other bitter taste signals from sensory neurons to the protocerebrum.

Results

Hugin neurons are required for avoidance response to caffeine. We first asked whether the hugin neurons make contacts with caffeine responsive GR66a neurons. Using the GRASP (GFP reconstitution across synaptic partners) approach[19], we could indeed observe a GRASP signal in the SEZ, indicating that caffeine receptor neurons and hugin neurons are in close proximity to each other (**Fig. 1a, b**). Activating the hugin neurons causes the larvae to stop feeding and move out of a strongly appetitive food source (yeast)[20], which could be due to activation of an aversive bitter taste pathway. We therefore tested behavioral response to caffeine in a two choice assay. When hugin neurons are activated with the temperature sensitive cation channel dTrpA1, the animals were almost impervious to caffeine stimuli (**Fig. 1c**). We next asked how the animals would behave if hugin neuronal activity was suppressed by ablating the hugin neurons. These animals showed significantly less avoidance to caffeine (**Fig. 1d, e**). To exclude potential developmental effects, we also expressed the temperature sensitive mutant form of dynamin (shibire[TS]) in the hugin neurons, which leads to a block of synaptic release in a temperature dependent manner. The loss of proper bitter aversion still persisted (**Fig 1d, f**).
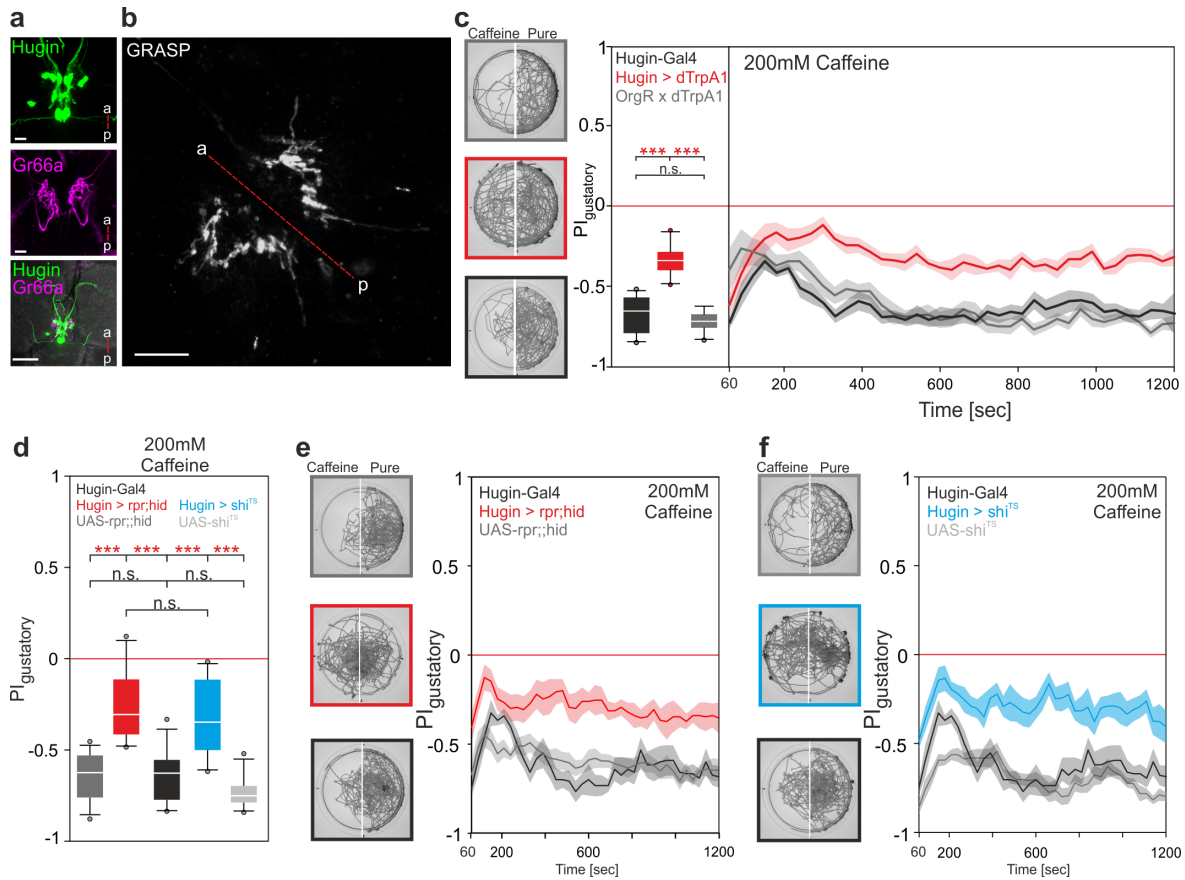
Fig. 1: Hugin neurons are part of bitter gustatory pathway

(**a**) Expression analysis of hugin neurons and GR66a positive dendrites in the SEZ using Hug-YFP;UAS-mRFP line crossed to GR66a-Gal4. Scale bars: 10µm for upper two panels, 50µm for lowest panel. (**b**) Close proximity of GR66a positive dendrites and hugin positive dendrites located in the SEZ using GRASP (Hug1.2lexA attp40 driving lexAop-CD4::spGFP11 crossed to GR66a-Gal4 driving UAS-CD4::spGFP1-10). Scale bar: 10µm. a -- p = anterior – posterior. (**c**) Two-choice assay with 200mM caffeine. Left representative plates are time projections of the last 5 min of the 20 min experiment. Activating hugin neurons with UAS-dTrpA1 (n=10) leads to impairment of choice behavior (p<0.001 compared to OrgR x dTrpA1 (n=10) and Hugin-Gal4 (n=11)). (**d-f**) Two-choice assay with 200mM caffeine. Ablation of hugin neurons by expression of UAS-rpr;;hid (n=10) leads to impairment of bitter substrate avoidance compared to HugS3-Gal4 (n=10) and UAS-rpr;;hid (n=14) controls (p<0.001). Silencing hugin neurons by expression of UAS-shibire^{TS} (n=10) shows same impairment on gustatory bitter choice compared to HugS3-Gal4 (n=10) and UAS-shi^{TS} (n=10) controls (p<0.001). All two-choice experiments were performed at 32°C. For statistics Mann-Whitney-Rank-Sum-Test was used. Boxplots were generated from PI values of the last 5 min of the 20 min experiment time. Significances are indicated as ***p<0.001, **p<0.01 and *p<0.05. Line plots showing the time course of the two choice experiments are displayed as mean (line) ± SEM (transparent areas). Details of descriptive statistics are shown in **Supplementary Table 1**.

We next asked if hugin neurons were involved in other taste modalities. We first tested high salt (2M NaCl), which is very aversive for larvae, in two-choice assays. As with caffeine, activation of the hugin neurons led to animals being almost impervious to high salt (**Fig 2a**). However, no difference to control was observed when hugin neurons were ablated,

indicating that hugin neurons are not required for behavioral response to high salt (**Fig. 2b**). High caffeine and salt levels are both aversive gustatory stimuli. To determine how manipulation of hugin neuronal activity affected response to an appetitive cue, we performed two-choice assays with 1M fructose. Similar result was obtained as with high salt, namely that activation led to refractory behavior, whereas ablation had no effect relative to control **(Fig. 2c, d; Supplementary Figure 1)**. Thus, when hugin

neurons are activated, the larvae become refractive to different taste modalities, as represented by yeast protein[20], fructose, high salt and caffeine. This chemosensory response was specific for taste, as olfactory behavior was not affected **(Fig 3)**, showing that activation of hugin neurons selectively disrupts gustatory chemosensory processing. However, inhibiting the hugin neurons results in the inability to respond appropriately to caffeine, indicating that hugin neurons process caffeine taste information.
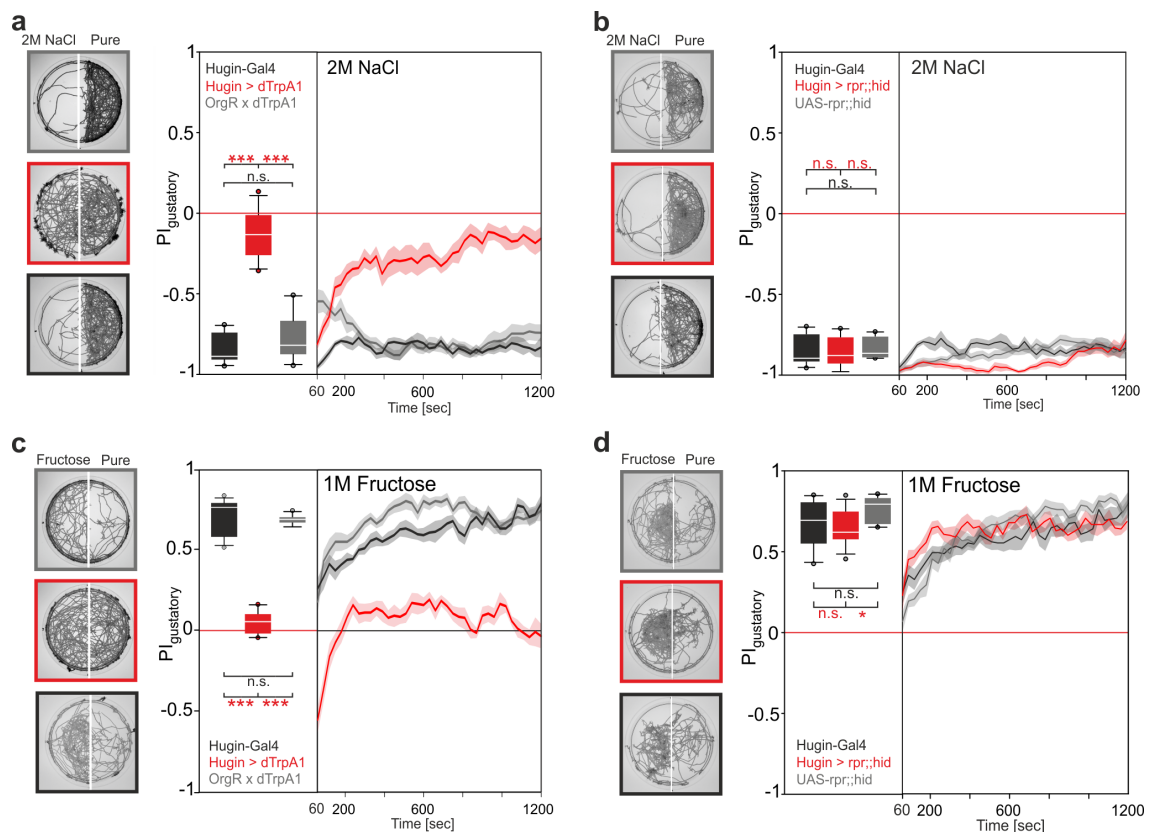
Fig. 2: Hugin neurons impair, but are not necessary for high salt or sweet taste processing

(**a**) Two choice assay with 2M NaCl. Activating hugin neurons with UAS-dTrpA1 (n=11) leads to impairment of choice behavior (p<0.001 compared to OrgR x dTrpA1 (n=10) and Hugin-Gal4 (n=10)). (**b**) No significant difference in avoidance behavior was observed on 2M NaCl between Hugin > rpr;;hid (n=10) and UAS-rpr;;-hid (n=10), p=0.165 or Hugin-Gal4 (n=10), p=0.838. (**c**) Two choice assay with 1M fructose. Activating hugin neurons with UAS-dTrpA1 (n=11) leads to impairment of choice behavior (p<0.001 compared to OrgR x dTrpA1 (n=11) and Hugin-Gal4 (n=13)). (**d**) There was no significant difference on 1M fructose choice behavior between Hugin

> rpr;;hid (n=12) and Hugin-Gal4 (n=10), p=0.306. UAS-rpr;;hid larvae (n=10) showed significant difference to Hugin > rpr;;hid (p=0.013). Sample two choice plates are shown on the left side of each experiment for each genotype for the last 5 min of the experiment. For statistics Mann-Whitney-Rank-Sum-Test was used. Boxplots were generated from PI values of the last 5 min of the 20 min experiment. Significances are indicated as ***p<0.001, **p<0.01 and *p<0.05. Line plots showing the time course of the two choice experiments are displayed as mean (line) ± SEM (transparent areas). Details of descriptive statistics are shown in **Supplementary Table 2**.

Fig. 3: Activation of hugin neurons does not impair attractive olfactory guidance

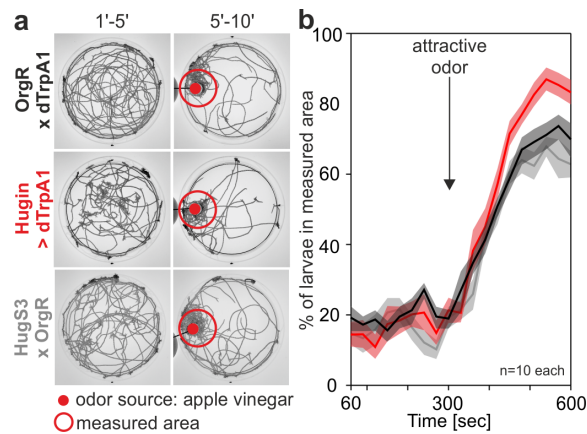(**a**) Olfactory assay for choice behavior in response to an attractive odor (apple vinegar). Shown are time projections of the pure agar plates for the first 5 min of the experiment and the last 5min of the experiment with the appetitive odor source apple vinegar. (**b**) Larvae of all three geneotypes (OrgR x dTrpA1, Hugin > dTrpA1 and HugS3 x OrgR) detected the appetitive odor at the same timepoint and were equally fast at reaching the nearby area beneath the apple vinegar spot above the plate.

Hugin neurons projecting to the protocerebrum modulate taste and feeding behavior. As the hugin neuronal cluster is composed of different classes with different projection targets[13,14], we next wanted to determine which class was responsible for taste processing and feeding regulation. Through promoter deletion analysis, we generated a hugin promoter-Gal4 line which showed target gene expression exclusively in the eight hugin cells (four per hemisphere) that project to the protocerebrum (HugPC-Gal4, **Fig. 4a**). To see whether this subset of hugin neurons (huginPC neurons) is necessary for proper bitter taste processing, we ablated

these neurons (**Fig. 4b**) and tested larvae in the caffeine two-choice experiment. Ablation of the huginPC neurons resulted in the inability to avoid caffeine as compared to control animals (**Fig. 4c**). Consistent with the ablation of all hugin neurons (**see Fig. 2**), ablating just the huginPC neurons had no effect compared to controls on high salt or fructose (**Fig. 4d, e**). We note that, in the case of 2M NaCl, there was a significant difference to one of the control animals (UAS-rpr;;hid control larvae). Therefore, we additionally tested the animals on a lower, but still aversive salt concentration (500mM), and this showed that huginPC neuron are not necessary for proper high salt

aversion (**Supplementary Figure 2**). Activating just the huginPC neurons was also sufficient to suppress food intake, induce wandering-like behavior (**Fig. 4f; Supplementary Figure 3**), as well as decrease the motor pattern of pharyngeal muscle contractions (**Fig. 4g**). These results indicated that the hugin neurons responsible for feeding and caffeine taste mediated behaviors are those that project to the protocerebrum.
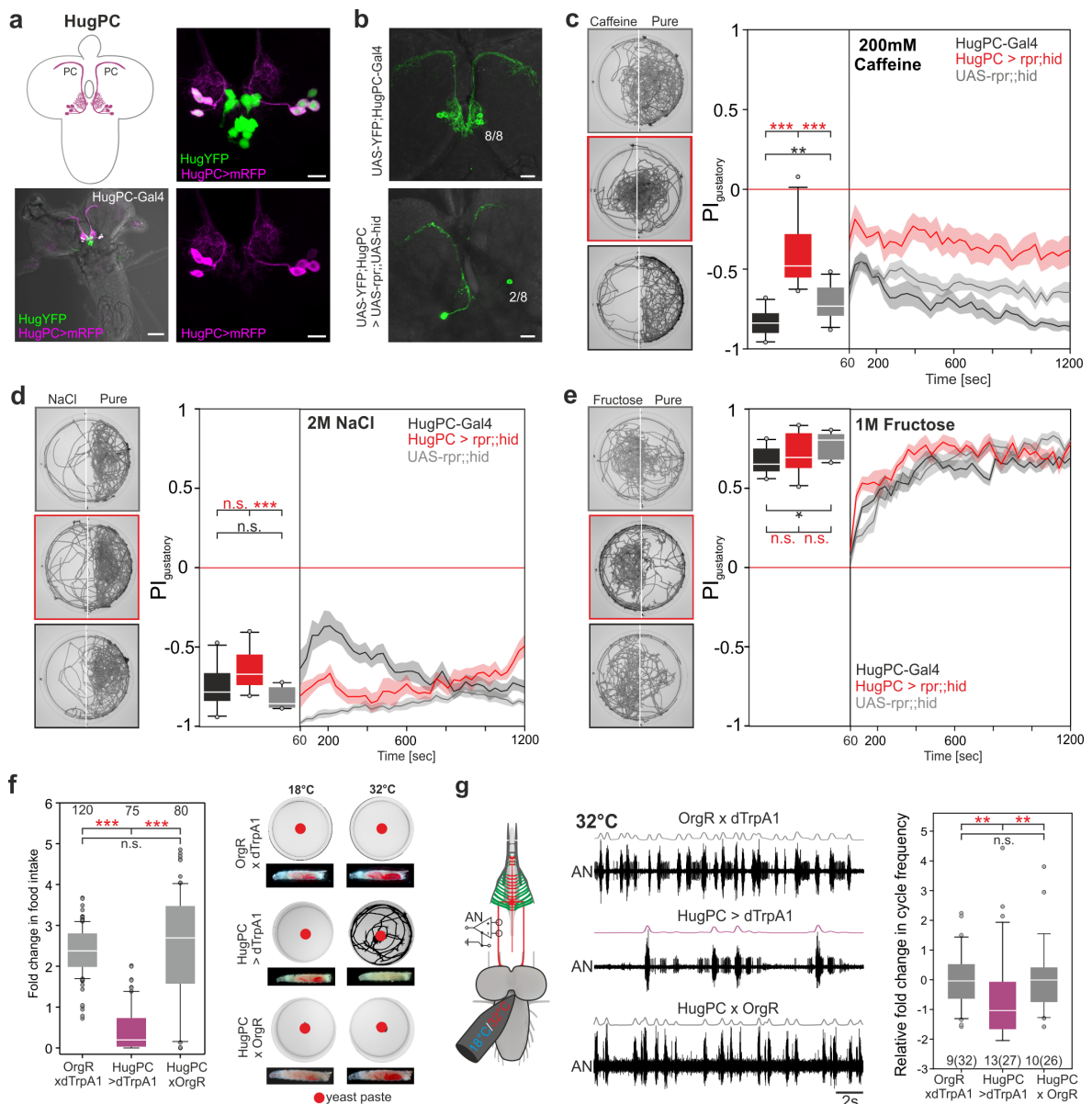

Fig. 4: HuginPC neurons modulate feeding and aversive gustatory behavior

(**a**) Expression of hugin neurons in HugPC-Gal4 line crossed to Hug-YFP;UAS-mRFP line. Eight hugin neurons that project to the protocerebrum are labelled by UAS-mRFP. Scale bars: 50µm for left and 10µm for right panels. (**b**) In HugPC > rpr;;hid larvae 6 of 8

huginPC neurons were ablated successfully (n=17); 2 (+/- 0.3 SE). (**c**) Two choice assay with caffeine after ablation of huginPC neurons with UAS-rpr;;hid (n=13). (p<0.001 compared to HugPC-Gal4 (n=10) and UAS-rpr;;hid (n=14). (**d**) Two-choice assay with 2M NaCl. Ablating huginPC neurons causes no impairment of high salt avoidance compared to HugPC-Gal4 (n=10) (p<0.001). A significant difference in salt avoidance occurred comparing HugPC > rpr;;hid with UAS-rpr;;hid larvae (n=10, p<0.001). (**e**) Two-choice assay with 1M fructose. Ablating huginPC neurons with UAS-rpr;;hid (n=10) causes no impairment in fructose attraction compared to HugPC-Gal4 (n=10, p=0.241) or UAS-rpr;;hid (n=10, p=0.450). Controls show significant difference to each other (p=0.013). (**f**) HugPC-Gal4 line driving UAS-dTrpA1 (n=75 larvae). Larvae show reduction in food intake compared to OrgR x dTrpA1 (n=120 larvae) and HugPC x OrgR (n=80 larvae) (p<0.001). Activation of huginPC neurons with dTrpA1 induces wandering like behavior, where larvae leave the appetitive food source yeast. Shown are time projections over 20 min of plates with apple juice agar and a red spot of yeast in the middle. Decrease of food intake was measured as % of red stained gut content compared to the area of the whole larva. (**g**) Extracellular recordings of the antennal nerve (AN). Activation of huginPC neurons leads to significant decrease in cycle frequency of the AN motor pattern compared to OrgR x dTrpA1 (n=9 larvae, 32 temperature steps) and HugPC x OrgR (n=10 larvae, 26 temperature steps) (p=0.003). For statistics Mann-Whitney-Rank-Sum-Test was used. Boxplots were generated from PI values of the last 5 min of the 20 min experiment time in two-choice assays. Significances are indicated as ***p<0.001, **p<0.01 and *p<0.05. Line plot shows the time course of the two choice experiment displayed as mean (line) ± SEM (transparent areas). Details of descriptive statistics are shown in **Supplementary Table 3.**

Calcium imaging of huginPC neurons upon bitter stimulation. To further investigate the connection between bitter taste and hugin neurons, we asked if the huginPC neurons could be activated by caffeine using CaMPARI (<u>Ca</u>lcium <u>M</u>odulated <u>P</u>hotoactivatable <u>R</u>atiometric <u>I</u>ntegrator), that allows monitoring of calcium activity in intact animal. Calcium activity and simultaneous presence of UV-Light (405nm) lead to an irreversible conversion from green to red fluorescence of the neurons of interest[21]. When we placed intact larvae in solutions containing water and water mixed with caffeine, fructose, high NaCl or yeast (**Fig. 5a**), huginPC neurons were strongly activated by caffeine (**Fig. 5b, c**). They also showed concentration dependent increase in calcium activity with increasing caffeine concentrations (**Fig. 5d**). Other bitter tastants, such as quinine and denatonium, also activated huginPC neurons (**Fig. 5e).** For denatonium, calcium activity in huginPC neurons was behaviorally relevant since ablation of these neurons resulted in larvae with impaired avoidance (**Fig. 5f**). Unexpectedly, we observed decrease in huginPC calcium activity in larvae placed in high salt, fructose and yeast relative to water alone (**Fig. 5c**). Although the functional significance of this repression is not clear, it has been shown that bitter taste pathways can inhibit sweet pathways[22], reflecting an interaction between pathways involving different taste modalities.
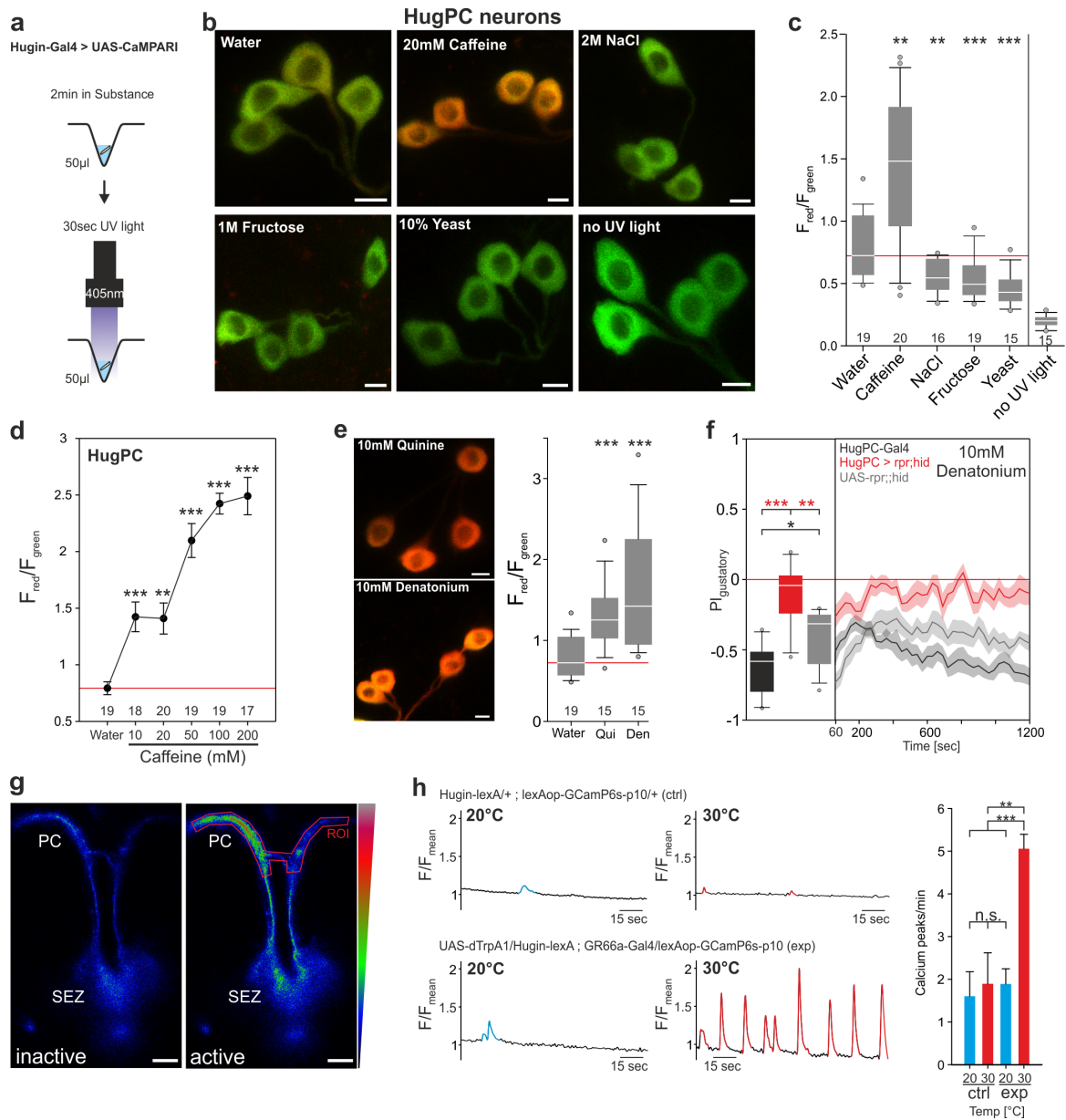
Fig. 5: HuginPC neurons relay bitter taste information

(**a**) Experimental setup (left panel). (**b**) Larvae expressing UAS-CaMPARI in huginPC neurons showed green to red photoconversion only when larvae were placed in caffeine solution. Scale bars: 5µm. (**c**) Quantification of F_{red} divided by F_{green} for z-projections of huginPC neurons (p=0.003 for caffeine, p=0.004 for NaCl, p<0.001 for fructose and p<0.001 for yeast mixed in water compared to pure water). Right most boxplot shows fluorescence ratio of huginPC neurons without UV light exposure. (**d**) Measurement of huginPC neurons expressing UAS-CaMPARI in larvae confronted with different concentrations of caffeine. HuginPC neurons display increasing red/green ration with increasing caffeine concentration (10mM: p<0.001, 20mM: p=0.003, 50mM: p<0.001, 100mM: p<0.001, 200mM: p<0.001 compared to water alone). Dots represent mean, whiskers represent SEM. (**e**) HuginPC neurons expressing UAS-CaMPARI display high calcium activity in 10mM quinine (p<0.001) or 10mM Denatonium (p<0.001). numbers indicate number of larvae used for each experiment. (**f**) Two-choice assay with 10mM denatonium. Ablating huginPC neurons with UAS-rpr;;hid leads to impairment of gustatory choice on denatonium compared to HugPC-Gal4 (n=10, p<0.001) or UAS-rpr;;hid (n=12, p=0.002). controls

show significant difference to each other (p=0.027). (**g**) Example of huginPC neuronal arborizations in the protocerebrum expressing GCamP6s in inactive and active state. (**h**) Activation of GR66a neurons by dTrpA1 in larvae expressing Hugin-lexA-lexAop-GCamP6s. Sample traces of calcium currents show rhythmic activity of huginPC projections when GR66a neurons are activated at 30°C. Quantification of calcium spikes/min showed no significant difference between control (ctrl, n=13) and experimental genotypes (exp, n=13) at 20°C (p=0.241); control at 20°C and 30°C (p=0.790); and control at 30°C and experimental genotype at 20°C (p=0.197). Significant difference could be shown for the experiment at 20°C and 30°C (p=0.004), as well as control at 20°C compared to experiment at 30°C (p<0.001). Scale bars: 20μm. For statistics Mann-Whitney-Rank-Sum-Test was used. Boxplots were generated from PI values of the last 5 min of the 20 min experiment time for two-choice experiment. Significances are indicated as ***p<0.001, **p<0.01 and *p<0.05. Line plots showing the time course of the two choice experiment and dot plots are displayed as mean (line) ± SEM (transparent areas). Details of descriptive statistics are shown in **Supplementary Table 4**.

Finally we asked if there is a functional connection, in addition to the anatomical connection (see **Fig. 1a, b**), between the caffeine sensing GR66a neurons and hugin neurons. To this end, we activated the GR66a neurons and then monitored the activity of hugin neurons using the calcium indicator GCaMP6s (**Fig. 5g**). Activation of GR66a by dTrpA1 and simultaneous calcium imaging of huginPC projections resulted in an induction of rhythmically occurring calcium peaks, demonstrating a functional connection between GR66a and huginPC neurons (**Fig. 5h**).

Discussion

Bitter taste rejection response is important for all animals that encounter toxic or harmful food in their environment. Here we could show that the hugin neurons in the *Drosophila* larval brain function as a relay between bitter sensory neurons and higher brain centers (**Fig. 6**). Strikingly, activation of the hugin neurons made the animals refractory to substrates with negative valence like bitter

(caffeine) and salty (high NaCl), as well as positive valence like sweet (fructose).
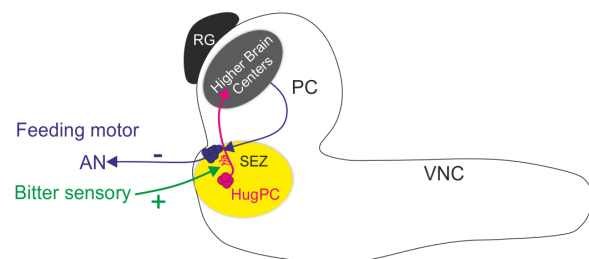
Fig. 6: HuginPC neurons act as gustatory interneurons for bitter taste

Bitter taste detected in peripheral taste organs activate huginPC neurons. Activity of huginPC neurons projecting to higher brain centers leads to a decrease in food intake and in the cycle frequency of feeding related motor patterns in the antennal nerve (AN). Activation of huginPC neurons also leads to aversion to different gustatory substrates, including yeast, thereby triggering aversive behavior. Thus, huginPC neurons act as relay of bitter taste to the protocerebrum in the Drosophila larval brain.

In other words, when the hugin neurons are active these animals "think" they are tasting bitter and therefore become insensitive to

other gustatory cues. This is in line with observations made in mice, where optogenetically activating bitter cortex neurons caused animals to avoid an empty chamber illuminated with blue light. In this situation, although mice do not actually taste something bitter, they avoid the empty chamber since the bitter flavor has been implanted into the CNS by optogenetic means[23]. In our previous work, activation of all hugin neurons led to behavioral and physiological phenotypes such as decreased feeding, decrease in neural activity of the antennal nerve, and induction of a wandering-like behavior[20]. We have now pinpointed the neurons responsible specifically to those that project to the protocerebrum. These neurons not only respond to bitter stimuli, but also show a concentration dependent increase in calcium activity in response to caffeine. The dose dependent coding of bitter taste stimuli has earlier been shown to be true for peripheral bitter sensory neurons, where bitter sensilla exhibit dose dependent responses to various bitter compounds[9]. Interestingly, the huginPC neurons are inhibited when larvae taste other modalities like salt (NaCL), sugar (fructose) or protein (yeast). This may indicate that taste pathways in the brain are segregated but influence each other, as previously suggested[10]. Bitter compounds may be able to inhibit the sweet-sensing response to ensure that bitter taste cannot be masked by sweet tasting food. This provides an efficient strategy for the detection of potentially harmful or toxic substances in food[24,25]. For appetitive tastes like fructose and yeast, bitter neurons may become inhibited to ensure appropriate behavior to food. Salt is a bivalent taste modality which in low doses drives appetitive behavior, whereas in high doses is aversive to larval[26,27] and adult[28,29] *Drosophila*. Inhibition of huginPC neurons when larvae are tasting salt might be due to a different processing circuits for different concentrations of salt and the decision to either take up low doses or reject high doses. Taken together, we propose that hugin neuropeptide neurons projecting to the protocerebrum represent a hub between bitter gustatory receptor neurons and higher brain centers that integrate bitter sensory information in the brain, and through its activity, influences the decision of the animal to avoid a bitter food source. The identification of second order gustatory neurons for bitter taste will not only provide valuable insights into bitter taste pathways in *Drosophila*, but may also help in assigning a potentially novel role of its mammalian homolog neuromedin U in taste processing.

Methods

Fly lines. Wild type (OrgR) crossed to UAS-dTrpA1 (Bloomington #26263) served as control in Fig.1 and Fig. 2. Hugin-Gal4 (HugS3-Gal4[13], Bloomington# 58769), GR66a-Gal4 (2nd Chr., gift from K.Scott[30](formerly described as GR66C1)), GR66a-Gal4 (3rd Chr., Bloomington# 57670 used in Fig. 3d), Hugin-lexA (Hug1.2-lexA attp40[31]), HugPC-Gal4 (see generation of this Gal4-line below), UAS-eNpHR-YFP ((Bloomington# 41753, referred here as UAS-YFP in Supplementary Fig. 3, since this homozygous line together with HugPC-Gal4

was used as fluorescent marker only), UAS-CaMPARI (Bloomington #58761), UAS-rpr;;UAS-hid (UAS-rpr (Bloomington# 5823) crossed homozygous to UAS-hid[32]), UAS-shibire[TS 33], lexAop-CD4::spGFP11 and UAS-CD4::spGFP1-10 were gifts from K. Scott[19], 13x LexAop2-IVS-GCaMP6s-p10 (Bloomington #44274).

Fly Care. Adult flies and larvae were kept on 25°C under 12h light/dark conditions. For electrophysiological and food intake experiments 4h egg collections were made on apple juice agar plates containing a spot of yeast-water paste. After 48h, larvae were transferred into food vials containing lab standard fly food. For other experiments (two-choice, CaMPARI, GCaMP) larvae were raised in vials containing standard fly food with a spot of yeast for 4 days. All larvae used for the experiments were 98 +/- 2 h old. Only feeding 3rd instar larvae were used for the experiments.

Generation of transgenic Flies. For HugPC-Gal4 line, a 544 bp Hugin fragment 155 bp upstream of the ATG was amplified with primer1 (AAG GGT TTG GTT TAA TTT ATT TAT GTC ATA) and primer2 (GAG CCT GAT TAG GTC CCT GAT GTT TAA ACT T) and cloned into pCaSpeR-AUG-Gal4-X vector (Addgene plasmid 8378. The construct was injected into w[[1118]]).

Two-choice gustatory assay. To measure the preference index of larvae towards given appetitive or aversive substrates, 9mm diameter petri dishes were filled with 20ml warm water agar (2.125% Agar-Agar, Kobe).

After 20min of air drying half of the agar was cut away and discarded. Compounds (2M NaCl, 1M Fructose, 200mM Caffeine, 10mM Denatonium) were diluted in warm agar in the given concentration until the agar fluid was clear, and filled in the other half of the petri dish (10ml). After air drying again for 20min, petri dishes were prewarmed in the 32°C incubator 1.5h prior to the experiment. All two-choice experiments were performed at 32°C for comparability between all genotypes. For each experiment 30 larvae were taken out of standard fly food and washed with tap water. Larvae were then placed on the water side of the two-choice dishes and videotaped for 20min. Videos were processed with FIJI (ImageJ) and analyzed using a custom written script for FIJI. Analysis of PI values started 60 seconds after the start of the experiment to ensure proper tracking of larvae due larval accumulation at the beginning by placing them on the pure agar side. $PI_{gustatory}$ was calculated as (#larvae$_{substrate}$ - #larvae$_{water}$)/#larvae$_{total}$.

One-choice olfactory assay. For testing response to an attractive odor (apple vinegar), a one-choice assay was performed. Agar plates were used (as described earlier for two-choice petri dishes) and placed into the incubator at 32°C for 1.5h. Larvae were videotaped at 32°C for 5 min, and then an Eppendorf cup (1.5ml) with filter paper soaked with apple vinegar was placed on one side of the water agar plate above the larvae such that they were not able to reach the odorant source. Movement of larvae was analyzed using the custom made FIJI macro.

Food intake assay. Apple juice agar plates were prepared with a spot of red yeast paste in the middle of the plate. Plates were then placed in incubators precooled to 18°C or prewarmed to 32°C for 2h. After 30min starvation, 5 larvae were transferred on top of the yeast paste of a plate and videotaped for 20min. After 20min of videotaping, larvae were transferred into a small cell strainer and washed with 60°C hot water. Larvae were then transferred to glass slides for photo documentation and analyzed with the open source software FIJI (ImageJ) and a custom written analysis macro, which calculated the percentage of the red stained surface of the body compared to the whole body of the larva. To calculate the fold change of food intake from 18°C to 32°C, the value of all 32°C values was divided by the mean value of all 18°C values.

Electrophysiology. 3rd instar larvae were dissected in 35mm petri dishes coated with 5ml two-component silicone (Elastosil RT). Larvae were pinned down dorsal side up at the anterior and posterior end using 77µm thick sharp etched tungsten needles. The larva was cut open longitudinally along the dorsal midline and the cuticle was pinned aside with 40µm tungsten needles. Interior organs like fat body, intestine or salivary glands were removed except for the cephalopharyngeal skeleton and CNS with attached nerves of interest. Eye and leg imaginal discs were also removed. A transversal cut of the cuticle was performed beneath the CNS to reveal the antennal nerve (AN). Nerves not needed for the respective recording were cut. A piece of thinned Parafilm was placed beneath the nerve of interest. This nerve was isolated from the surrounding solution with two adjacent jelly pools. Motor output of the AN was measured using custom made silver wire electrodes connected to a preamplifier (Model MA103, Ansgar Büschges group electronics lab). The preamplifier was connected to a four-channel amplifier/signal conditioner (Model MA 102, Ansgar Büschges group electronics lab). All recorded signals were amplified (amplification factor: 5000) and filtered (bandpass: 0.1-3 kHz). Recordings were sampled at 20 kHz. Data was acquired with Micro3 1401 A/D board (Cambridge Electronic Design) and Spike2 software (Cambridge Electronic Design).

Calcium imaging with CaMPARI. 405nm high power LED (Thorlabs, M405L2 - UV (405 nm) Mounted LED, 1000 mA, 410 mW) was driven with a LED controller (Thorlabs, LEDDB1 driven with 1000mA) and positioned 18cm above the solution with the larva. 96-well PCR plate was filled with 50µl containing the given taste stimuli in tap water. Larvae were placed into the solution for 2min and then UV light was applied for 30sec.

Afterwards brains were dissected in PBS and mounted onto a Poly-L-lysine (Sigma, Lot # SLBG4596V) coated cover slide with a drop of PBS. All z-stacks of the HugPC neurons were aquired using a ZEISS LSM 780 Laser scanning microscope with LCI Plan-Neofluar 25x/0.8Imm Korr DIC M27. For quantification of green to red photoconversion maximum intensity projections of the acquired z-stacks

were used and a portion of the cytoplasmatic region of each cell was analyzed to obtain data for green and red fluorescence intensity. Red fluorescence intensity was divided by green fluorescence intensity to get F_{red}/F_{green} ratio. A "no UV light" control was included to show that scanning of the CNS without being exposed to UV light does not convert green to red fluorescence.

GRASP. Genotypes used for GRASP (GFP reconstitution across synaptic partners) method[19] were: Hug1.2lexA;lexAop-CD4::spGFP11 and GR66a-Gal4;UAS-CD4::spGFP1-10. Larval CNS was dissected and stained with anti-mouse-GFP (Abcam, 1:500, secondary antibody was anti-mouse-AI488 (Invitrogen, 1:500)). Images were acquired using a ZEISS LSM 780 Laser scanning microscope with LCI Plan-Neofluar 25x/0.8Imm Korr DIC M27.

Calcium imaging with GCaMP. Freshly dissected CNS of feeding third instar larvae of the genotypes UAS-dTrpA1/Hug1.2lexA; GR66a-Gal4/lexAop-GCamP6s-p10 (experiment) and Hug1.2lexA/CyO; lexAop-GCamP6s/TM3, Sb (control) were placed with the SEZ region up on a Poly-L-lysine coated coverslide in a drop of saline. Coverslide was attached to a custom built heating device consisting of a 1.5cm^2 Peltier element for shifting the temperature from 20°C to 30°C by applying specific voltage values. Images were acquired with a Zeiss LSM 780 laser scanning microscope as time series with a speed of 781.96ms (approx. 1.28Hz) using a Zeiss LCI "Plan-Neofluar" 25x/0.8 Imm Korr DIC M27

objective dipped in the saline solution. Region of interest covered the complete HugPC neuronal "sprinkler-like" arborization pattern in the protocerebrum.

Statistics. For comparison of two groups in the two choice assays Mann-Whitney-Rank-Sum-Test was used. Statistical data was acquired as cumulative PI values of the last 5 min of the 20min experiment and displayed as boxplots. For food intake analysis 32°C values (% of red yeast in gut relative to whole body) were divided by the mean of all 18°C values to gather the fold change of food intake. Fold changes were then compared with the Mann-Whitney-Rank-sum-Test. For electrophysiological data cycle frequencies were analyzed at 18°C for 60sec and 32°C for 60sec. The fold change was calculated between 18°C and 32°C. Per larva a maximum of 4 temperature steps could be applied to the CNS during recordings. All fold changes of one genotype were then compared with the Mann-Whitney-Rank-Sum-Test with the other genotypes. The relative fold change is displayed as subtraction of the mean of OrgR x dTrpA1 control values from the fold change values of all genotypes (OrgR x dTrpA1 set to 0). CaMPARI data were analyzed by calculating the mean F_{red}/F_{green} value of all 8 HuginPC neurons of one larvae to determine one mean F_{red}/F_{green} value per larva. Values were then compared with the Mann-Whitney-Rank-Sum-Test to water control.

References

1. Kwon, J. Y., Dahanukar, A., Weiss, L. a & Carlson, J. R. Molecular and cellular organization of the taste system in the *Drosophila* larva. *J. Neurosci.* **31,** 15300–15309 (2011).

2. Apostolopoulou, A. A., Rist, A. & Thum, A. S. Taste processing in *Drosophila* larvae. *Front. Integr. Neurosci.* **9,** 1–9 (2015).

3. Breslin, P. A. S. & Spector, A. C. Mammalian taste perception. *Curr. Biol.* **18,** R148–55 (2008).

4. Yarmolinsky, D. A., Zuker, C. S. & Ryba, N. J. P. Common sense about taste: From mammals to insects. *Cell* **139,** 234–244 (2009).

5. Joseph, R. M. & Carlson, J. R. *Drosophila* Chemoreceptors: A molecular interface between the chemical world and the brain. *Trends Genet.* **31,** 683–695 (2015).

6. Clyne, P. J. Candidate taste receptors in *Drosophila*. *Science* **287,** 1830–1834 (2000).

7. Scott, K. *et al.* A chemosensory gene family encoding candidate gustatory and olfactory receptors in *Drosophila Cell* **104,** 661–673 (2001).

8. Dunipace, L., Meister, S., McNealy, C. & Amrein, H. Spatially restricted expression of candidate taste receptors in the *Drosophila* gustatory system. *Curr. Biol.* **11,** 822–835 (2001).

9. Weiss, L. A., Dahanukar, A., Kwon, J. Y., Banerjee, D. & Carlson, J. R. The molecular and cellular basis of bitter taste in *Drosophila*. *Neuron* **69,** 258–272 (2011).

10. Harris, D. T., Kallman, B. R., Mullaney, B. C. & Scott, K. Representations of taste modality in the *Drosophila* brain. *Neuron* **86,** 1449–1460 (2015).

11. Carleton, A., Accolla, R. & Simon, S. A. Coding in the mammalian gustatory system. *Trends Neurosci.* **33,** 326–334 (2010).

12. Kain, P. & Dahanukar, A. Secondary taste neurons that convey sweet taste and starvation in the *Drosophila* brain. *Neuron* **85,** 819–32 (2015).

13. Melcher, C. & Pankratz, M. J. Candidate gustatory interneurons modulating feeding behavior in the *Drosophila* brain. *PLoS Biol.* **3,** e305 (2005).

14. Bader, R. *et al.* Genetic dissection of neural circuit anatomy underlying feeding behavior in *Drosophila*: distinct classes of hugin-expressing neurons. *J. Comp. Neurol.* **502,** 848–56 (2007).

15. Marella, S. *et al.* Imaging taste responses in the fly brain reveals a functional map of taste category and behavior. *Neuron* **49,** 285–295 (2006).

16. Moon, S. J., Köttgen, M., Jiao, Y., Xu, H. & Montell, C. A Taste receptor required for the caffeine response in vivo. *Curr. Biol.* **16,** 1812–1817 (2006).

17. Thorne, N., Chromey, C., Bray, S. & Amrein, H. Taste perception and coding in *Drosophila*. *Curr. Biol.* **14,** 1065–1079 (2004).

18. Hernandez-Nunez, L. *et al.* Reverse-correlation analysis of navigation dynamics in *Drosophila* larva using optogenetics. *Elife* **4,** 1–4 (2015).

19. Gordon, M. D. & Scott, K. Motor control in a *Drosophila* taste circuit. *Neuron* **61,** 373–84 (2009).

20. Schoofs, A. *et al.* Selection of motor programs for suppressing food intake and inducing locomotion in the *Drosophila* brain. *PLoS Biol.* **12,** e1001893 (2014).

21. Fosque, B. F. *et al.* Neural circuits. Labeling of active neural circuits in vivo with designed calcium integrators. *Science* **347,** 755–60 (2015).

22. Chu, B., Chui, V., Mann, K. & Gordon, M. D. Presynaptic gain control drives sweet and bitter taste integration in *Drosophila*. *Curr. Biol.* **24,** 1978–1984 (2014).

23. Peng, Y. *et al.* Sweet and bitter taste in the brain of awake behaving animals. *Nature* 1–12 (2015)

24. French, A. S. *et al.* Dual mechanism for bitter avoidance in *Drosophila*. *J. Neurosci.* **35,** 3990–4004 (2015).

25. Meunier, N., Marion-Poll, F., Rospars, J.-P. & Tanimura, T. Peripheral coding of bitter taste in *Drosophila*. *J. Neurobiol.* **56,** 139–152 (2003).

26. Niewalda, T. *et al.* Salt processing in larval *Drosophila*: choice, feeding, and learning shift from appetitive to aversive in a concentration-dependent way. *Chem. Senses* **33,** 685–692 (2008).

27. Alves, G., Sallé, J., Chaudy, S., Dupas, S. & Manière, G. High-NaCl perception in *Drosophila melanogaster*. *J. Neurosci.* **34,** 10884–10891 (2014).

28. Zhang, Y. V., Ni, J. & Montell, C. The molecular basis for attractive salt-taste coding in *Drosophila*. *Science (80-.).* **340,** 1334–1338 (2013).

29. Nakamura, M., Baldwin, D., Hannaford, S., Palka, J. & Montell, C. Defective proboscis extension response (DPR), a member of the Ig superfamily required for the gustatory response to salt. *J. Neurosci.* **22,** 3463–3472 (2002).

30. Wang, Z., Singhvi, A., Kong, P. & Scott, K. Taste representations in the *Drosophila* brain. *Cell* **117,** 981–991 (2004).

31. Bader, R. *et al.* The IGFBP7 homolog Imp-L2 promotes insulin signaling in distinct neurons of the *Drosophila* brain. *J. Cell Sci.* **126,** 2571–2576 (2013).

32. Zhou, L. *et al.* Cooperative functions of the reaper and head involution defective genes in the programmed cell death of *Drosophila* central nervous system midline cells. *Proc. Natl. Acad. Sci.* **94,** 5131–5136 (1997).

33. Kitamoto, T. Conditional modification of behavior in *Drosophila* by targeted expression of a temperature-sensitive shibire allele in defined neurons. *J. Neurobiol.* **47,** 81–92 (2001).

Author contributions

S.H. and M.J.P. designed experiments and wrote the manuscript. S.H. carried out the experiments and analyzed the data. M.P. performed the GRASP experiment.

Supplementary material: Hückesfeld et al. (2016)
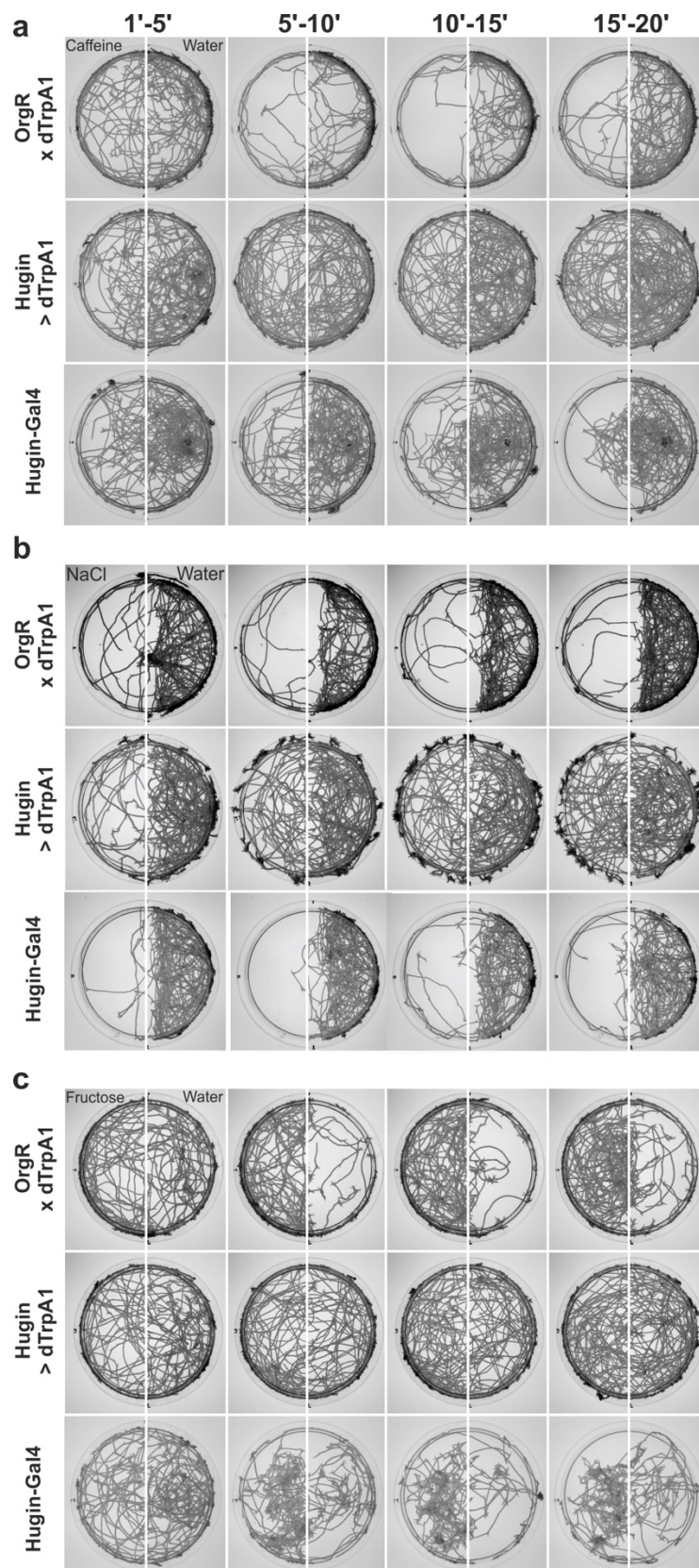
Supplementary Fig. 1: Attraction and aversion to taste substrates over time

Examples of 5 min time projections for each genotype in the 20 min two-choice experiments. **(a)** Two-choice plates with caffeine on the left side shown for Hugin-Gal4 line, Hugin > dTrpA1 and OrgR > dTrpA1. Graphs of at least 10 (for exact n numbers, see Fig. 1). Petri dishes with 30 larvae each, is shown on the right side with Hugin > dTrpA1 larvae showing less aversion to the caffeine substrate than controls. **(b)** Hugin > dTrpA1 larvae show less aversion to the NaCl substrate than controls. **(c)** Hugin > dTrpA1 larvae show less attraction to the fructose substrate. Activation of Hugin neurons causes general loss of appropriate substrate choice for aversive and attractive substrates.
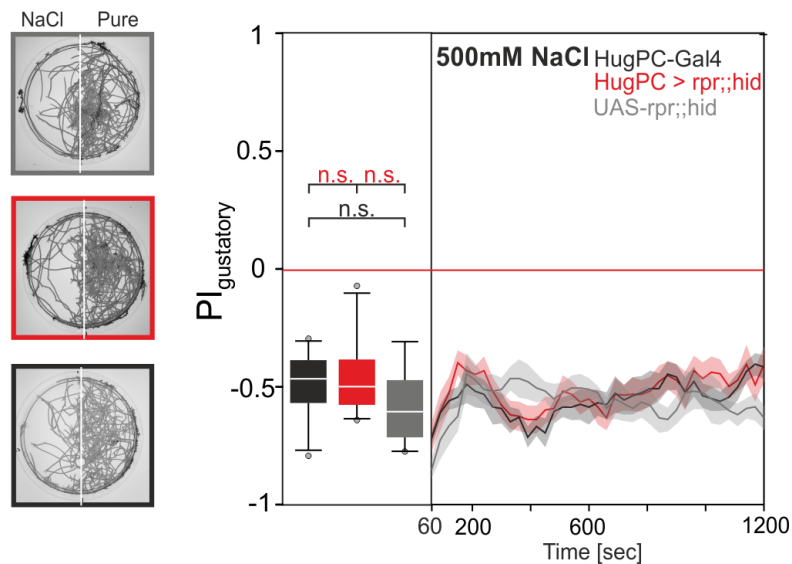
Supplementary Fig. 2: HuginPC are not necessary for salt avoidance

Two-Choice experiments on 500mM NaCl substrate on the left side of the plate verify the lack of phenotype shown in Figure 5. Larvae with the genotypes HugPC-Gal4, HugPC > rpr;;hid and UAS rpr;;hid did not show a difference in their avoidance behavior towards 500mM NaCl substrate. Plates on the left show 5min time projections of the last 5 min of the 20 min long experiment. Mann-Whitney-Rank-Sum-Test was used to compare always two groups in graphs showing boxplots. Significances are indicated as ***p<0.001, **p<0.01 and *p<0.05. Line plots showing the time course of the experiments are displayed as mean (line) ± SEM (transparent areas). Details of descriptive statistics are shown in **Supplemetary Table 5**.
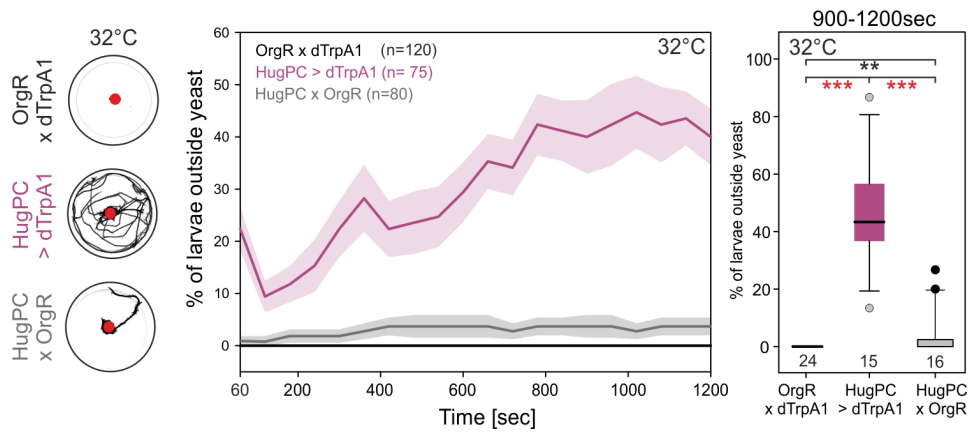
Supplementary Fig. 3: Activation of huginPC neurons causes wandering like phenotype

In the food intake assay larvae in which the huginPC neurons are activated (via UAS-dTrpA1 for 20 minutes), leave a strongly attractive food source (yeast). Control larvae (OrgR x dTrpA1 and HugPC x OrgR) did not leave extensively the yeast (red spot in the middle of the petri dish) at any time point during the assay. Numbers below boxplots represent number of petri dishes analyzed (5 larvae per dish). For statistics Mann-Whitney-Rank-Sum-Test was used. Significances are indicated as ***$p<0.001$, **$p<0.01$ and *$p<0.05$. Line plots showing the time course of the experiments are displayed as mean (line) ± SEM (transparent areas). Details of descriptive statistics are shown in **Supplemetary Table 5**.

Supplementary Table 1: Descriptive statistics to Figure 1

All statistical tests were performed with Mann-Whitney-U-Rank-Sum-Test

Green p-values indicate significance
Red p-values indicate no significance

p ≤ 0.05 = * / p ≤ 0.01 = ** / p ≤ 0.001 = ***

Statistics to Fig. 1c   Hugin activation 200mM Caffeine (box plots)

Experimental cross	Hugin-Gal4	Hugin > dTrpA1	OrgR > dTrpA1
n (plates)	11	10	10
mean	-0.6629	-0.3315	-0.7115
median	-0.6455	-0.3333	-0.7121
Std.err.	0.0352	0.0306	0.0208
Std. dev.	0.1167	0.0968	0.0657
p-value	<0.001		
p-value		<0.001	
p-value	←------------------ 0.275 ------------------→		

Statistics to Fig. 1d   Hugin loss of function 200mM Caffeine (box plots)

Experimental cross	UAS-rpr;;hid	Hugin > rpr;;hid	Hugin-Gal4	Hugin > shi^{TS}	UAS-shi^{TS}
n (plates)	14	10	10	10	10
mean	-0.7056	-0.2685	-0.6667	-0.3217	-0.7552
median	-0.7303	-0.3061	-0.6485	-0.3485	-0.7515
Std.err.	0.0299	0.0591	0.0346	0.0668	0.0161
Std. dev.	0.1118	0.1868	0.1147	0.2114	0.0508
p-value	<0.001				
p-value		<0.001			
p-value			<0.001		
p-value				<0.001	
p-value	←------------ 0.728 ------------→				
p-value				←------------ 0.168 ------------→	
p-value	←---------------------------------- 0.082 ----------------------------------→				

Supplementary Table 2: Descriptive statistics to Figure 2

Statistics to Fig. 2a	Hugin activation 2M NaCl (box plots)		
Experimental cross	Hugin-Gal4	Hugin > dTrpA1	OrgR > dTrpA1
n (plates)	10	11	10
mean	-0.8497	-0.1466	-0.7710
median	-0.8697	-0.1333	-0.8199
Std.err.	0.0295	0.0450	0.0462
Std. dev.	0.0933	0.1494	0.1461
p-value	<0.001		
p-value		<0.001	
p-value	←----------------- 0.241 -----------------→		

Statistics to Fig. 2b	Hugin ablation 2M NaCl (box plots)		
Experimental cross	Hugin-Gal4	Hugin > rpr;;hid	UAS-rpr;;hid
n (plates)	10	10	10
mean	-0.8497	-0.8361	-0.82
median	-0.8697	-0.8848	-0.8545
Std.err.	0.0295	0.0291	0.0213
Std. dev.	0.0933	0.0919	0.0674
p-value	0.838		
p-value		0.165	
p-value	←----------------- 0.241 -----------------→		

Statistics to Fig. 2c	Hugin activation 1M Fructose (box plots)		
Experimental cross	Hugin-Gal4	Hugin > dTrpA1	OrgR > dTrpA1
n (plates)	13	11	11
mean	0.7066	0.0533	0.693
median	0.7697	0.0600	0.693
Std.err.	0.0311	0.0222	0.002
Std. dev.	0.1120	0.0737	0.082
p-value	<0.001		
p-value		<0.001	
p-value	←----------------- 0.384 -----------------→		

Statistics to Fig. 2d	Hugin ablation 1M Fructose (box plots)		
Experimental cross	Hugin-Gal4	Hugin > rpr;;hid	UAS-rpr;;hid
n (plates)	10	12	10
mean	0.6810	0.6584	0.7764
median	0.7033	0.6273	0.8030
Std.err.	0.0455	0.0317	0.0251
Std. dev.	0.1439	0.1097	0.0793
p-value	0.668		
p-value		0.013	
p-value	←----------------- 0.104 -----------------→		

Supplementary Table 3: Descriptive statistics to Figure 4

Statistics to Fig. 4c	HugPC ablation 200mM Caffeine (box plots)		
Experimental cross	HugPC-Gal4	HugPC > rpr;;hid	UAS-rpr;;hid
n (plates)	10	13	14
mean	-0.8345	-0.3981	-0.7056
median	-0.8367	-0.4788	-0.7303
Std.err.	0.026	0.0559	0.0299
Std. dev.	0.0837	0.2135	0.1118
p-value	<0.001		
p-value		<0.001	
p-value	←----------------- 0.006 ------------------→		

Statistics to Fig. 4d	HugPC ablation 2M NaCl (box plots)		
Experimental cross	HugPC-Gal4	HugPC > rpr;;hid	UAS-rpr;;hid
n (plates)	10	10	10
mean	-0.7509	-0.6376	-0.82
median	-0.7818	-0.6697	-0.8545
Std.err.	0.043	0.0420	0.0213
Std. dev.	0.1360	0.1379	0.0674
p-value	0.076		
p-value		<0.001	
p-value	←----------------- 0.167 ------------------→		

Statistics to Fig. 4e	HugPC ablation 1M Fructose (box plots)		
Experimental cross	HugPC-Gal4	HugPC > rpr;;hid	UAS-rpr;;hid
n (plates)	10	10	10
mean	0.6667	0.7194	0.7764
median	0.6515	0.6939	0.8030
Std.err.	0.0201	0.0402	0.0251
Std. dev.	0.0824	0.1271	0.0793
p-value	0.241		
p-value		0.450	
p-value	←----------------- 0.013 ------------------→		

Statistics to Fig. 4f	HugPC activation - food intake (box plots)		
Experimental cross	OrgR x dTrpA1	HugPC > dTrpA1	HugPC x OrgR
n (larvae)	120	75	80
mean fold change	2.3738	0.4515	2.4567
median fold change	2.3767	0.1966	2.6939
Std.err.	0.0532	0.0636	0.1511
Std. dev.	0.5823	0.5511	1.3511
p-value	<0.001		
p-value		<0.001	
p-value	←----------------- 0.107 ------------------→		

Statistical tests were performed comparing the mean fold changes.

Supplementary Table 3 continued…

Statistics to Fig. 4g	HugPC activation – AN nerve recordings (box plots)		
Experimental cross	OrgR x dTrpA1	HugPC > dTrpA1	HugPC x OrgR
n larvae (n temperature steps)	9(32)	13(27)	10(26)
mean fold change/relative fold change	2.0490 / 0	1.4147 / -0.6343	2.1191 / 0.0701
median fold change/relative fold change	2.0109 / -0.0381	1.0123 / -1.0367	2.0378 / -0.0112
Std.err.	0.1688	0.2599	0.0701
Std. dev.	0.9550	1.4932	1.1807
p-value	0.003		
p-value		0.003	
p-value	←----------------- 0.969 ------------------→		

Statistical tests were performed comparing the mean fold changes. Relative fold changes are displayed as boxplots in Fig. 4g!

Supplementary Table 4: Descriptive statistics to Figure 5

Statistics to Fig. 5c   HugPC neurons - CaMPARI (box plots)

Taste substance	Water	20mM Caffeine	2M NaCl	1M Fructose	10% yeast	no UV light
n (larvae)	19	20	17	19	15	15
mean	0.7931	1.4093	0.5609	0.5419	0.4566	0.1847
median	0.7232	1.4816	0.5445	0.4944	0.4399	0.1870
Std.err.	0.0569	0.1373	0.0342	0.0387	0.0299	0.0122
Std. dev.	0.2481	0.6138	0.1366	0.1685	0.1305	0.0472
p-values		0.003	0.004	<0.001	<0.001	<0.001

Statistics to Fig. 5d   HugPC neurons – Caffeine concentrations - CaMPARI

Taste substance	Water	10mM	20mM	50mM	100mM	200mM
n (larvae)	19	18	20	19	19	17
mean	0.7931	1.4236	1.4093	2.1257	2.4236	2.4904
Std.err.	0.0569	0.1310	0.1373	0.1891	0.0916	0.1651
p-values		<0.001	0.003	<0.001	<0.001	<0.001

Statistics to Fig. 5e   HugPC - other bitter substances – CaMPARI (box plots)

Experimental cross	Water	10mM Quinine	10mM Denatonium
n (larvae)	19	15	15
mean	0.7931	1.3247	1.5921
median	0.7232	1.2527	1.4228
Std.err.	0.0569	0.1055	0.2030
Std. dev.	0.2481	0.4087	0.7863
p-value		<0.001	<0.001

Statistics to Fig. 5f   HugPC ablation 10mM Denatonium (box plots)

Experimental cross	HugPC-Gal4	HugPC > rpr;;hid	UAS-rpr;;hid
n (plates)	10	10	12
mean	-0-6412	-0.1073	-0.4141
median	-0-5818	-0.0424	-0.3152
Std.err.	0-0570	0.0663	0.0557
Std. dev.	0-1802	0.2096	0.1931
p-value	<0.001		
p-value		0.002	
p-value	←------------------ 0.027 ------------------→		

Supplementary Table 4 continued…

Statistics to Fig. 5h   GR66a activation – HugPC calcium imaging – peaks/min (bar plots)

Experimental cross	20°C control	30°C control	20°C experiment	30°C experiment
n (larvae)	13	13	14	14
mean	1.6035	1.8941	1.8893	5.0571
Std.err.	0.5730	0.7254	0.3553	0.3372
p-value	0.790			
p-value		0.197		
p-value			<0.001	
p-value	←------------- 0.241 -------------→			
p-value		←------------- 0.004 -------------→		
p-value	←-------------------------- <0.001 --------------------------→			

Supplementary Table 5: Descriptive statistics to Supplementary Figure 2 and 3

Statistics to Supplementary Fig. 2   HugPC ablation 500mM NaCl (box plots)

Experimental cross	HugPC-Gal4	HugPC > rpr;;hid	UAS-rpr;;hid
n (plates)	11	10	11
mean	-0.4937	-0.46	-0.5753
median	-0.4667	-0.5	-0.6061
Std.err.	0.0446	0.0526	0.0485
Std. dev.	0.1478	0.1665	0.1609
p-value	0.944		
p-value		0.130	
p-value	←----------------- 0.189 ------------------→		

Statistics to Supplementary Fig. 3   HugPC activation – % larvae leaving yeast (5 per plate) (box plots)

Experimental cross	OrgR x dTrpA1	HugPC > dTrpA1	HugPC x OrgR
n (plates)	15	24	16
mean	0	47.3333	3.8333
median	0	43.3333	-
Std.err.	0	5.1249	1.7816
Std. dev.	0	19.8486	7.9674
p-value	<0.001		
p-value		<0.001	
p-value	←----------------- 0.003 ------------------→		

5.3   Summary

The previous findings showed that activation of Hugin neurons decreases food intake in the presence of an otherwise appetitive food source, yeast [SEE CHAPTER 4]. The question arose how the Hugin neuronal network operates. Does activity of Hugin neurons regulate the state of satiety in larvae, which makes the protein source less attractive for the animals? Or is the neural processing of gustatory information disrupted, so that larvae cannot discriminate the valence of the food substrate?

In a previous study it was shown, that Hugin neurons are located in an area of the brain, the SEZ, where sensory taste afferents show dendritic arborizations [MELCHER & PANKRATZ, 2005]. This was shown for sensory neurons expressing the bitter (caffeine) gustatory receptor GR66a. Now, GRASP analysis verified that Hugin neurons display dendritic arborizations in close proximity (or even synaptic contact) to GR66a positive dendrites. Two choice assays showed that larvae with activated Hugin neurons display less aversion to the bitter caffeine substrate. Ablation of the Hugin neurons and synaptic silencing revealed that they are necessary for appropriate processing of bitter taste. Whereas activation of all 20 Hugin neurons led also to disruption in gustatory choice behavior on salt and fructose, larvae showed normal aversion and attraction to these substrates when all Hugin neurons were ablated, respectively. Since olfactory guidance was not altered in the Hugin activated state, it was concluded that Hugin neurons take part in bitter taste processing.

It has been demonstrated that certain Hugin neuron subclasses have different functions in the CNS [SEE CHAPTER 4]. To analyze the function of these subclasses in gustatory choice behavior, a *hugin* promoter driver line was generated, which restricts expression to the eight Hugin^{PC} neurons projecting to the protocerebrum. In line with the findings of all Hugin neurons being part of the bitter taste pathway, ablation of only the Hugin^{PC} neurons resulted in impaired gustatory choice behavior on caffeine substrate. No behavioral difference was observed when tested on salt or fructose substrates. It was also shown that the Hugin^{PC} neurons elicit the same phenotypic effects on feeding and wandering like behavior as all 20 Hugin neurons. Furthermore, activation of the Hugin^{PC} neurons led to a decrease in the cycle frequency of the AN motor pattern.

Measuring calcium activity in intact larvae using CaMPARI demonstrated that Hugin^{PC} neurons respond exclusively to bitter taste in a concentration dependent manner. Other taste modalities like sweet (fructose), salty (NaCl) and umami (yeast) decreased calcium activity in Hugin^{PC} neurons. Finally, GCaMP6s analysis demonstrated that Hugin^{PC} neurons show enhanced calcium influx upon artificial activation of neurons expressing the bitter receptor GR66a.

The initial question of how the Hugin neuronal network operates in the brain could be pinpointed to the Hugin[PC] neuronal cluster. This study clearly showed that the Hugin neurons that project to the protocerebrum are second order gustatory neurons for bitter taste in the *Drosophila* larval brain.

6   Conclusion

Basic components of the feeding motor system, the motor neurons, for *Drosophila* larval feeding behavior, were identified and neural populations modulating the activity of these motor neurons were analyzed. For the neurotransmitter serotonin it was shown that serotonergic neurons in the CNS of larvae serve as general up regulator of feeding related movements of the CPS, pharynx and esophagus. Emphasis relied on the functional role of the Hugin neuropeptide in modulation of feeding behavior, resulting in decline of food intake. It was revealed, that one subset of Hugin neurons projecting to the protocerebrum (Hugin^{PC}), serve as gustatory interneurons for bitter taste in the *Drosophila* larval CNS. Among the pleiotropic physiological roles assigned to its mammalian homolog NMU, a function in taste processing has not yet been assigned. Thus findings gathered about the Hugin^{PC} neurons in *Drosophila* larvae might help assigning a new role to NMU in the mammalian system.

Further investigations of the Hugin neuropeptide and its local actions should not end with the insights about the function of the Hugin^{PC} neurons, but expand to two directions for future research. On the one hand, recently the full synaptic first order connectome of all Hugin neurons in the larval CNS was mapped [SCHLEGEL ET AL., 2016]. This enables future work on the Hugin^{PC} connectivity to identify up and downstream synaptic partners of the Hugin^{PC} neurons in order to anatomically and functionally tackle the next step in bitter processing within the brain. On the other hand, since Hugin neurons can be divided into four subclasses, based on their projections targets in and outside the CNS, investigations concerning the functions of the other Hugin neurons should help to better understand how local actions of a neuropeptide might lead to different behavioral outcomes [SEE CHAPTER 4, function of Hugin^{VNC} neurons separated from the other neurons].

The deconstruction of neural networks, shown here with specific examples in *Drosophila* larvae, will help to understand basic principles of biological processes, especially when they are compared to other model organisms. Conserved neural circuits, as described here for NMU in mammals and Hugin in flies offer this opportunity. Yet the genetic accessibility of *Drosophila* and the technological advance like single cell manipulation and synaptic connectomic analysis will further enhance our ability to understand specific components of a neural network in the central nervous system.

7 Publications

7.1 Research Articles

7.1.1 PhD Period

Hückesfeld, S., Peters, M. and Pankratz, M. J. (2016). Central relay of bitter taste to the protocerebrum by peptidergic interneurons in the *Drosophila* brain. (peer reviewed, in revision) *Nature Communications*.

Hückesfeld, S., Schoofs, A., Schlegel, P., … Pankratz, M. J. (2015). Localization of Motor Neurons and Central Pattern Generators for Motor Patterns Underlying Feeding Behavior in *Drosophila* Larvae. *PLOS ONE*, *10*(8), e0135011.

Schoofs, A., Hückesfeld, S., Schlegel, P., … Pankratz, M. J. (2014). Selection of Motor Programs for Suppressing Food Intake and Inducing Locomotion in the *Drosophila* Brain. *PLoS Biology*, *12*(6), e1001893.

Schoofs, A., Hückesfeld, S., Surendran, S., & Pankratz, M. J. (2014). Serotonergic pathways in the *Drosophila* larval enteric nervous system. *Journal of Insect Physiology*, *69*, 118–125.

7.1.2 Additional Publications

Hückesfeld, S., Niederegger, S., Schlegel, P., … Spieß, R. (2011). Feel the heat: The effect of temperature on development, behavior and central pattern generation in 3rd instar *Calliphora vicina* larvae. *Journal of Insect Physiology*, *57*(1), 136–146.

Hückesfeld, S., Niederegger, S., Heinzel, H.-G., & Spieß, R. (2010). The cephalic and pharyngeal sense organs of *Calliphora vicina* 3rd instar larvae are mechanosensitive but have no profound effect on ongoing feeding related motor patterns. *Journal of Insect Physiology*, *56*(11), 1530–1541.

7.2   Scientific Talks

Hückesfeld, S., Schoofs, A., Schlegel, P., Klumpp, M., Pankratz, M.J. (2014). Feeding motor programs in *Drosophila*. *2014 ESF-EMBO Symposium – Flies, worms and robots.*

Hückesfeld, S., Schlegel, P., Pankratz, M.J. (2013). Central Neurons Modulate Feeding Behavior in *Drosophila*: Potential Role in Pathogen avoidance. *Science Days 2013 of the Bonn Cluster of Excellence Immunosensation.*

-   This talk was awarded as winner of the 1st price category fo excellent presentation

7.3   Posters

Hückesfeld, S., Schoofs, A., Schlegel, P., Pankratz, M.J. (2012). Manipulation of central neurons modulating the feeding behavior of *Drosophila* larvae. *Janelia conferences – Behavioral Neurogenetics of Drosophila larvae.*

Hückesfeld, S., Schlegel, P., Miroschnikow, A., …Pankratz, M.J. (2014). Hugin: A neural circuit involved in feeding regulation and gustatory processing in the *Drosophila* larval brain. *24th European Drosophila Research Conference.*

References

Adams, M. D., Celniker, S. E., Holt, R. A., Evans, C. A., … Venter, J. C. (2000). The Genome Sequence of *Drosophila* melanogaster. *Science (New York, N.Y.)*, *287*(5461), 2185–95.

Al-Anzi, B., Armand, E., Nagamei, P., Olszewski, M., … Benzer, S. (2010). The Leucokinin Pathway and Its Neurons Regulate Meal Size in *Drosophila*. *Current Biology*, *20*(11), 969–978.

Apostolopoulou, A. A., Mazija, L., Wüst, A., & Thum, A. S. (2014). The Neuronal and Molecular Basis of Quinine-Dependent Bitter Taste Signaling in *Drosophila* Larvae. *Frontiers in Behavioral Neuroscience*, *8*(January), 6.

Apostolopoulou, A. A., Rist, A., & Thum, A. S. (2015). Taste Processing in Drosophila Larvae. *Frontiers in Integrative Neuroscience*, *9*(October), 1–9.

Argilés, J. M., Olivan, M., Busquets, S., & López-Soriano, F. J. (2010). Optimal Management of Cancer Anorexia – Cachexia Syndrome. *Cancer Management and Research*, (2), 27–38.

Augood, S. J., Keast, J. R., & Emson, P. C. (1988). Distribution and Characterisation of Neuromedin U-like Immunoreactivity in Rat Brain and Intestine and in Guinea Pig Intestine. *Regulatory Peptides*, *20*(4), 281–292.

Austin, C., Lo, G., Nandha, K. A., Meleagros, L., & Bloom, S. R. (1995). Cloning and Characterization of the cDNA Encoding the Human Neuromedin U (NmU) Precursor: NmU Expression in the Human Gastrointestinal Tract. *Journal of Molecular Endocrinology*, *14*(2), 157–169.

Austin, C., Oka, M., Nandha, K. A., Legon, S., … Bloom, S. R. (1994). Distribution and Developmental Pattern of Neuromedin Expression in the Rat Gastrointestinal Tract. *J Molecular Endocrinol*, *12*(3), 257–263.

Ayali, A. (2004). The Insect Frontal Ganglion and Stomatogastric Pattern Generator Networks. *NeuroSignals*, *13*(1-2), 20–36.

Bader, R., Colomb, J., Pankratz, B., Schröck, A., … Pankratz, M. J. (2007). Genetic Dissection of Neural Circuit Anatomy Underlying Feeding Behavior in *Drosophila*: Distinct Classes of Hugin-Expressing Neurons. *The Journal of Comparative Neurology*, *502*(5), 848–56.

Ballesta, J., Carlei, F., Bishop, A. E., Steel, J. H., … Polak, J. M. (1988). Occurrence and Developmental Pattern of Neuromedin U-Immunoreactive Nerves in the Gastrointestinal Tract and Brain of the Rat. *Neuroscience*, *25*(3), 797–816.

Bargmann, C. I. (2012). Beyond the Connectome: How Neuromodulators Shape Neural Circuits. *BioEssays*, *34*(6), 458–465.

Barretto, R. P. J., Gillis-Smith, S., Chandrashekar, J., Yarmolinsky, D. A., … Zuker, C. S. (2015). The Neural Representation of Taste Quality at the Periphery. *Nature*, *517*(7534), 373–6.

Bässler, U., & Büschges, A. (1998). Pattern Generation for Stick Insect Walking Movements—Multisensory Control of a Locomotor Program. *Brain Research Reviews*, *27*(1), 65–88.

Baxter, D. A., & Byrne, J. H. (2006). Feeding Behavior of *Aplysia*: A Model System for Comparing Cellular Mechanisms of Classical and Operant Conditioning. *Learning & Memory*, *13*(6), 669–680.

Bechtold, D. A., Ivanov, T. R., & Luckman, S. M. (2009). Appetite-Modifying Actions of Pro-Neuromedin U-Derived Peptides. *Am J Physiol Endocrinol Metab*, *297*, 545–551.

Bellen, H. J., Tong, C., & Tsuda, H. (2010). 100 Years of *Drosophila* Research and its Impact on Vertebrate Neuroscience: A History Lesson for the Future. *Nature Reviews Neuroscience*, *11*(7), 514–522.

Benton, R., Vannice, K. S., Gomez-Diaz, C., & Vosshall, L. B. (2009). Variant Ionotropic Glutamate Receptors as Chemosensory Receptors in *Drosophila*. *Cell*, *136*(1), 149–162.

Bharucha, K. N., Tarr, P., & Zipursky, S. L. (2008). A Glucagon-Like Endocrine Pathway in *Drosophila* Modulates Both Lipid and Carbohydrate Homeostasis. *Journal of Experimental Biology*, *211*(19), 3103–3110.

Bjordal, M., Arquier, N., Kniazeff, J., Pin, J. P., & Léopold, P. (2014). Sensing of Amino Acids in a Dopaminergic Circuitry Promotes Rejection of an Incomplete Diet in *Drosophila*. *Cell*, *156*(3), 510–521.

Blundell, J. (1991). Pharmacological Approaches to Appetite Suppression. *Trends in Pharmacological Sciences*, *12*(4), 147–157.

Brand, A. H., & Perrimon, N. (1993). Targeted Gene Expression as a Means of Altering Cell Fates and Generating Dominant Phenotypes. *Development (Cambridge, England)*, *118*(2), 401–15.

Bray, S. (2006). Notch Signalling: A Simple Pathway Becomes Complex. *Nature reviews. Molecular Cell Biology*, *7*(September), 678–689.

Breslin, P. A. S., & Spector, A. C. (2008). Mammalian Taste Perception. *Current Biology*, *18*(4), R148–55.

Brighton, P. J., Szekeres, P. G., & Willars, G. B. (2004). Neuromedin U and Its Receptors: Structure, Function, and Physiological Roles. *Pharmacological Reviews*, *56*(2), 231–248.

Brown, M. R., Crim, J. W., Arata, R. C., Cai, H. N., … Shen, P. (1999). Identification of a *Drosophila* Brain-Gut Peptide Related to the Neuropeptide Y Family. *Peptides*, *20*(9), 1035–1042.

Callewaert, G., Eilers, J., & Konnerth, A. (1996). Axonal Calcium Entry During Fast "Sodium" Action Potentials in Rat Cerebellar Purkinje Neurones. *Journal of Physiology*, *495.3*, 641–647.

Carleton, A., Accolla, R., & Simon, S. A. (2010). Coding in the Mammalian Gustatory System. *Trends in Neurosciences*, *33*(7), 326–334.

Carter, M. E., Han, S., & Palmiter, R. D. (2015). Parabrachial Calcitonin Gene-Related Peptide Neurons Mediate Conditioned Taste Aversion. *Journal of Neuroscience*, *35*(11), 4582–4586.

Carter, M. E., Soden, M. E., Zweifel, L. S., & Palmiter, R. D. (2013). Genetic Identification of a Neural Circuit that Suppresses Appetite. *Nature*, *503*(7474), 111–4.

Chandrashekar, J., Hoon, M. a, Ryba, N. J. P., & Zuker, C. S. (2006). The Receptors and Cells for Mammalian Taste. *Nature*, *444*(7117), 288–294.

Chandrashekar, J., Kuhn, C., Oka, Y., Yarmolinsky, D. A., … Zuker, C. S. (2010). The Cells and Peripheral Representation of Sodium Taste in Mice. *Nature*, *464*(7286), 297–301.

Chandrashekar, J., Mueller, K. L., Hoon, M. a, Adler, E., … Ryba, N. J. . (2000). T2Rs Function as Bitter Taste Receptors. *Cell*, *100*(6), 703–711.

Chen, T.-W., Wardill, T. J., Sun, Y., Pulver, S. R., … Kim, D. S. (2013). Ultrasensitive Fluorescent Proteins for Imaging Neuronal Activity. *Nature*, *499*(7458), 295–300.

Chu, B., Chui, V., Mann, K., & Gordon, M. D. (2014). Presynaptic Gain Control Drives Sweet and Bitter Taste Integration in *Drosophila*. *Current Biology*, *24*(17), 1978–1984.

Clyne, P. J., Warr, C. G., & Carlson, J. R. (2000). Candidate Taste Receptors in *Drosophila*. *Science*, *287*(5459), 1830–1834.

Cohen, A. H. (1987). Intersegmental Coordinating System of the Lamprey Central Pattern Generator for Locomotion. *Journal of Comparative Physiology A*, *160*(2), 181–193.

Colomb, J., Grillenzoni, N., Ramaekers, A., & Stocker, R. F. (2007). Architecture of the Primary Taste Center in *Drosophila melanogaster* Larvae. *Journal of Comparative Neurology*, *502*(5), 834–847.

Colomb, J., & Stocker, R. F. (2007). Combined Rather than Separate Pathways for Hedonic and Sensory Aspects of Taste in Fly Larvae? *Journal of Comparative Neurology*, (August), 232–234.

Cooper, P. D., & He, P.-H. (1994). Control of Foregut Contraction in the Black Field Cricket, *Teleogryllus commodus* Walker (Gryllidae, Orthoptera). *Journal of Insect Physiology*, *40*(6), 475–481.

Copenhaver, P. F. (2007). How to Innervate a Simple Gut: Familiar Themes and Unique Aspects in the Formation of the Insect Enteric Nervous System. *Developmental Dynamics*, *236*(7), 1841–1864.

Couto, A., Alenius, M., & Dickson, B. J. (2005). Molecular, Anatomical, and Functional Organization of the *Drosophila* Olfactory System. *Current Biology*, *15*(17), 1535–1547.

Cowley, M. a, Smart, J. L., Rubinstein, M., Cerdán, M. G., … Low, M. J. (2001). Leptin Activates Anorexigenic POMC Neurons Through a Neural Network in the Arcuate Nucleus. *Nature*, *411*(6836), 480–484.

Dahanukar, A., Lei, Y.-T., Kwon, J. Y., & Carlson, J. R. (2007). Two Gr Genes Underlie Sugar Reception in *Drosophila*. *Neuron*, *56*(3), 503–516.

de Araujo, I. E., & Simon, S. a. (2009). The Gustatory Cortex and Multisensory Integration. *International Journal of Obesity*, *33*(S2), S34–S43.

Delcomyn, F. (1980). Neural Basis of Rhythmic Behavior in Animals. *Science (New York, N.Y.)*, *210*(4469), 492–8.

Di Lorenzo, P. M., Platt, D., & Victor, J. D. (2009). Information Processing in the Parabrachial Nucleus of the Pons. *Annals of the New York Academy of Sciences*, *1170*(1), 365–371.

Duffy, J. B. (2002). GAL4 System in *Drosophila*: A Fly Geneticist's Swiss Army Knife. *Genesis*, *34*(1-2), 1–15.

Dunipace, L., Meister, S., McNealy, C., & Amrein, H. (2001). Spatially Restricted Expression of Candidate Taste Receptors in the *Drosophila* Gustatory System. *Current Biology*, *11*(11), 822–835.

Edgecomb, R. S., Harth, C. E., & Schneiderman, A. M. (1994). Regulation of Feeding Behavior in Adult Drosophila Melanogaster Varies With Feeding Regime and Nutritional State, *235*, 215–235.

El-Keredy, A., Schleyer, M., König, C., Ekim, A., & Gerber, B. (2012). Behavioural Analyses of Quinine Processing in Choice, Feeding and Learning of Larval *Drosophila*. *PloS one*, *7*(7), e40525.

Ellisen, L. W., Bird, J., West, D. C., Soreng, A. L., … Sklar, J. (1991). TAN-1, the Human Homolog of the *Drosophila* Notch Gene, is Broken by Chromosomal Translocations in T Lymphoblastic Neoplasms. *Cell*, *66*(4), 649–661.

Elmquist, J. K., Elias, C. F., & Saper, C. B. (1999). From Lesions to Leptin: Hypothalamic Control of Food Intake and Body Weight. *Neuron*, *22*(2), 221–32.

Ertekin, C., & Aydogdu, I. (2003). Neurophysiology of Swallowing. *Clinical Neurophysiology*, *114*(12), 2226–2244.

Feany, M. B., & Bender, W. W. (2000). A *Drosophila* Model of Parkinson ' s Disease. *Nature*, *404*(March), 394–398.

Flood, J. F., & Morley, J. E. (1991). Increased Food Intake by Neuropeptide Y is Due to an Increased Motivation to Eat. *Peptides*, *12*(6), 1329–1332.

Fosque, B. F., Sun, Y., Dana, H., Yang, C.-T., … Schreiter, E. R. (2015). Labeling of Active Neural Circuits in Vivo with Designed Calcium Integrators. *Science (New York, N.Y.)*, *347*(6223), 755–60.

French, A. S., Sellier, M.-J., Ali Agha, M., Guigue, A., … Marion-Poll, F. (2015). Dual Mechanism for Bitter Avoidance in *Drosophila*. *Journal of Neuroscience*, *35*(9), 3990–4004.

Friedman, J. M., & Halaas, J. L. (1998). Leptin and the Regulation of Body Weight in Mammals. *Nature*, *395*, 763–770.

Fujii, R., Hosoya, M., Fukusumi, S., Kawamata, Y., … Fujino, M. (2000). Identification of Neuromedin U as the Cognate Ligand of the Orphan G Protein-coupled Receptor FM-3. *Journal of Biological Chemistry*, *275*(28), 21068–21074.

Funes, S., Hedrick, J. a, Yang, S., Shan, L., … Gustafson, E. L. (2002). Cloning and Characterization of Murine Neuromedin U Receptors. *Peptides*, *23*(9), 1607–1615.

Gasque, G., Conway, S., Huang, J., Rao, Y., & Vosshall, L. B. (2013). Small Molecule Drug Screening in *Drosophila* Identifies the 5HT2A Receptor as a Feeding Modulation Target. *Scientific Reports*, *3*, srep02120.

Gershon, M. D. (2008). Functional Anatomy of the Enteric Nervous System. In *Hirschsprung`s Diesease and Allied Disorders* (pp. 21–49).

Glendinning, J. I. (1994). Is the Bitter Rejection Response Always Adaptive? *Physiology and Behavior*, *56*(6), 1217–1227.

Gordon, M. D., & Scott, K. (2009). Motor Control in a *Drosophila* Taste Circuit. *Neuron*, *61*(3), 373–84.

Green, C. H., Burnet, B., & Connolly, K. J. (1983). Organization and Patterns of Inter- and Intraspecific Variation in the Behaviour of *Drosophila* Larvae. *Animal Behaviour*, *31*(1), 282–291.

Grillner, S., & Zangger, P. (1979). On the Central Generation of Locomotion in the Low Spinal Cat. *Experimental Brain Research*, *34*(2), 241–261.

Griss, C. (1990). Mandibular Motor Neurons of the Caterpillar of the Hawk Moth *Manduca Sexta*. *The Journal of Comparative Neurology*, *296*(3), 393–402.

Grönke, S., Müller, G., Hirsch, J., Fellert, S., … Kühnlein, R. P. (2007). Dual Lipolytic Control of Body Fat Storage and Mobilization in *Drosophila*. *PLoS Biology*, *5*(6), e137.

Halford, J. C. G., & Blundell, J. E. (2000). Separate Systems for Serotonin and Leptin in Appetite Control. *Annals of Medicine*, *32*(3), 222–232.

Hamada, F. N., Rosenzweig, M., Kang, K., Pulver, S. R., … Garrity, P. a. (2008). An Internal Thermal Sensor Controlling Temperature Preference in *Drosophila*. *Nature*, *454*(7201), 217–220.

Hanada, R., Nakazato, M., Murakami, N., Sakihara, S., … Sakata, T. (2001). A Role for Neuromedin U in Stress Response. *Biochemical and Biophysical Research Communications*, *289*(1), 225–228.

Hanada, R., Teranishi, H., Pearson, J. T., Kurokawa, M., … Kojima, M. (2004). Neuromedin U Has a Novel Anorexigenic Effect Independent of the Leptin Signaling Pathway. *Nature Medicine*, *10*(10), 1067–1073.

Hanada, T., Date, Y., Shimbara, T., Sakihara, S., … Nakazato, M. (2003). Central Actions of Neuromedin U via Corticotropin-releasing Hormone. *Biochemical and Biophysical Research Communications*, *311*(4), 954–958.

Harris, D. T., Kallman, B. R., Mullaney, B. C., & Scott, K. (2015). Representations of Taste Modality in the *Drosophila* Brain. *Neuron*, *86*(6), 1449–1460.

Harrold, J. A., Dovey, T. M., Blundell, J. E., & Halford, J. C. G. (2012). CNS Regulation of Appetite. *Neuropharmacology*, *63*(1), 3–17.

Hartenstein, V. (2006). The Neuroendocrine System of Invertebrates: A Developmental and Evolutionary Perspective. *Journal of Endocrinology*, *190*(3), 555–570.

Hashimoto, T., Masui, H., Uchida, Y., Sakura, N., & Okimura, K. (1991). Agonistic and Antagonistic Activities of Neuromedin-U8 Analogs Substituted with Glycine or D-Amino acid on Contractile Activity of Chicken Crop Smooth Muscle Preparations. *Chem. Pharm. Bull.*, *39*(9), 2319–2322.

Hergarden, A. C., Tayler, T. D., & Anderson, D. J. (2012). Allatostatin-A Neurons Inhibit Feeding Behavior in Adult *Drosophila*. *Proceedings of the National Academy of Sciences of the United States of America*, *109*(10), 3967–72.

Hernádi, L., Erdélyi, L., Hiripi, L., & Elekes, K. (1998). The Organization of Serotonin-, Dopamine-, and FMRFamide-containing Neuronal Elements and their Possible Role in the Regulation of Spontaneous Contraction of the Gastrointestinal Tract in the Snail Helix pomatia. *Journal of neurocytology*, *27*(10), 761–75.

Hoebel, B. G., & Teitelbaum, P. (1962). Hypothalamic Control of Feeding and Self-Stimulation. *Science (New York, N.Y.)*, *135*, 375–377.

Hornstein, N. J., Pulver, S. R., & Griffith, L. C. (2009, January). Channelrhodopsin 2 Mediated Stimulation of Synaptic Potentials at *Drosophila* Neuromuscular Junctions. *Journal of visualized experiments : JoVE*.

Howard, A. D., Wang, R., Pong, S. S., Mellin, T. N., … Liu, Q. (2000). Identification of Receptors for Neuromedin U and its Role in Feeding. *Nature*, *406*(6791), 70–4.

Hückesfeld, S., Schoofs, A., Schlegel, P., Miroschnikow, A., & Pankratz, M. J. (2015). Localization of Motor Neurons and Central Pattern Generators for Motor Patterns Underlying Feeding Behavior in *Drosophila* Larvae. *PLOS ONE*, *10*(8), e0135011.

Inada, K., Kohsaka, H., Takasu, E., Matsunaga, T., & Nose, A. (2011). Optical Dissection of Neural Circuits Responsible for *Drosophila* Larval Locomotion with Halorhodopsin. *PloS one*, *6*(12), e29019.

Inagaki, H. K. K., Ben-Tabou de-Leon, S., Wong, A. M., Jagadish, S., … Anderson, D. J. J. (2012). Visualizing Neuromodulation In Vivo: TANGO-Mapping of Dopamine Signaling Reveals Appetite Control of Sugar Sensing. *Cell*, *148*(3), 583–595.

Ishimaru, Y., Inada, H., Kubota, M., Zhuang, H., … Matsunami, H. (2006). Transient Receptor Potential Family Members PKD1L3 and PKD2L1 Form a Candidate Sour Taste Receptor. *Proceedings of the National Academy of Sciences*, *103*(33), 12569–12574.

Ja, W. W., Carvalho, G. B., Mak, E. M., de la Rosa, N. N., … Benzer, S. (2007). Prandiology of Drosophila and the CAFE Assay. *Proc Natl Acad Sci U S A*, *104*(20), 8253–8256.

Jean, A. (2001). Brain Stem Control of Swallowing: Neuronal Network and Cellular Mechanisms. *Physiological reviews*, *81*(2), 929–969.

Jethwa, P. H. (2005). Neuromedin U Has a Physiological Role in the Regulation of Food Intake and Partially Mediates the Effects of Leptin. *AJP: Endocrinology and Metabolism*, *289*(2), E301–E305.

Jethwa, P. H., Smith, K. L., Small, C. J., Abbott, C. R., … Bloom, S. R. (2006). Neuromedin U Partially Mediates Leptin-induced Hypothalamo-pituitary Adrenal (HPA) Stimulation and Has a Physiological Role in the Regulation of the HPA Axis in the Rat. *Endocrinology*, *147*(6), 2886–2892.

Kabotyanski, E. A., Baxter, D. a, Cushman, S. J., & Byrne, J. H. (2000). Modulation of Fictive Feeding by Dopamine and Serotonin in *Aplysia*. *Journal of Neurophysiology*, *83*(1), 374–92.

Kain, P., & Dahanukar, A. (2015). Secondary Taste Neurons that Convey Sweet Taste and Starvation in the *Drosophila* Brain. *Neuron*, *85*(4), 819–32.

Kamisoyama, H., Honda, K., Saneyasu, T., Sugahara, K., & Hasegawa, S. (2007). Central Administration of Neuromedin U Suppresses Food Intake in Chicks. *Neuroscience Letters*, *420*(1), 1–5.

Kasuya, J. (2009). Neuronal Mechanisms of Learning and Memory Revealed by Spatial and Temporal Suppression of Neurotransmission Using *shibire ts1*, a Temperature-sensitive Dynamin Mutant Gene in *Drosophila melanogaster*. *Frontiers in Molecular Neuroscience*, *2*(August), 11.

Katz, P. S., & Frost, W. N. (1995). Intrinsic Neuromodulation in the Tritonia Swim CPG: The Serotonergic Dorsal Swim Interneurons Act Presynaptically to Enhance Transmitter Release from Interneuron C2. *The Journal of neuroscience : the official journal of the Society for Neuroscience*, *15*(9), 6035–45.

Kim, S. K., & Rulifson, E. J. (2004). Conserved Mechanisms of Glucose Sensing and Regulation by *Drosophila* Corpora Cardiaca Cells. *Nature*, *431*(7006), 316–320.

Kirkhart, C., & Scott, K. (2015). Gustatory Learning and Processing in the Drosophila Mushroom Bodies. *The Journal of Neuroscience*, *35*(15), 5950–8.

Kitamoto, T. (2001). Conditional Modification of Behavior in *Drosophila* by Targeted Expression of a Temperature-sensitive *Shibire* Allele in Defined Neurons. *Journal Neurobiology*, *47*(2), 81–92.

König, C., Schleyer, M., Leibiger, J., El-Keredy, A., & Gerber, B. (2015). Bitter-Sweet Processing in Larval *Drosophila*. *Chemical Senses*, *40*(6), 445–445.

Kowalski, T. J., Spar, B. D., Markowitz, L., Maguire, M., … Gustafson, E. L. (2005). Transgenic Overexpression of Neuromedin U Promotes Leanness and Hypophagia in Mice. *Journal of Endocrinology*, *185*(1), 151–164.

Kwon, J. Y., Dahanukar, A., Weiss, L. a, & Carlson, J. R. (2011). Molecular and Cellular Organization of the Taste System in the *Drosophila* Larva. *Journal of Neuroscience*, *31*(43), 15300–15309.

Lai, J. S.-Y., Lo, S.-J., Dickson, B. J., & Chiang, A.-S. (2012). Auditory Circuit in the *Drosophila* Brain. *Proceedings of the National Academy of Sciences of the United States of America*, *109*(7), 2607–12.

Lanyi, J. K. (1986). Halorhodopsin: A Light-Driven Chloride Ion Pump. *Annual Review of Biophysics and Biomolecular Structure*, *15*(1), 11–28.

Lee, K.-S., Kwon, O.-Y., Lee, J. H., Kwon, K., … Yu, K. (2008). *Drosophila* Short Neuropeptide F Signalling Regulates Growth by ERK-mediated Insulin Signalling. *Nature Cell Biology*, *10*(4), 468–475.

Lee, K.-S., You, K.-H., Choo, J.-K., Han, Y.-M., & Yu, K. (2004). *Drosophila* Short Neuropeptide F Regulates Food Intake and Body Size. *Journal of Biological Chemistry*, *279*(49), 50781–50789.

Li, Z., Chalazonitis, A., Huang, Y. -y., Mann, J. J., … Gershon, M. D. (2011). Essential Roles of Enteric Neuronal Serotonin in Gastrointestinal Motility and the Development/Survival of Enteric Dopaminergic Neurons. *Journal of Neuroscience*, *31*(24), 8998–9009.

Lindemann, B. (2002). The Discovery of Umami. *Chemical Senses*, *27*(9), 843–844.

Lo, G., Legon, S., Austin, C., Wallis, S., … Bloom, S. R. (1992). Characterization of Complementary DNA Encoding the Rat Neuromedin U Precursor. *Molecular Endocrinology*, *6*(10), 1538–44.

Lowne, B. (1890). *The Anatomy, Physiology, Morphology, and Development of the Blow-Fly (*Calliphora erythrocephala*) : A Study in the Comparative Anatomy and Morphology of Insects. published for the author by R.H. Porter, 18 Princes Street, Cavedish Square, London* (Vol. 2).

Luffy, D., & Dorn, A. (1991). Serotoninergic Elements in the Stomatogastric Nervous System of the Stick Insect, *Carausius morosus*, Demonstrated by Immunohistochemistry. *Journal of Insect Physiology*, *37*(4), 269.

Manzo, a., Silies, M., Gohl, D. M., & Scott, K. (2012). Motor Neurons Controlling Fluid Ingestion in *Drosophila. Proceedings of the National Academy of Sciences*, 1–6.

Marder, E. (2012). Neuromodulation of Neuronal Circuits: Back to the Future. *Neuron*, *76*(1), 1–11.

Marder, E., & Bucher, D. (2001). Central Pattern Generators and the Control of Rhythmic Movements. *Current Biology*, *11*(23), R986–R996.

Marder, E., O'Leary, T., & Shruti, S. (2014). Neuromodulation of Circuits with Variable Parameters: Single Neurons and Small Circuits Reveal Principles of State-dependent and Robust Neuromodulation. *Annual review of Neuroscience*, *37*, 329–46.

Marella, S., Fischler, W., Kong, P., Asgarian, S., … Scott, K. (2006). Imaging Taste Responses in the Fly Brain Reveals a Functional Map of Taste Category and Behavior. *Neuron*, *49*(2), 285–295.

Marella, S., Mann, K., & Scott, K. (2012). Dopaminergic Modulation of Sucrose Acceptance Behavior in Drosophila. *Neuron*, *73*(5), 941–950.

Martinez, V. G., & O'Driscoll, L. (2015). Neuromedin U: A Multifunctional Neuropeptide with Pleiotropic Roles. *Clinical chemistry*, *61*(3), 471–482.

Maruyama, K., Konno, N., Ishiguro, K., Wakasugi, T., … Matsuda, K. (2008). Isolation and Characterisation of Four cDNAs Encoding Neuromedin U (NMU) From the Brain and Gut of Goldfish, and the Inhibitory Effect of a Deduced NMU on Food Intake and Locomotor Activity. *Journal of Neuroendocrinology*, *20*(1), 71–78.

Matsuo, K., & Palmer, J. B. (2009). Anatomy and Physiology of Feeding and Swallowing-Normal and Abnormal. *Phys Med Rehabil Clin N Am.*, *19*(4), 691–707.

Meister, B. (2007). Neurotransmitters in Key Neurons of the Hypothalamus that Regulate Feeding Behavior and Body Weight. *Physiology and Behavior*, *92*, 263–271.

Melcher, C., Bader, R., Walther, S., Simakow, O., & Pankratz, M. J. (2006). Neuromedin U and Its Putative *Drosophila* Homolog *hugin. PLoS Biology*, *4*(3), e68.

Melcher, C., & Pankratz, M. J. (2005). Candidate Gustatory Interneurons Modulating Feeding Behavior in the *Drosophila* Brain. *PLoS Biology*, *3*(9), e305.

Meng, X., Wahlström, G., Immonen, T., Kolmer, M., … Roos, C. (2002). The *Drosophila hugin* Gene Codes for Myostimulatory and Ecdysis-modifying Neuropeptides. *Mechanisms of Development*, *117*(1-2), 5–13.

Meunier, N., Marion-Poll, F., Rospars, J.-P., & Tanimura, T. (2003). Peripheral Coding of Bitter Taste in *Drosophila*. *Journal of Neurobiology*, *56*(2), 139–152.

Miles, & Booker. (1998). The Role of the Frontal Ganglion in the Feeding and Eclosion Behavior of the Moth *Manduca sexta*. *The Journal of Experimental Biology*, *201 (Pt 11*, 1785–98.

Miles, C. I., & Booker, R. (1994). The Role of the Frontal Ganglion in Foregut Movements of the Moth, *Manduca sexta*. *Journal of Comparative Physiology A*, *174*(6), 1785–98.

Minamino, N., Kangawa, K., & Matsuo, H. (1985b). Neuromedin U-8 and U-25: Novel Uterus Stimulating and Hypertensive Peptides Identified in Porcine Spinal Cord. *Biochemical and Biophysical Research Communications*, *130*(3), 1078–1085.

Minamino, N., Sudoh, T., Kangawa, K., & Matsuo, H. (1985a). Neuromedins: Novel Smooth-Muscle Stimulating Peptides Identified in Porcine Spinal Cord. *Peptides*, *6*(SUPPL. 3), 245–248.

Mishra, D., Miyamoto, T., Rezenom, Y. H., Broussard, A., … Amrein, H. (2013). The Molecular Basis of Sugar Sensing in *Drosophila* Larvae. *Current Biology*, *23*(15), 1466–1471.

Miyazaki, T., Lin, T.-Y., Ito, K., Lee, C.-H., & Stopfer, M. (2015). A Gustatory Second-order Neuron that Connects Sucrose-sensitive Primary Neurons and a Distinct Region of the Gnathal Ganglion in the Drosophila Brain. *Journal of Neurogenetics*, *7063*(October), 1–12.

Moon, S. J., Köttgen, M., Jiao, Y., Xu, H., & Montell, C. (2006). A Taste Receptor Required for the Caffeine Response In Vivo. *Current Biology*, *16*(18), 1812–1817.

Morgan, T. H. (1910). Sex Limited Inheritance in *Drosophila*. *Science*, *32*, 120–122.

Morgan, T. H., & Bridges, C. B. (1916). Sex-linked Inheritance in *Drosophila*. *Publs Carnegie Instn*, *237*, 1–88.

Morley, J. E., & Levine, A. S. (1982). Corticotropin Releasing Factor, Grooming and Ingestive Behavior. *Life Sciences*, *31*, 1459–1464.

Morton, G. J., Meek, T. H., & Schwartz, M. W. (2014). Neurobiology of Food Intake in Health and Disease. *Nature Reviews Neuroscience*, *15*(6), 367–378.

Murphy, A. D. (2001). The Neuronal Basis of Feeding in the Snail, *Helisoma*, with Comparisons to Selected Gastropods. *Progress in Neurobiology*, *63*(4), 383–408.

Nagel, G., Szellas, T., Huhn, W., Kateriya, S., … Bamberg, E. (2003). Channelrhodopsin-2, a Directly Light-gated Cation-selective Membrane Channel. *Proceedings of the National Academy of Sciences*, *100*(24), 13940.

Nakahara, K., Katayama, T., Maruyama, K., Ida, T., … Murakami, N. (2010). Comparison of Feeding Suppression by the Anorexigenic Hormones Neuromedin U and Neuromedin S in Rats. *The Journal of Endocrinology*, *207*(2), 185–93.

Nakai, J., Ohkura, M., & Imoto, K. (2001). A High Signal-to-Noise Ca(2+) Probe Composed of a Single Green Fluorescent Protein. *Nature Biotechnology*, *19*(2), 137–41.

Neckameyer, W. S., & Bhatt, P. (2012). Neurotrophic Actions of Dopamine on the Development of a Serotonergic Feeding Circuit in Drosophila melanogaster. *BMC Neuroscience*, *13*(1), 26.

Nelson, G., Chandrashekar, J., Hoon, M. A., Feng, L., … Zuker, C. S. (2002). An Amino-Acid Taste Receptor. *Nature*, *416*(6877), 199–202.

Nelson, G., Hoon, M. a, Chandrashekar, J., & Ryb. (2001). Mammalian Sweet Taste Receptors. *Cell*, *106*, 381–390.

Neuner, P., Peier, A. M., Talamo, F., Ingallinella, P., … Pessi, A. (2014). Development of a Neuromedin U-human Serum Albumin Conjugate as a Long-acting Candidate for the Treatment of Obesity and Diabetes. Comparison with the PEGylated Peptide. *Journal of Peptide Science*, *20*(1), 7–19.

Nichols, R., Schneuwly, S. A., & Dixon, J. E. (1988). Identification and Characterization of a *Drosophila* Homologue to the Vertebrate Neuropeptide Cholecystokinin. *Journal of Biological Chemistry*, *263*(25), 12167–12170.

Niewalda, T., Singhal, N., Fiala, A., Saumweber, T., … Gerber, B. (2008). Salt Processing in Larval *Drosophila*: Choice, Feeding, and Learning Shift from Appetitive to Aversive in a Concentration-Dependent Way. *Chemical Senses*, *33*(8), 685–692.

Nüsslein-Volhard, C., & Wieschaus, E. (1980). Mutations Affecting Segment Number and Polarity in *Drosophila*. *Nature*, *287*(5785), 795–801.

Ongur, D. (2000). The Organization of Networks within the Orbital and Medial Prefrontal Cortex of Rats, Monkeys and Humans. *Cerebral Cortex*, *10*(3), 206–219.

Oppliger, F. Y., M. Guerin P., P., & Vlimant, M. (2000). Neurophysiological and Behavioural Evidence for an Olfactory Function for the Dorsal Organ and a Gustatory One for the Terminal Organ in *Drosophila melanogaster* Larvae. *Journal of Insect Physiology*, *46*(2), 135–144.

Park, D., Veenstra, J. A., Park, J. H., & Taghert, P. H. (2008). Mapping Peptidergic Cells in *Drosophila*: Where DIMM Fits In. *PLoS ONE*, *3*(3).

Park, Y., Kim, Y.-J., & Adams, M. E. (2002). Identification of G Protein-coupled Receptors for *Drosophila* PRXamide Peptides, CCAP, Corazonin, and AKH Supports a Theory of Ligand-Receptor Coevolution. *Proceedings of the National Academy of Sciences of the United States of America*, *99*(17), 11423–11428.

Patterson, G. H., Lippincott-Schwartz, J., Momethylase, C.-, Patterson, G. H., … Momethylase, C.-. (2002). A Photoactivatable GFP for Selective Photolabeling of Proteins and Cells. *Science*, *297*(5588), 1873–1877.

Penzlin, H. (1985). Stomatogastric Nervous System. In G. A. Kerkut & L. I. GIlbert (Eds.), *Comp. Insect Physiol. Biochem. Pharmacol.* (vol 5., pp. 371–406). Oxford, UK: Pergammon.

Peter, M., Bathellier, B., Fontinha, B., Pliota, P., … Rumpel, S. (2013). Transgenic Mouse Models Enabling Photolabeling of Individual Neurons In Vivo. *PLoS ONE*, *8*(4).

Pool, A.-H., Kvello, P., Mann, K., Cheung, S. K., … Scott, K. (2014a). Four GABAergic Interneurons Impose Feeding Restraint in *Drosophila*. *Neuron*, *83*(1), 164–177.

Pool, A.-H., & Scott, K. (2014b). Feeding Regulation in *Drosophila*. *Current Opinion in Neurobiology*, *29*, 57–63.

Prüßing, K., Voigt, A., & Schulz, J. B. (2013). *Drosophila melanogaster* as a Model Organism for Alzheimer ' s Disease. *Molecular Neurodegeneration*, *8*(35).

Pulver, S. R., Pashkovski, S. L., Hornstein, N. J., Garrity, P. a, & Griffith, L. C. (2009). Temporal Dynamics of Neuronal Activation by Channelrhodopsin-2 and TRPA1 Determine Behavioral Output in *Drosophila* Larvae. *Journal of neurophysiology*, *101*(6), 3075–3088.

Radford, J. C. (2002). Systematic G-protein-coupled Receptor Analysis in *Drosophila melanogaster* Identifies a Leucokinin Receptor with Novel Roles. *Journal of Biological Chemistry*, *277*(41), 38810–38817.

Rajan, A., & Perrimon, N. (2013). Of Flies and Men: Insights on Organismal Metabolism from Fruit Flies. *BMC biology*, *11*, 38.

Rohwedder, A., Wenz, N. L., Stehle, B., Huser, A., … Thum, A. S. (2016). Four Individually Identified Paired Dopamine Neurons Signal Reward in Larval *Drosophila*. *Current Biology*, *26*(5), 661–669.

Rosenkilde, C., Cazzamali, G., Williamson, M., Hauser, F., … Grimmelikhuijzen, C. J. . (2003). Molecular Cloning, Functional Expression, and Gene Silencing of Two *Drosophila* Receptors for the *Drosophila* neuropeptide Pyrokinin-2. *Biochemical and Biophysical Research Communications*, *309*(2), 485–494.

Rulifson, E. J., Kim, S. K., & Nusse, R. (2002). Ablation of Insulin-producing Neurons in Flies: Growth and Diabetic Phenotypes. *Science*, *296*(5570), 1118–1120.

Schlegel, P., Texada, M. J., Miroschnikow, A., Peters, M., … Pankratz, M. J. (2016). Synaptic Transmission Parallels Neuromodulation in a Central Food-Intake Circuit. *bioRxiv*.

Schleyer, M., Miura, D., Tanimura, T., & Gerber, B. (2015). Learning the Specific Quality of Taste Reinforcement in Larval *Drosophila*. *eLife*, *2015*(4), 1–10.

Schoofs, A., Hückesfeld, S., Schlegel, P., Miroschnikow, A., … Pankratz, M. J. (2014). Selection of Motor Programs for Suppressing Food Intake and Inducing Locomotion in the *Drosophila* Brain. *PLoS Biology*, *12*(6), e1001893.

Schoofs, A., Hückesfeld, S., Surendran, S., & Pankratz, M. J. (2014). Serotonergic Pathways in the *Drosophila* Larval Enteric Nervous System. *Journal of Insect Physiology*, *69*, 118–125.

Schoofs, A., Niederegger, S., van Ooyen, A., Heinzel, H.-G., & Spieß, R. (2010). The Brain Can Eat: Establishing the Existence of a Central Pattern Generator for Feeding in Third Instar Larvae of Drosophila virilis and Drosophila melanogaster. *Journal of Insect Physiology*, *56*(7), 695–705.

Schoofs, A., & Spieß, R. (2007). Anatomical and Functional Characterisation of the Stomatogastric Nervous System of Blowfly (*Calliphora vicina*) Larvae. *Journal of Insect Physiology*, *53*(4), 349–60.

Schroll, C., Riemensperger, T., Bucher, D., Ehmer, J., … Fiala, A. (2006). Light-induced Activation of Distinct Modulatory Neurons Triggers Appetitive or Aversive Learning in Drosophila Larvae. *Current Biology*, *16*(17), 1741–1747.

Schröter, U., & Menzel, R. (2003). A New Ascending Sensory Tract to the Calyces of the Honeybee Mushroom Body, the Subesophageal-Calycal Tract. *Journal of Comparative Neurology*, *465*(2), 168–178.

Schwartz, M. W., Seeley, R. J., Woods, S. C., Weigle, D. S., … Baskin, D. G. (1997). Leptin Increases Hypothalamic Pro-opiomelanocortin mRNA Expression in the Rostral Arcuate Nucleus. *Diabetes*, *46*(12), 2119–2123.

Scott, K., Brady, R., Cravchik, J., Morozov, A., … Axel, R. (2001). A Chemosensory Gene Family Encoding Candidate Gustatory and Olfactory Receptors. *Cell*, *104*, 661–673.

Segal-Lieberman, G., Trombly, D. J., Juthani, V., Wang, X., & Maratos-Flier, E. (2003). NPY Ablation in C57BL/6 Mice Leads to Mild Obesity and to an Impaired Refeeding Response to Fasting. *American Journal of Physiology - Endocrinology And Metabolism*, *284*(6), E1131–E1139.

Selverston, A. I. (2010). Invertebrate Central Pattern Generator circuits. *Philosophical Transactions of the Royal Society B: Biological Sciences*, *365*(1551), 2329–2345.

Selverston, A. I., & Moulins, M. (1987). *The Crustacean Stomatogastric Nervous System*. Springer Verlag.

Shousha, S., Nakahara, K., Miyazato, M., Kangawa, K., & Murakami, N. (2005). Endogenous Neuromedin U Has Anorectic Effects in the Japanese Quail. *General and Comparative Endocrinology*, *140*(3), 156–163.

Sillar, K. (1993). Dynamic Biological Networks: The Stomatogastric Nervous System. *Trends in Neurosciences*, *16*(5), 198–199.

Singh, R. N. (1997). Neurobiology of the Gustatory Systems of *Drosophila* and Some Terrestrial Insects. *Microscopy Research and Technique*, *39*(6), 547–563.

Söderberg, J. A. E., Carlsson, M. A., & Nässel, D. R. (2012). Insulin-Producing Cells in the *Drosophila* Brain also Express Satiety-Inducing Cholecystokinin-Like Peptide, Drosulfakinin. *Frontiers in Endocrinology*, *3*(August), 1–13.

Sohn, J.-W., Elmquist, J. K., & Williams, K. W. (2013). Neuronal Circuits that Regulate Feeding Behavior and Metabolism. *Trends in Neurosciences*, *36*(9), 504–512.

Spector, A. C. (2005). The Representation of Taste Quality in the Mammalian Nervous System. *Behavioral and Cognitive Neuroscience Reviews*, *4*(3), 143–191.

Spieß, R., Schoofs, A., & Heinzel, H.-G. (2008). Anatomy of the Stomatogastric Nervous System Associated With the Foregut in *Drosophila melanogaster* and *Calliphora vicina* Third Instar Larvae. *Journal of Morphology*, *282*(October 2007), 272–282.

Stocker, R. F. (1994). The Organization of the Chemosensory System in *Drosophila melanogaster*: A Review. *Cell Tissue Research*, *275*, 3–26.

Stocker, R. F. (2009). The Olfactory Pathway of Adult and Larval *Drosophila*: Conservation or Adaptation to Stage-specific Needs. *Annals of the New York Academy of Sciences*, *1170*, 482–486.

Strader, A. D., & Woods, S. C. (2005). Gastrointestinal Hormones and Food Fntake. *Gastroenterology*, *128*(1), 175–191.

Straub, V. a, & Benjamin, P. R. (2001). Extrinsic Modulation and Motor Pattern Generation in a Feeding Network: A Cellular Study. *The Journal of Neuroscience*, *21*(5), 1767–78.

Szekeres, P. G., Muir, A. I., Spinage, L. D., Miller, J. E., … Chambers, J. K. (2000). Neuromedin U is a Potent Agonist at the Orphan G Protein-coupled Receptor FM3. *Journal of Biological Chemistry*, *275*(27), 20247–20250.

Thomas, A. L., Davis, S. M., & Dierick, H. A. (2015). Of Fighting Flies, Mice, and Men: Are Some of the Molecular and Neuronal Mechanisms of Aggression Universal in the Animal Kingdom? *PLoS Genetics*, *11*(8), 1–14.

Thorne, N., Chromey, C., Bray, S., & Amrein, H. (2004). Taste Perception and Coding in *Drosophila*. *Current Biology*, *14*(12), 1065–1079.

Tissot, M., Gendre, N., & Stocker, R. F. (1998). Drosophila P[Gal4] lines Reveal that Motor Neurons Involved in Feeding Persist Through Metamorphosis. *Journal of Neurobiology*, *37*(2), 237–250.

Tokita, K., Inoue, T., & Boughter, J. D. (2009). Afferent Connections of the Parabrachial Nucleus in C57BL/6J Mice. *Neuroscience*, *161*(2), 475–488.

Travagli, R. A., Hermann, G. E., Browning, K. N., & Rogers, R. C. (2006). Brainstem Circuits Regulating Gastric Function. *Annual Review of Physiology*, *68*(1), 279–305.

Umeda, K., Shoji, W., Sakai, S., Muto, A., … Yawo, H. (2013). Targeted Expression of a Chimeric Channelrhodopsin in Zebrafish under Regulation of Gal4-UAS System. *Neuroscience Research*, *75*(1), 69–75.

von Euler, C. (1983). On the Central Pattern Generator for the Basic Breathing Rhythmicity. *Journal of applied physiology: respiratory, environmental and exercise physiology*, *55*(6), 1647–59.

Vosshall, L. B., & Stocker, R. F. (2007). Molecular Architecture of Smell and Taste in *Drosophila*. *Annual Review of Neuroscience*, *30*(1), 505–533.

Watanabe, K., Toba, G., Koganezawa, M., & Yamamoto, D. (2011). Gr39a, a Highly Diversified Gustatory Receptor in *Drosophila*, has a Role in Sexual Behavior. *Behavior Genetics*, *41*(5), 746–753.

Weiss, L. A., Dahanukar, A., Kwon, J. Y., Banerjee, D., & Carlson, J. R. (2011). The Molecular and Cellular Basis of Bitter Taste in *Drosophila*. *Neuron*, *69*(2), 258–272.

Wilson, D. M. (1961). The Central Nervous Control of Flight in a Locust. *J. Exp. Biol.*, *38*(2), 471–490.

Woods, S. C., Seeley, R. J., Jr, D. P., & Schwartz, M. W. (1998). Signals That Regulate Food Intake and Energy Homeostasis. *Science, 280*(May).

Wren, A. M., Small, C. J., Abbott, C. R., Jethwa, P. H., … Bloom, S. R. (2002). Hypothalamic Actions of Neuromedin U. *Endocrinology*, *143*(11), 4227–4234.

Wu, Q., Boyle, M. P., & Palmiter, R. D. (2009). Loss of GABAergic Signaling by AgRP Neurons to the Parabrachial Nucleus Leads to Starvation. *Cell*, *137*(7), 1225–1234.

Wu, Q., Clark, M. S., & Palmiter, R. D. (2012). Deciphering a Neuronal Circuit that Mediates Appetite. *Nature*, *483*(7391), 594–597.

Wu, Q., Wen, T., Lee, G., Park, J. H., … Shen, P. (2003). Developmental Control of Foraging and Social Behavior by the *Drosophila* neuropeptide Y-like system. *Neuron*, *39*(1), 147–161.

Wu, Q., Zhang, Y., Xu, J., & Shen, P. (2005). Regulation of Hunger-driven Behaviors by Neural Ribosomal S6 Kinase in *Drosophila*. *Proceedings of the National Academy of Sciences of the United States of America*, *102*(37), 13289–94.

Yamamoto, T. (2008). Central Mechanisms of Taste: Cognition, Emotion and Taste-elicited Behaviors. *Japanese Dental Science Review*, *44*(2), 91–99.

Yarmolinsky, D. A., Zuker, C. S., & Ryba, N. J. P. (2009). Common Sense about Taste: From Mammals to Insects. *Cell*, *139*(2), 234–244.

Zhang, F., Aravanis, A. M., & Adamantidis, A. (2007). Circuit-breakers: Optical Technologies for Probing Neural Signals and Systems. *Nature*, *8*(August), 577–581.

Zhang, Y., Proenca, R., Maffei, M., Barone, M., … Friedman, J. M. (1994). Positional Cloning of the Mouse Obese Gene and its Human Homologue. *Nature*, *372*(6505), 425–432.

Zhao, S., Ting, J. T., Atallah, H. E., Qiu, L., … Feng, G. (2011). Cell-type Specific Optogenetic Mice for Dissecting Neural Circuitry Function. *Nature Methods*, *8*(9), 745–752.

Zinke, I., Kirchner, C., Chao, L. C., Tetzlaff, M. T., & Pankratz, M. J. (1999). Suppression of Food Intake and Growth by Amino Acids in *Drosophila*: the Role of *pumpless*, a Fat Body Expressed Gene with Homology to Vertebrate Glycine Cleavage System. *Development*, *126*(23), 5275–84.

Abbreviations

5-HT	5-hydroxytryptamin
A/D	analog/digital
AbN	abdominal nerve
Ach	acetylcholine
AGRP	agouti related protein
AKH, *akh*	adipokinetic hormone
AMMC	antennal mechanosensory motor center
AMY	amygdala
AN	antennal nerve
ARC, Arc	arcuate nucleus
AstA	allatostatin A
Ca^{2+}	calcium ions
CAM	calmodulin
CaMPARI	calcium modulated photoactivatable ratiometric integrator
CCK	cholecystokinin
CDM	cibarial dilator muscles
ChR2	channelrhodopsin 2
Cl^-	chloride ions
cm	centimeter
CNS	central nervous system
CPG	central pattern generator
CPS	cephalo-pharyngeal skeleton
CRH	corticotropin-releasing hormone
cry- dNPF	cryptochrome negative *Drosophila* neurpeptide F
CRZ	corazonin
CTA	conditioned taste aversion
ctrl	control
DA	dorsal arm
DA	dopamine
DCSO	dorsal cibarial sense organ
Den	denatonium
dilP	*Drosophila* insulin like peptide
DILP2	*Drosophila* insulin like peptide 2
DMH	dorsomedial hypothalamic nucleus
DO	dorsal organ
DopECR	dopamine/ecdysteroid receptor
DPS	dorsal pharyngeal sensilla
DSK	drosulfakinin
dTrpA1	*Drosophila* transient receptor potential A1

e.g.	exempli gratia
ENaC	epithelial sodium channel
eNpHR	enhanced *Natronomonas pharaonis* halorhodopsin
ENS	enteric nervous system
es	esophagus
exp	experiment
eYFP	enhanced yellow fluorescent protein
FG	frontal ganglion
FN	frontal nerve
FNJ	frontal nerve junction
GABA	gamma amino butyric acid
GCN2	general control nonderepressable 2
GFP	green fluorescent protein
GI	gastrointestinal
Glu	glutamate
GR	gustatory receptor
GRASP	gfp reconstitution across synaptic partners
GRN	gustatory receptor neuron
H	hypothalamus
HCG	hypocerebral ganglion
Hug	Hugin
IPCs	insulin producing cells
KCl	potassium chloride
kHz	kilo hertz
Kir	potassium inward rectifying
klu	klumpfuß
KO	knock out
LbO	labial organ
LED	light emitting diode
LES	lower esophageal sphincter
LK	leucokinin
LPS	lipopolysaccharide
LSO	labral sense organ
MB	mushroom body
MCH	melanin-concentrating hormone
MeN	mesothoracic nerve
mg	midgut
MgCl	magnesium chloride
MHD	mouth hook depressor
MHE	mouth hook elevator
µM	micomolar
min	minute
mM	millimolar
MN	maxillary nerve

mNSC	median neurosecretory cells
MOhm	mega ohm
mRFP	membrane tethered red fluorescent protein
n.s.	not significant
NaCl	sodium chloride
NCS	nervus cardiacus stomatogastricus
nm	nano meter
NMU	neuromedin U
NPY	neuropeptide Y
NTS, NST	nucleus tractus solitarius
OA	octopamine
OFC	orbifrontal cortex
P, ph	pharynx
PaGFP	photoactivatable GFP
PaN	prothoracic accessory nerve
PBN, PbN	parabrachial nucleus
PBT	phosphate buffered saline with tween
PC	protocerebrum
PFA	paraformaldehyde
PI	pars intercerebralis
Pit	pituitary gland
PK2	pyrokinin 2
PK2R1	pyrokinin 2 receptor 1
PKD2L1	polycystic kidney disease 2-like 1 protein
PL	pars lateralis
POMC	pro-opiomelanocortin
ppl	pumpless
PPS	posterior pharyngeal sensilla
ProdoA	dorsal protractor muscle A
ProN	prothoracic nerve
PSP	postsynaptic potential
PV, pv	proventriculus
PVG	proventricular ganglion
PVN	paraventricular nucleus
Qui	quinine
RG	ring gland
RN	recurrent nerve
RNA	ribonucleic acid
ROI	region of interest
SCN	suprachiasmic nucleus
SEA	antennal nerve serotonergic neurons
sec	second
SEM	standard error of the mean
SEZ	subesophageal zone

shi^{TS}	temperature sensitives allel von *shibire*
sNPF	short neuropeptide F
SNS	satellite nervous system
SOG	subesophageal ganglion
STG	stomatogastric ganglion
T1R2	taste receptor type 1 member 2
T1R3	taste receptor type 1 member 3
T2R	taste receptor type 2
TH-VUM	ventral unpaired medial dopaminergic neuron
Tmr-D	tetramethylrhodamine dextran
TO	terminal organ
TPH1/2	tryptophan-hydroxylase 1/2
TRC	taste receptor cell
TRH	tryptophan-hydroxylase
UAS	upstream activating sequence
UES	upper esophageal sphincter
UV	ultra violet
VCSO	ventral cibarial sense organ
VDRC	Vienna *Drosophila* resource center
VMH	ventromedial hypothalamus
VNC	ventral nerve cord
VO	ventral organ
VPM	ventral posteromedial nucleus
VPS	ventral pharyngeal sensilla
ZMG	Zentraler Mustergenerator
ZNS	Zentrales Nervensystem

Copyright and Licensing of Figures and Research Articles

The presented research articles in this cumulative thesis underlie the following copyright:

Chapter 2:   Hückesfeld et al, 2015 (PloS One)

Chapter 3:   Schoofs, A.; Hückesfeld, S. et al., 2014 (J. Insect Physiol.)

Chapter 4:   Schoofs, A.; Hückesfeld, S. et al., 2014 (Plos Biology)

Parts of figures presented in the General Introduction underlie the following copyright:

Figure 1.1 a: Adapted from [MATSUO & PALMER, 2009].

DOI: 10.1016/j.pmr.2008.06.001.Anatomy

Obtained single user license.

Figure 1.1 b: Adapted from [ERTEKIN & AYDOGDU, 2003]

DOI: 10.1016/S1388-2457(03)00237-2

obtained single user license.

This is a License Agreement between Sebastian Hückesfeld ("You") and Elsevier ("Elsevier") provided by Copyright Clearance Center ("CCC"). The license consists of your order details, the terms and conditions provided by Elsevier, and the payment terms and conditions.

All payments must be made in full to CCC. For payment instructions, please see information listed at the bottom of this form.

Supplier	Elsevier Limited
	The Boulevard,Langford Lane
	Kidlington,Oxford,OX5 1GB,UK
Registered Company Number	1982084
Customer name	Sebastian Hückesfeld
Customer address	Carl-Troll-Str. 31
	Bonn, NRW 53175
License number	3853450289204
License date	Apr 21, 2016
Licensed content publisher	Elsevier
Licensed content publication	Clinical Neurophysiology
Licensed content title	Neurophysiology of swallowing
Licensed content author	Cumhur Ertekin,Ibrahim Aydogdu
Licensed content date	December 2003
Licensed content volume number	114
Licensed content issue number	12
Number of pages	19
Start Page	2226
End Page	2244
Type of Use	reuse in a thesis/dissertation
Intended publisher of new work	other
Portion	figures/tables/illustrations
Number of figures/tables/illustrations	1
Format	both print and electronic
Are you the author of this Elsevier article?	No
Will you be translating?	No
Original figure numbers	2
Title of your thesis/dissertation	The Control of Food Intake and Bitter Taste Information Processing in the Drosophila Larval Brain
Expected completion date	Apr 2016
Estimated size (number of pages)	170
Elsevier VAT number	GB 494 6272 12
Permissions price	0.00 USD
VAT/Local Sales Tax	0.00 USD / 0.00 GBP
Total	0.00 USD

for terms and conditions, see https://www.elsevier.com/about/company-information/policies/open-access-licenses/elsevier-user-license

Figure 1.2 b: Adapted from [Zɪɴᴋᴇ ᴇᴛ ᴀʟ., 1999]

at http://dev.biologists.org/content/126/23/5275.long

open access article, see http://dev.biologists.org/content/rights-permissions

additional permission from author Michael J. Pankratz to adapt figure for use in this thesis.

Figure 1.2 f: Adapted from [Sᴄʜᴏᴏғs & Sᴘɪᴇß, 2007]

DOI: 10.1016/j.jinsphys.2006.12.009

obtained single user license.

This is a License Agreement between Sebastian Hückesfeld ("You") and Elsevier ("Elsevier") provided by Copyright Clearance Center ("CCC"). The license consists of your order details, the terms and conditions provided by Elsevier, and the payment terms and conditions.

All payments must be made in full to CCC. For payment instructions, please see information listed at the bottom of this form.

Supplier	Elsevier Limited
	The Boulevard,Langford Lane
	Kidlington,Oxford,OX5 1GB,UK
Registered Company Number	1982084
Customer name	Sebastian Hückesfeld
Customer address	Carl-Troll-Str. 31
	Bonn, NRW 53175
License number	3853511458849
License date	Apr 21, 2016
Licensed content publisher	Elsevier
Licensed content publication	Journal of Insect Physiology
Licensed content title	Anatomical and functional characterisation
	of the stomatogastric nervous system of blowfly (Calliphora vicina) larvae
Licensed content author	Andreas Schoofs,Roland Spieß
Licensed content date	April 2007
Licensed content volume number	53
Licensed content issue number	4
Number of pages	12
Start Page	349
End Page	360
Type of Use	reuse in a thesis/dissertation
Intended publisher of new work	other
Portion	figures/tables/illustrations
Number of figures/tables/illustrations	1
Format	both print and electronic
Are you the author of this Elsevier article?	No
Will you be translating?	No
Original figure numbers	Figure 2 A
Title of your thesis/dissertation	The Control of Food Intake and Bitter Taste Information Processing
	in the Drosophila Larval Brain
Expected completion date	Apr 2016
Estimated size (number of pages)	170
Elsevier VAT number	GB 494 6272 12
Permissions price	0.00 EUR
VAT/Local Sales Tax	0.00 EUR / 0.00 GBP
Total	0.00 EUR

Figure 1.4: taken from [POOL & SCOTT, 2014]

DOI: 10.1016/j.conb.2014.05.008

obtained single user license

This is a License Agreement between Sebastian Hückesfeld ("You") and Elsevier ("Elsevier") provided by Copyright Clearance Center ("CCC"). The license consists of your order details, the terms and conditions provided by Elsevier, and the payment terms and conditions.

All payments must be made in full to CCC. For payment instructions, please see information listed at the bottom of this form.

Supplier	Elsevier Limited
	The Boulevard,Langford Lane
	Kidlington,Oxford,OX5 1GB,UK
Registered Company Number	1982084
Customer name	Sebastian Hückesfeld
Customer address	Carl-Troll-Str. 31
	Bonn, NRW 53175
License number	3851811199070
License date	Apr 18, 2016
Licensed content publisher	Elsevier
Licensed content publication	Current Opinion in Neurobiology
Licensed content title	Feeding regulation in Drosophila
Licensed content author	Allan-Hermann Pool,Kristin Scott
Licensed content date	December 2014
Licensed content volume number	29
Licensed content issue number	n/a
Number of pages	7
Start Page	57
End Page	63
Type of Use	reuse in a thesis/dissertation
Portion	figures/tables/illustrations
Number of figures/tables/illustrations	2
Format	both print and electronic
Are you the author of this Elsevier article?	No
Will you be translating?	No
Original figure numbers	Figures 1 and 3
Title of your thesis/dissertation	The Control of Food Intake and Bitter Taste Information Processing in the Drosophila Larval Brain
Expected completion date	Apr 2016
Estimated size (number of pages)	170
Elsevier VAT number	GB 494 6272 12
Permissions price	0.00 EUR
VAT/Local Sales Tax	0.00 EUR / 0.00 GBP

Figure 1.6 b: adapted from [MELCHER & PANKRATZ, 2005]

This is an open-access article distributed under the terms of the Creative Commons Attribution License, which permits unrestricted use, distribution, and reproduction in any medium, provided the original work is properly cited.

Figure 1.7 and 1.8 a: adapted from [Yᴀʀᴍᴏʟɪɴsᴋʏ ᴇᴛ ᴀʟ., 2009]

DOI: 10.1016/j.cell.2009.10.001

obtained single user license.

This is a License Agreement between Sebastian Hückesfeld ("You") and Elsevier ("Elsevier") provided by Copyright Clearance Center ("CCC"). The license consists of your order details, the terms and conditions provided by Elsevier, and the payment terms and conditions.

All payments must be made in full to CCC. For payment instructions, please see information listed at the bottom of this form.

Supplier	Elsevier Limited
	The Boulevard,Langford Lane
	Kidlington,Oxford,OX5 1GB,UK
Registered Company Number	1982084
Customer name	Sebastian Hückesfeld
Customer address	Carl-Troll-Str. 31
	Bonn, NRW 53175
License number	3851811410070
License date	Apr 18, 2016
Licensed content publisher	Elsevier
Licensed content publication	Cell
Licensed content title	Common Sense about Taste: From Mammals to Insects
Licensed content author	David A. Yarmolinsky,Charles S. Zuker,Nicholas J.P. Ryba
Licensed content date	16 October 2009
Licensed content volume number	139
Licensed content issue number	2
Number of pages	11
Start Page	234
End Page	244
Type of Use	reuse in a thesis/dissertation
Intended publisher of new work	other
Portion	figures/tables/illustrations
Number of figures/tables/illustrations	3
Format	both print and electronic
Are you the author of this Elsevier article?	No
Will you be translating?	No
Original figure numbers	figures 1,3 and 5
Title of your thesis/dissertation	The Control of Food Intake and Bitter Taste Information Processing in the Drosophila Larval Brain
Expected completion date	Apr 2016
Estimated size (number of pages)	170
Elsevier VAT number	GB 494 6272 12
Permissions price	0.00 USD
VAT/Local Sales Tax	0.00 USD / 0.00 GBP
Total	0.00 USD

Figure 1.9 b: adapted and modified from [Kᴀsᴜʏᴀ, 2009]

This is an open-access article subject to an exclusive license agreement between the authors and the Frontiers Research Foundation, which permits unrestricted use, distribution, and reproduction in any medium, provided the original authors and source are credited.

Figure 1.9 d: adapted from [F. Zhang et al., 2007]

obtained single user license.

This is a License Agreement between Sebastian Hückesfeld ("You") and Nature Publishing Group ("Nature Publishing Group") provided by Copyright Clearance Center ("CCC"). The license consists of your order details, the terms and conditions provided by Nature Publishing Group, and the payment terms and conditions.

All payments must be made in full to CCC. For payment instructions, please see information listed at the bottom of this form.

License Number	3853460769164
License date	Apr 21, 2016
Licensed content publisher	Nature Publishing Group
Licensed content publication	Nature Reviews Neuroscience
Licensed content title	Circuit-breakers: optical technologies for probing neural signals and systems
Licensed content author	Feng Zhang,Alexander M. Aravanis,Antoine Adamantidis, Luis de Lecea and Karl Deisseroth
Licensed content date	Aug 1, 2007
Volume number	8
Issue number	8
Type of Use	reuse in a dissertation / thesis
Requestor type	academic/educational
Format	print and electronic
Portion	figures/tables/illustrations
Number of figures/tables/illustrations	1
High-res required	no
Figures	Figure 1 a
Author of this NPG article	no
Your reference number	None
Title of your thesis / dissertation	The Control of Food Intake and Bitter Taste Information Processing in the Drosophila Larval Brain
Expected completion date	Apr 2016
Estimated size (number of pages)	170
Total	0.00 USD